COMPUTATIONAL FLUID DYNAMICS (CFD) STUDY ON AIR FLOW CHARACTERISTICS OF CEILING AIR DIFFUSER IN ROOM

YEE CHUN KIET

A project report submitted in partial fulfilment of the requirements for the award of Master of Engineering (Mechanical)

Lee Kong Chian Faculty of Engineering and Science
Universiti Tunku Abdul Rahman

May 2015

DECLARATION

I hereby declare that this project report is based on my original work except for citations and quotations which have been duly acknowledged. I also declare that it has not been previously and concurrently submitted for any other degree or award at UTAR or other institutions.

Signature	:	
Name	:	YEE CHUN KIET
ID No.	:	13UEM02090
Date	:	13 April 2015

APPROVAL FOR SUBMISSION

I certify that this project report entitled **"COMPUTATIONAL FLUID DYNAMICS (CFD) ON AIR FLOW CHARACTERISTICS OF CEILING AIR DIFFUSER IN ROOM"** was prepared by **YEE CHUN KIET** has met the required standard for submission in partial fulfilment of the requirements for the award of Master of Engineering (Mechanical) at Universiti Tunku Abdul Rahman.

Approved by,

Signature	:	
Supervisor	:	Dr. Lai Soon Onn
Date	:	13 April 2015

Specially dedicated to

my beloved wife and daughter

ACKNOWLEDGEMENTS

I would like to thank everyone who had contributed to the successful completion of this project. I would like to express my gratitude to my research supervisor, Dr. Lai Soon Onn for his invaluable advice, guidance and his enormous patience throughout the development of the research.

In addition, I would also like to express my gratitude to my loving parent and friends who had helped and given me encouragement particularly Mr. Lee Sze Shin and Mr. Chay Kwok Goon who have guided me through the program used for computational work in this project.

COMPUTATIONAL FLUID DYNAMICS STUDY ON AIR FLOW CHARACTERISTICS OF CEILING AIR DIFFUSER IN ROOM

ABSTRACT

This project was aimed to investigate the air flow characteristics and temperature distribution of various round ceiling air diffusers installed at various outlet positions in a room utilising a CFD software package, i.e., ANSYS FLUENT. The results of proposed 5 and 7-blade air diffusers were compared with that of commercial 4-blade air diffuser by varying several factors such as diffuser blade types, blade angles, outlets position, inlet air velocities and temperatures to determine their improvement on the uniformity of air and temperature distribution at the air diffuser. The standard k–ε turbulent model was adopted in the three-dimensional simulation analysis to investigate the turbulent air flow characteristics. It was found that the proposed 5 and 7-blade air diffusers could exhibit more uniform air flow behaviour and temperature distribution within the room, while the 7-blade diffuser provided relatively more consistent air flow and temperature distribution than other models in this project. In addition, the model with two outlets near the wall bottom of the room allowed more effective air flow throughout the room than other outlet positions. An inlet air velocity of 1.0 m/s and temperature of 287 K were concluded to be optimal operating conditions for the 5 and 7-blade diffusers. Besides, the results of the dimensionless average room velocity and temperature were compatible with the CFD predicted results. Additionally, an effective energy consumption was observed, particularly for the proposed 7-blade air diffuser, to achieve required thermal comfort level according to the results of overall ventilation effectiveness and effective draft temperature.

TABLE OF CONTENTS

LIST OF TABLES

LIST OF FIGURES

LIST OF SYMBOLS / ABBREVIATIONS

°C	degree Celsius
C_p	specific heat capacity, J/(kg·K)
V	velocity, m/s
P	pressure, kPa
T	temperature, K
g	gravity acceleration, N/m^2
M	mass flow rate, kg/s
ρ	density, kg/m^3
β	thermal expansion coefficient of air, K^{-1}
μ	dynamic viscosity, N s/m^2
λ	thermal conductivity, W/m K
ASHRAE	American Society of Heating, Refrigerating, and Air-Conditioning Engineers
CAD	computer-aided design
CFD	computational fluid dynamics
CPU	central processing unit
HVAC	heating, ventilation and air conditioning
RAM	random-access memory
RH	relative humidity

LIST OF APPENDICES

CHAPTER 1

INTRODUCTION

1.1 Background on Round Ceiling Air Diffuser

The ceiling air diffuser is the mechanical device that controls the characteristics of air flow to an enclosure (such as room, hall, corridor, and etc.) for air conditioning or ventilation purpose, where it will reduce the supply air velocity at the terminal in order to enhance the mixing of supply air and surrounding air within the enclosure. It usually consists of a number of deflection blades or vanes, which will direct the air to the desired direction or orientation (Tavakoli & Hosseini, 2013).

There are various type of ceiling air diffusers available in the market, in which round ceiling air diffuser is one of the widely used diffusers in commercial buildings to obtain intended air flow rate and even air distribution within a room or open space in order to achieve required indoor air quality and thermal comfort after the delivered air mixes with room air at optimized noise level (Aziz et al., 2012).

1.2 Background on Computational Fluid Dynamics (CFD)

Computational fluid dynamics (CFD) can be one of the subjects of fluid dynamics that applies the numerical methods and algorithms to analyse and resolve issues regarding the fluid flows in laminar or turbulent approach for any geometry. It is one of the popular tools for modelling, simulating, predicting and reporting flow characteristics or performance of air, gases and liquids, temperature, heat transfer, acoustic, mass flow rate of static or dynamics bodies in simple or complex design (Moukalled et al., 2011).

Pre-processing, solving and post-processing are the three stages involved in the CFD simulation. Pre-processing mainly used to create and analyse the flow model using the computer-aided design (CAD) package, i.e. ANSYS FLUENT, GAMBIT, COMSOL, etc., which constructs and forms acceptable computational mesh, and inputs the properties of fluid materials and flow boundary conditions in order to produce suitable and fine mesh for the model with unique curvature and proximity features (ANSYS, 2015).

The CFD solver performs the flow calculations and produces the results at solving stage, where the FLUENT CFD code permits modification to be conducted over the analysis when necessary in high speed, accuracy, and flexibility. The post-processing stage of CFD simulation organises and interprets the predicted flow technical data and generates the CFD images and animations (ANSYS, 2015).

1.3 Problem Statement

Round ceiling air diffuser with four blades or vanes are commonly used to supply and distribute conditioned air in any room in the industry due to their capability to achieve desired air flow rate in competitive cost. However, uneven supply air distribution to the room occurred on a particular 4-blade round ceiling air diffuser design based on a sample trial testing by others (but the testing results were not available). The aforesaid situation will affect the room thermal comfort or create unpleasant condition where the room temperature underneath the air diffuser may be relatively low (approximate 17°C) and occupants around the air diffuser may feel uncomfortable. A design of round ceiling air diffuser with better air flow and temperature distribution is therefore required.

1.4 Aim and Objectives

The aim of this project was to identify the issue of uneven air distribution from the previous mentioned four blades round ceiling air diffuser, and to conduct numerical simulation study to minimise the aforesaid issue by proposing diffusers with different blade configuration in order to provide uniform air distribution to improve the air flow behaviour and temperature distribution in a room via CFD. Meanwhile, the project objectives are stated as below:

1. To evaluate the performance of 5 and 7-blade round ceiling air diffusers with an average blade angle of 40° and 5-blade round ceiling air diffuser with blade angle of 30° in providing uniform air distribution and achieving thermal comfort required in a room.

2. To compare the performance of each type of proposed diffuser with commercial 4-blade air diffuser in terms of air flow behaviour and temperature distribution.

3. To determine an optimum outlet position, inlet velocity and inlet temperature of air diffuser to obtain better thermal comfort level in a room.

4. To assess the effectiveness of the proposed air diffusers in reducing energy consumption by air handling unit to cool down the supply air.

1.5 Scope of Work

The round ceiling air diffuser with various types of blades was mounted on top of central of a room (2 m length × 2 m width × 2 m height), with one or two outlets on top of the room or near wall bottoms. The models were drafted, meshed, and simulated for their air flow behaviour and temperature distribution using ANSYS FLUENT 15.0. The CFD simulation was conducted on the existing 4-blade diffuser and also the proposed 5 and 7-blade diffusers.

The grid independence was conducted to optimize the mesh size used in the simulation models. The standard k–ε turbulence model was chosen as it has been proven to be the most appropriate or proper model to study the turbulent air flow characteristics in ventilated spaces (Zhao et al., 2003).

The results of velocity and temperature in the room were presented in contour and X-Y plot. The dimensionless average room velocity and temperature were calculated to compare with the CFD predicted results. Lastly, the overall ventilation effectiveness and effective draft temperature were used to determine the energy consumption of the proposed diffusers.

CHAPTER 2

LITERATURE REVIEW

2.1 Ceiling Air Diffusers

The ceiling mounted air diffuser or grille can be the mechanical device adopted for controlling or adjusting air flow behaviour at air inlet to an open system of thermodynamic, which is commonly used in air conditioning or mechanical ventilation system, where they are serving several purposes for room air distribution (Mohammed, 2013):

1. To deliver required air flow for air conditioning in any space.
2. To return or remove required air flow from air conditioning or mechanical ventilated space respectively.
3. To direct air flow uniformly to any designated position.
4. To ensure mixing of primary supply air and room air effectively.
5. To create air jet effect for longer air flow distance.
6. To lower down air velocity movement in order to minimise noise level generation.

There are many types of ceiling air diffusers available in the market as indicated in Figures 2.1 to 2.6. Each of them has its particular function besides the aesthetic or appearance features to meet the interior design requirement.

2.1.1 Round Ceiling Air Diffuser

The round ceiling air diffuser is capable of a high aspiration rate and handle large amount of air flow rate at relatively low noise levels for supply and return air applications, which is useful to be installed in open spaces with high ceiling level such as auditorium, airport lobby, hypermarket, multi-purpose hall and factory (Ruskin, 2014).

The multi core or blade design is mainly for high flow requirement and suitable for high end interior design and also adequate for both ceiling mounted i.e. 600 × 600 or 1200 × 600 mm ceiling grid system or plaster ceiling system and exposed installation on ductwork for horizontal or vertical air throw pattern by adjustment via rotation of centre core. The outer diameter of the air diffuser frame can be 300, 400, 500 and 600 mm with varied neck size for ductwork connection based on air flow volume required. It is made of extruded aluminium sheet metal in 1.0 to 1.2 mm thickness with powder coated epoxy paint in white colour or other colour for surface finishes to match the surrounding ceiling or wall colour (Ruskin, 2014).

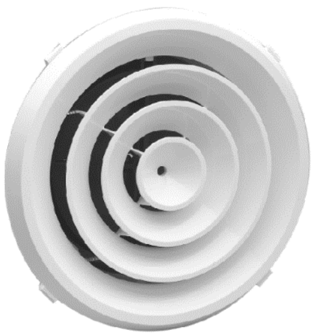

Figure 2.1: Round ceiling air diffuser (Hart & Cooley, 2014)

2.1.2 Square Ceiling Air Diffuser

The ceiling mounted square diffuser has wide range of deflection designs and is able to provide air throw pattern in horizontal, angle or vertical direction. By arranging the blade vanes in pre-determine orientation, the air diffuser is able to create multi directional air flow from a single outlet, which to be in 1, 2, 3 or 4 different way flow directions. It is usually used at those rooms, spaces or corridors where the ceiling height is around 2 to 3 m high. It can be mounted on 600 × 600 or 1200 × 600 mm ceiling grid system or plaster ceiling system and exposed installation on ductwork (PrudentAire, 2014).

The air diffuser frame outer size is usually 600 × 600 mm with varied neck size for ductwork connection based on air flow volume required. The centre core of the air diffuser can be removed for maintenance access. Its frame and vanes materials can be 1.2 mm thick extruded aluminium or 0.6 mm thick galvanised steel sheet metal respectively. Its surface finishes can be either epoxy polyester powder spray coated paint or naturally anodized (PrudentAire, 2014).

Figure 2.2: Square ceiling air diffuser (Hart & Cooley, 2014)

2.1.3 Ceiling Swirl Air Diffuser

The ceiling swirl air diffuser (Figure 2.3) is designed to optimise air distribution effectiveness, where it has high air induction from diffuser to extract stagnant room air, and 360° swirl air throw pattern for better Coanda effect to circulate the air masses for flushing the whole room in order to achieve quicker mixing of supply air and room air as indicated in Figure 2.4 (HC-Barcol-Air, 2012). The Coanda effect can also be illustrated as air jet from the air diffuser to room space and can move in contact with the adjacent surface of the ceiling or wall (Tavakoli & Hosseini, 2013). It is usually used at those rooms or spaces where the ceiling height is around 2 to 3 m high. It can be mounted on 600 × 600 or 1200 × 600 mm ceiling grid system or plaster ceiling system and exposed installation on ductwork (PrudentAire, 2014).

The air diffuser frame outer size is usually 600 × 600 mm with varied neck size for ductwork connection based on air flow volume required. Its frame and vanes materials can be 0.7 mm thick and 1.0 mm thick stainless steel or galvanised steel sheet metal respectively. Its surface finishes can be coated with 9010 RAL silver grey paint (PrudentAire, 2014).

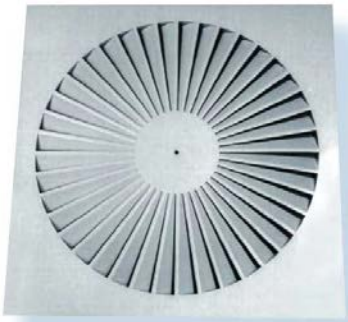

Figure 2.3: Swirl ceiling air diffuser (JPR Services, 2015)

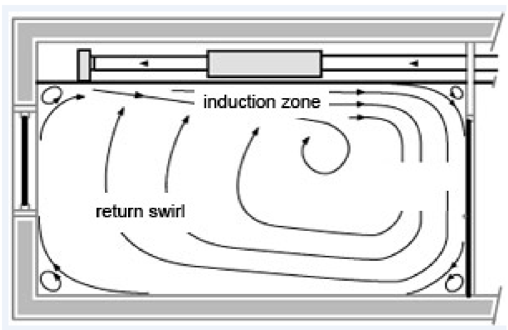

Figure 2.4: Coanda effect of air distribution (HC-Barcol-Air, 2012)

2.1.4 Jet Air Diffuser

The jet air diffuser is commonly used at wide open spaces i.e. convention hall, airport check in counter hall, etc., where ductwork can't be extended to the desire spot, to deliver air to localised target area over large distance up to 50 m. The air flow direction from the air diffuser deflectors can be adjusted in either one plane or two planes, and its aerodynamic design enables producing air flow at high outlet velocity without increasing the noise level of surrounding area. In addition, its fully rotatable centre core allows both narrow and wide throw configurations where the wider throw provides better air induction but at a shorter throw distance. Hence, it can be adjusted to throw the air to the desire distance within the 50 m span (PrudentAire, 2014).

The outer diameter of diffuser frame can be ranged from 280 to 430 mm with varied neck size for ductwork connection based on air flow volume required. Its frame and vanes materials can be 1.0 mm thick aluminium or 0.8 mm thick galvanised steel sheet metal, respectively. Its surface finishes can be epoxy polyester powder spray coated paint (PrudentAire, 2014).

Figure 2.5: Jet air diffuser (PrudentAire, 2014)

2.1.5 Linear Slot Ceiling Air Diffuser

The linear slot ceiling air diffuser with adjustable deflector blades can be used for horizontal and vertical flow in low noise and pressure loss operating conditions. It is mostly used at show rooms, hotel lobbies, conference rooms or spaces that required executive level of interior design plaster ceiling finishes due to its versatile and aesthetic, as it is available in highly customisable shapes. It can be detached individually for allowing cleaning of the terminal unit and ductwork (Halton, 2014).

The air diffuser frame nominal size can range from 600 to 1800 mm depends on the ceiling profile. Its slots can be range from 1 to 4 numbers where higher air flow rate can be provided on larger number of slots. . Its frame and deflector materials can be 1.2 mm thick and 1.0 mm thick extruded aluminium sheet metal respectively. Its surface finishes can be either anodised polyester paint or coated with 9010 RAL silver grey paint (Halton, 2014).

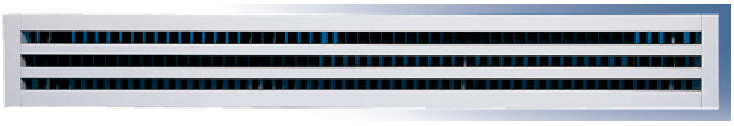

Figure 2.6: Linear slot ceiling air diffuser (Scottaire, 2014)

2.2 Flow Characteristics Study on Ceiling Air Diffusers

Design conditions of HVAC for human occupied in a conditioned room or space are usually specifying the room temperature to be maintained at 20 – 24°C, relative humidity (RH) to be maintained at 50 – 60% RH, and air flow velocity to be around 0.1 – 0.3 m/s respectively according to ASHRAE design guideline as indicated on Appendix A. While, those healthcare facilities required more stringent room condition control might prefer positive or negative room air pressure to be maintained with all room air to be exhausted without any recirculation in order to achieve the room air cleanliness or prevent any bacteria/virus spread to nearest space according to healthcare requirement (Aziz, et al. 2012).

Substantial amount of research on flow characteristics of ceiling air diffusers have been conducted previously for achieving the room conditions as specified by ASHRAE in which numerical method for CFD simulation is one of the major approach that being applied by many researchers besides experimental testing facilities. Meanwhile, the predicted results of CFD simulation were verified or validated with tested experimental data.

2.2.1 Experimental Approach and Numerical Method for CFD Simulation on Air Flow Characteristics of Ceiling Mounted Diffusers

The experimental and numerical air flow patterns for round, square, and vortex ceiling air diffuser had been investigated and identified for thermal comfort effect in the room with ventilation as revealed in Figures 2.7, 2.8 and 2.9. Two kinds of thermal comfort criteria such as effective draft temperature, and overall ventilation effectiveness were applied for predicting the thermal comfort level within the room space. A test room was established to measure and collected the temperature data, as well as used the unstructured grids to discretize the numerical domain. The conservation equations such as equations of continuity, momentum, energy, standard k–ε model, etc. were applied for solving the air flow analysis by using commercial FLUENT solver (Aziz et al., 2012).

a) Equation of continuity (Aziz et al., 2012)

$$\nabla . V = 0 \tag{2.1}$$

b) Equation of momentum (Aziz et al., 2012)

$$-\nabla P + \mu_{eff} \nabla^2 V + \rho g \beta (T - T_{ref}) = \rho V . \nabla V \tag{2.2}$$

where

ρ = Density, kg/m^3

V = Velocity, m/s

P = Pressure, Pa or N/m^2

μ_{eff} = Effective Dynamic Viscosity, N s/m^2 or kg/(m s)

β = Thermal Expansion Coefficient for air, K^{-1}

T_{ref} = Reference point temperature, K

T = Temperature for air, K

g = Gravity acceleration for air, N or kg/m^2

c) Equation of Effective Dynamic Viscosity (Aziz et al., 2012)

$$\mu_{eff} = \mu_t + \mu_l \tag{2.3}$$

where

μ_t = Turbulent Viscosity, kg/(m s) or N s/m^2

μ_l = Laminar Viscosity, kg/(m s) or N s/m^2

d) Equation of energy (Aziz et al., 2012)

$$\rho C_p V.\nabla T = \lambda_{eff} \nabla^2 T \tag{2.4}$$

where

C_p = Specific heat for constant pressure, J/kg K

λ_{eff} = Effective Thermal Conductivity, (W/m K)

e) Equation of Effective Thermal Conductivity (Aziz et al., 2012)

$$\lambda_{eff} = \lambda_t + \lambda_l \tag{2.5}$$

where

λ_t = Turbulent Thermal Conductivity, W/m K

λ_l = Laminar Thermal Conductivity, W/m K

f) Equation of standard *k*–*ε* turbulent model (Aziz et al., 2012)

$$\frac{\partial}{\partial x_i}(\rho u_i k) = (\mu + \frac{\mu_t}{\sigma_k})\nabla^2 k + \mu_t S^2 - \rho\varepsilon \tag{2.6}$$

$$\frac{\partial}{\partial x_i}(\rho u_i \varepsilon) = (\mu + \frac{\mu_t}{\sigma_\varepsilon})\nabla^2 \varepsilon + C_{\varepsilon 1}\frac{\varepsilon}{k}\mu_t S^2 - C_{\varepsilon 2}\rho\frac{s^2}{k} \tag{2.7}$$

$$u_t = \frac{\rho C_\mu k^2}{\varepsilon} \tag{2.8}$$

The coefficients of C_{μ}, σ_k, σ_{ε}, $C_{\varepsilon 1}$, $C_{\varepsilon 2}$ = 0.09, 1.0, 1.3, 1.44, 1.44 respectively and $S=(S_{ij}S_{ij})^{0.5}$(Aziz et al., 2012).

g) Equation of Overall Ventilation Effectiveness (E) (Aziz et al., 2012)

$$E = \frac{t_e - t_s}{t_m - t_s} \times 100 \tag{2.9}$$

The overall ventilation effectiveness is defined as efficiency of energy usage, which is provided in the room space to obtain thermally comfortable zone, where t_e is exit or outlet air temperature (K), t_m is mean or average temperature (K), and t_s is supply or inlet air temperature (K) (Aziz et al., 2012).

h) Equation of Effective Draft Temperature (EDT) (Aziz et al., 2012)

$$EDT = (t_x - t_m) - 8(V_x - 0.15) \tag{2.10}$$

The *EDT* is described as merging the velocity and temperature of air in which the *EDT* values between -1.7 and 1.1 are considered as thermally comfortable zone. It is cold impression if the values are below -1.7, and warm impression if the values are above 1.1. t_x is local air stream temperature (K), t_e is mean or average temperature (K), and V_x is local airstream velocity (m/s) (Aziz et al., 2012).

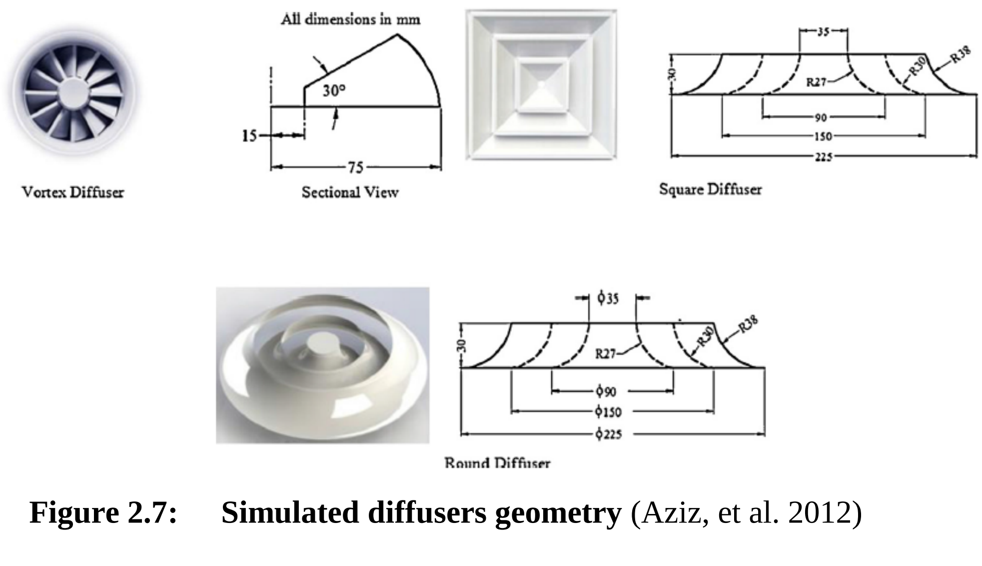

Figure 2.7: Simulated diffusers geometry (Aziz, et al. 2012)

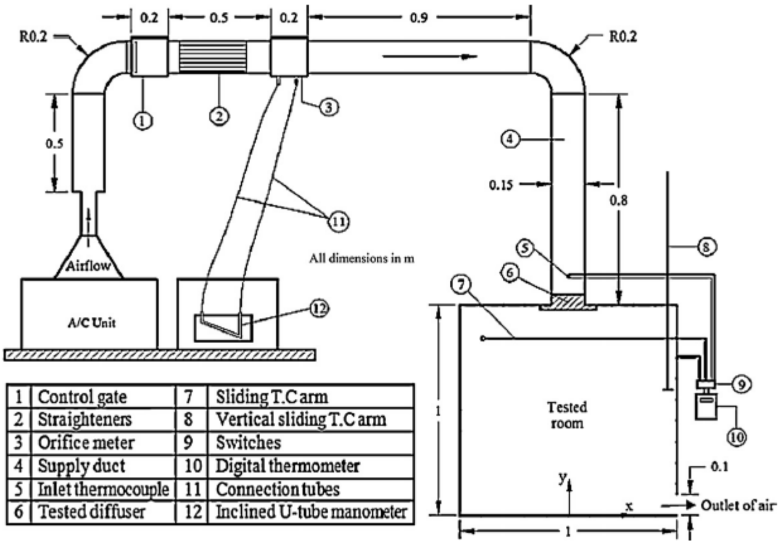

1	Control gate	7	Sliding T.C arm
2	Straighteners	8	Vertical sliding T.C arm
3	Orifice meter	9	Switches
4	Supply duct	10	Digital thermometer
5	Inlet thermocouple	11	Connection tubes
6	Tested diffuser	12	Inclined U-tube manometer

Figure 2.8: The experimental set-up schematic diagram (Aziz et al., 2012)

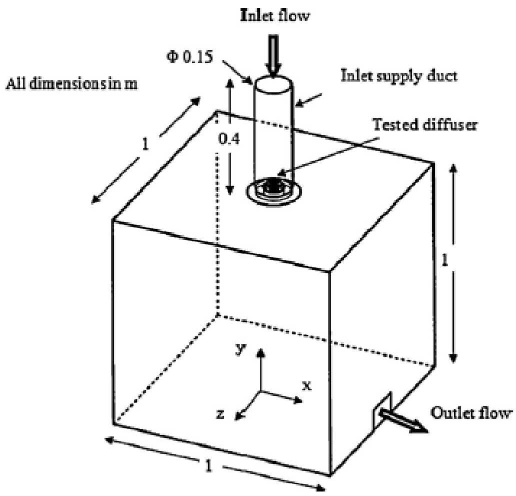

Figure 2.9: The computational schematic (Aziz et al., 2012)

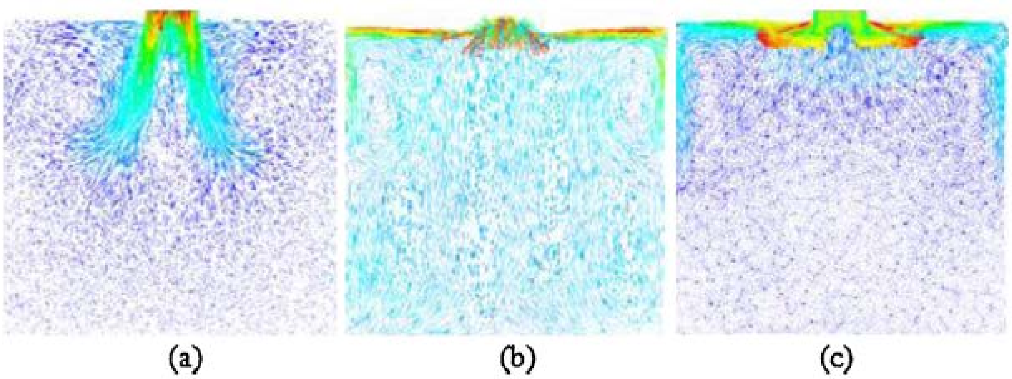

Figure 2.10: Vertical plane velocity vector for diffuser (a) vortex (b) round(c) square at V_o = 1 m/sand t_o = 18 °C (Aziz et al., 2012)

The study has been validated by comparing the obtained experimental data with the numerical outcomes of three kinds of turbulence model, which concluded that the standard *k–ε* turbulence model could be adopted for analysing the case studies effectively. The consequences of inlet velocity of air, thermal comfort, and energy consumption were investigated (Aziz et al., 2012).

From Figure 2.10 (b) & (c), the throw from these diffuser are long since the flow turned 90° downward when reached the wall while swirling flow effect around central of room as illustrated in Figure 2.10 (a). The CFD outcomes have shown that the vortex diffuser could save energy for 1.5 times below the round diffuser and square diffuser as reflected in Figures 2.11 and 2.12 since it have achieved thermal comfort level and its EDT is the highest (Aziz et al., 2012).

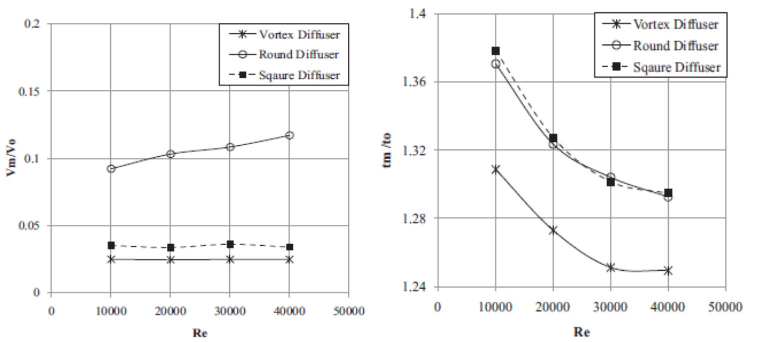

Figure 2.11: The dimensionless average velocity and room temperature at various Reynolds number for tested diffusers (Aziz et al., 2012)

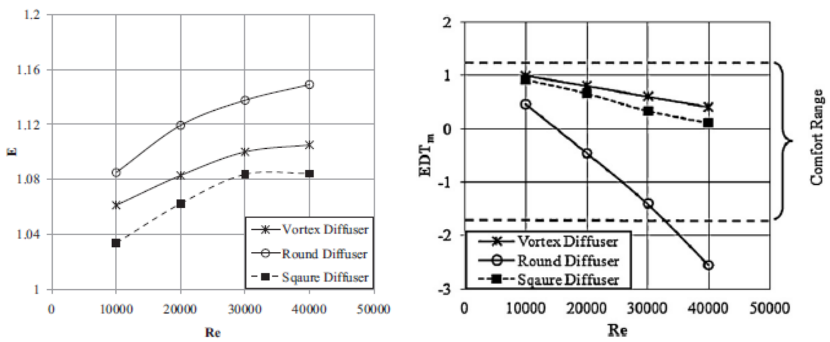

Figure 2.12: The EDT and overall ventilation effectiveness (E) at various Reynolds number for tested diffusers (Aziz et al., 2012)

The simplified method was proposed for inlet air opening to speed up the ceiling diffusers simulation process. A test room equipped with simplified diffuser (without inlet neck) was established for measuring and recording room temperature data, as well as numerical study for comparing with non-simplified diffuser (with inlet neck). The conservation equations stated in previous section were solved by using the commercial FLUENT package. The numerical results were also validated with the experimental data, where the model of standard *k*–*ε* turbulence could be applied for simulating the simplified air inlet on square and round diffusers effectively (Mohammed, 2013).

From Figures 2.13 to 2.15, the results of simplified and non-simplified models are compatible with each other on air velocity and temperature distribution simulation as well as graphical plot on dimensionless room temperature with Reynolds number. The results reflected that the air flow characteristics were similar even though the air diffuser have neck or not (Mohammed, 2013).

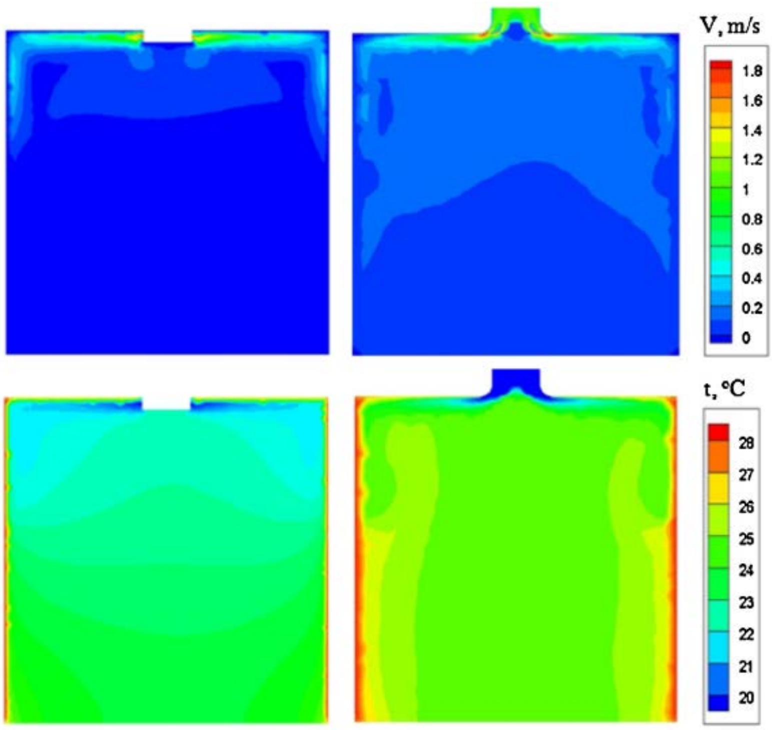

Figure 2.13: Air velocity and temperature distribution for (a) simplified and (b) non-simplified round diffuser model (Mohammed, 2013)

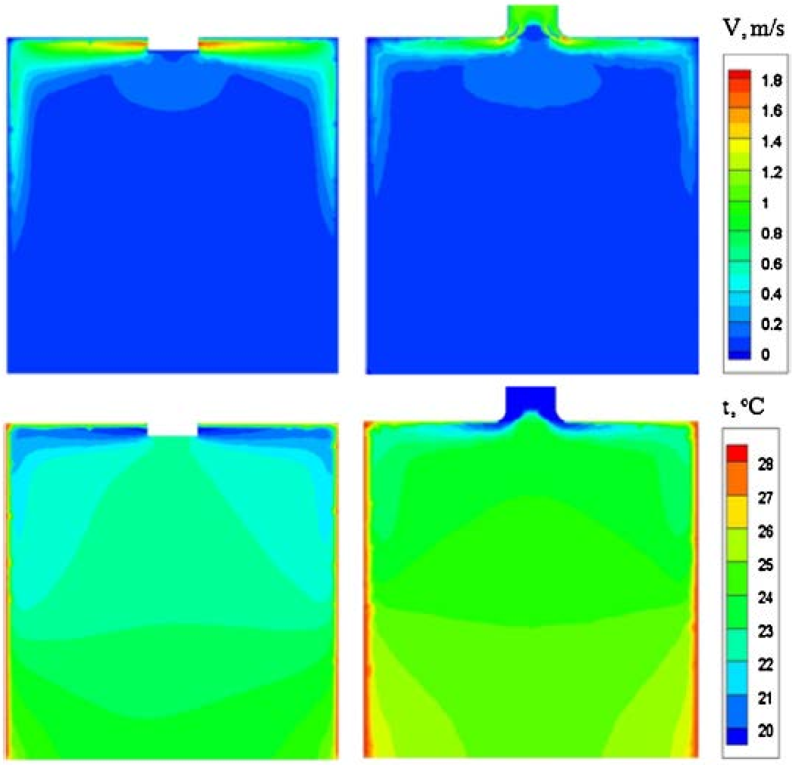

Figure 2.14: Air velocity and temperature distribution for (a) simplified and (b) non-simplified square diffuser model (Mohammed, 2013)

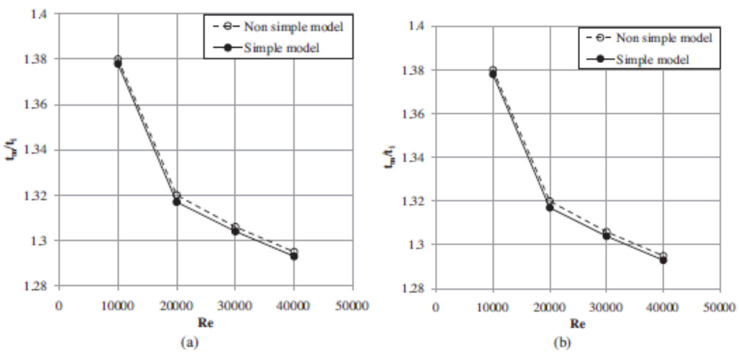

Figure 2.15: Dimensionless room temperature against Reynolds number for simplified and non-simplified diffusers (a) round (b) square (Mohammed, 2013)

The simplified model could be easily and accurately predicted the indoor air flow condition outcomes in quick manner since it could obtain similar results as that of non-simplified model. It could be applied at practical simulations of room air flow to expedite the modelling process of several kind of diffusers on a room (Mohammed, 2013).

In addition, CFD simulation study on air flow characteristics of a room with square diffuser was conducted as expressed in Figure 2.16 to identify the effects of air flow behaviours at discharge angle near the air diffuser area. The same model was also developed by infrared visualisation for verification purpose. The room air flow was evaluated with several geometries i.e. air discharged angles at 30°, 45°, 60° & 75° at the lip and offset of diffuser, and also boundary conditions such as inlet velocity at 0.49 to 0.52 m/s and wall temperature of 294 K (Sun & Smith, 2011).

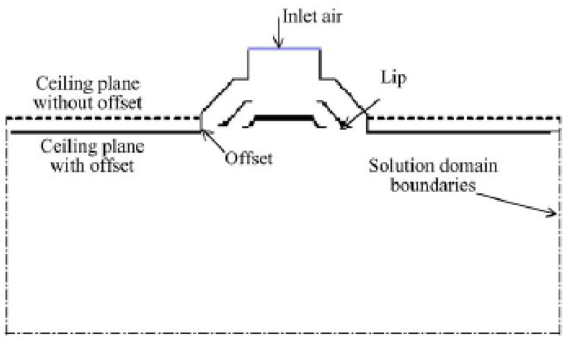

Figure 2.16: The square diffuser on a room (Sun & Smith, 2011)

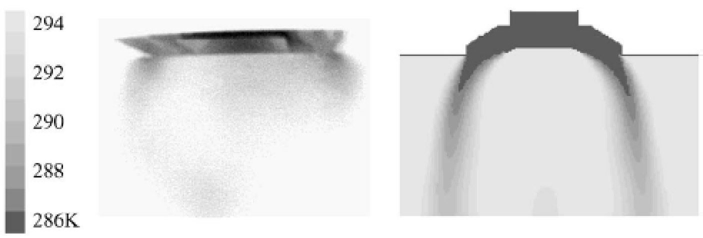

(a) (b)

Figure 2.17: (a) infrared visualisation (b) simulation results for temperature distribution (Sun & Smith, 2011)

From Figure 2.17, the darken spot of both results illustrated the air flow for both cases has similar discharged angles, which reflected the simulation results could be validated by the infrared visualisation results. The same procedures also conducted on other discharged angles and inlet velocities, where the results of simulation were also similar to that of infrared visualisation. Hence, the air discharged angle of the lip and offset of diffuser as well as buoyancy effect of air flow played significant role to determine the room air flow behaviours (Sun & Smith, 2011).

2.2.2 Numerical Investigation of Swirl Air Diffuser Blades Angle

The geometric parameters effect over the performance of the swirl air diffuser was investigated by numerical method as showed in Figure 2.18. The results indicated that the blade angle and aspect ratio of diffuser slots geometry could be impressive on the performance, which was quite consistent in wide range of diffuser slot specifications (Sajadi, et al., 2011).

The outcomes revealed that the performance of diffuser and resultant of room air flow distribution prominently depended on the blade angle, where the sensitivity was important for angle in between 30° and 35° as stated in Figure 2.19. The optimal angle is 32°, which did not dependent on diffuser’s air flow rate as illustrated in Figure 2.20 if compared with model without swirl angle or 40° blade angle. However, Figure 2.21 indicated inverse proportional between evacuation time and diffuser discharge velocity, where the performance of diffuser at high slots angles and aspect ratio were not directly improved although the discharged velocity was increased. Meanwhile, the performance of diffuser did not depend much on the wide range of geometry of slots, where slots angles below 25° or aspect ratio below 3, the air flow behaviour was similar as revealed in Figure 2.20 since air flow into the room was without rotation although there were swirl blades. Hence, the Coanda effect was reduced due to diminishing of discharged air rotation, which made air flow detached from ceiling and affected the uniform air flow distribution. These results were significant for gaining better considerate of the swirl diffuser air flow and how diffuser geometry could influence on its function besides the effect of optimal blades angle (Sajadi, et al., 2011).

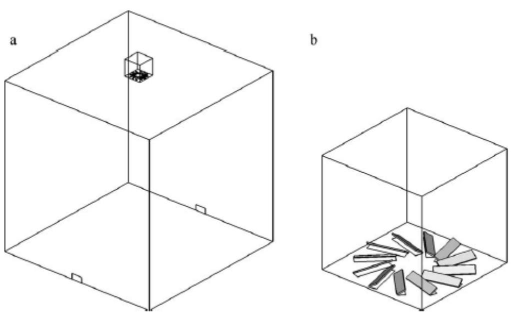

Figure 2.18: (a) The computational schematic, (b) The swirl diffuser (Sajadi, et al., 2011)

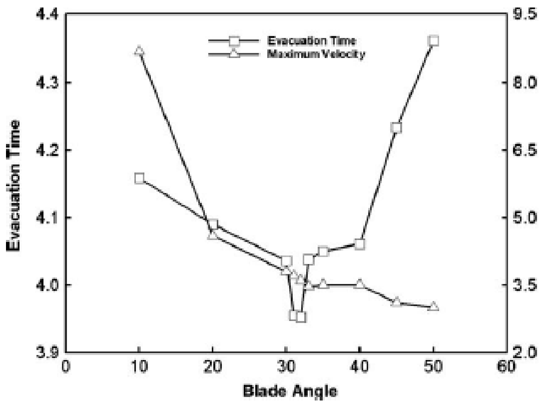

Figure 2.19: **The blades angle effect on maximum discharge velocity and evacuation time** (Sajadi, et al., 2011)

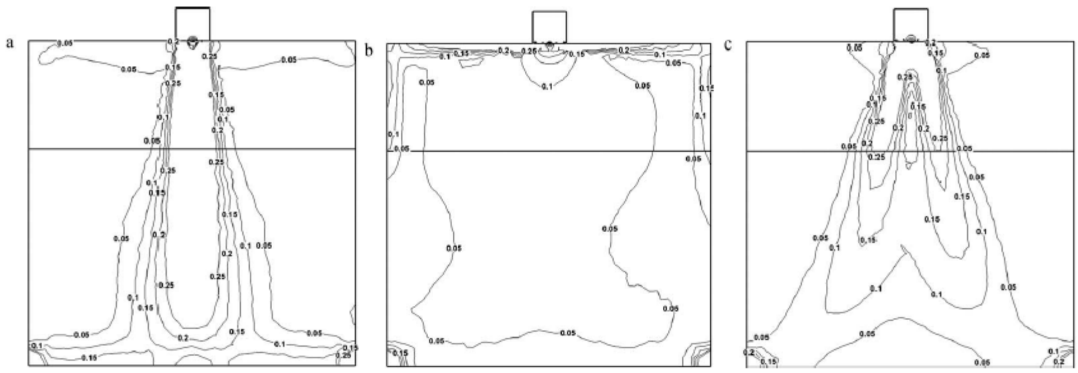

Figure 2.20: **The blades angle effect on distribution of air velocity through room for (a) no swirl blade, (b) 32° blades angle, (c) 40° blades angle** (Sajadi, et al., 2011)

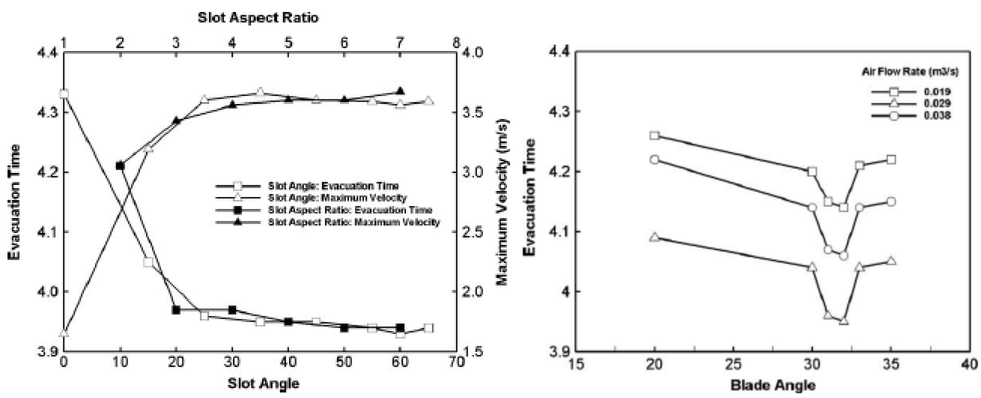

Figure 2.21: **The slot geometry effect on maximum discharged velocity and evacuation time, and air flow rate effect on the optimal swirl blades angle** (Sajadi, et al., 2011)

In addition, numerical study was conducted on ventilation characteristics, turbulent flow structure, and mass transfer of swirl diffusers at various swirling angles (α) between 45° and 65° as indicated in Figure 2.22. The large eddy simulation (LES) was applied and the scheme of second order finite differences was conducted to gain the outcomes together with the application of procedure of dynamic Smagorinsky in sub-grid modelling scale. While, the local and overall air qualities, the mass transfer transient evolution, and the distribution of average and instantaneous velocity were evaluated (Tavakoli & Hosseini, 2013).

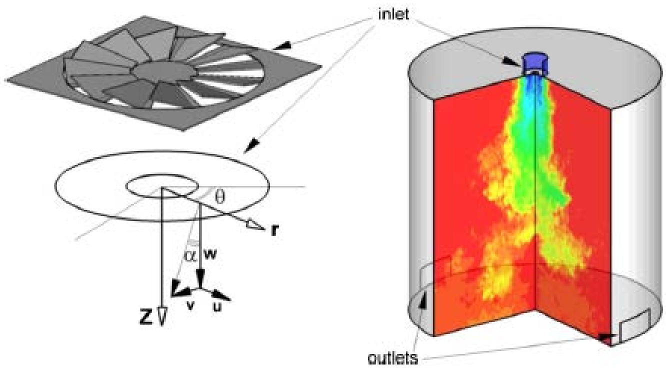

Figure 2.22: The swirl diffuser geometry schematics and cylindrical coordinates (*r*, *θ*, *z*) with (*u*, *v*, *w*) as its velocity components respectively; *α* is the swirl angle (Tavakoli & Hosseini, 2013)

From Figures 2.23 and 2.24, the simulations of three main secondary flow configurations were obtained where the bubble vortex is breakdown at α ≤ 45°, while, the toroid recirculation zone occurred on top of room corners at α ≤ 50°, and the toroid central recirculation zone attached to floor. Meanwhile, the jet type changed from open swirling to Coanda jet between 50° ≤ α ≤ 55°, where they depicted the characteristics of improved ventilation. However, the open swirl jet with highest swirling angle distributed the age of air in more effective manner and also indicated enhanced local air quality in the central room region at α = 50°. Furthermore, the Coanda jet with lowest swirling angle mixed the fresh air throughout the room effectively and enhanced the average air quality at α = 55°. Therefore, these results were essential to obtain considerate swirl diffuser functions (Tavakoli & Hosseini, 2013).

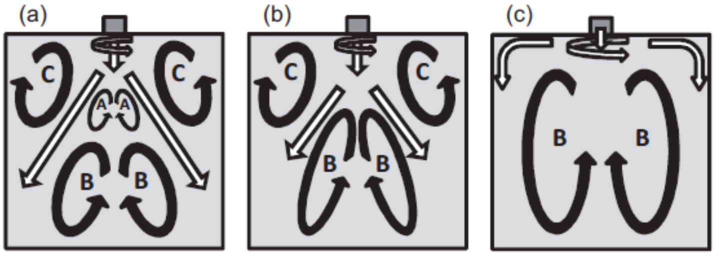

Figure 2.23: **The main flow structures schematics in hollow arrows and types A, B & C secondary flow structure in solid black arrows: (a) low swirling open jet (b) high swirling open jet (c) Coanda jet** (Tavakoli & Hosseini, 2013)

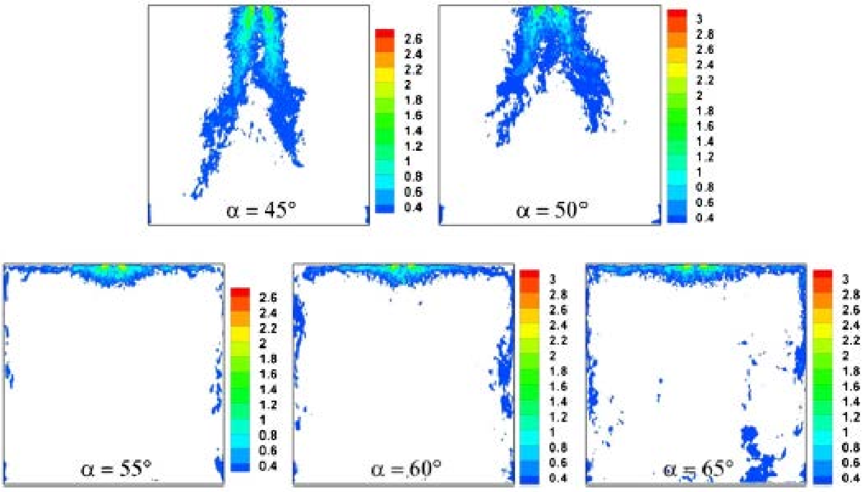

Figure 2.24: **Instantaneous velocity magnitude contours at various swirl angles** (Tavakoli & Hosseini, 2013)

CHAPTER 3

METHODOLOGY

3.1 Air flow and temperature simulation by CFD in ANSYS FLUENT

The air flow distribution from the air diffuser and temperature distribution patterns within the room space were simulated using ANSYS FLUENT version 15.0 software package.

The Design Modeller was used for sketching the geometry models of this project. Once the geometry modelling was completed, the Meshing function was operated subsequently for assigning the inlet and outlet positions, as well as suitable mesh element size for the geometry model. Upon completion of meshing, the FLUENT solver was conducted for solving the flow characteristics in iteration with fluid properties and boundary conditions.

The inlet air velocity could be high and inconsistent, possibly leading to turbulent air flow in the room space. Therefore, the standard k-ε turbulent model, which was one of the most common turbulence models used in the CFD, was applied in this project. In addition, the fluid used in the analysis was assumed to be steady, incompressible, and Newtonian fluid. The basic model specifications, and fluid material properties are tabulated in Table 3.1.

Table 3.1: Basic model specifications and fluid material properties

Item	Value
Room dimensions	2 m × 2 m × 2 m (H)
Diffuser dimensions	600 mm Ø
Inlet dimensions, d_i	350 mm Ø
Outlet dimensions	600 mm × 600 mm, except for ceiling outlet which was 400 mm × 400 mm
Inlet velocity, V_i	1.0 m/s
Inlet Temperature, T_i	287 K (14 °C)
Average Room Temperature, T_a	296 K (23 °C)
Density of air, ρ	1.225 kg/m^3
Dynamics viscosity of air, μ	1.7894 × 10^{-5} kg/m-s
Specific heat of air, C_p	1006.43 J/kg-K
Thermal conductivity of air, k	0.0242 W/m-K
Thermal expansion coefficient of air, β	0.0034 K^{-1}
Turbulent intensity	5%
Turbulent viscosity ratio	10
Reynolds number at inlet Re_i (= $\rho V_i d_i/\mu$)	23,961

Table 3.2: Diffuser outlet velocity (based on inlet velocity of 1.0 m/s &assuming Q_1 = Q_2)

Item	4-blade	5-blade (40°)	5-blade (30°)	7-blade
Cross section area of inlet duct A_1 (m^2)	0.0963	0.0963	0.0963	0.0963
Inlet Velocity V_1 (m/s)	1.0	1.0	1.0	1.0
Flow rate $Q_1 = A_1V_1$ (m^3/s)	0.0963	0.0963	0.0963	0.0963
Cross section area of diffuser air gap A_2 (m^2)	0.2781	0.2754	0.2749	0.2737
Diffuser Outlet Velocity V_2 (m/s)	0.3461	0.3494	0.3502	0.3517
Flow rate $Q_2 = A_2V_2$ (m^3/s)	0.0963	0.0963	0.0963	0.0963

The equations for conservation of mass, momentum and energy are Equations (2.1) to (2.3). Other equations used in ANSYS FLUENT for this project are expressed in Equations (2.4) to (2.8).

3.2 Geometry Modelling

The 3D view schematic diagram of the ceiling air round diffuser in a room of 2 m length × 2 m width × 2 m height, and each blade type of round diffuser were modelled using AutoCAD version 15.0 (Figures 3.1 to 3.7). All these schematic diagrams were used as reference for preparing the graphics of geometry modelling in the Design Modeller of ANSYS FLUENT as illustrated in Figures 3.8 to 3.10 for meshing and numerical analysis subsequently.

The air flow inlet to the room via inlet ductwork and diffusers was indicated at the middle part of the ceiling level of the room. While, the outlet can be on the ceiling level, i.e., 50 mm away from the perimeter edge of vertical wall and in this case the left hand side vertical wall's perimeter edge was selected. Meanwhile, single outlet can be near either left or right hand side wall bottom in which 150 mm above the bottom edge of the vertical wall, however, right hand side wall was chosen for this project. Besides, the double outlets can be near the left and right hand side wall bottoms respectively, which are 150 mm above the bottom edge of the vertical wall. In addition, the air outlets or return air diffusers will be installed on either ceiling level or near bottom of walls in industry normal practice, and thus this project applied the similar concept to place the air outlets on either ceiling level or near bottom of walls to identify the effect of outlet position on air flow behaviour.

The round ceiling air diffusers 5 (blade angles of 30° and 40°) and 7-blade were proposed to compare with the commercial 4-blade air diffuser in which uneven air distribution could occur.

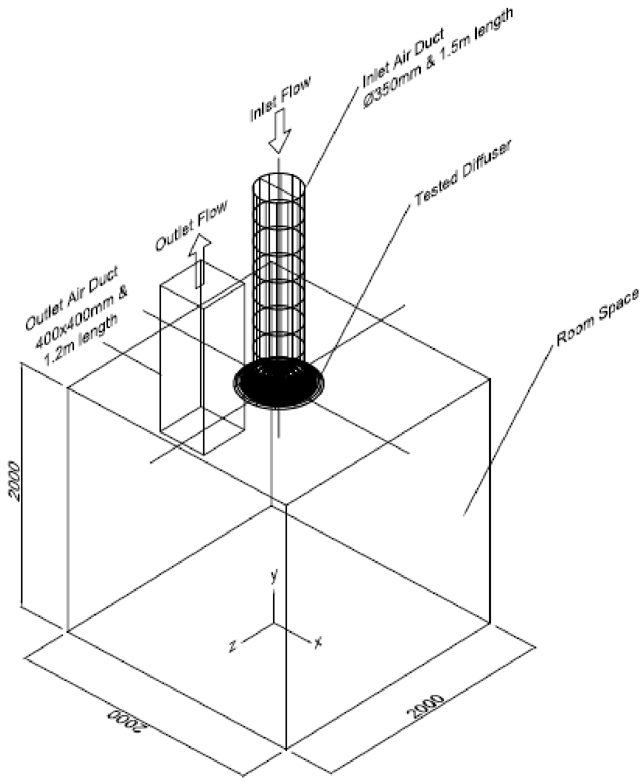

Figure 3.1: **The 3D view of ceiling air round diffuser in room with air flow inlet and outlet on ceiling level**

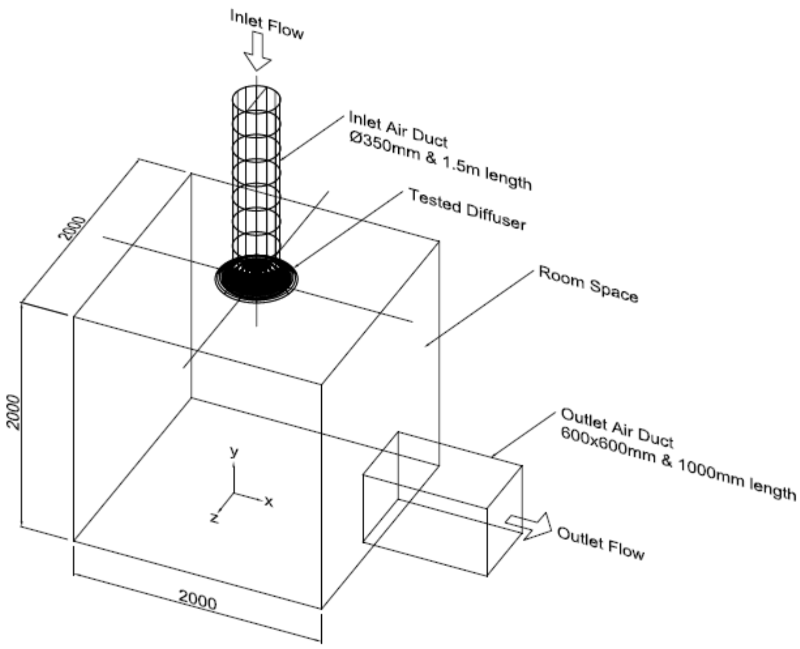

Figure 3.2: **The 3D view of ceiling air round diffuser in room with air flow inlet on ceiling level and air flow outlet near right hand side wall bottom**

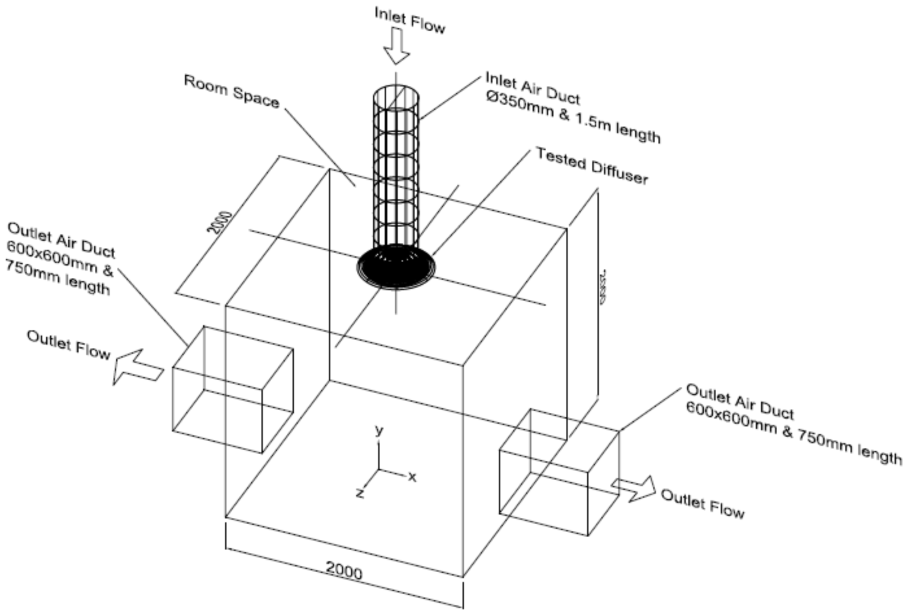

Figure 3.3: **The 3D view of ceiling air round diffuser in room with air flow inlet on ceiling level and two air flow outlets near left and right hand side wall bottoms, respectively**

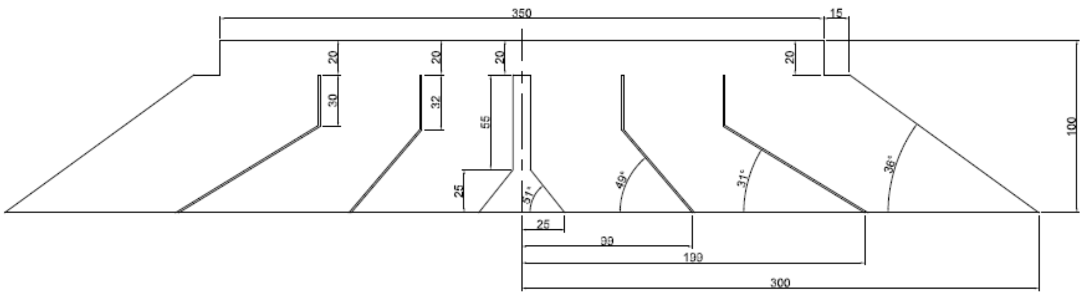

Figure 3.4: **The sectional view of 4-blade ceiling air round diffuser with an average blade angle of 40°**

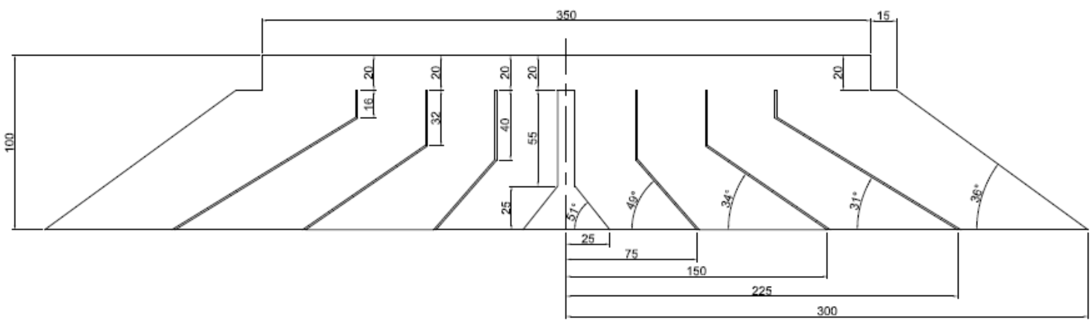

Figure 3.5: **The sectional view of 5-blade ceiling air round diffuser with an average blade angle of 40°**

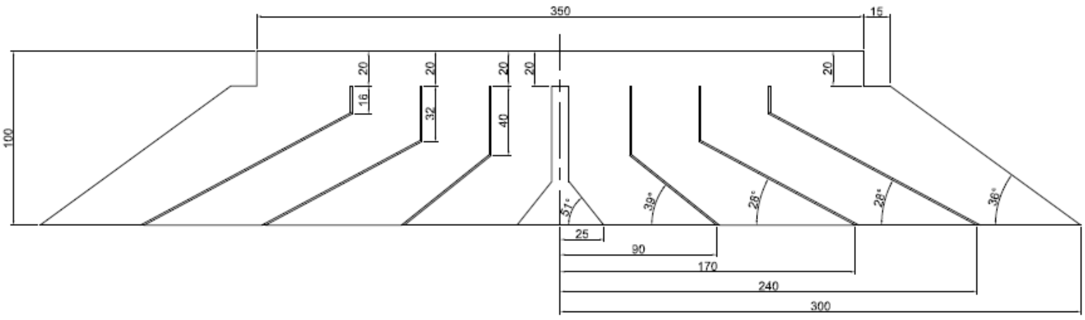

Figure 3.6: The sectional view of 5-blades ceiling air round diffuser with an average blade angle of 30°

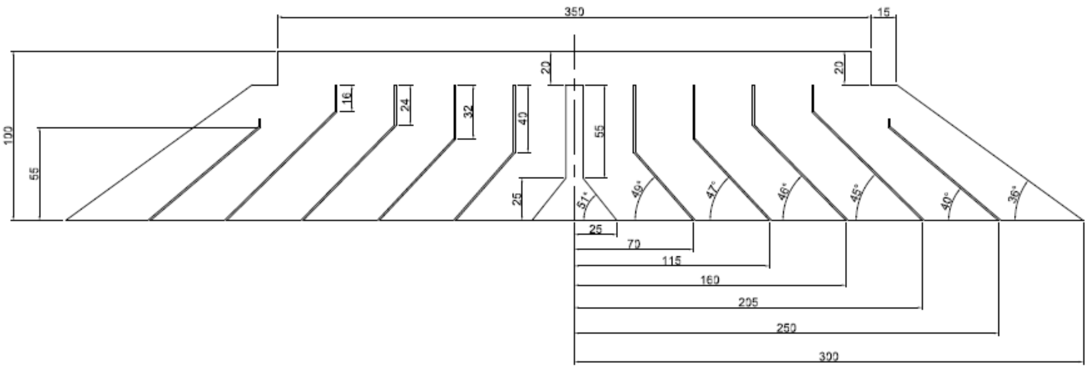

Figure 3.7: The sectional view of 7-blades ceiling air round diffuser with an average blade angle of 40°

The models used in this project were scaled down to 1:2, compared to the physical round air diffuser installed on a room ceiling, in order to reduce cell numbers of mesh element. For example, the mesh element of 13,989,508 cells was reduced to 4,481,032 cells after scaling down.

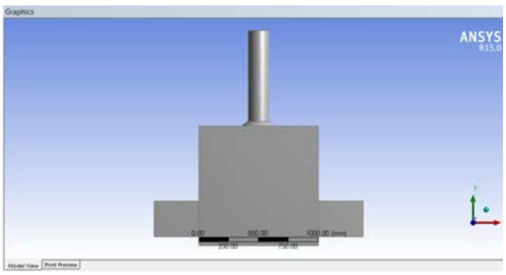

Figure 3.8: ANSYS FLUENT geometry of ceiling air round diffuser in room with air flow inlet on ceiling level and two air flow outlets near left and right hand side wall bottoms, respectively

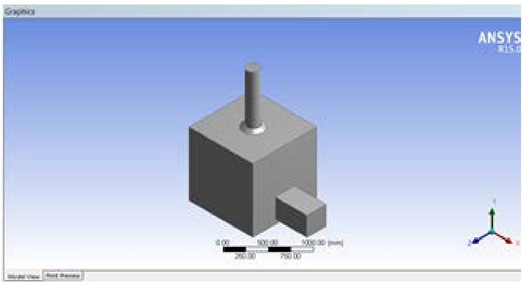

Figure 3.9: ANSYS FLUENT geometry of ceiling air round diffuser in room with air flow inlet on ceiling level and air flow outlet near the right hand side wall bottom

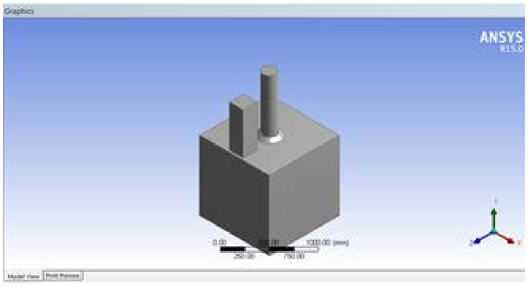

Figure 3.10: ANSYS FLUENT geometry of ceiling air round diffuser in room with air flow inlet and outlet on ceiling level

3.3 Meshing configuration

The meshing process was assigned upon generating of single volume of geometry modelling of ceiling round air diffuser in room. The inlet and outlet of the models were also identified on meshing function.

3.3.1 Meshing faces

The meshing faces element or cell sizes were assigned according to proximity and curvature, while maximum and minimum grid sizes, maximum face size, proximity size, etc. under the mesh sizing function are presented in Figure 3.11, which could furnish suitable orthogonal quality of mesh sizes for FLUENT analysis subsequently.

The interval size of the face was set as 0.01 m, which ranged from 0.09 m to 0.01 m with maximum and minimum grid size of 0.1 and 0.001 m, respectively in order to suit all faces for uniformity since the grid size used in meshing the surfaces would govern the cell sizes or mesh sizes filling up the volume of the fluid model. Once the mesh sizing data were set, they were updated in order to obtain the total mesh size and orthogonal quality.

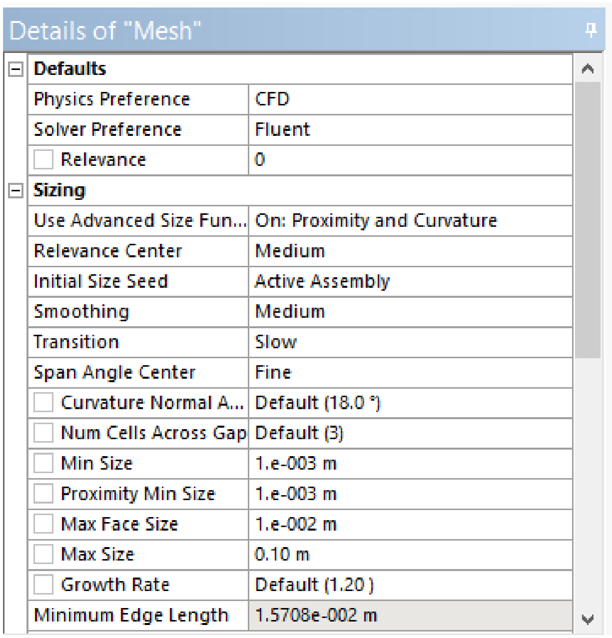

Details of "Mesh"

Defaults	
Physics Preference	CFD
Solver Preference	Fluent
Relevance	0
Sizing	
Use Advanced Size Fun...	On: Proximity and Curvature
Relevance Center	Medium
Initial Size Seed	Active Assembly
Smoothing	Medium
Transition	Slow
Span Angle Center	Fine
Curvature Normal A...	Default (18.0 °)
Num Cells Across Gap	Default (3)
Min Size	1.e-003 m
Proximity Min Size	1.e-003 m
Max Face Size	1.e-002 m
Max Size	0.10 m
Growth Rate	Default (1.20)
Minimum Edge Length	1.5708e-002 m

Figure 3.11: The meshing operation data set up

3.3.2 Meshing quality

The preferable minimum orthogonal quality of mesh sizes would be 0.05 or above, where 0.196 was obtained for the case of round air diffuser of 7 blades/vane in room with generated total mesh cells of 4,481,032 as shown in Figure 3.12. Figure 3.13 depicts the fine meshes generated for air volume of 7-blade air diffuser. More accurate calculation could be obtained for smaller interval size. However, the smallest mesh face sizes could be limited by the computer memory, i.e. 0.009 or below.

Statistics	
Nodes	820007
Elements	4481032
Mesh Metric	Orthogonal Quality
Min	0.195721020625131
Max	0.997132383132774
Average	0.856318382896484
Standard Deviation	8.51002627664289E-02

Figure 3.12: The orthogonal quality of generated mesh size for 7-blade air diffuser in meshing operation

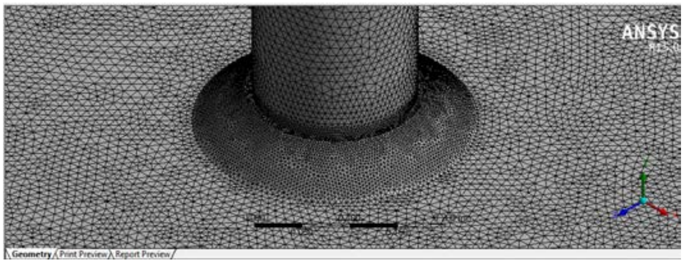

Figure 3.13: Fine mesh generated for air volume of 7-blade air diffuser

3.4 ANSYS FLUENT analysis

3.4.1 ANSYS FLUENT configuration

The solution setup was established in ANSYS FLUENT solver configuration, where the standard *k-ε* model of viscous model and energy equation were defined. Meanwhile, the viscous model parameters are specified in Figure 3.14. Meanwhile, the working fluid of the project was defined as air, whose property parameters are revealed in Figure 3.15. In addition, the atmospheric pressure of air was set as 101325 Pa.

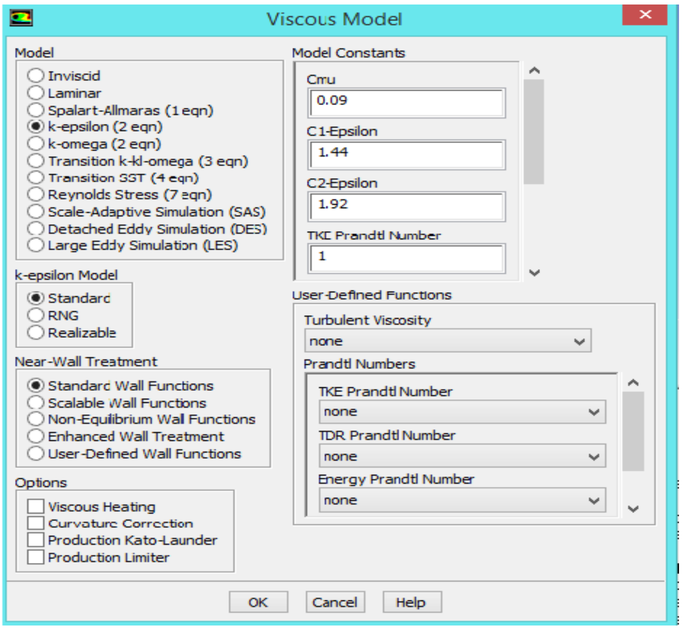

Figure 3.14: The Viscous Model setting

The boundary conditions were set with inlet velocity at 1.0 m/s for low air flow rate study, while air flow was defined in a direction normal to the inlet. The turbulent intensity and turbulent viscosity ratio were specified as 5% and 10 respectively, whereas the temperature of inlet air and wall were defined as 287 K (14 °C) and 296 K (23 °C), respectively, since these temperature are normally used as supply air temperature and room temperature as stated in Appendix A.

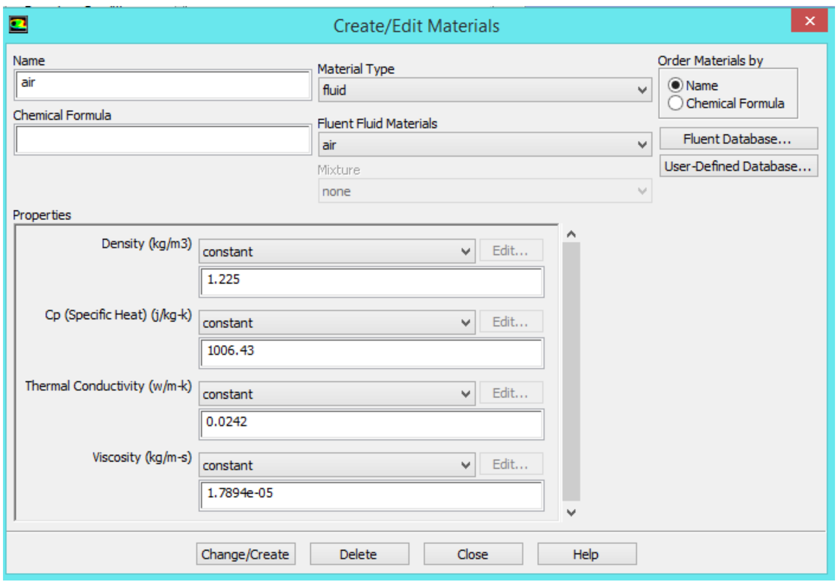

Figure 3.15: The fluid material properties setting

3.4.2 ANSYS FLUENT problems solver

The parameters of ANSYS FLUENT solution methods and solution controls were identified and the standard solution initialization was specified subsequently for problems solving, which was computed from inlet of the model. The iteration process was conducted subsequently based on 500 iterations since the higher number of iteration might obtain accurate results prior to convergence.

3.4.3 ANSYS FLUENT post processing

Any iterative solution process can provide converged solution which is relative to some criteria, i.e., when all discretize transport equations have complied with the specified tolerance defined by ANSYS FLUENT residuals or the solution will not vary further with subsequent iterations. However, convergence may not have similar accuracy if it does not match with any similar simulation data (Stamou & Katsiris, 2006). In addition, the parameters of solution convergence are specified in residual monitors.

The scaled residuals can be plotted with the iterations calculation until the solution has converged. Figure 3.16 reflects one of the scaled residuals plots with solution convergence among the simulations conducted in this project. It was observed that the residuals did not vary much when approaching 100^{th} iterations.

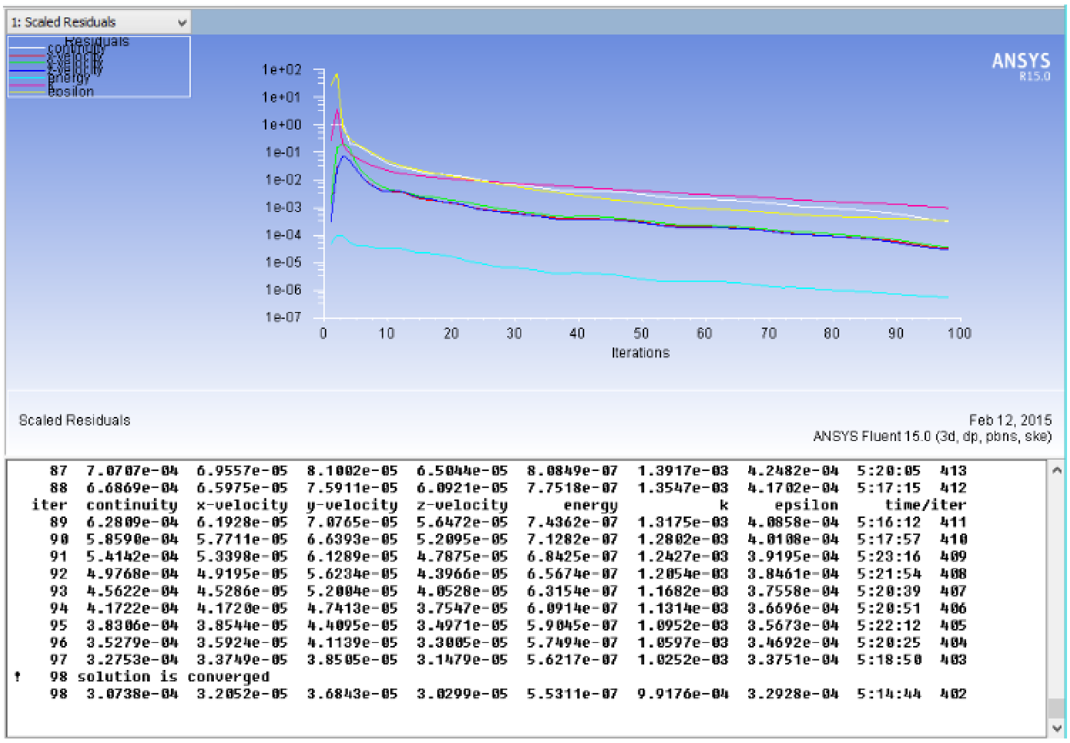

Figure 3.16: ANSYS FLUENT scaled residuals plot with solution convergence

Since the geometry model was prepared in 3D, the boundary results could only be observed when viewing the interior result, which could be shaded by boundaries if the whole volume was shown on screen. Therefore, specific planes or lines views within the room were created in order to view the results within the room.

The graphical results of velocity, temperature, etc. could be viewed upon completion of iteration process via contours or vectors graphical display. Meanwhile, the ANSYS FLUENT surface integrate or volume integrate were used to provide average velocity magnitude or static temperature on surface of any selected plane or point of a solid for reporting purpose. In addition, the results of contours and XY plots of velocity magnitude, Y velocity and static temperature will be discussed further in Chapter 4.

3.5 Grid independence

Grid independence can be termed as the improvement of results via assigning successive smaller cell sizes for calculation, which should be approaching the accurate result as the mesh size becomes finer. When the results are identical to each other for two consecutive cell sizes, the ANSYS FLUENT solution is considered as converged, and the grid can be treated as independence (Wang & Zhai, 2012).

The ANSYS FLUENT solution used for comparison of two different cells size for mesh sensitivity was the velocity magnitude at a line along the central and outer edge of the 7 blades/vane ceiling air round diffuser on room ceiling level as illustrated in Figure 3.17. For case 1, the grid size used was 0.01 m with the number of cells generated as 4,481,032 cells. For case 2, the mesh size used was 0.02 m with the number of cells generated as 2,985,116 cells.

From facet average of ANSYS FLUENT surface integrate, the average velocity magnitude of Case 1 was 0.5578 m/s, and Case 2 was 0.5693 m/s, suggesting a small difference percentage of 2.02%.

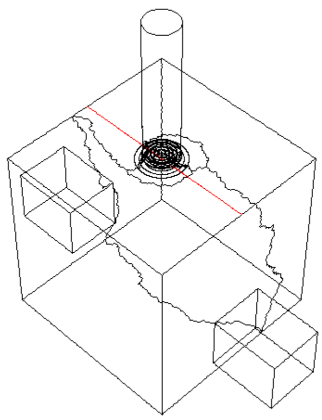

Figure 3.17: The section line (red colour) on *x*-axis extending from the centre of the 7-blade ceiling air round diffuser on a room to the edge of walls

In addition, the ANSYS FLUENT solution for comparison of two different cells size for mesh sensitivity was also conducted on velocity magnitude at the plane surface on top of the room as expressed in Figure 3.18. From facet average of ANSYS FLUENT surface integrate, the average velocity magnitude of Case 1 was 0.5186 m/s, and Case 2 was 0.5450 m/s. Hence, the average velocity magnitude of Case 1 and Case 2 was different by 4.84%.

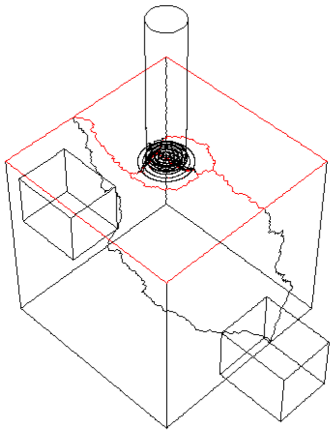

Figure 3.18: The plane surface (red colour) on top of the room

The velocity magnitude profiles on X-Y plot for section line of Figure 3.17 for Cases 1 and 2 are reflected in Figure 3.19 for comparing the results of the aforesaid two different mesh sizes. Both of the results revealed that they were almost similar at most of the positions.

Since the differences of the section line or plane surface for average velocity magnitude on selected position of Cases 1 and 2 were approximately 2% and 4.8%, respectively, and the velocity magnitude profiles on X-Y plot for both cases were almost similar, the CFD results were considered to be grid independent.

As the finer mesh could generate relatively precise solution for the number of cells created within the computational capability of the computer used, the grid size of 0.01 m was adopted for all models to be simulated in this project.

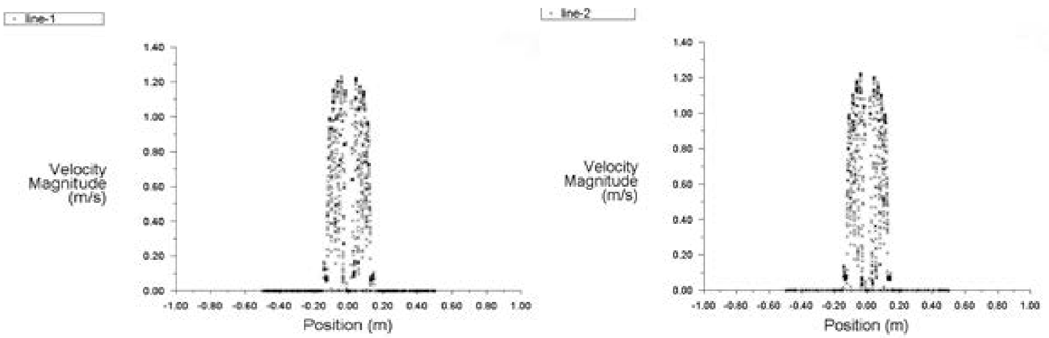

Figure 3.19: The X-Y plot of velocity magnitude at section line on *x*-axis extending from the centre of the 7-blade ceiling air round diffuser on a room to the edge of walls for Cases 1 and 2

3.6 Dimensionless average room air velocity or temperature

Dimensionless analysis is considered for determining the relationship between few variables when actual functional relationship is not known. The dimensionless average room air velocity or temperature distribution in a room for 5 and 7-blade diffusers was evaluated in this project by plotting the dimensionless average room air velocity or temperature against the Reynolds number at various inlet air velocities. This study was aimed to compare their results with the CFD predicted results of 5 and 7-blade diffusers (Aziz et al., 2012).

In this project, the dimensionless average room velocity was defined as a ratio of average room air velocity to the inlet air velocity (V_a/V_i). The average room air velocity was calculated based on ANSYS FLUENT volume integrals on velocity magnitude for various inlet air velocities at same inlet air temperature of 287 K. Meanwhile, the dimensionless average room temperature was defined as a ratio of average room temperature of various inlet velocities to the same inlet air temperature of 287 K (T_a/T_i). The dimensionless average room temperature was calculated based on ANSYS FLUENT volume integrals on static temperature at various inlet air velocities at same inlet air temperature of 287 K. The results of dimensionless average room velocity or temperature will be further discussed in Chapter 4.

3.7 Overall ventilation effectiveness and effective draft temperature

The overall ventilation effectiveness (*E*) in room was evaluated to identify whether the proposed 5 and 7-blade air diffusers could obtain effective energy consumption to achieve required thermal comfort in a room (Aziz et al., 2012). The minimum requirement on overall ventilation effectiveness for acceptable indoor supply air distribution should be $E = 1$ according to the ASHRAE Indoor Air Quality (2013) as indicated on Appendix E. It was calculated via Equation 2.9 for both 5 and 7-blade air diffusers with the average room and inlet air temperature at various inlet air velocities and same inlet temperature, and outlet air temperature was obtained from the average static temperature of surface integrals for 5 and 7-blade round air diffuser with 2 outlets near bottom of walls generated by ANSYS FLUENT.

Meanwhile, the effective draft temperature (*EDT*) in room was studied to determine whether the proposed 5 and 7-blade air diffusers could achieve thermal comfort level in a room within the value of 1.1 and -1.7 (Aziz et al., 2012). It was calculated via Equation 2.10 for both 5 and 7-blade air diffusers with the average room air temperature, local airstream temperature and velocity at various inlet air velocities. The local airstream temperature and velocity were obtained from surface integrals on static temperature and velocity magnitude within the room for 5 and 7-blade air diffusers with 2 outlets near bottom of walls generated by ANSYS FLUENT. The results of overall ventilation effectiveness and *EDT* will be further discussed in Chapter 4.

CHAPTER 4

RESULTS AND DISCUSSION

4.1 The CFD simulation of air flow behaviour and temperature distribution

This section discusses the vertical view of CFD simulation of air flow patterns and temperature distribution from air inlet duct on ceiling level via each type of round ceiling air diffusers, throughout the room space, and flow to the various types of air outlet duct at various inlet velocities and temperatures. The contours of velocity magnitude, Y velocity and static temperature of each model as well as their X-Y plot are illustrated in this chapter, while the velocity vectors of each model can be found in Appendix B.

4.1.1 Inlet velocity at 1.0 m/s for the round ceiling air diffuser with two outlets near wall bottoms

The air flow behaviours and temperature distribution of round ceiling air diffusers in room with inlet on ceiling and 2 outlets near wall bottoms for inlet velocity at 1.0 m/s and, inlet temperature of 287 K are illustrated in Figures 4.1 to 4.6.

From sections (a) of Figures 4.1 and 4.2, the 4-blade/vane round ceiling air diffuser indicated that the air flow distribution (0 – 0.6 m/s) was not evenly throughout the room as most of the distributed air was concentrated around the middle spot of the room. It might be due to high volumetric flow rate or static pressure around the central core blade, where the air tended to release from the air diffuser on the shorter distance. As such, the occupants nearby the air diffuser may not feel comfortable due to higher air flow toward their body continuously.

Compared to 4-blade/vane round ceiling air diffuser, the air flow distribution from the 5-blade/vane round ceiling air diffuser (0 – 0.3 m/s) was relatively more uniform throughout the room (0 – 0.6 m/s) since air flow via the blades of 5-blade air diffuser was smoother (sections (b) of Figures 4.1 and 4.2). They did not display any concentration of air distribution around the middle spot of the room, and Coanda effect of air distribution was observed where the flow emerged radically and approached the wall and then turned into 90° downward, which reflected the throw of air could be longer in Figures 4.1 (b). It is therefore expected that the occupants nearby the air diffuser may feel comfortable as the air from the air diffuser was uniformly distributed throughout the room.

Although the CFD results of sections (c) of Figures 4.1 and 4.2 showed that the air flow distribution from the 5 blades round ceiling air diffuser with an average blade angle of 30° was similar to those of 5 blades round ceiling air diffuser with an average blade angle of 40° in sections (b) of Figures 4.1 and 4.2, the air diffuser with 40° blade angle exhibited slightly more consistent air flow (0 – 0.3 m/s) than that (0 – 0.3 m/s) of diffusers with 30° blade angle since air flow via the air diffuser with 40° blade angle had less direct impact with the air diffuser blades, and was able to flow more smoothly if compared with the air diffuser of 30° blade angle. Nevertheless, the air flow distribution from 5-blade air diffuser with 30° blade angle (0 – 0.3 m/s) relatively uniform throughout the room, leading to a more consistent velocity profile within the room than that of the 4-blade diffuser (0 – 0.6 m/s). Both 5-blade air diffusers were therefore found to create comfortable indoor environment as the air from the air diffusers was uniformly distributed throughout the room without high flow concentration around the air diffuser.

The CFD results of sections (d) of Figures 4.1 and 4.2 for 7-blade/vane round ceiling air diffuser revealed that the air flow behaviours (0 – 0.3 m/s) were slightly consistent than those of the 4 (0 – 0.6 m/s) or 5- (0 – 0.3 m/s) blade round ceiling air diffusers since the air flow via the 7-blade diffuser was relatively more equal than that that via 4 or 5-blade diffuser. Coanda effect of air distribution was noticed where the flow emerged radically and reached the wall and then directed into 90° downward, which revealed the throw of air could be longer in Figures 4.1 (d). These results would result in the occupants' comfort with more uniform air flow distribution in the room.

In addition, line 1 of all the X-Y plots in Figure 4.2 revealed the fluctuation of velocity profile around the centre position due to the air flow through the air gap (constricted area) between the air diffuser blades with Venturi effect where air velocity was increased and pressure was reduced. The velocity profile within the room of lines 2 to 5 for 5 or 7-blade diffuser reflected that the air velocity was within 0.3 m/s, while velocity profile within the room of lines 2 to 5 for 4-blade air diffuser indicated air velocity was up to 0.6 m/s around centre position, suggesting an uneven air flow distribution.

Furthermore, the contour views of velocity magnitude of 5 and 7-blade diffusers with two outlets near the wall bottoms were compared with those of round ceiling air diffusers obtained by Mohammed (2013) as illustrated in Figure 2.13. It was noticed that the air velocity distribution through the blades of the proposed air diffusers in this project was slightly consistent and uniform with less contact between the air flow and blade surfaces than that reported by Mohammed (2013).

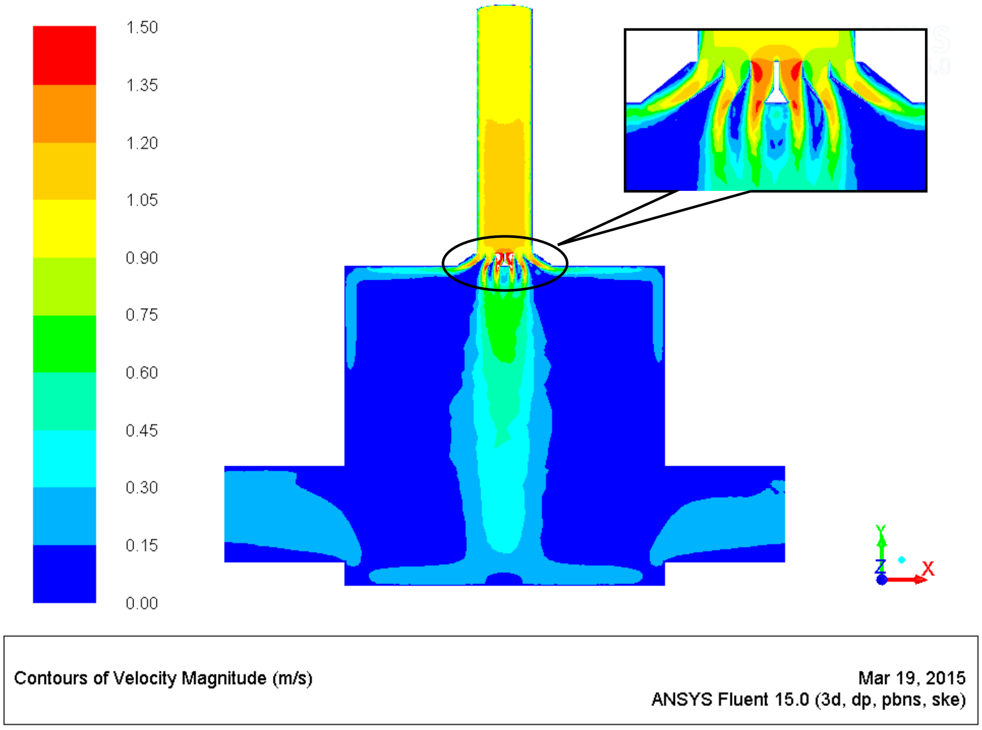
1.50
1.35
1.20
1.05
0.90
0.75
0.60
0.45
0.30
0.15
0.00
Contours of Velocity Magnitude (m/s)
Mar 19, 2015
ANSYS Fluent 15.0 (3d, dp, pbns, ske)

(a)

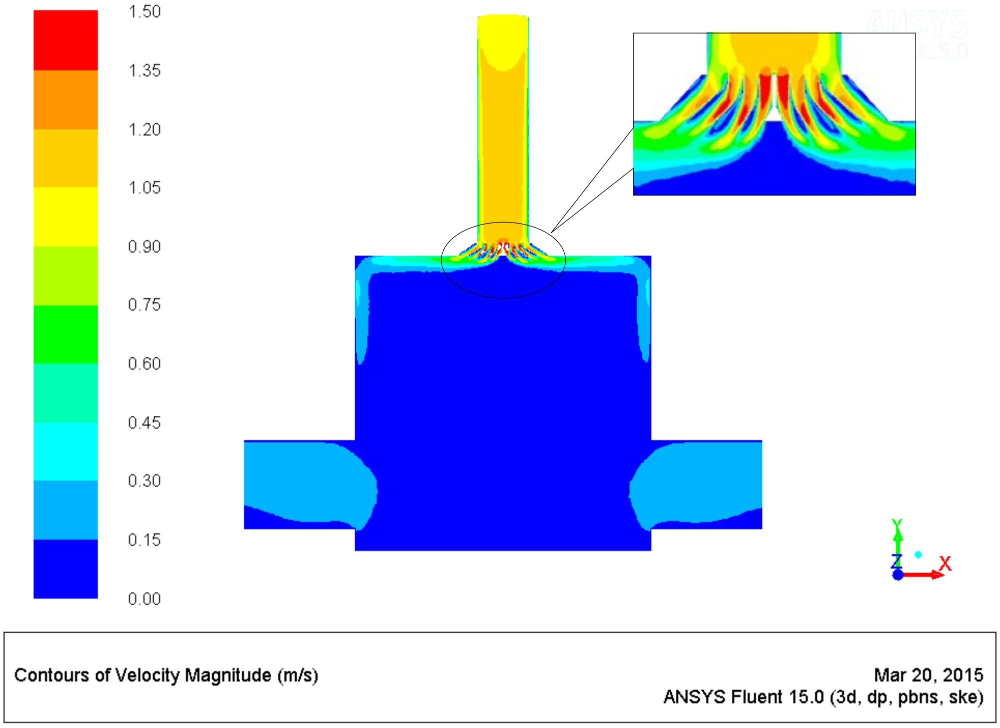
1.50
1.35
1.20
1.05
0.90
0.75
0.60
0.45
0.30
0.15
0.00
Contours of Velocity Magnitude (m/s)
Mar 20, 2015
ANSYS Fluent 15.0 (3d, dp, pbns, ske)

(b)

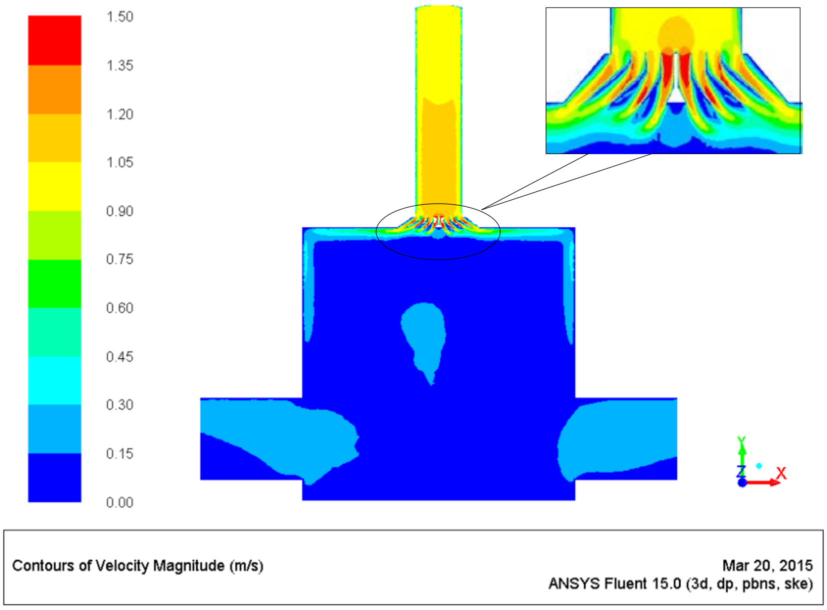

(c)

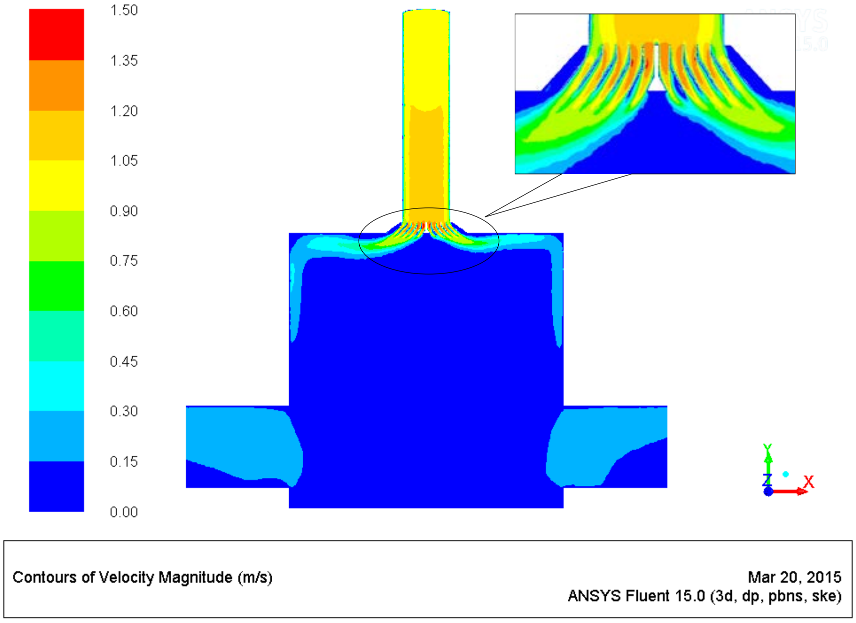

(d)

Figure 4.1: **Contours of velocity magnitude in the room with inlet on ceiling and 2 outlets near wall bottoms: (a) 4-blade, (b) 5-blade at 40° blade angle, (c) 5-blade at 30° blade angle, & (d) 7-blade round ceiling air diffuser**

The X-Y plots for velocity magnitude, Y velocity and static temperature were illustrated according to red colour lines 1 to 5 depicted in a small figure beside the X-Y plots. Those lines were extended from the centre of the room to the edges of the walls and they were 0.2 m apart vertically. The line 1 was extended from the centre of the air diffuser to the edges of the walls, and line 5 was extended from the centre of the room to the edges of the outlets.

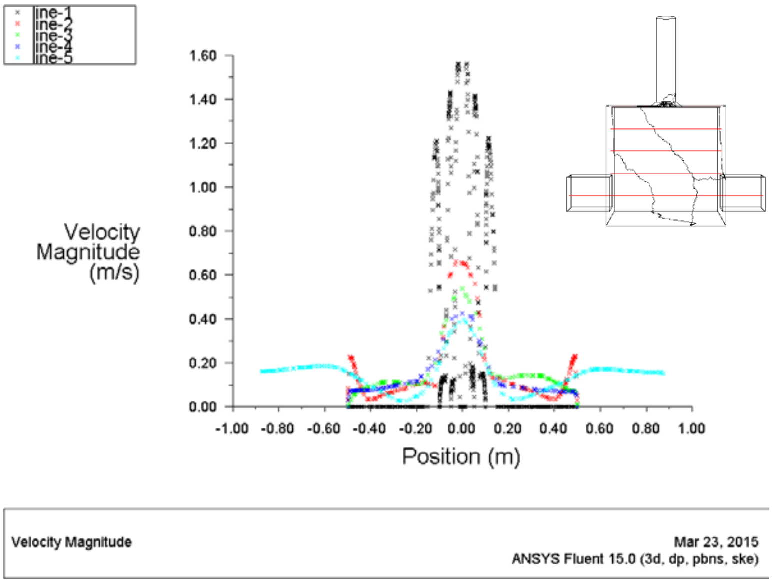

(a)

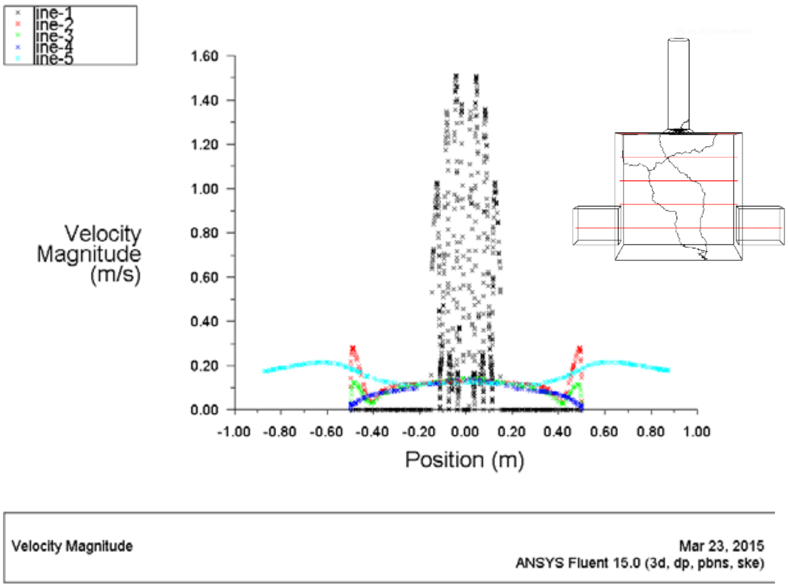

(b)

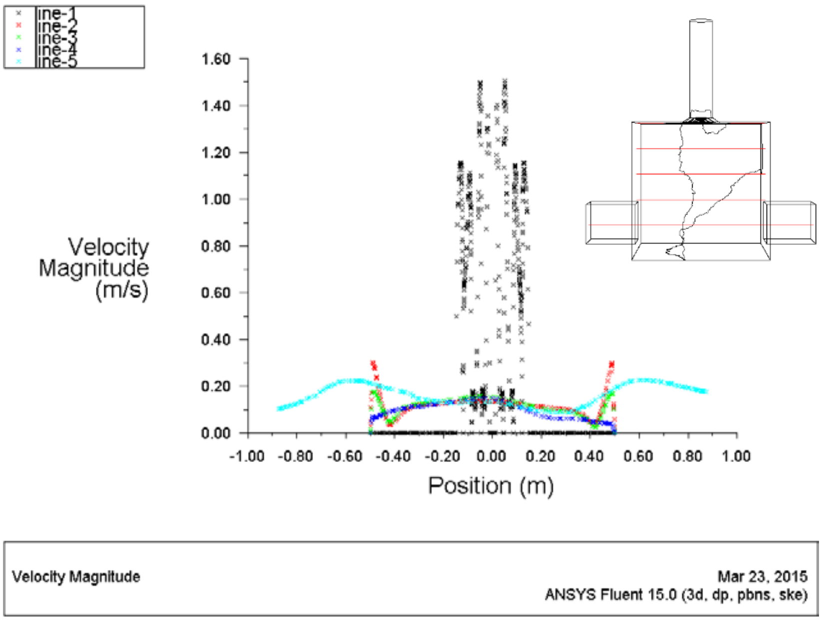

(c)

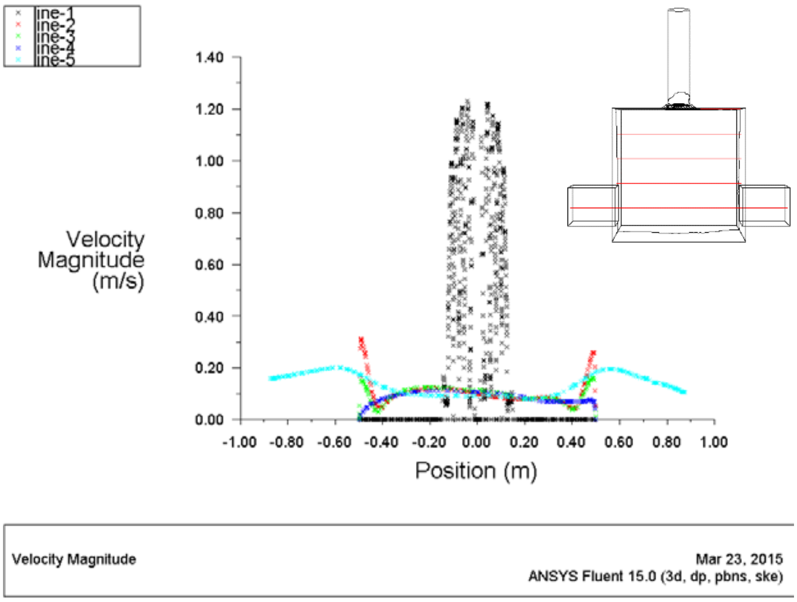

(d)

Figure 4.2: The X-Y plots of velocity magnitude at section lines (red colour line 1 to 5 depicted in small figure beside the XY plot) on *x*-axis extending from the centre of the room to the edge of walls with 2 outlets near wall bottoms: (a) 4-blade, (b) 5-blade, (c) 5-blade with blade angle change, & (d) 7-blade round ceiling air diffuser

Based on sections (a) of Figures 4.3 and 4.4, the 4-blade/vane round ceiling air diffuser showed that the air flow distribution (-0.48 – 0.2 m/s) was not uniformly throughout the room as most of the distributed air was concentrated around the middle spot of the room. It might be due to high volumetric flow rate or static pressure around the central core blade where the air tended to release from the air diffuser at shorter distance. The higher air flow toward the occupants' bodies continuously will lead to discomfort.

From sections (b) of Figures 4.3 and 4.4, the air flow distribution from the 5-blade/vane round ceiling air diffuser was relatively more uniform (0.03 – 0.2 m/s) throughout the room than that of 4-blade/vane round ceiling air diffuser (-0.48 – 0.2 m/s) since the air flow through the blades of 5-blade air diffuser was smoother. Hence, the occupants nearby the air diffuser may feel comfortable without high flow concentration around the air diffuser.

The sections (c) of Figures 4.3 and 4.4 showed that the air flow distribution from the 5-blade round ceiling air diffuser with an average blade angle of 30° was similar to those of 5-blade round ceiling air diffuser with an average blade angle of 40° in sections (b) of Figures 4.3 to 4.4. However, the air diffuser with 40° blade angle (0.03 – 0.2 m/s) exhibited slightly consistent air flow than that of diffuser with 30° blade angle (0.03 – 0.2 m/s) since the air flow through the air diffuser with 40° blade angle have less direct impact the air diffuser blades, and was able to flow smoothly if compared with the air diffuser with 30° blade angle. The air flow of 5-blade air diffuser with 30° blade angle was able to distribute effectively throughout the room, leading to a more consistence velocity profile (0.03 – 0.2 m/s) within the room than that of 4-blade air diffuser (-0.48 – 0.2 m/s) since it provided similar effect if compared to that of 5-blade air diffuser with 40° blade angle. The occupants nearby the air diffuser may enjoy relative comfort as the air from the air diffuser was uniformly distributed throughout the room without high flow concentration around the air diffuser.

The CFD results of sections (d) of Figures 4.3 and 4.4 for 7-blade/vane (0.03 – 0.2 m/s) air diffuser revealed that the air flow behaviours was slightly consistent than those of the 4 (-0.48 – 0.2 m/s) or 5- (0.03 – 0.2 m/s) blade air diffusers since the air flow through the 7-blade air diffuser was relatively more equal than that through 4 or

5-blade air diffuser. It implied that the 7-blade air diffuser might be able to create more thermal comfort for occupants within the room since the air flow rate from the 7-blade air diffuser was relatively higher and was able to distribute to further space uniformly if compared with the other air diffusers.

In addition, line 1 of all the X-Y plots in Figure 4.4 showed that the fluctuation of velocity profile around the centre position due to the air flow through the air gap (constricted area) between the air diffuser blades with Venturi effect where air velocity was increased and pressure was reduced. The velocity profile within the room of lines 2 to 5 for 5 or 7-blade air diffuser reflected that the air velocity was within 0.2 m/s, while velocity profile within the room of lines 2 to 5 for 4-blade air diffuser indicated air velocity up to -0.6 m/s around the centre position due to uneven air distribution.

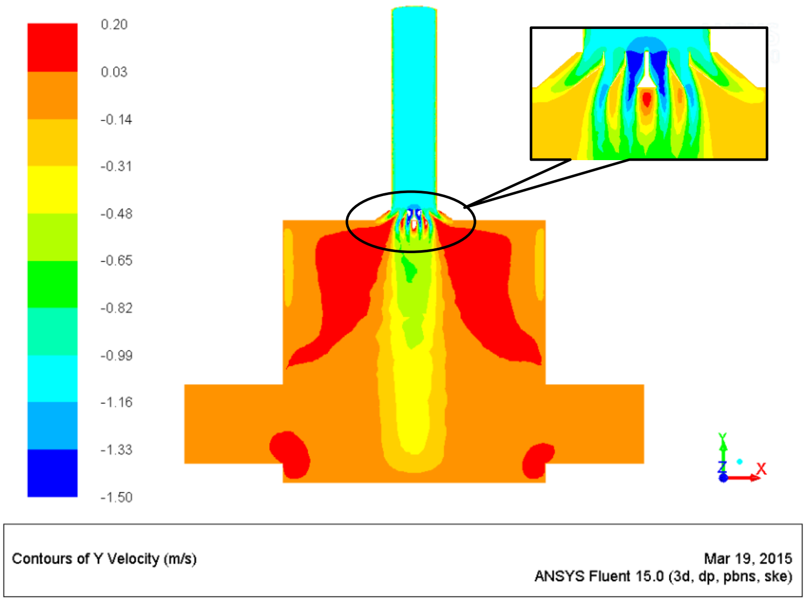
0.20
0.03
-0.14
-0.31
-0.48
-0.65
-0.82
-0.99
-1.16
-1.33
-1.50
Contours of Y Velocity (m/s)
Mar 19, 2015
ANSYS Fluent 15.0 (3d, dp, pbns, ske)

(a)

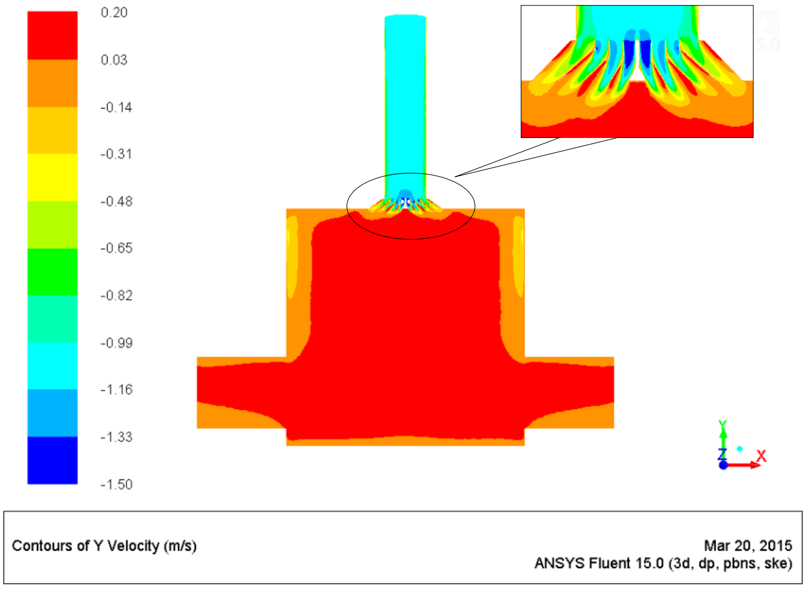
0.20
0.03
-0.14
-0.31
-0.48
-0.65
-0.82
-0.99
-1.16
-1.33
-1.50
Contours of Y Velocity (m/s)
Mar 20, 2015
ANSYS Fluent 15.0 (3d, dp, pbns, ske)

(b)

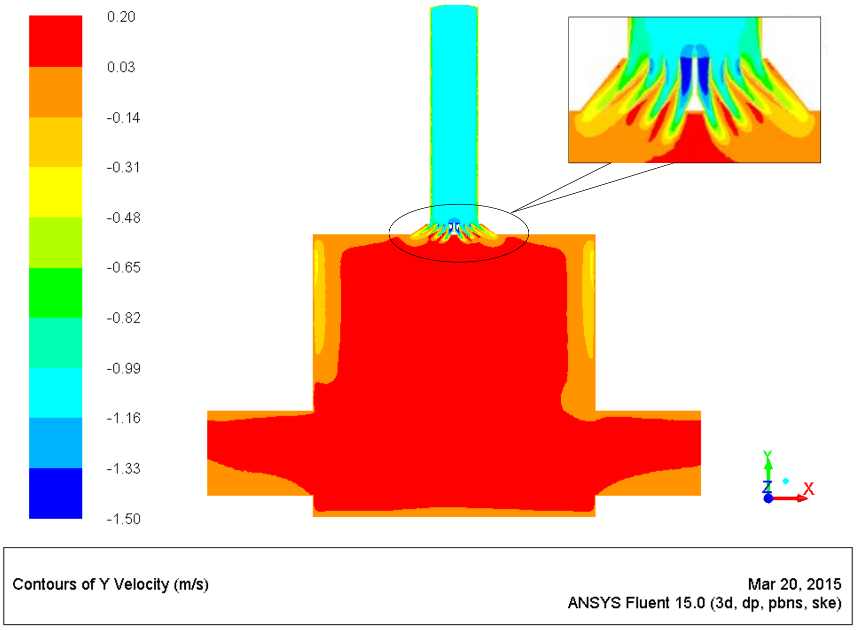

(c)

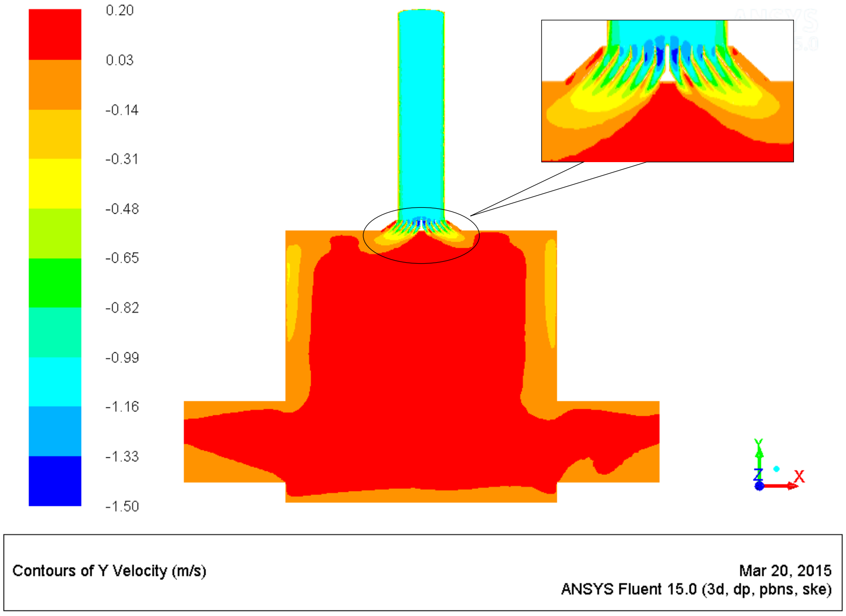

(d)

Figure 4.3: **Contours of Y velocity in the room with inlet on ceiling and 2 outlets near wall bottoms: (a) 4-blade, (b) 5-blade, (c) 5-blade with blade angle change, & (d) 7-blade round ceiling air diffuser**

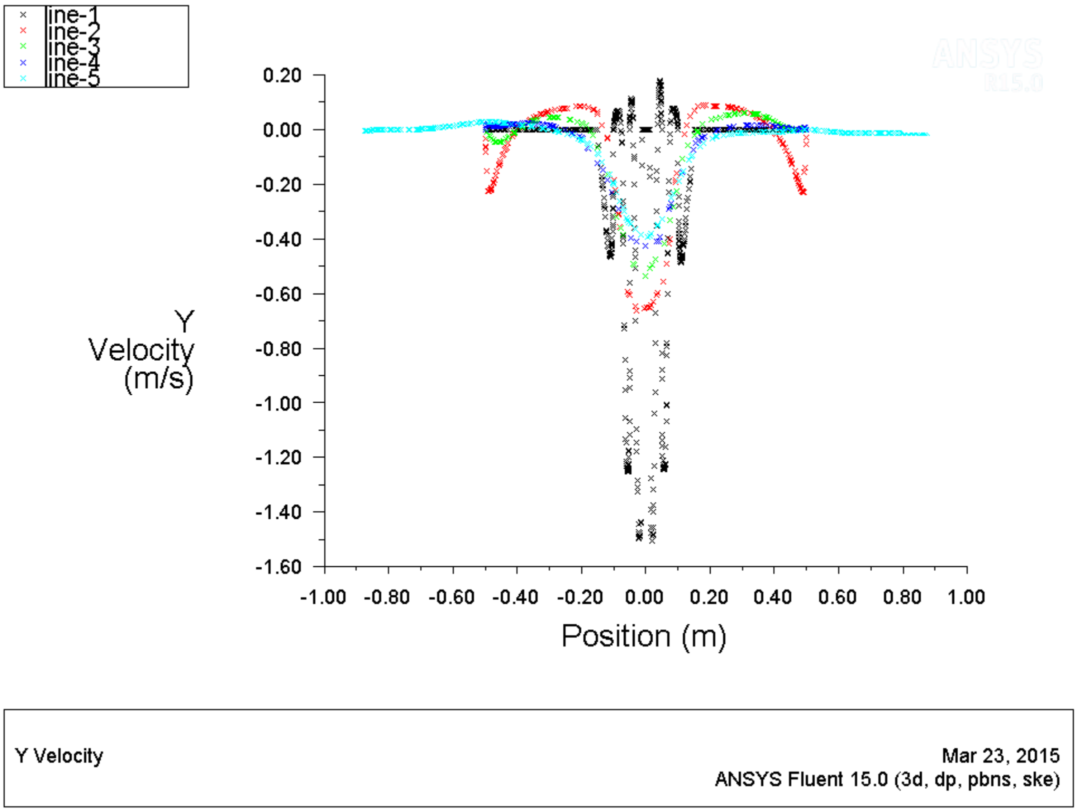
line-1
line-2
line-3
line-4
line-5
ANSYS
R15.0
0.20
0.00
-0.20
-0.40
-0.60
-0.80
-1.00
-1.20
-1.40
-1.60
Y
Velocity
(m/s)
-1.00
-0.80
-0.60
-0.40
-0.20
0.00
0.20
0.40
0.60
0.80
1.00
Position (m)
Y Velocity
Mar 23, 2015
ANSYS Fluent 15.0 (3d, dp, pbns, ske)

(a)

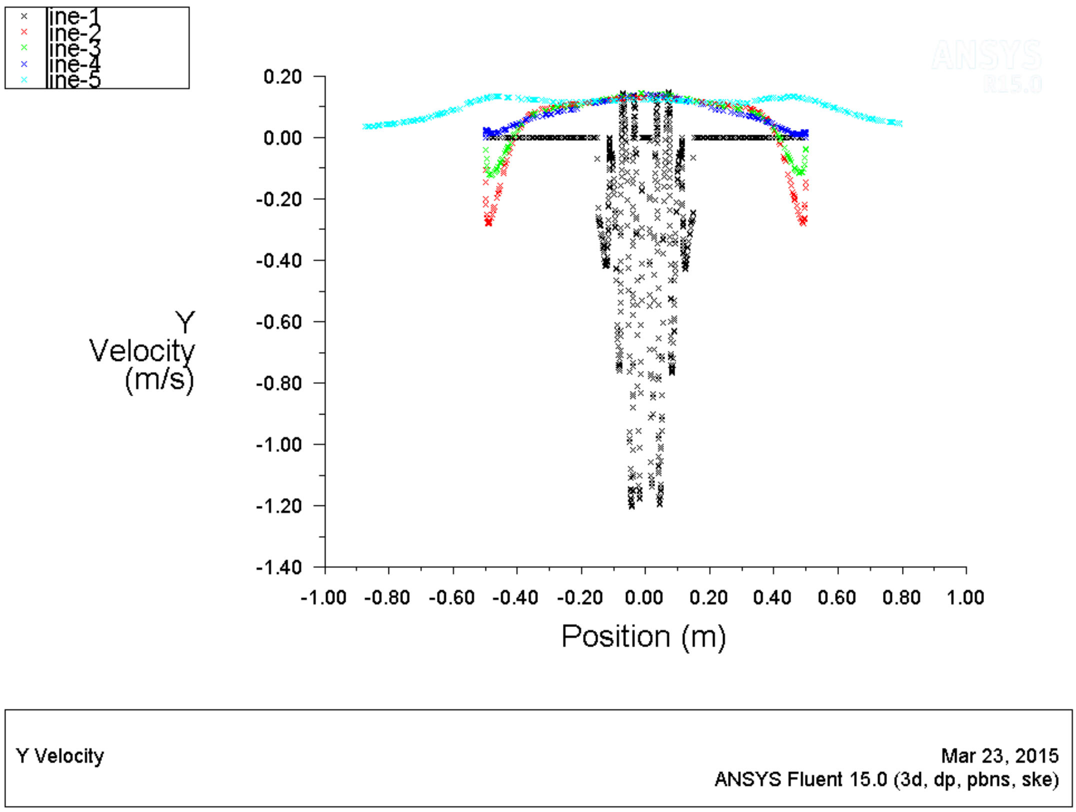
line-1
line-2
line-3
line-4
line-5
ANSYS
R15.0
0.20
0.00
-0.20
-0.40
-0.60
-0.80
-1.00
-1.20
-1.40
Y
Velocity
(m/s)
-1.00
-0.80
-0.60
-0.40
-0.20
0.00
0.20
0.40
0.60
0.80
1.00
Position (m)
Y Velocity
Mar 23, 2015
ANSYS Fluent 15.0 (3d, dp, pbns, ske)

(b)

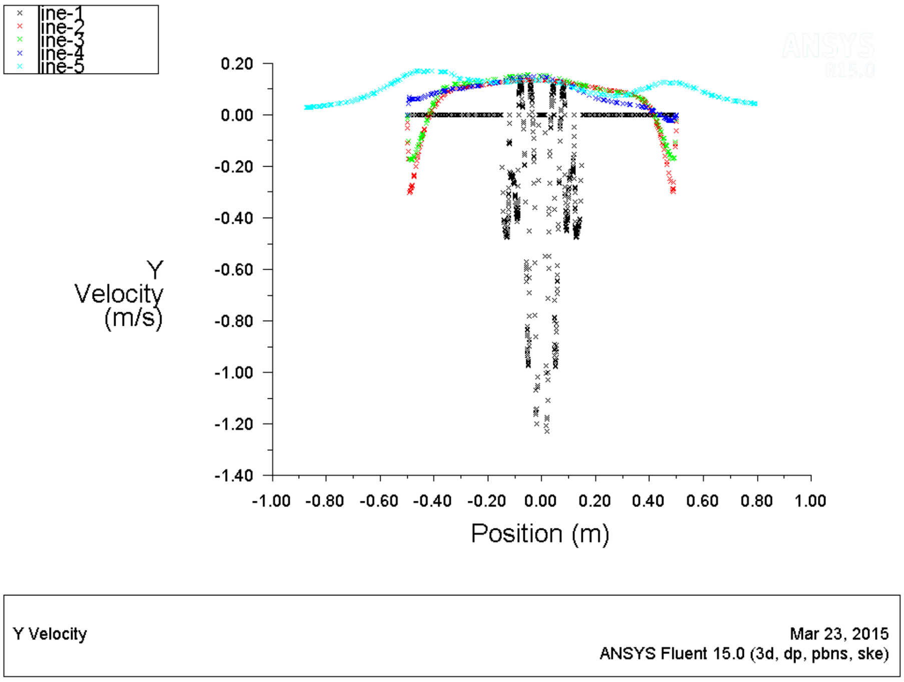

(c)

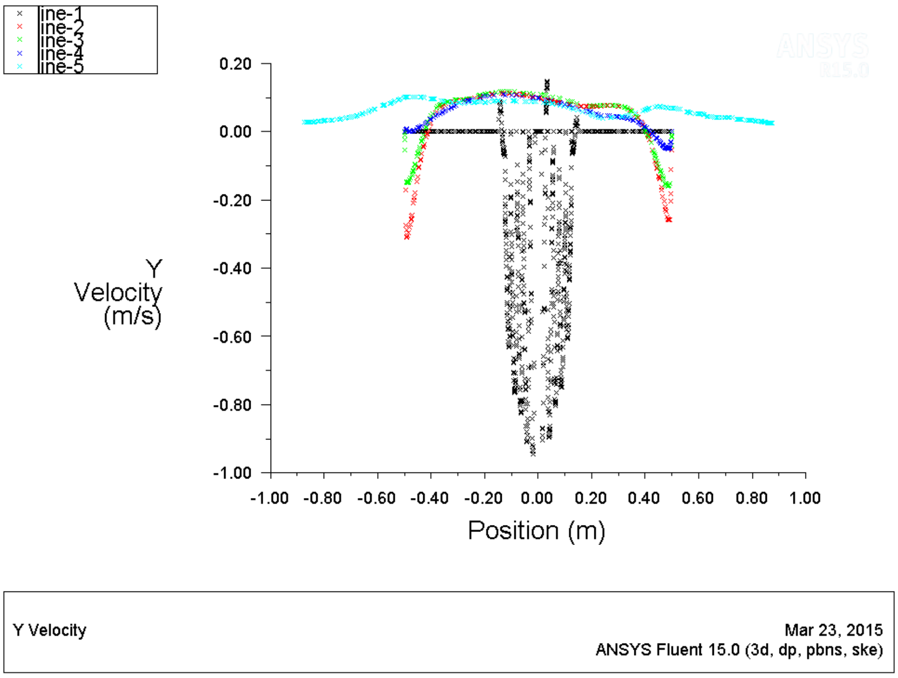

(d)

Figure 4.4: **The X-Y plots of velocity magnitude at section lines on *x*-axis extending from the centre of the room to the edge of walls with 2 outlets near wall bottoms: (a) 4-blade, (b) 5-blade, (c) 5-blade with blade angle change, & (d) 7-blade round ceiling air diffuser**

Based on sections (a) of Figures 4.5 and 4.6, the 4-blade/vane air diffuser indicated that the temperature distribution was not evenly throughout the room as most of the distributed air was concentrated around the middle spot of the room due to the reasons as stated in the previous section, resulting in cooler air (289.7 – 290.6 K) for the occupants nearby the air diffuser.

From sections (b) of Figures 4.5 and 4.6, the temperature distribution from the 5-blade/vane round ceiling air diffuser was relatively more consistent (292.4 – 294.2 K) throughout the room than that (289.7 – 293.3 K) of 4-blade/vane round ceiling air diffuser (Figures 4.5 (a)) since the air flow through the blades of 5-blade air diffuser was uniform. This result will lead to good thermal comfort among the occupants nearby the air diffuser.

The sections (c) of Figures 4.5 and 4.6 revealed that the air flow distribution from the 5-blade round ceiling air diffuser with an average blade angle of 30° was similar to those of 5-blade round ceiling air diffuser with an average blade angle of 40° in sections (b) of Figures 4.5 and 4.6. However, the air diffuser with 40° blade angle (sections (b) of Figures 4.5 and 4.6) exhibited slightly consistent temperature distribution (292.4 – 294.2 K) than that (292.4 – 294.2 K) of diffusers with 30° blade angle (sections (c) of Figures 4.5 and 4.6) since the air flow through the air diffuser with 40° blade angle had less direct impact with the air diffuser blades, and was able to flow smoothly if compared with the air diffuser of 30° blade angle. The air flow of 5-blade air diffuser with 30° blade angle was able to distribute effectively throughout the room, leading to a more consistent room temperature profile (292.4 – 294.2 K) within the room than that of 4-blade air diffuser (289.7 – 293.3 K) since it provided similar effect if compared to that of 5-blade air diffuser with 40° blade angle. A good thermal comfort can also be predicted among the occupants nearby the air diffuser without high flow concentration the air diffuser.

The CFD results of sections (d) of Figures 4.5 and 4.6 for 7-blade/vane air diffuser (292.4 – 293.3 K) revealed that the temperature distribution was slightly consistent if compared with that of the 4 (289.7 – 293.3 K) or 5- (292.4 – 294.2 K) blade air diffusers since the air flow through the 7-blade air diffuser was relatively more equal than that through 4 or 5-blade air diffuser. Meanwhile, the 7-blade air diffuser provided relatively lower temperature profile of 292.4 – 293.3 K throughout the room (Figure 4.5 (d)) if compared with that of 4 or 5-blade air diffuser, implying that the 7-blade air diffuser could create better thermal comfort for the occupants within the room, and assist in reducing energy consumption by the air handling unit to cool the supply air since the air flow rate from the 7-blade air diffuser was relatively higher and was able to distribute to further space more uniformly if compared with the other air diffusers.

The line 1 of all the X-Y plots in Figure 4.6 reflected that fluctuation of temperature profile around the centre position due to air flow through the air gap (constricted area) between the air diffuser blades with Venturi effect where air velocity was increased and pressure was reduced, and air velocity could affect the temperature distribution. The temperature profile within the room of lines 2 to 5 for 5 and 7-blade air diffusers reflected that the room temperature was within 293 K, and 292 – 293 K, respectively, while velocity profile within the room of lines 2 to 5 for 4-blade air diffuser indicated the room temperature up to 288 K around the centre position due to uneven air distribution.

In addition, it can be observed that the models with two air outlets near the wall bottoms were able to provide more effective air flow behaviour and temperature distribution throughout the room as the air was equally directed from the inlet to the two outlets, if compared with those models with either one outlet near the wall bottom or one outlet on ceiling level. However, the actual position of air outlets, i.e., return air diffusers, are normally installed on the ceiling level of a room or space in the building instead of near the bottom of any walls due to lack of space to box-up those duct droppers, which are extended from the main ductwork on ceiling space. The effect of air outlet mounted on ceiling level will be further discussed in Section 4.1.7.

Furthermore, the contour views of static temperature of 5 and 7-blade air diffusers with two outlets near the wall bottoms were compared with those of air diffuser obtained by Mohammed (2013) as depicted in Figure 2.13. It was noticed that the temperature distribution of the proposed air diffusers was slightly consistent than that of air diffuser reported by Mohammed (2013) since the air flow distribution through the blades of the proposed air diffusers was more uniformly distributed due to less contact between the air flow and blade surfaces.

The range of velocity magnitude, Y velocity and static temperature distribution within the room for each model with two outlets near the wall bottoms, are summarised in Table 4.1.

Table 4.1: Range of velocity magnitude, Y velocity and static temperature distribution within the room with two outlets near the wall bottoms

Item	Diffuser Model			
	4-blade	5-blade (40°)	5-blade (30°)	7-blade
Velocity Magnitude (m/s)	0 – 0.75	0 – 0.60	0 – 0.60	0 – 0.60
Y Velocity (m/s)	-0.65 – 0.20	-0.14 – 0.20	-0.14 – 0.20	-0.14 – 0.20
Static Temperature (K)	289.7 – 293.3	292.4 – 294.2	292.4 – 294.2	292.4 – 293.3

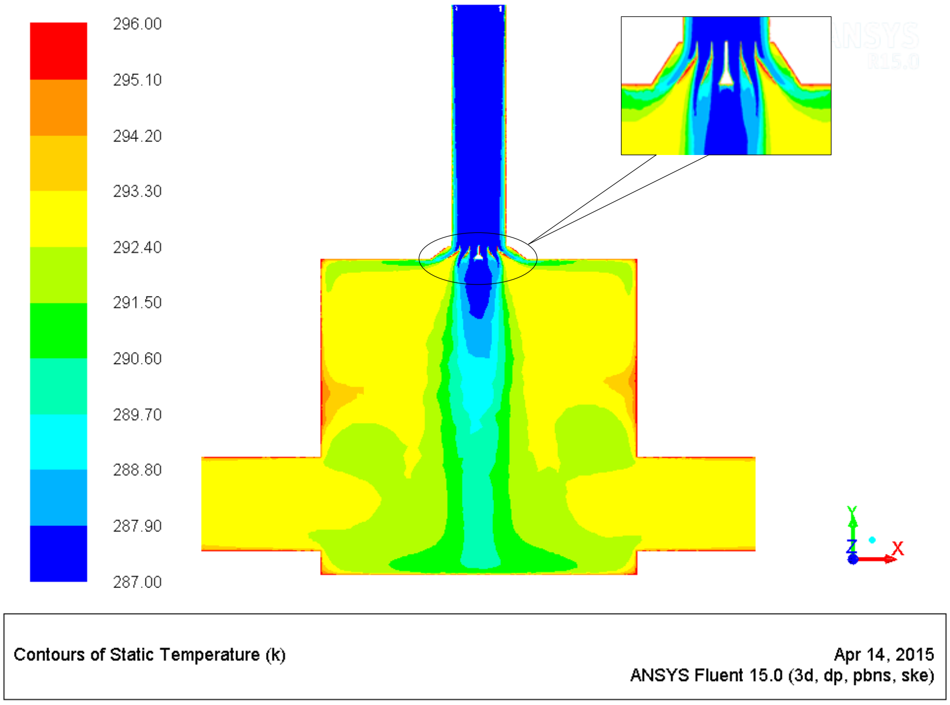
296.00
295.10
294.20
293.30
292.40
291.50
290.60
289.70
288.80
287.90
287.00
Contours of Static Temperature (k)
Apr 14, 2015
ANSYS Fluent 15.0 (3d, dp, pbns, ske)

(a)

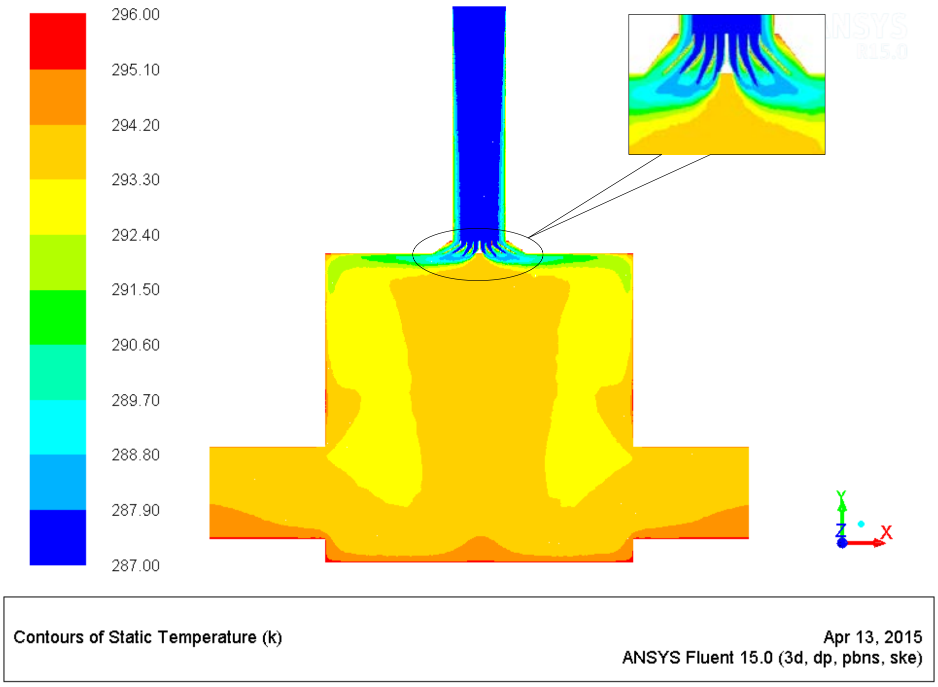
296.00
295.10
294.20
293.30
292.40
291.50
290.60
289.70
288.80
287.90
287.00
Contours of Static Temperature (k)
Apr 13, 2015
ANSYS Fluent 15.0 (3d, dp, pbns, ske)

(b)

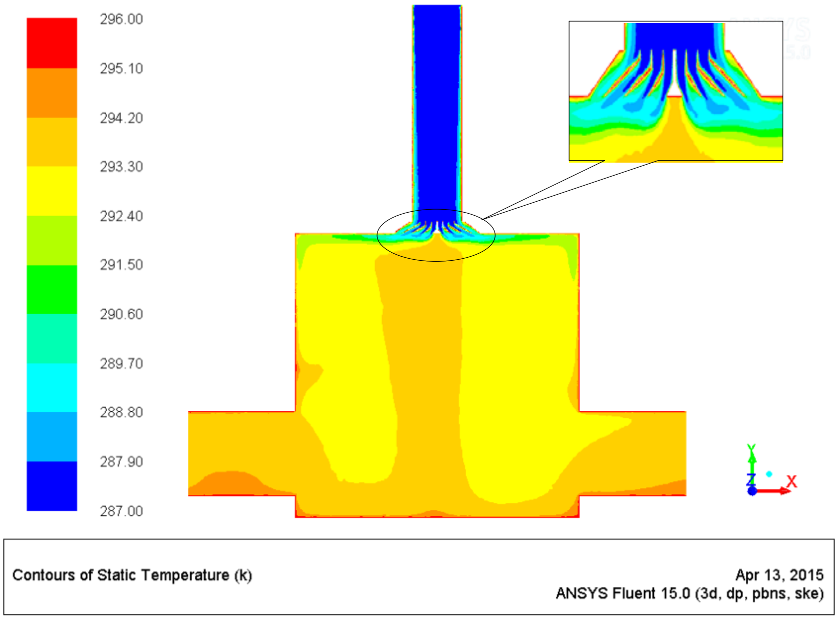

(c)

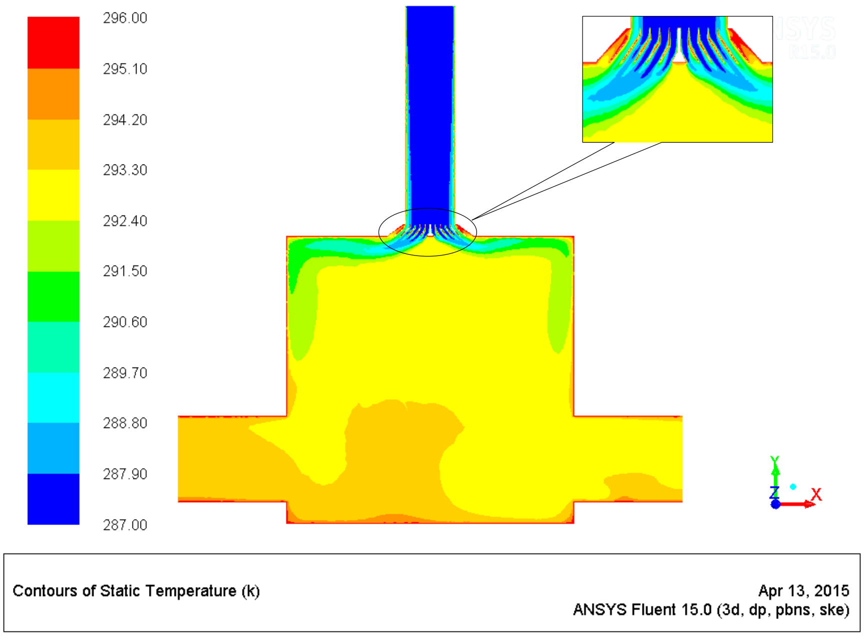

(d)

Figure 4.5: Contours of static temperature in the room with inlet on ceiling and 2 outlets near wall bottoms: (a) 4-blade, (b) 5-blade, (c) 5-blade with blade angle change, & (d) 7-blade round ceiling air diffuser

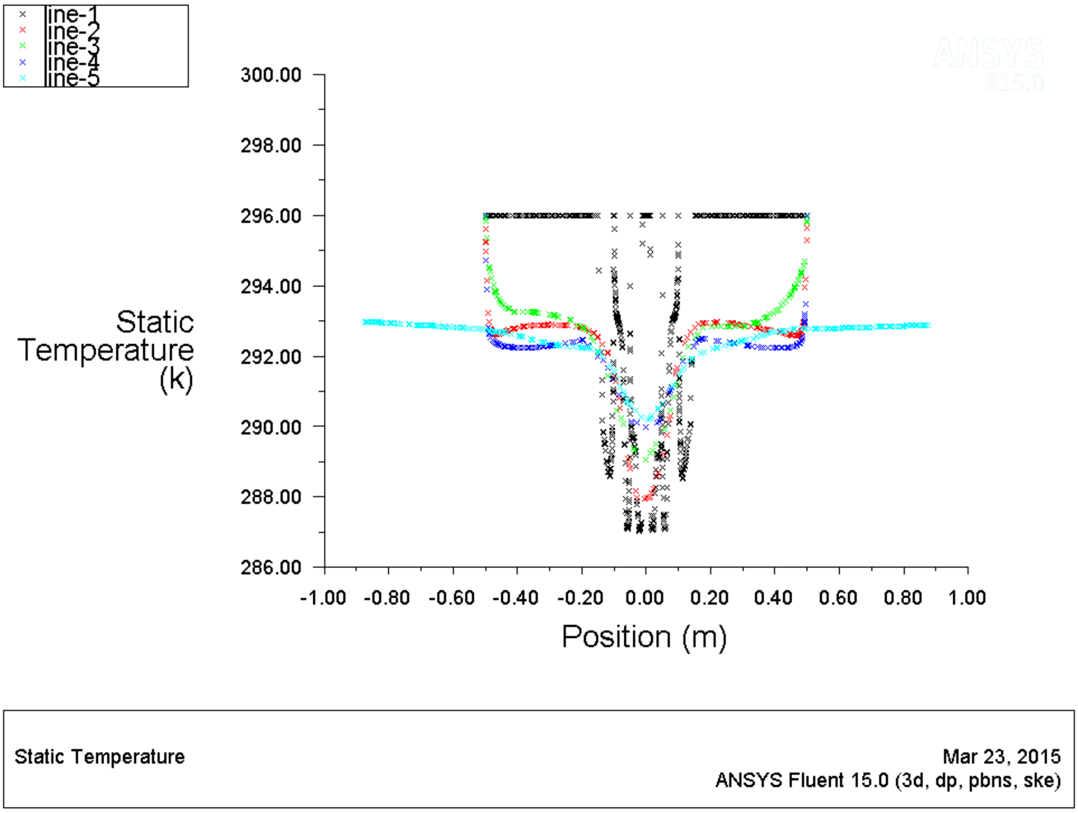
line-1
line-2
line-3
line-4
line-5
Static Temperature (k)
Position (m)
Static Temperature
Mar 23, 2015
ANSYS Fluent 15.0 (3d, dp, pbns, ske)

(a)

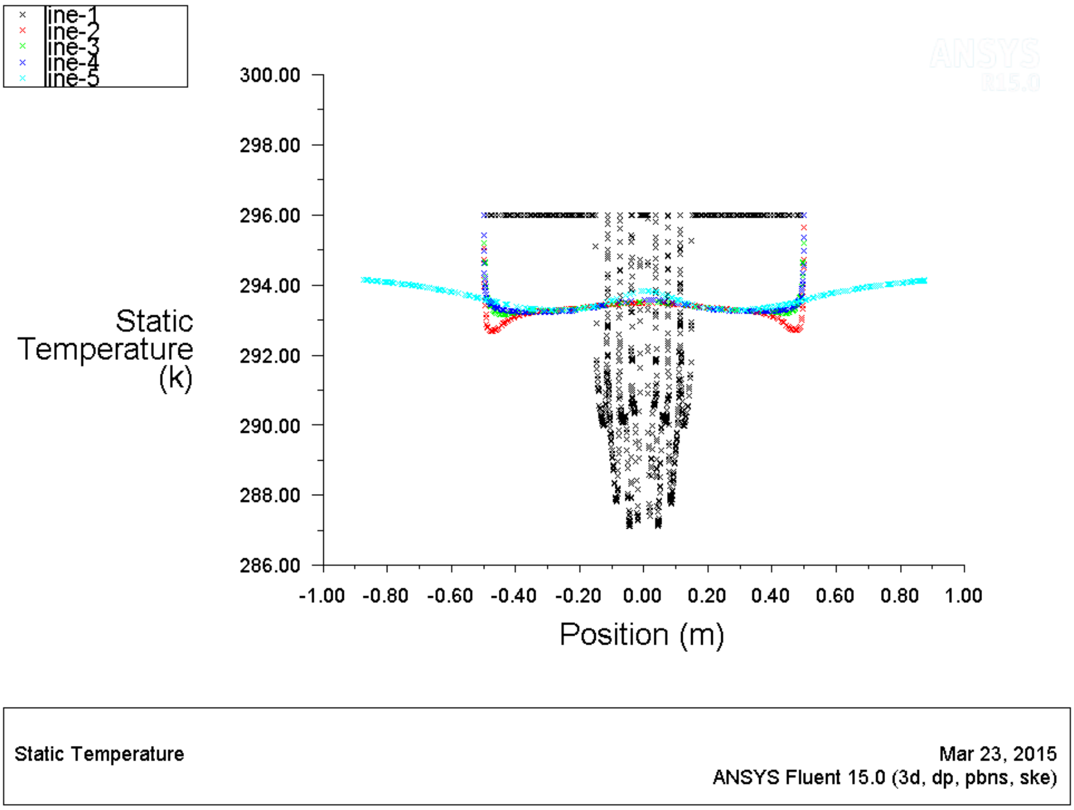
line-1
line-2
line-3
line-4
line-5
Static Temperature (k)
Position (m)
Static Temperature
Mar 23, 2015
ANSYS Fluent 15.0 (3d, dp, pbns, ske)

(b)

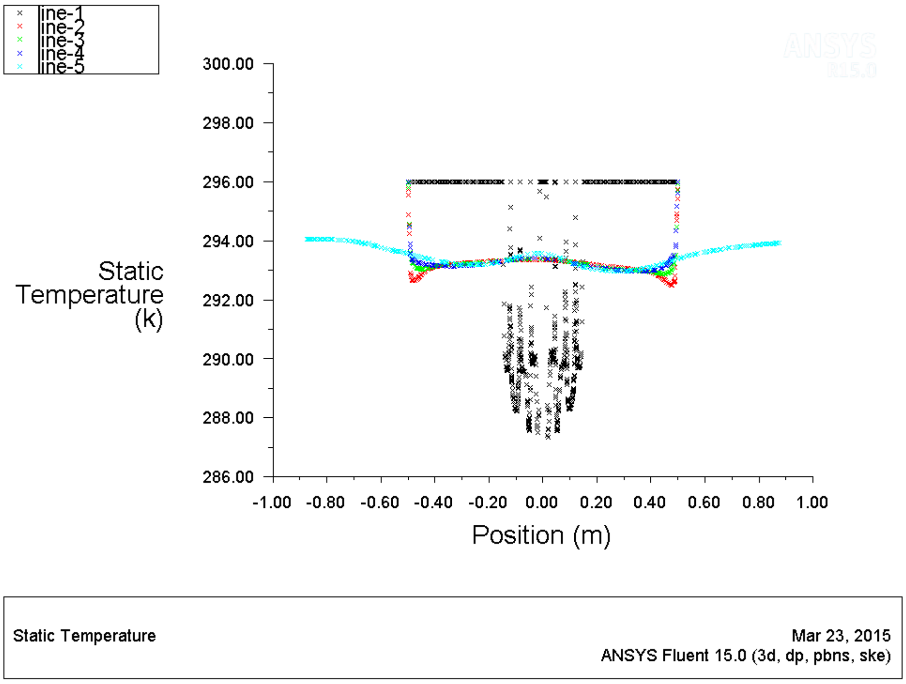

(c)

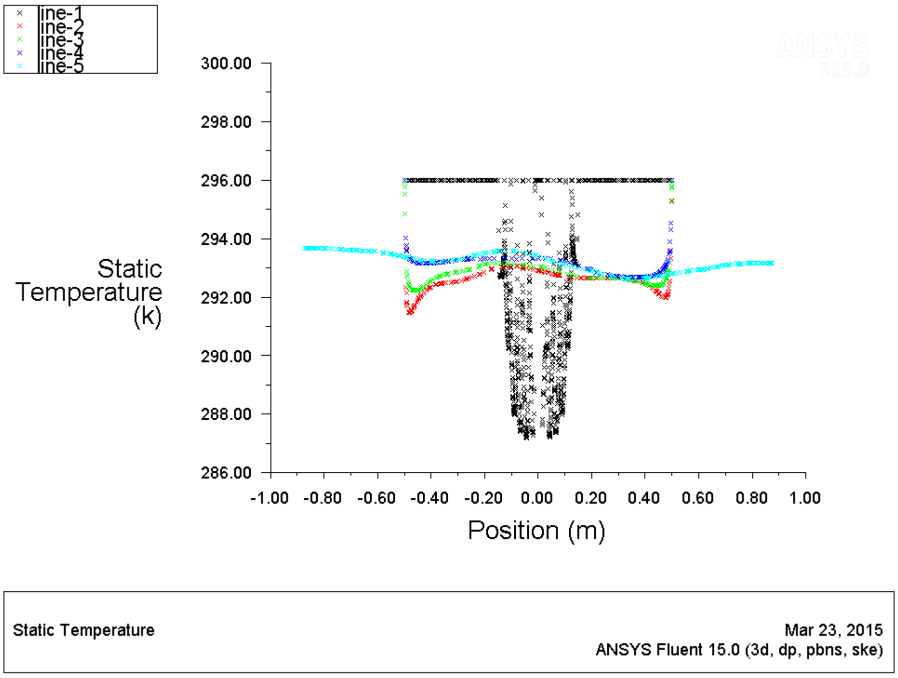

(d)

Figure 4.6: **X-Y plots of static temperature at section lines on *x*-axis extending from the centre of the room to the edge of walls with 2 outlets near wall bottoms: (a) 4-blade, (b) 5-blade, (c) 5-blade with blade angle change, & (d) 7-blade round ceiling air diffuser**

4.1.2 Inlet velocity at 0.5 m/s for the round ceiling air diffuser with two outlets near bottom of walls

The study of various inlet air velocities for round ceiling air diffuser was focused on 5 and 7-blade air diffusers with two outlets near wall bottoms since these two models have provided most consistent air flow distribution and temperature distribution among the 4 types of the air diffuser models as discussed in the previous sections.

The air flow patterns and temperature distribution behaviours of round ceiling air diffusers in room with inlet on ceiling and 2 outlets near bottom of walls were observed for inlet air velocity at 0.5, 2.0 and 3.0 m/s, while inlet air temperature was maintained at 287 K as indicated in Figures 4.7 and 4.12. The aforesaid velocities are sometimes applied for inlet air velocity for supply air diffusers in industry besides 1.0 m/s, whereas the 287 K inlet air temperature is the optimal temperature for supply air diffusers.

Based on sections (a) of Figures 4.7 and 4.8, the air flow behaviours throughout the room for 7-blade/vane air diffuser at 0.5 m/s inlet air velocity (0 – 0.16 m/s) were uniform than that of 5-blade/vane air diffuser (0 – 0.16 m/s) since the air flow through the 7-blade air diffuser was more consistent than that through 5-blade air diffuser. Meanwhile, the 5 or 7-blade air diffuser with 0.5 m/s inlet air velocity has lower velocity profile (0 – 0.16 m/s) within the room than that of 5 or 7-blade air diffuser with 1.0 m/s inlet velocity (0 – 0.30 m/s). It was because the air flow rate from the air diffuser with an inlet velocity of 0.5 m/s was lower than that of diffuser with an inlet velocity of 1.0 m/s. Therefore, the air flow distribution with an inlet velocity of 0.5 m/s to further end of a room was slower than that with an inlet velocity of 1.0 m/s. In addition, Coanda effect of air distribution was observed in Figure 4.7 where the flow emerged radically and reached the wall and then directed into 90° downward, suggesting that the throw of air could be longer.

The line 1 of all the X-Y plots in Figure 4.8 revealed that the fluctuation of velocity profile around the centre position was due to the air flow through the air gap (constricted area) between the air diffuser blades with Venturi effect where air velocity was increased and pressure was reduced. In addition, the velocity profile within the room of lines 2 to 5 for 5 or 7-blade air diffuser showed that the air velocity was within 0.16 m/s, which slightly lower than (0.2 m/s) those of 5 or 7-blade air diffuser at 1.0 m/s inlet velocity.

Furthermore, the air velocity distribution of 5 and 7-blade air diffusers with two outlets near wall bottoms at 0.5 m/s inlet velocity were slightly consistent if compared with that of round diffuser obtained by Mohammed (2013) as illustrated in Figure 2.13 since the air flow distribution via the blades of proposed models was relatively more uniform distributed although the inlet velocity of proposed models might be lower than those air diffusers established by Mohammed (2013).

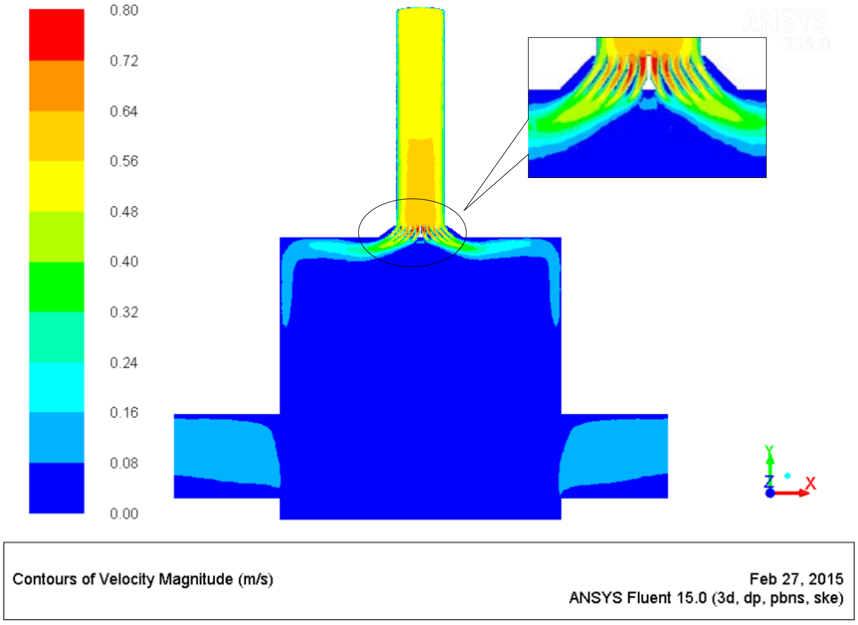

(a)

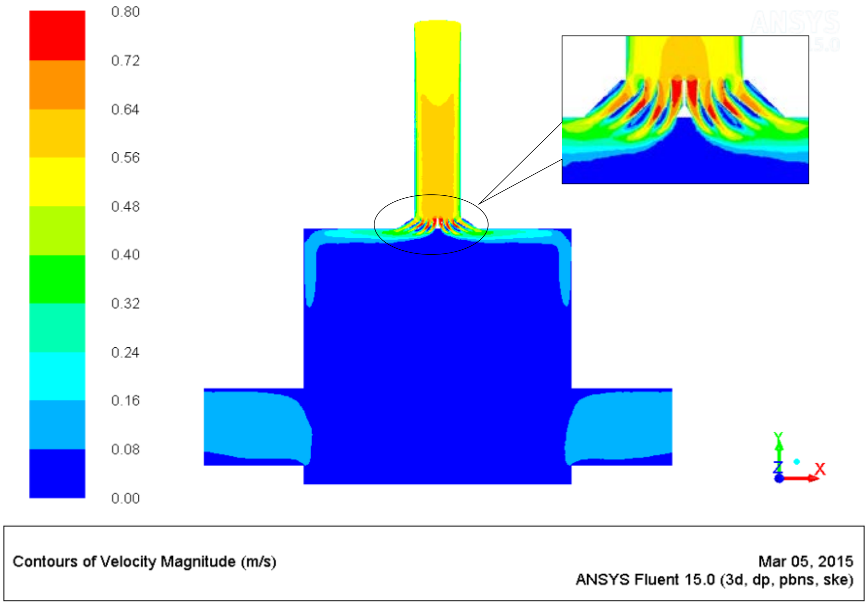

(b)

Figure 4.7: Contours of velocity magnitude in the room with inlet on ceiling and 2 outlets near wall bottoms at 0.5 m/s inlet velocity: (a) 7-blade, & (b) 5-blade round ceiling air diffuser

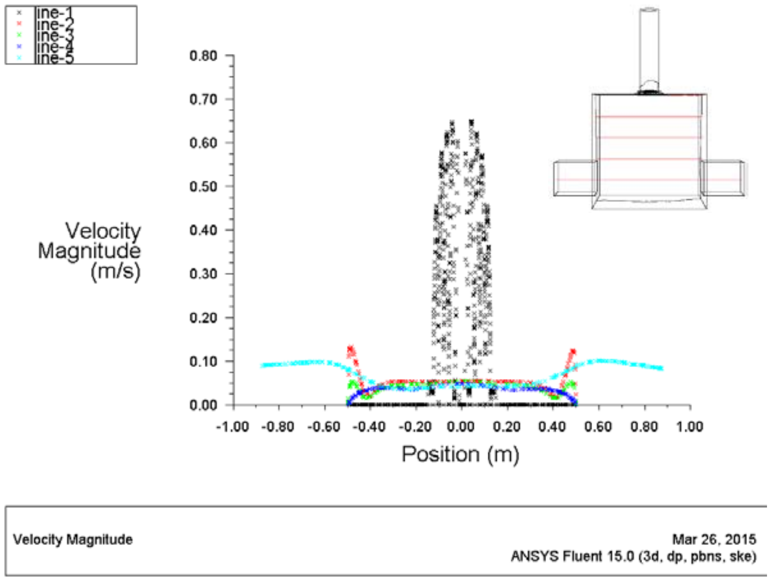

(a)

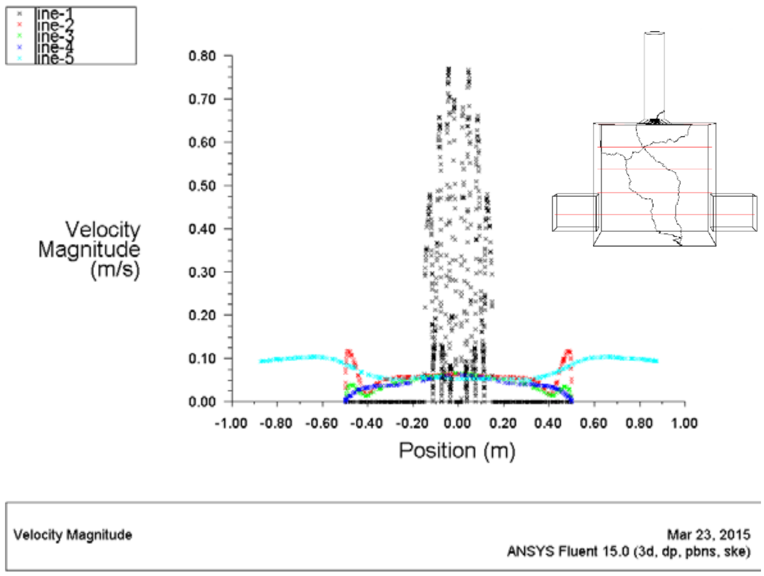

(b)

Figure 4.8: **The X-Y plots of velocity magnitude at section lines (red colour line 1 to 5 depicted in small figure beside the XY plot) on *x*-axis extending from the centre of the room to the edge of walls with 2 outlets near wall bottoms at 0.5 m/s inlet velocity: (a) 7-blade, & (b) 5-blade round ceiling air diffuser**

From sections (a) of Figures 4.9 and 4.10, the air flow distribution throughout the room for 7-blade/vane round ceiling air diffuser at 0.5 m/s inlet air velocity (0.01 – 0.1 m/s) was slightly consistent than that of 5-blade/vane round ceiling air diffuser (0.01 – 0.1 m/s) since the air flow via the 7-blade air diffuser was more equal or even than that via 5-blade air diffuser.

Meanwhile, the 5 or 7-blade round ceiling air diffuser with 0.5 m/s inlet air velocity had lower velocity profile (0.01 – 0.1 m/s) within the room than that of 5 or 7-blade air diffuser with 1.0 m/s inlet velocity (0.03 – 0.2 m/s). It was due to the air flow rate from the air diffuser with inlet velocity at 0.5 m/s was lower than that from the air diffuser with inlet velocity at 1.0 m/s. Therefore, the air flow distribution by the air diffuser with 0.5 m/s inlet velocity to further end of a room was slower than that of diffuser with 1.0 m/s inlet velocity. However, those occupants around the air diffuser will experience better thermal comfort because of the slower air flow since the air flow from diffuser could uniformly distributed throughout the room.

In addition, line 1 of all the X-Y plots in Figure 4.10 showed that the fluctuation of velocity profile around the centre position was due to air flow through the air gap (constricted area) between the air diffuser blades with Venturi effect where air velocity was increased and pressure was reduced. Moreover, the velocity profile within the room of lines 2 to 5 for 5 or 7-blade air diffuser reflected that the air velocity was within 0.1 m/s, which slightly lower than (0.2 m/s) that of 5 or 7-blade air diffuser at 1.0 m/s inlet velocity.

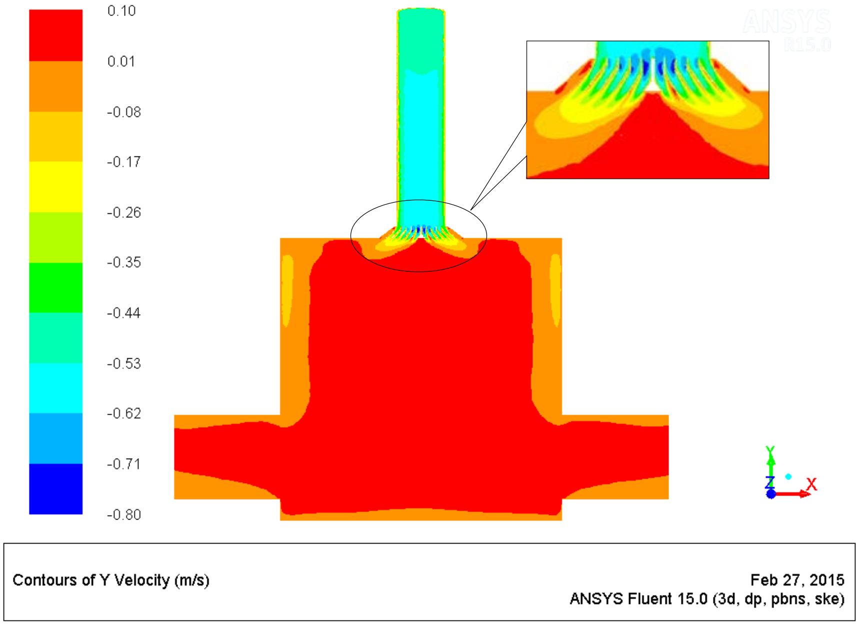

(a)

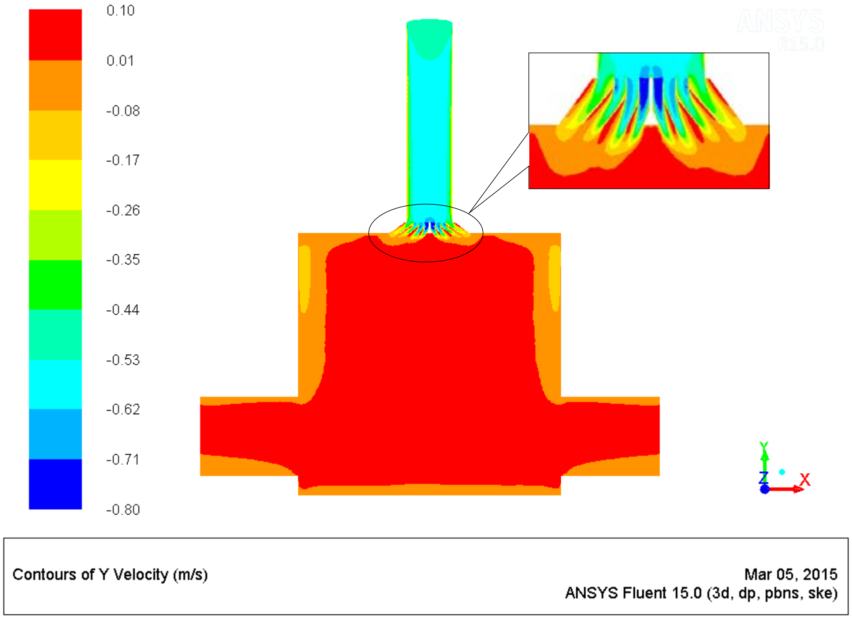

(b)

Figure 4.9: Contours of Y velocity in the room with inlet on ceiling and 2 outlets near wall bottoms at 0.5 m/s inlet velocity: (a) 7-blade, & (b) 5-blade round ceiling air diffuser

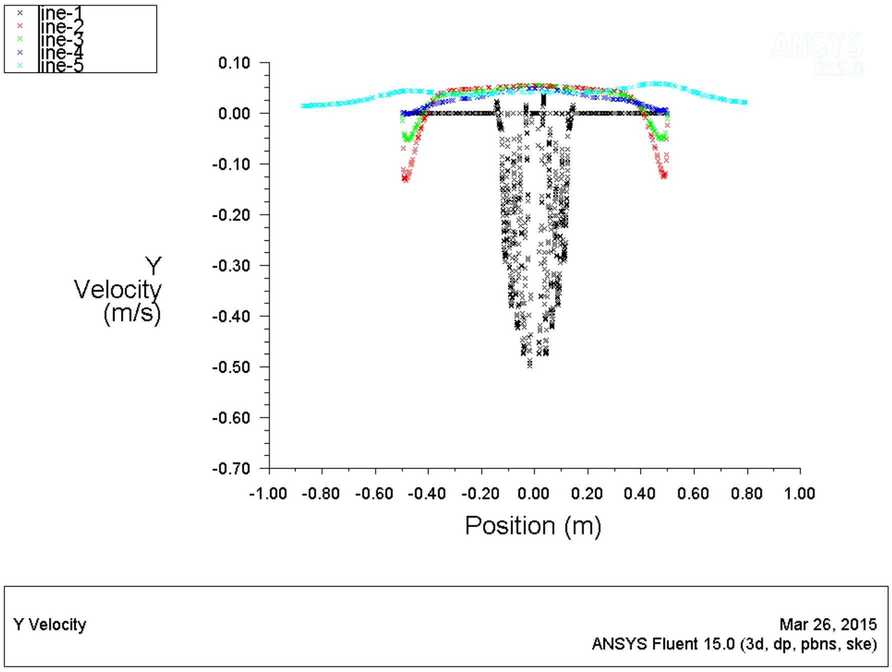

(a)

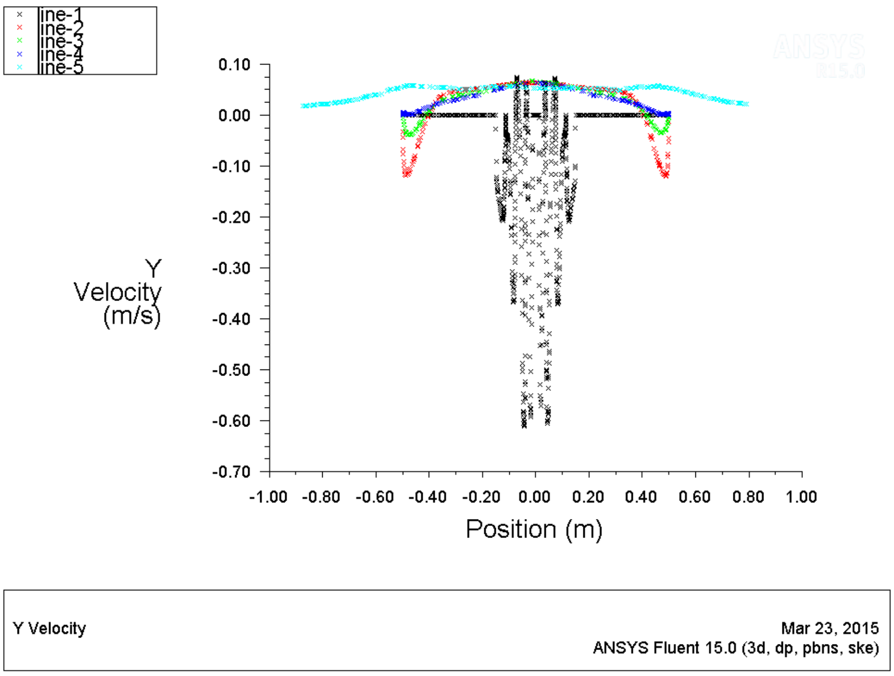

(b)

Figure 4.10: X-Y plots of Y velocity at section lines on *x*-axis extending from the centre of the room to the edge of walls with 2 outlets near wall bottoms at 0.5 m/s inlet velocity: (a) 7-blade, & (b) 5-blade round ceiling air diffuser

From sections (a) of Figures 4.11 and 4.12, the temperature distribution throughout the room for 7-blade/vane round ceiling air diffuser at 0.5 m/s inlet air velocity (293.3 – 295.1 K) was slightly more uniform than that of 5-blade/vane round ceiling air diffuser (293.3 – 295.1 K) since the air flow via the 7-blade air diffuser was more even or smooth than that via 5-blade air diffuser.

Meanwhile, the 5 or 7-blade round ceiling air diffuser with 0.5 m/s inlet air velocity had higher temperature profile (293.2 – 295.1 K) within the room than that of 5 or 7-blade air diffuser with 1.0 m/s inlet velocity (292.4 – 294.2 K). It was due to the air flow rate from the air diffuser with inlet velocity at 0.5 m/s was lower than that of the air diffuser with inlet velocity at 1.0 m/s. Therefore, the room temperature generated by the air diffuser with 0.5 m/s inlet velocity was warmer than that with 1.0 m/s inlet velocity. However, the thermal comfort might not seem to be an issue since the average room temperature did not exceed the recommended room temperature of 296 K, and the air from diffuser was uniformly distributed throughout the room.

In addition, the line 1 of all the X-Y plots in Figure 4.12 reflected that the fluctuation of temperature profile around the centre position was due to air flow through the air gap (constricted area) between the air diffuser blades with Venturi effect where air velocity was increased and pressure was reduced, and air velocity could affect the temperature distribution. Besides, the temperature profile within the room of lines 2 to 5 for 5 or 7-blade air diffuser reflected that the room temperature was within 294 K, which slightly higher than that (293 K) of 5 or 7-blade air diffuser.

Furthermore, the temperature distribution of 5 and 7-blade air diffusers with two outlets near wall bottoms at 0.5 m/s inlet velocity was slightly consistent if compared with that of round diffuser obtained by Mohammed (2013) as illustrated in Figure 2.13 since the air flow distribution via the blades of proposed models was relatively more uniform although the inlet velocity of proposed models might be lower than those diffusers established by Mohammed (2013).

The range of velocity magnitude, Y velocity and static temperature distribution within the room for round ceiling air diffuser with inlet velocity at 0.5 m/s are summarised in Table 4.2.

Table 4.2: Range of velocity magnitude, Y velocity and static temperature distribution within the room for 0.5 m/s inlet velocity

Item	Diffuser Model	
	5-blade	7-blade
Velocity Magnitude (m/s)	0 – 0.32	0 – 0.32
Y Velocity (m/s)	-0.08 – 0.10	-0.08 – 0.10
Static Temperature (K)	293.3 – 295.1	293.3 – 295.1

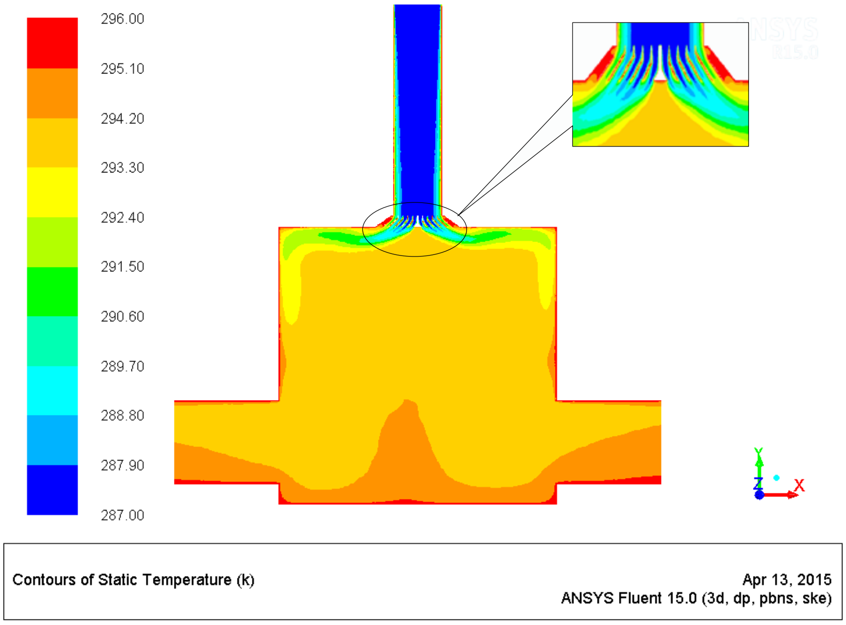

(a)

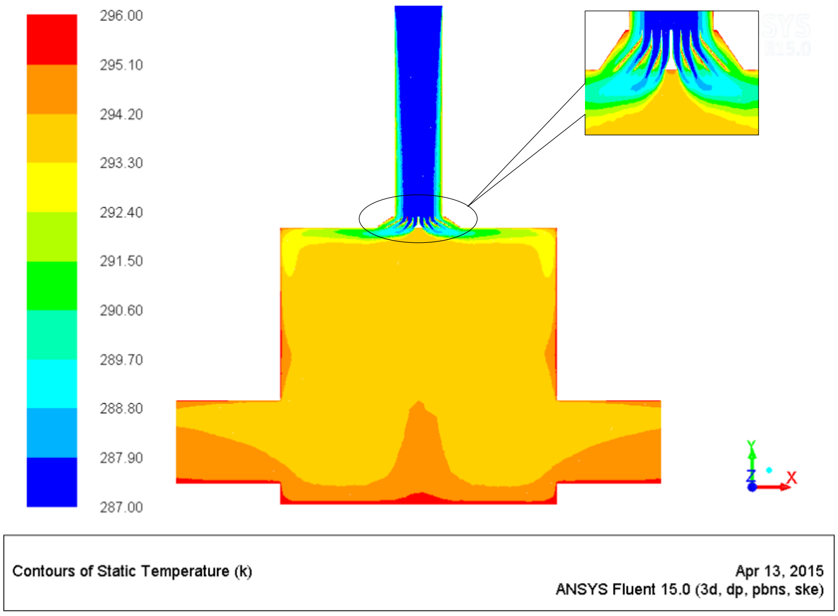

(b)

Figure 4.11: Contours of static temperature in the room with inlet on ceiling and 2 outlets near wall bottoms at 0.5 m/s inlet velocity: (a) 7-blade, & (b) 5-blade round ceiling air diffuser

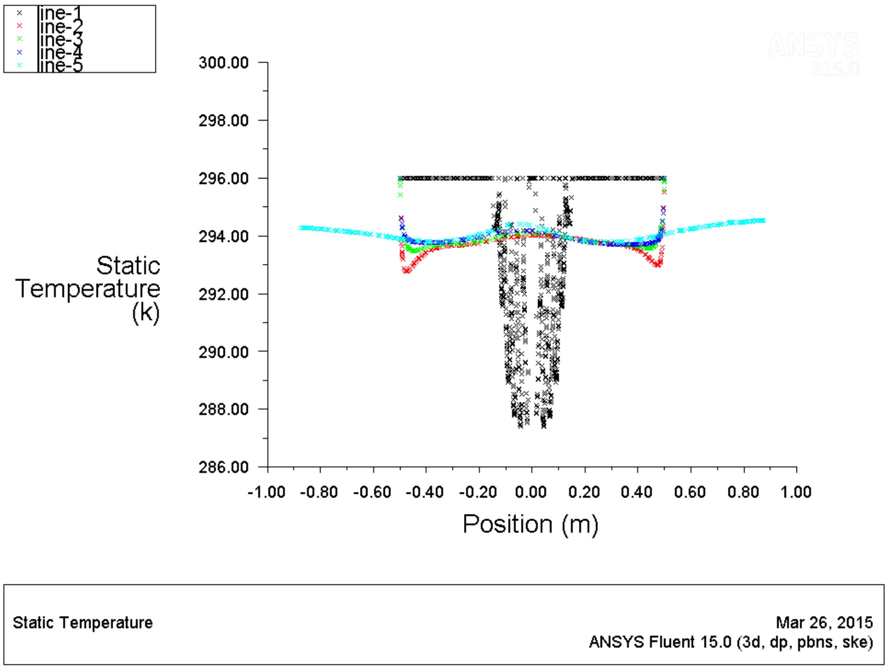

(a)

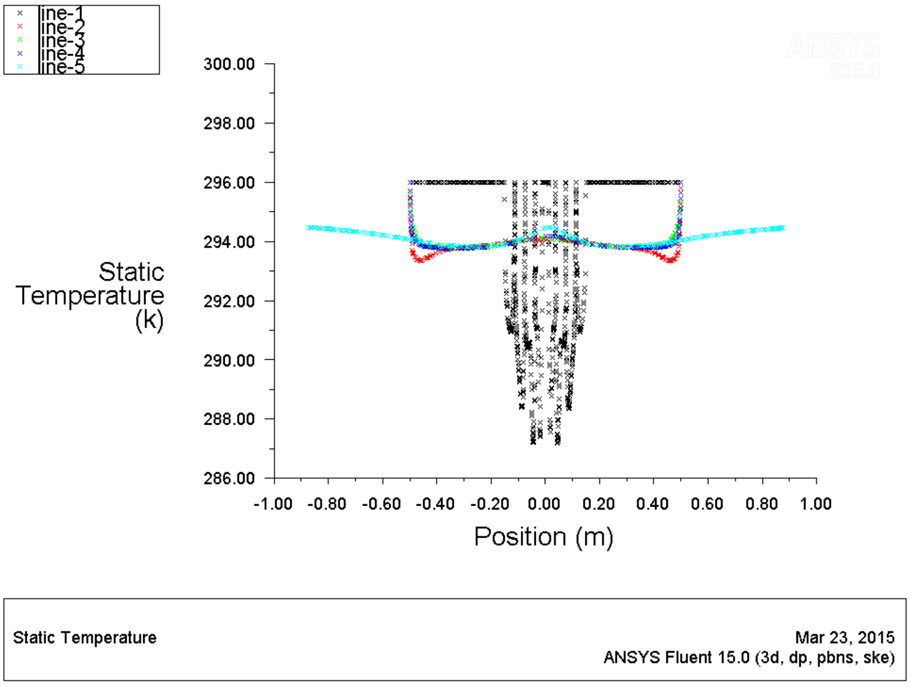

(b)

Figure 4.12: **X-Y plots of static temperature at section lines on *x*-axis extending from the centre of the room to the edge of walls with 2 outlets near wall bottoms at 0.5 m/s inlet velocity: (a) 7-blade, & (b) 5-blade round ceiling air diffuser**

4.1.3 Inlet velocity at 2.0 m/s for the round ceiling air diffuser with two outlets near bottom of walls

From sections (a) of Figures 4.13 and 4.14, the air flow behaviours throughout the room for 7-blade/vane round ceiling air diffuser at 2.0 m/s inlet velocity (0 – 0.6 m/s) was consistent than that of 5-blade/vane round ceiling air diffuser (0 – 0.6 m/s) since the air flow via the 7-blade air diffuser was more uniform than that via 5-blade air diffuser.

Meanwhile, the 5 or 7-blade round ceiling air diffuser with 2.0 m/s inlet air velocity had higher velocity profile (0 – 0.6 m/s) within the room than that of 5 or 7-blade air diffuser with 1.0 m/s inlet velocity (0 – 0.3 m/s). It was because the air flow rate from the air diffusers with inlet velocity at 2.0 m/s was relatively higher than those of the air diffusers with inlet velocity at 1.0 m/s. In addition, Coanda effect of air distribution was observed in Figure 4.13 where the flow emerged radically and approached the wall and then turned into 90° downward, which revealed the throw of air could be longer.

In addition, line 1 of all the X-Y plots in Figure 4.14 revealed that the fluctuation of velocity profile around the centre position due to air flow through the air gap (constricted area) between the air diffuser blades with Venturi effect where air velocity was increased and pressure was reduced. The velocity profile within the room of lines 2 to 5 for 5 or 7-blade air diffuser reflected that the air velocity was within 0.3 m/s, which was slightly higher than that (0.2 m/s) of 5 or 7-blade air diffuser at 1.0 m/s inlet velocity.

Furthermore, the air velocity distribution of 5 and 7-blade air diffusers with two outlets near wall bottoms at 2.0 m/s inlet velocity was slightly consistent if compared with that of round diffuser obtained by Mohammed (2013) as illustrated in Figure 2.13 since the air flow distribution via the blades of proposed models was relatively more uniform distributed although their inlet velocity might be similar to those diffusers established by Mohammed (2013).

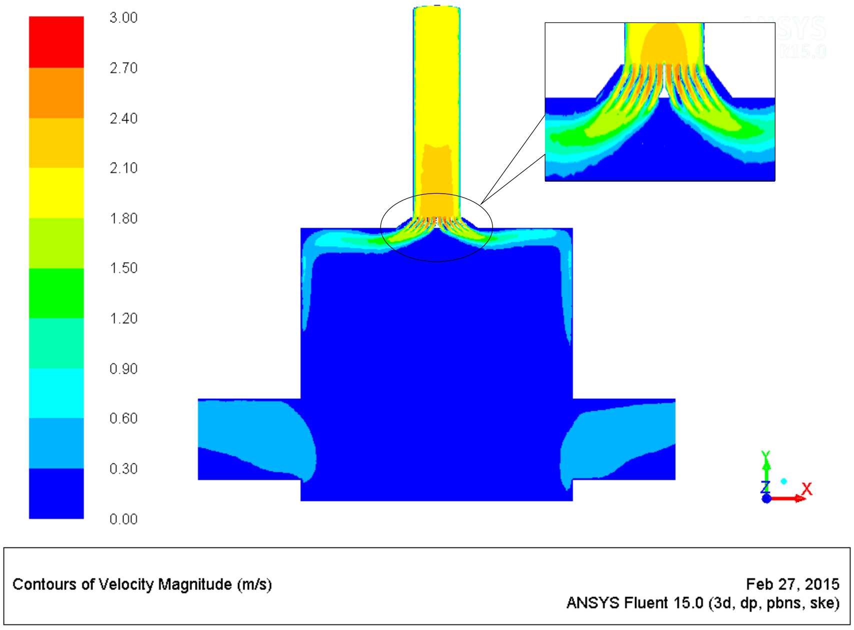

(a)

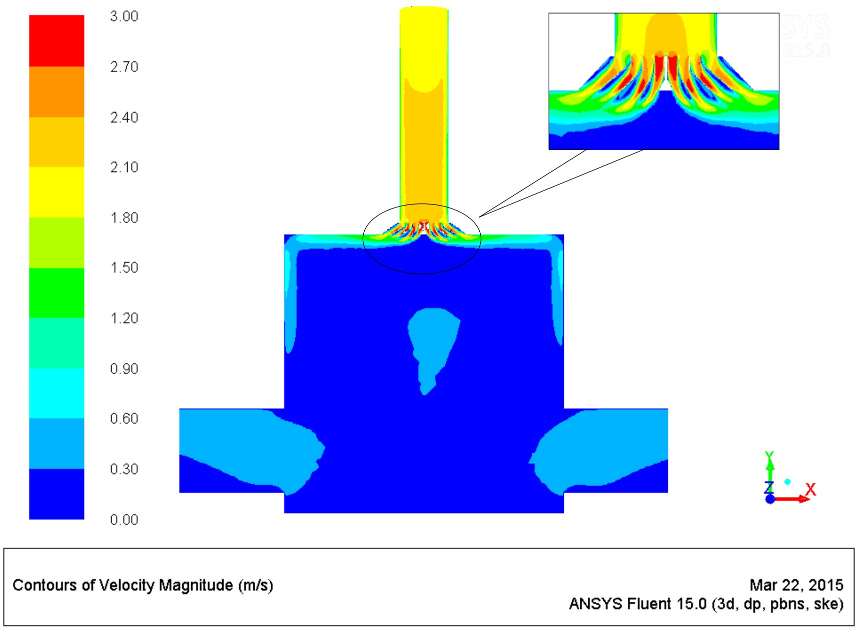

(b)

Figure 4.13: Contours of velocity magnitude in the room with inlet on ceiling and 2 outlets near wall bottoms at 2.0 m/s inlet velocity: (a) 7-blade, & (b) 5-blade round ceiling air diffuser

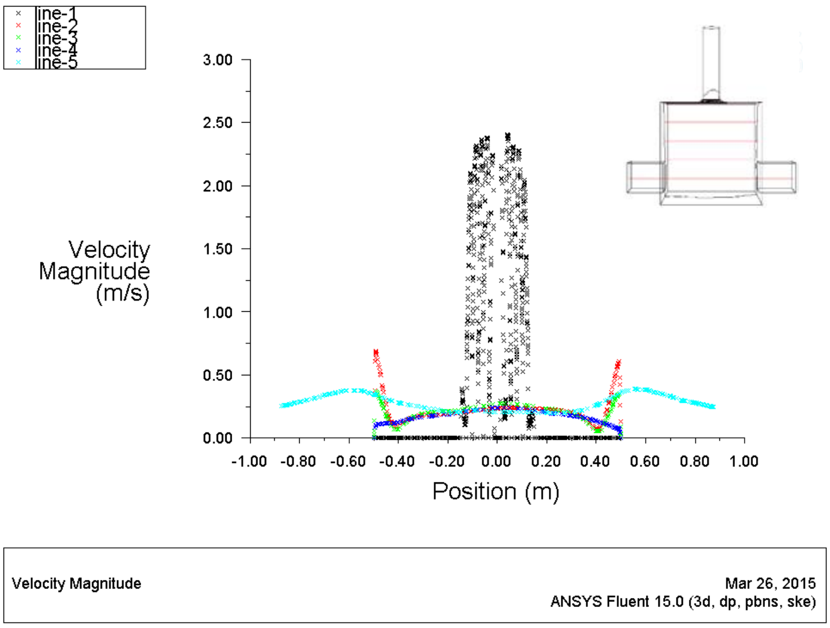

(a)

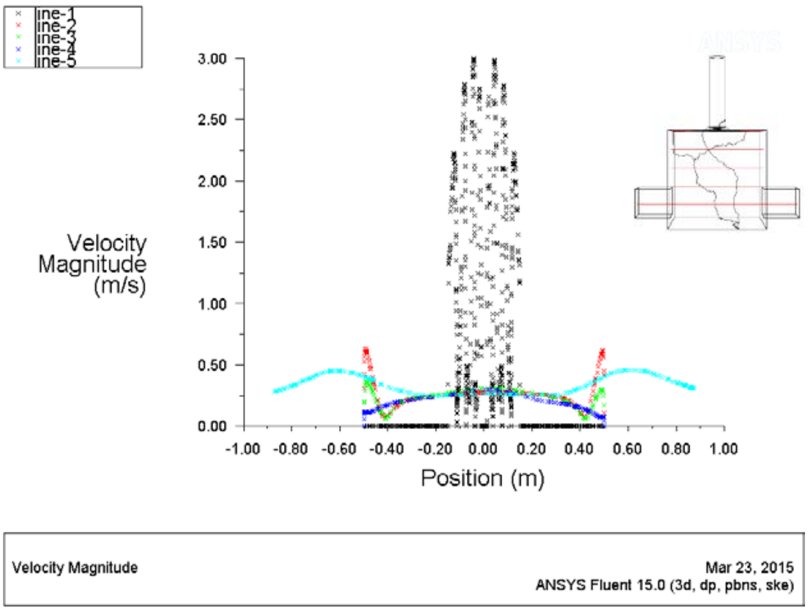

(b)

Figure 4.14: **X-Y plots of velocity magnitude at section lines (red colour line 1 to 5 depicted in small figure beside the XY plot) on *x*-axis extending from the centre of the room to the edge of walls with 2 outlets near wall bottoms at 2.0 m/s inlet velocity: (a) 7-blade, & (b) 5-blade round ceiling air diffuser**

Based on sections (a) of Figures 4.15 and 4.16, the air flow distribution throughout the room for 7-blade/vane round ceiling air diffuser (0.06 – 0.4 m/s) at 2.0 m/s inlet velocity was uniform than that of 5-blade/vane round ceiling air diffuser (0.06 – 0.4 m/s) since the air flow via the 7-blade air diffuser was more smooth than that via 5-blade air diffuser.

Meanwhile, the 5 or 7-blade round ceiling air diffuser with 2.0 m/s inlet air velocity had higher velocity profile (0.06 – 0.4 m/s) within the room than that of 5 or 7-blade air diffuser with 1.0 m/s inlet velocity (0.03 – 0.2 m/s). It was because the air flow rate from the air diffusers with inlet velocity at 2.0 m/s was relatively higher than those of the air diffusers with inlet velocity at 1.0 m/s. Therefore, the air flow distribution by the air diffuser with 2.0 m/s inlet velocity to further end of a room was faster than that with 1.0 m/s inlet velocity. The occupants around the air diffuser might feel slightly uncomfortable due to higher air flow toward their body continuously, although the air from the air diffuser was uniformly distributed throughout the room.

In addition, line 1 of all the X-Y plots in Figure 4.16 showed that the fluctuation of velocity profile around the centre position due to air flow through the air gap (constricted area) between the air diffuser blades with Venturi effect where air velocity was increased and pressure was reduced. The velocity profile within the room of lines 2 to 5 for 5 or 7-blade air diffuser reflected that the air velocity was within 0.3 m/s, which was slightly higher than that (0.2 m/s) of 5 or 7-blade air diffuser at 1.0 m/s inlet velocity.

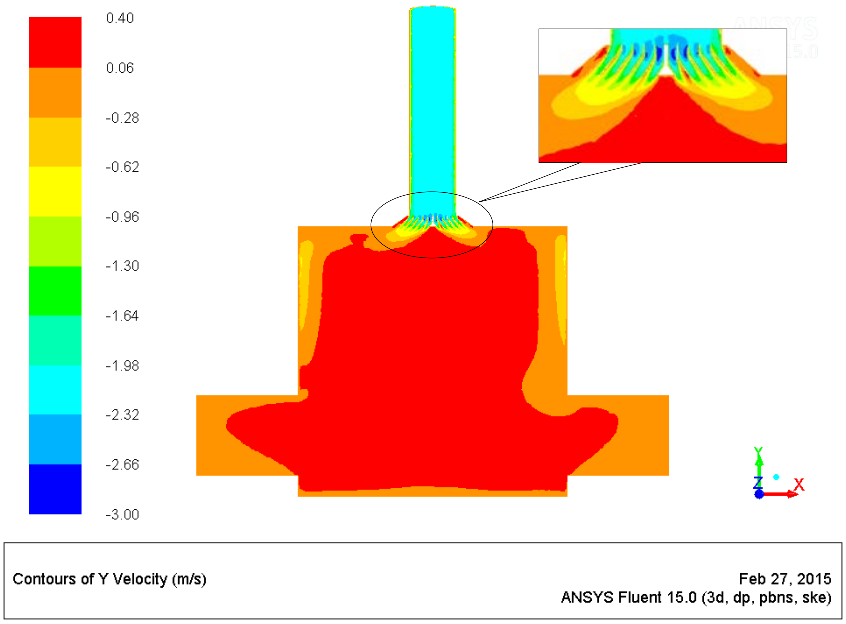

(a)

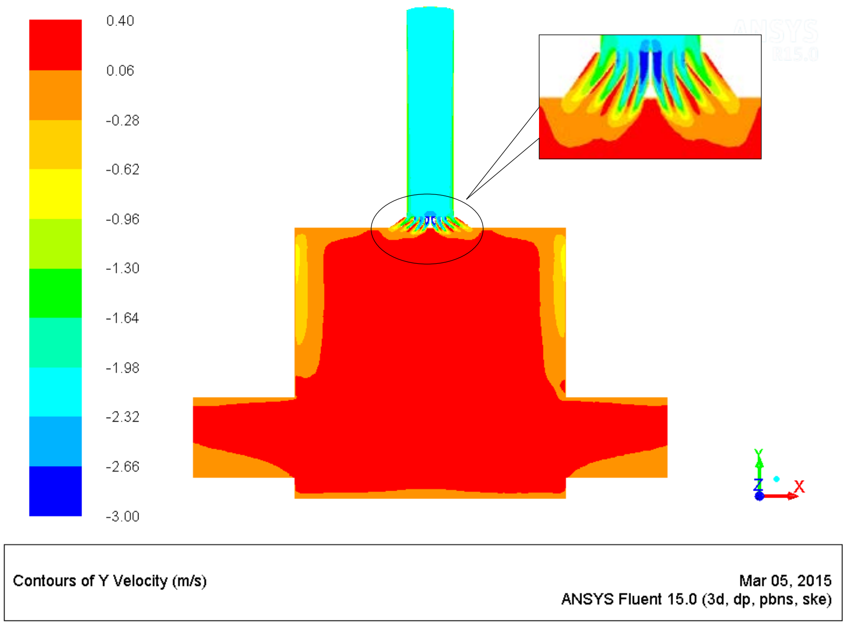

(b)

Figure 4.15: Contours of Y velocity in the room with inlet on ceiling and 2 outlets near wall bottoms at 2.0 m/s inlet velocity: (a) 7-blade, & (b) 5-blade round ceiling air diffuser

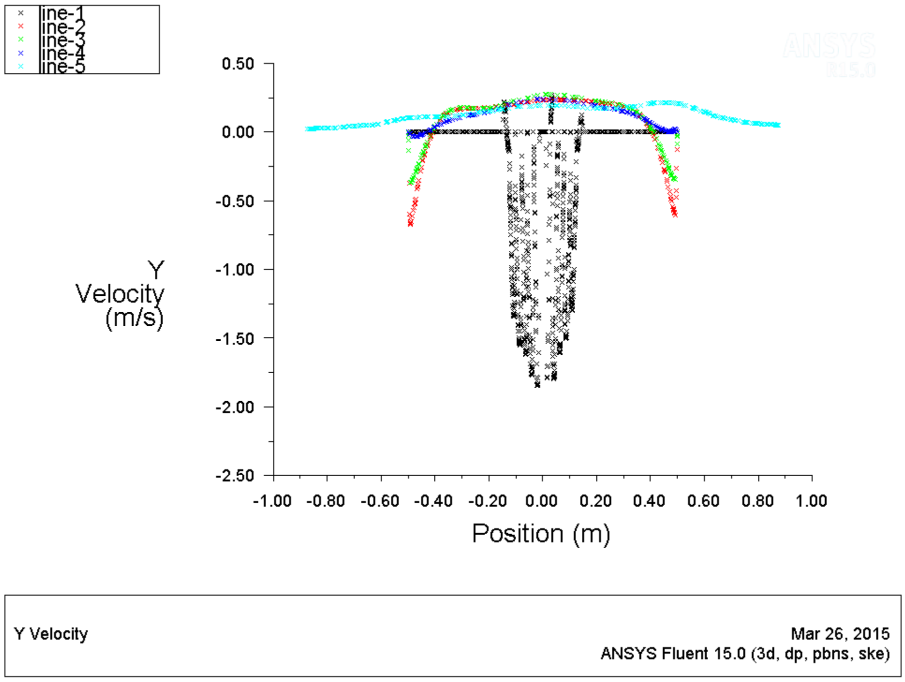

(a)

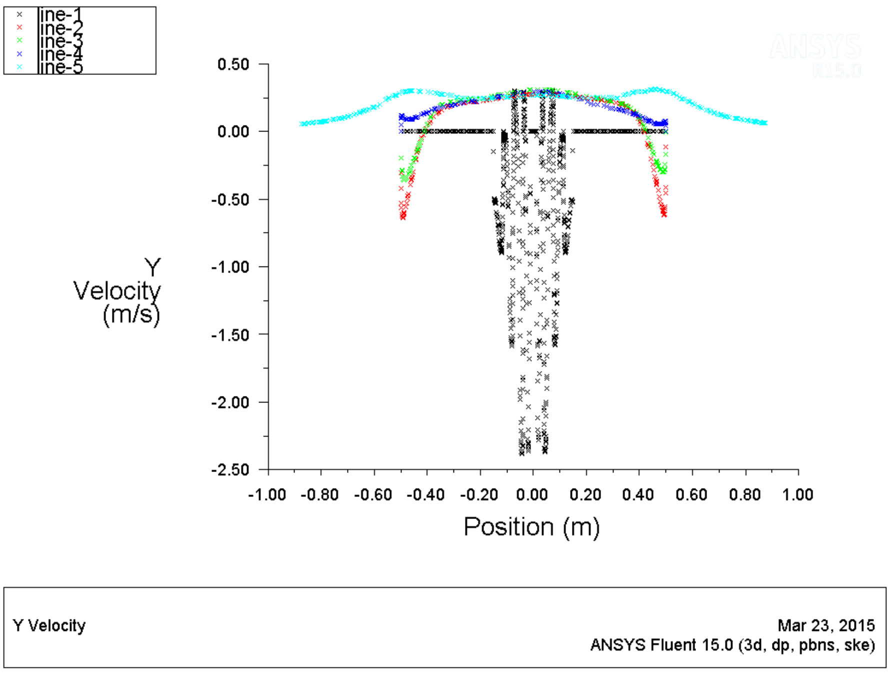

(b)

Figure 4.16: **X-Y plots of Y velocity at section lines on *x*-axis extending from the centre of the room to the edge of walls with 2 outlets near wall bottoms at 2.0 m/s inlet velocity: (a) 7-blade, & (b) 5-blade round ceiling air diffuser**

From sections (a) of Figures 4.17 and 4.18, the temperature distribution throughout the room for 7-blade/vane round ceiling air diffuser at 2.0 m/s inlet velocity (291.5 – 292.4 K) was consistent than that of 5-blade/vane round ceiling air diffuser (292.4 – 293.3 K) since the air flow via the 7-blade air diffuser was more uniform than that via 5-blade air diffuser. In addition, the 7-blade air diffuser had created slightly colder room temperature profile (291.5 – 292.4 K) within the room than that of 5-blade air diffuser (292.4 – 293.3 K), and therefore the colder air could be supplied by 7-blade air diffuser.

Meanwhile, the 5 or 7-blade round ceiling air diffuser with 2.0 m/s inlet air velocity provided lower temperature profile of 291.5 – 293.3 K within the room than that of 5 or 7-blade air diffuser with 1.0 m/s inlet velocity (292.4 – 294.2 K). It was due to air flow rate from the air diffusers with inlet velocity at 2.0 m/s is relatively higher than those of air diffusers with inlet velocity at 1.0 m/s. Therefore, the room temperature generated by the air diffuser with 2.0 m/s inlet velocity was slightly colder than that of the air diffuser with 1.0 m/s inlet velocity. A thermal discomfort will be detected at this colder room temperature since the air from air diffuser was uniformly distributed throughout the room, and the air diffuser could assist in reducing the energy consumption by air handling unit to cool the supply air.

In addition, line 1 of all the X-Y plots in Figure 4.18 reflected that the fluctuation of temperature profile around the centre position due to air flow through the air gap (constricted area) between the air diffuser blades with Venturi effect where air velocity was increased and pressure was reduced, and air velocity could affect the temperature distribution. In addition, the temperature profile within the room of lines 2 to 5 for 5 or 7-blade air diffusers showed that the room temperature was within 292 K, which was slightly lower than that (293 K) of 5 or 7-blade air diffuser at 1.0 m/s inlet velocity.

Furthermore, the temperature distribution of 5 and 7-blade air diffusers with two outlets near wall bottoms at 2.0 m/s inlet velocity was slightly consistent if compared with that of round diffuser obtained by Mohammed (2013) as illustrated in Figure 2.13 since the air flow distribution via the blades of proposed models was relatively more uniform although their inlet velocity might be similar to those diffusers established by Mohammed (2013).

The range of velocity magnitude, Y velocity and static temperature distribution within the room for round ceiling air diffuser with inlet velocity at 2.0 m/s are summarised in Table 4.3.

Table 4.3: Range of velocity magnitude, Y velocity and static temperature distribution within the room for 2.0 m/s inlet velocity

Item	Diffuser Model	
	5-blade	7-blade
Velocity Magnitude (m/s)	0 – 1.40	0 – 1.20
Y Velocity (m/s)	-0.28 – 0.40	-0.28 – 0.40
Static Temperature (K)	292.4 – 293.3	291.5 – 292.4

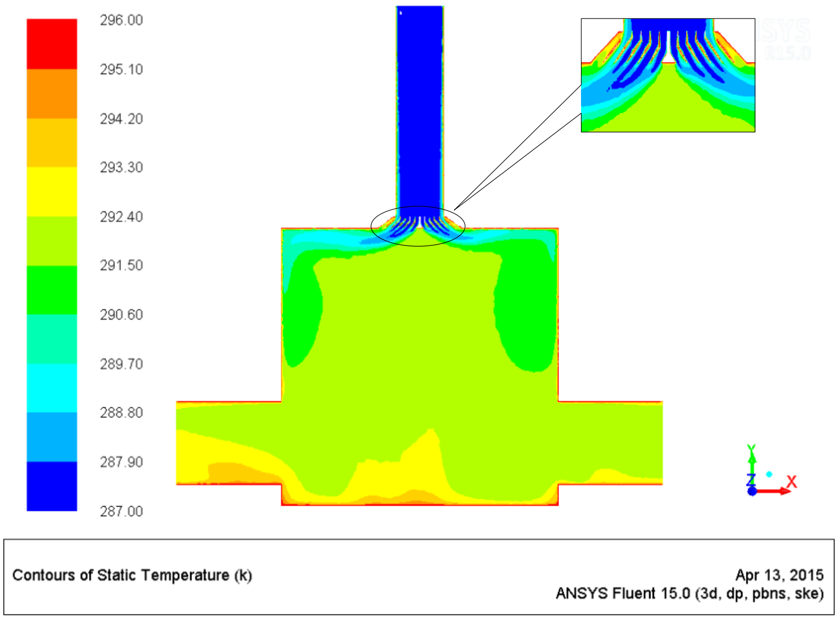

(a)

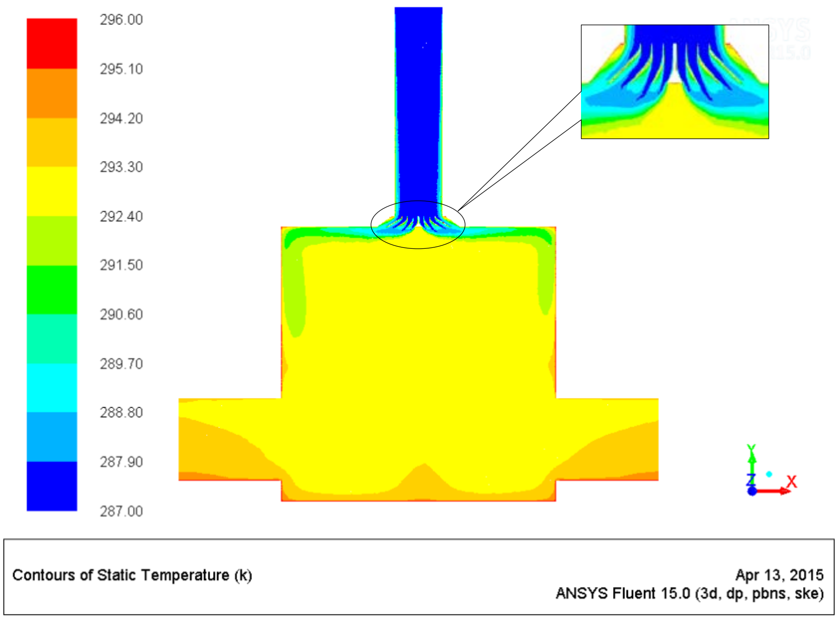

(b)

Figure 4.17: Contours of static temperature in the room with inlet on ceiling and 2 outlets near wall bottoms at 2.0 m/s inlet velocity: (a) 7-blade, & (b) 5-blade round ceiling air diffuser

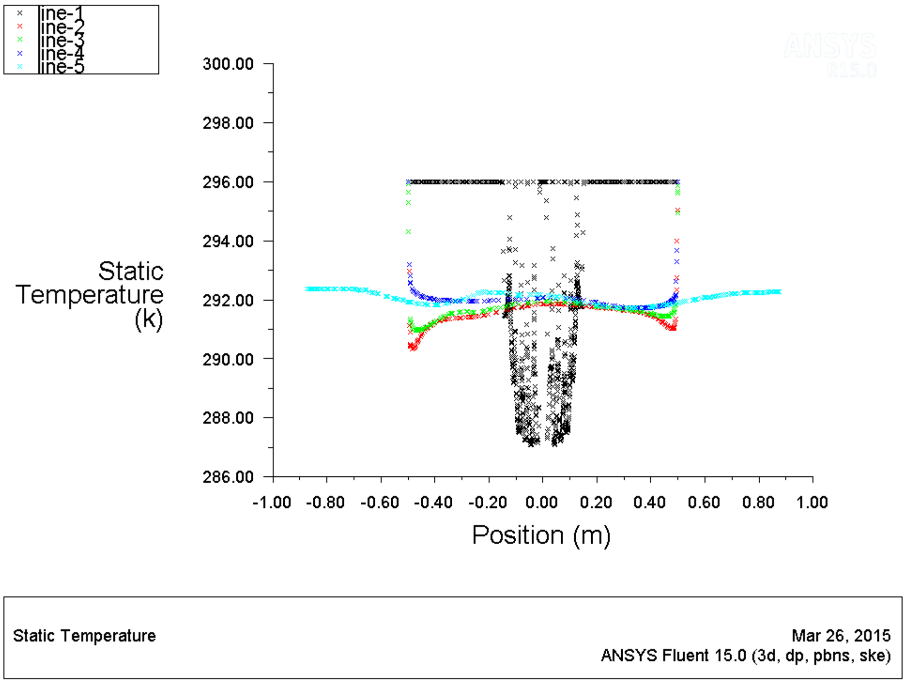

(a)

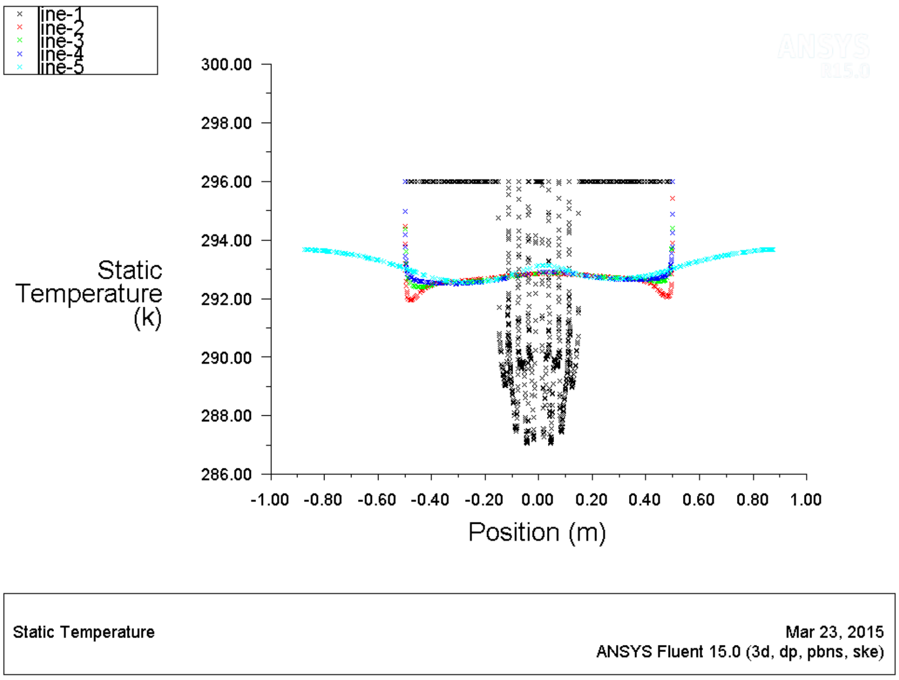

(b)

Figure 4.18: **X-Y plots of static temperature at section lines on *x*-axis extending from the centre of the room to the edge of walls with 2 outlets near wall bottoms at 2.0 m/s inlet velocity: (a) 7-blade, & (b) 5-blade round ceiling air diffuser**

4.1.4 Inlet velocity at 3.0 m/s for the round ceiling air diffuser with two outlets near bottom of walls

Based on sections (a) of Figures 4.19 and 4.20, the air flow behaviours throughout the room for 7-blade/vane round ceiling air diffuser at 3.0 m/s inlet velocity (0 – 1.0 m/s) was slightly uniform than that of 5-blade/vane round ceiling air diffuser (0 – 1.0 m/s) since the friction across the vanes of 7-blade air diffuser might be lower and the air flow through the air diffuser blade was smoother.

Meanwhile, the 5 or 7-blade round ceiling air diffuser with 3.0 m/s inlet velocity provided higher velocity profile (0 – 1.0 m/s) within the room than that of 5 or 7-blade air diffuser with 2.0 m/s inlet velocity (0 – 0.6 m/s). It was because the air flow rate from 5 or 7-blade air diffuser with 3.0 m/s inlet velocity was relatively higher than that of with 2.0 m/s inlet velocity. In addition, Coanda effect of air distribution was noticed in Figure 4.19 where the flow emerged radically and reached the wall and then directed into 90° downward, which reflected the throw of air could be longer.

In addition, line 1 of all the X-Y plots in Figure 4.20 indicated that the fluctuation of velocity profile around the centre position due to air flow through the air gap (constricted area) between the air diffuser blades with Venturi effect where air velocity was increased and pressure was reduced. Moreover, the velocity profile within the room of lines 2 to 5 for 5 or 7-blade air diffuser reflected that the air velocity ranged from 0.3 to 0.5 m/s, which was slightly higher than that (0.3 m/s) of 5 or 7-blade air diffuser at 2.0 m/s inlet velocity.

Furthermore, the air velocity distribution of 5 and 7-blade air diffusers with two outlets near wall bottoms at 3.0 m/s inlet velocity were slightly consistent if compared with that of round diffuser gained by Mohammed (2013) as observed in Figure 2.13 since the air flow distribution via the blades of proposed models was relatively more even although their inlet velocity might be similar to those diffusers established by Mohammed (2013).

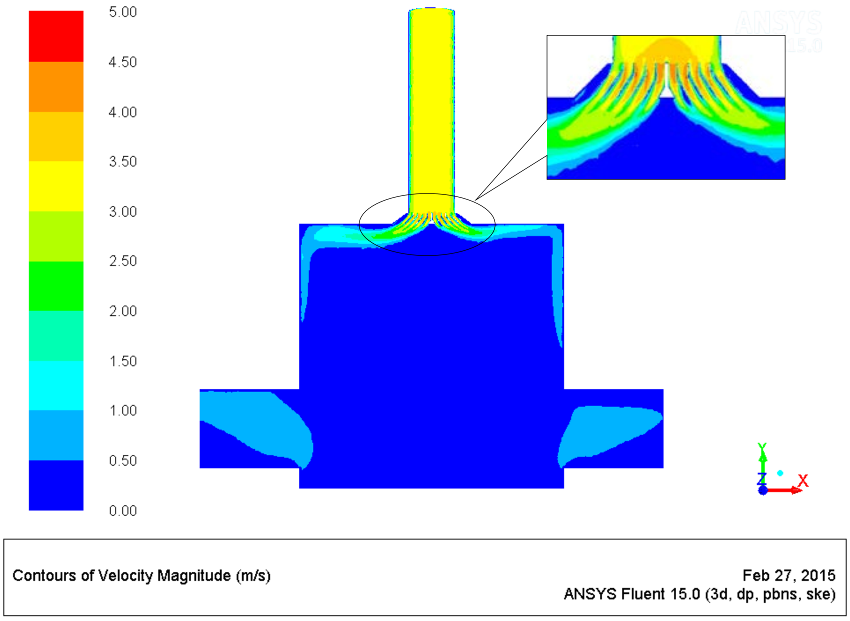

(a)

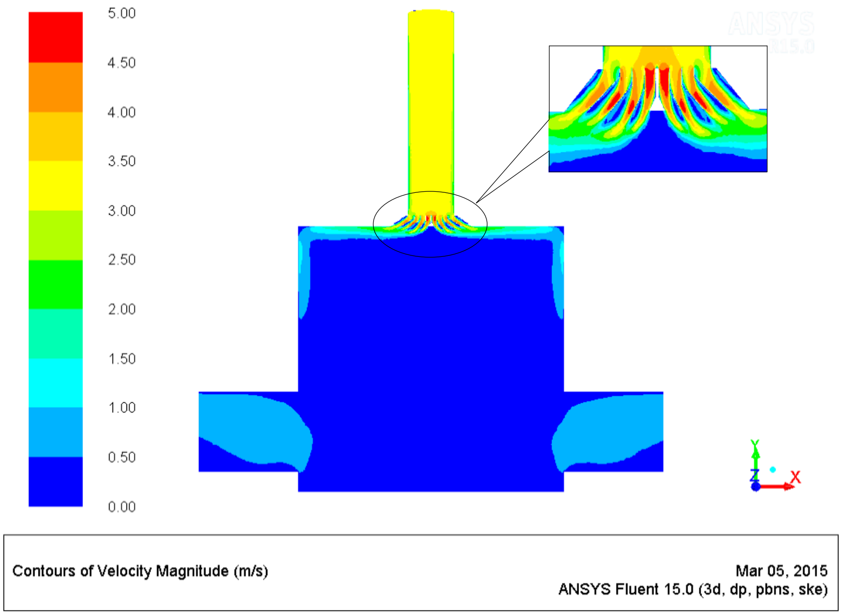

(b)

Figure 4.19: Contours of velocity magnitude in the room with inlet on ceiling and 2 outlets near wall bottoms at 3.0 m/s inlet velocity: (a) 7-blade, & (b) 5-blade round ceiling air diffuser

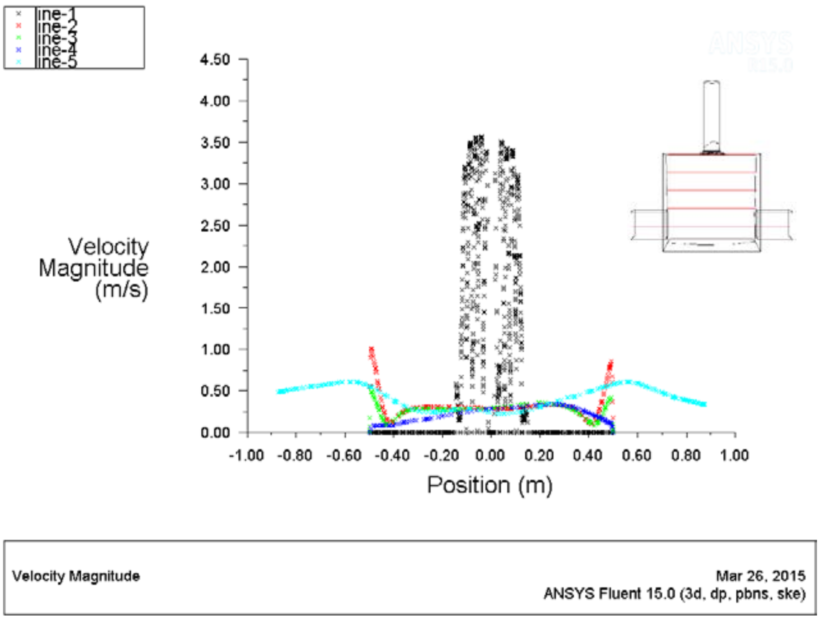

(a)

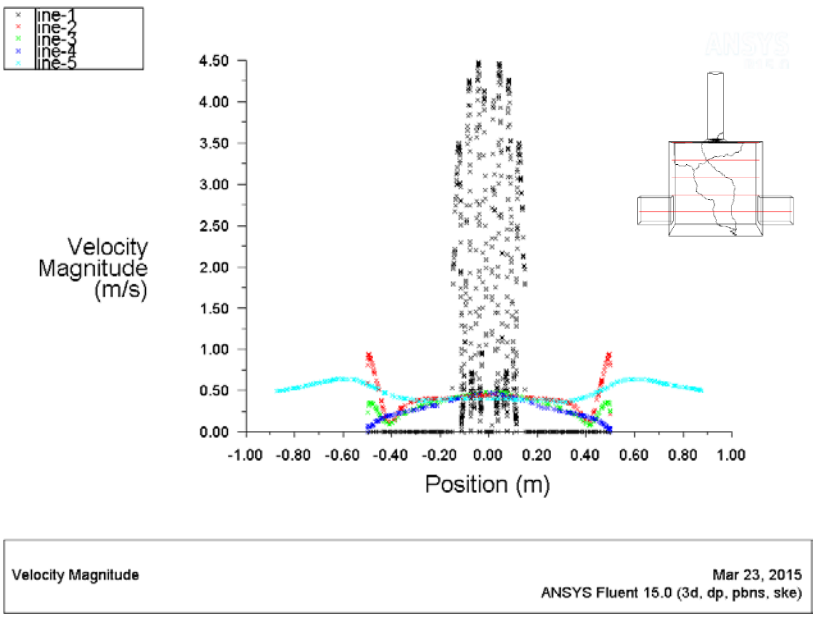

(b)

Figure 4.20: **X-Y plots of velocity magnitude at section lines (red colour line 1 to 5 depicted in small figure beside the XY plot) on *x*-axis extending from the centre of the room to the edge of walls with 2 outlets near wall bottoms at 3.0 m/s inlet velocity: (a) 7-blade, & (b) 5-blade round ceiling air diffuser**

From sections (a) of Figures 4.21 and 4.22, the air flow distribution throughout the room for 7-blade/vane round ceiling air diffuser at 3.0 m/s inlet velocity (0.09 – 0.6 m/s) was slightly consistent than that of 5-blade/vane round ceiling air diffuser (0.09 – 0.6 m/s) since the air flow via blades of 7 blade air diffuser has lesser contact on blade surface and it can flow smoother.

Meanwhile, the 5 or 7-blade round ceiling air diffuser with 3.0 m/s inlet velocity furnished higher velocity profile (0.09 – 0.6 m/s) within the room than that of 5 or 7-blade air diffuser with 2.0 m/s inlet velocity (0.06 – 0.4 m/s). It was because the air flow rate from 5 or 7-blade air diffuser with 3.0 m/s inlet velocity was relatively higher than that of 5 or 7-blade air diffuser with 2.0 m/s inlet velocity. Therefore, the air flow distribution by diffuser with 3.0 m/s inlet velocity to further end of a room was faster than that with 2.0 m/s inlet velocity. A discomfort may be encountered, although the air from the air diffuser was uniformly distributed throughout the room.

In addition, line 1 of all the X-Y plots in Figure 4.22 showed that the fluctuation of velocity profile around the centre position due to air flow through the air gap (constricted area) between the air diffuser blades with Venturi effect where air velocity was increased and pressure was reduced. The velocity profile within the room of lines 2 to 5 for 5 or 7-blade air diffuser reflected that the air velocity was within 0.3 – 0.5 m/s, which was slightly higher than that (0.3 m/s) of 5 or 7-blade air diffuser at 2.0 m/s inlet velocity.

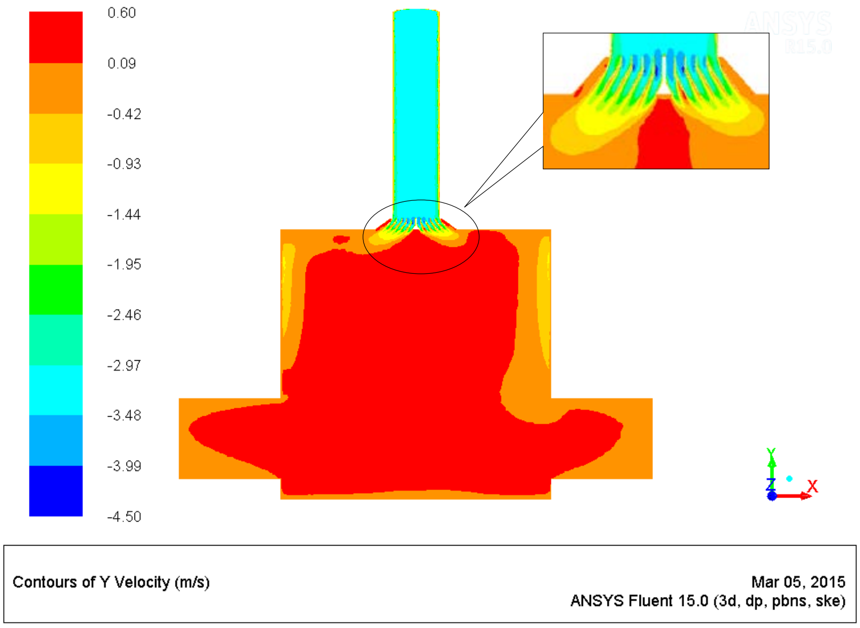

(a)

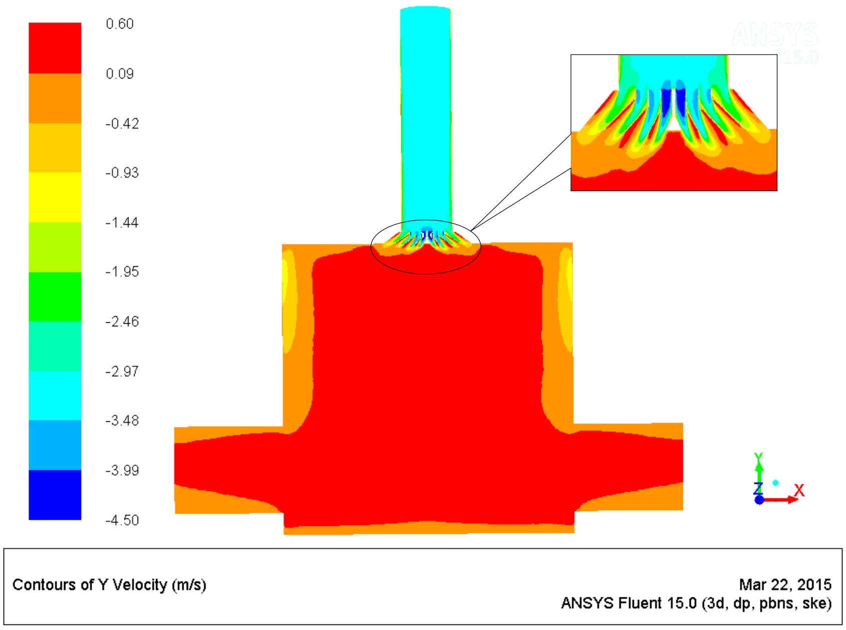

(b)

Figure 4.21: **Contours of Y velocity in the room with inlet on ceiling and 2 outlets near wall bottoms at 3.0 m/s inlet velocity: (a) 7-blade, & (b) 5-blade round ceiling air diffuser**

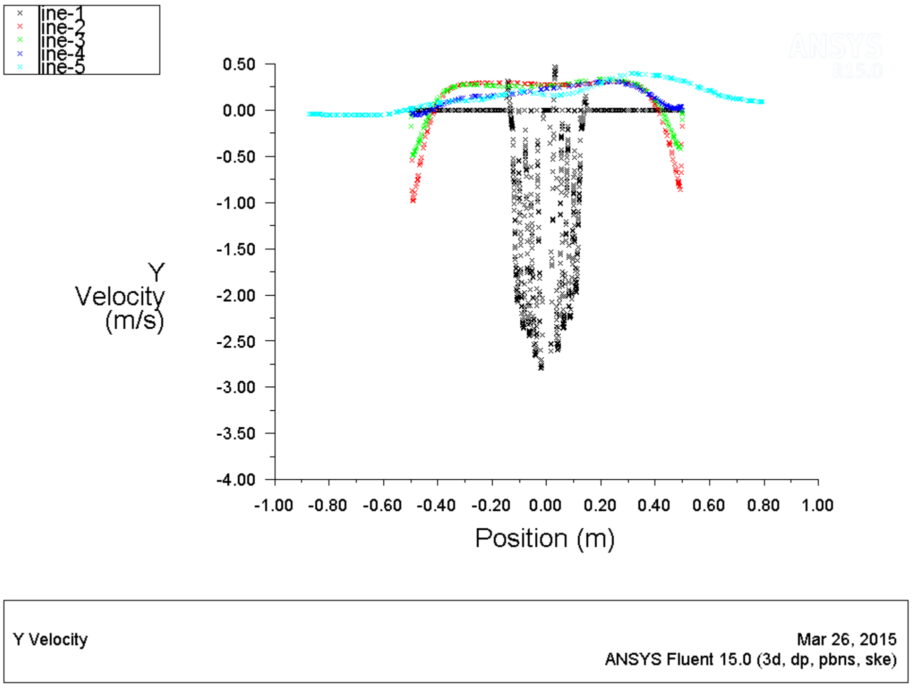

(a)

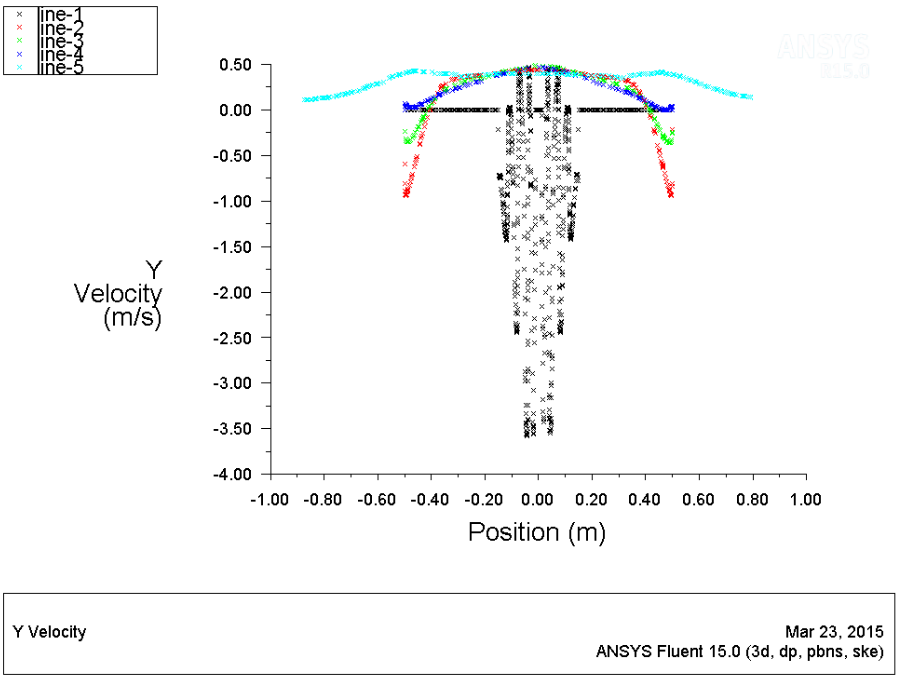

(b)

Figure 4.22: X-Y plots of Y velocity at section lines on *x*-axis extending from the centre of the room to the edge of walls with 2 outlets near wall bottoms at 3.0 m/s inlet velocity: (a) 7-blade, & (b) 5-blade round ceiling air diffuser

Based on sections (a) of Figures 4.23 and 4.24, the temperature distribution throughout the room for 7-blade/vane round ceiling air diffuser at 3.0 m/s inlet velocity (290.6 – 291.5 K) was more uniform than that of 5-blade/vane round ceiling air diffuser (291.5 – 293.3) since the air flow via the vanes of 7-blade air diffuser was more consistent than that of 5-blade air diffuser. Besides, the 7-blade air diffuser could provide slightly cooler air in a room (290.6 – 291.5 K) than that of 5-blade air diffuser (291.5 – 293.3).

Meanwhile, the 5 or 7-blade round ceiling air diffuser with 3.0 m/s inlet velocity furnished relatively more lower temperature profile (290.5 – 291.6 K) within the room than that of 5 or 7-blade air diffuser with 2.0 m/s inlet velocity (291.6 – 292.7 K). It was because air flow rate from 7-blade air diffuser with 3.0 m/s inlet velocity was relatively higher than that with 2.0 m/s inlet velocity. Thus, the room temperature generated by the air diffuser with 3.0 m/s inlet velocity was relatively colder than that with 2.0 m/s inlet velocity. The occupants around the air diffuser might feel uncomfortable at this colder room temperature although the air from diffuser was uniformly distributed throughout the room. However, the air diffuser is believed to be able to assist in reducing the energy consumption by air handling unit to cool the supply air volume.

In addition, line 1 of all the X-Y plots in Figure 4.24 showed that the fluctuation of temperature profile around the centre position due to air flow through the air gap (constricted area) between the air diffuser blades with Venturi effect where air velocity was increased and pressure was reduced, and air velocity could affect the temperature distribution. Besides, the temperature profile within the room of lines 2 to 5 for 5 or 7-blade air diffusers showed that the room temperature was within 291 - 292 K, which was slightly lower than that (292 K) of 5 or 7-blade air diffuser at 2.0 m/s inlet velocity.

Furthermore, the temperature distribution of 5 and 7-blade air diffusers with two outlets near wall bottoms at 3.0 m/s inlet velocity was slightly consistent if compared with that of round diffuser gained by Mohammed (2013) as found in Figure 2.13 since the air flow distribution via the blades of proposed models are relatively more uniform distributed although their inlet velocity might be similar to those diffusers established by Mohammed (2013).

The range of velocity magnitude, Y velocity and static temperature distribution within the room for round ceiling air diffuser with inlet velocity at 3.0 m/s are summarised in Table 4.4.

Table 4.4: Range of velocity magnitude, Y velocity and static temperature distribution within the room for 3.0 m/s inlet velocity

Item	**Diffuser Model**	
	5-blade	**7-blade**
Velocity Magnitude (m/s)	0 – 2.00	0 – 2.00
Y Velocity (m/s)	-0.42 – 0.60	-0.42 – 0.60
Static Temperature (K)	291.5 – 293.3	290.6 – 291.5

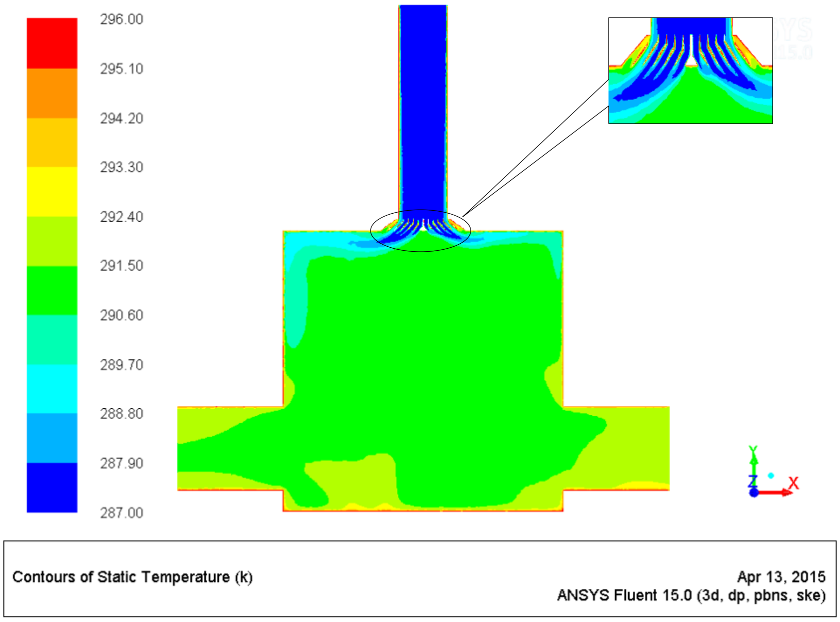

(a)

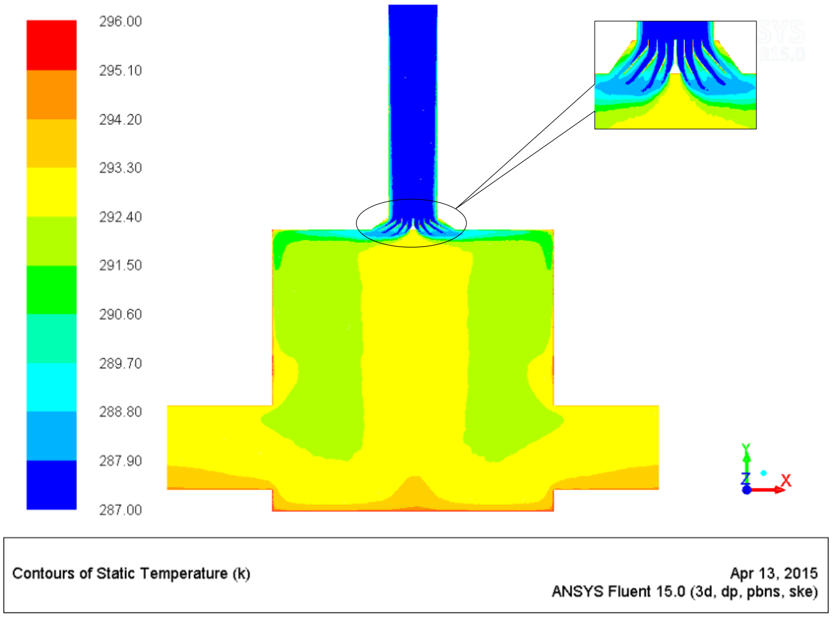

(b)

Figure 4.23: Contours of static temperature in the room with inlet on ceiling and 2 outlets near wall bottoms at 3.0 m/s inlet velocity: (a) 7-blade, & (b) 5-blade round ceiling air diffuser

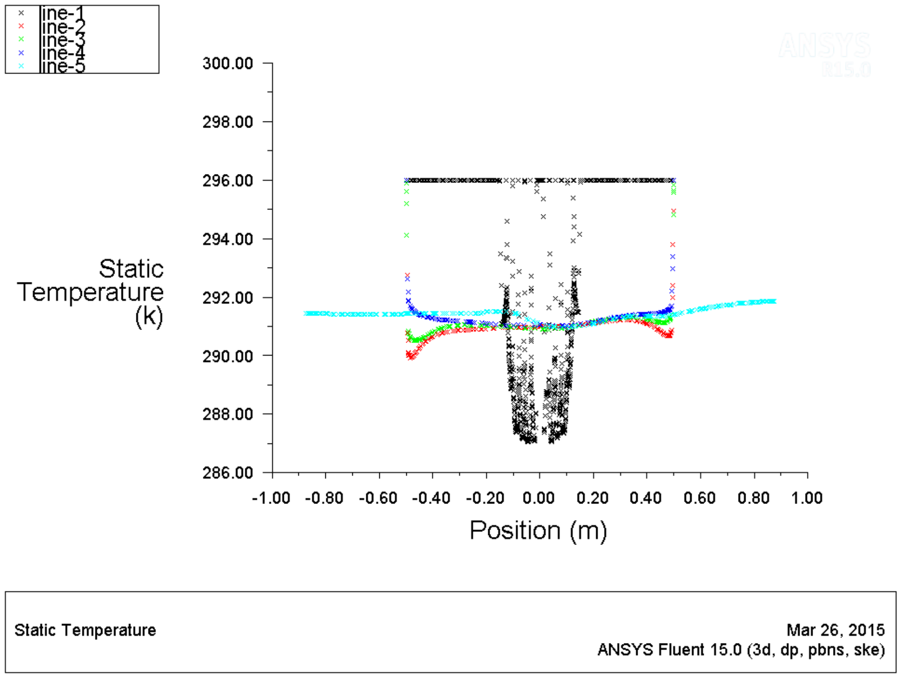

(a)

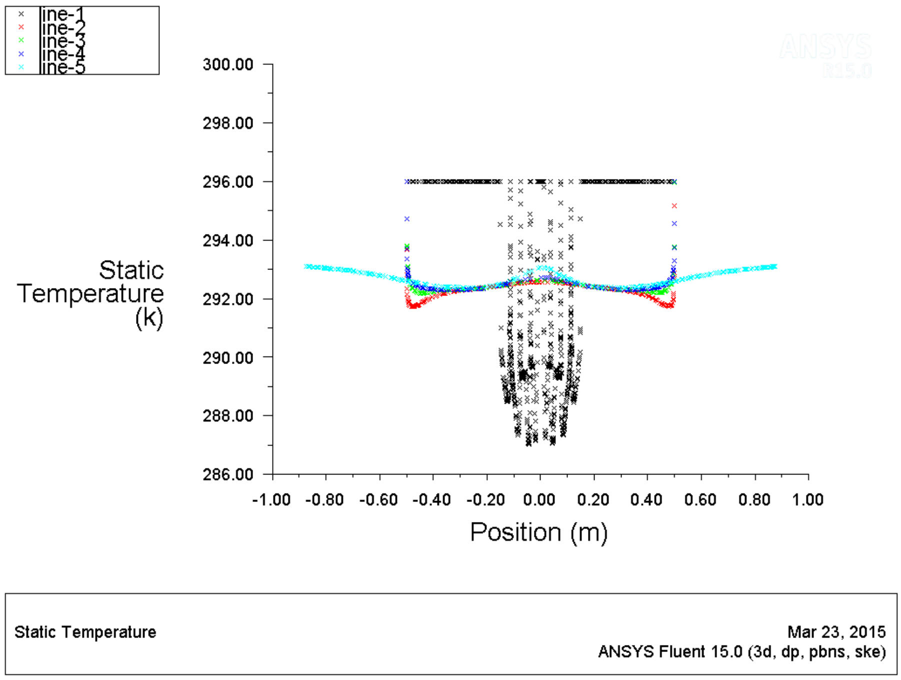

(b)

Figure 4.24: X-Y plots of static temperature at section lines on *x*-axis extending from the centre of the room to the edge of walls with 2 outlets near wall bottoms at 3.0 m/s inlet velocity: (a) 7-blade, & (b) 5-blade round ceiling air diffuser

4.1.5 Inlet temperature of 285 K for the round ceiling air diffuser with two outlets near bottom of walls

The study of various inlet air temperatures for the round ceiling air diffuser was focused on the 5 and 7-blade air diffusers with two outlets near wall bottoms since these two models would be able to provide consistent air flow behaviours and temperature distribution among the 4 types of diffuser model as discussed in the previous sections.

The temperature distribution of round ceiling air diffusers in room with inlet on ceiling and 2 outlets near bottom of walls was observed for inlet air temperature of 285 K (12 °C) and 289 K (16 °C), while inlet air velocity was maintained at 1.0 m/s as illustrated in Figures 4.25 to 4.28. The aforesaid temperature are sometimes applied for inlet air temperature for supply air diffusers in industry besides 287 K (14 °C), whereas 1.0 m/s inlet air velocity is optimal velocity for supply air diffusers.

From Figures 4.25 and 4.26, the 7-blade round ceiling air diffuser with inlet air temperature of 285 K provided lower temperature profile (291.6 – 292.7 K) within the room than that of 5-blade air diffuser (292.7 – 293.8 K). This temperature profile was also below the temperature profile of 7-blade air diffuser at inlet air temperature of 287 K (292.7 – 293.8 K) since air flow via the vanes of 7-blade air diffuser was consistent and associated with lower temperature. In addition, the velocity magnitude and Y velocity for current case were similar to those of others 5 or 7-blade air diffuser at 1.0 m/s inlet velocity although their inlet temperatures were different. Therefore, the inlet air flow velocity would play a major role on affecting the air condition in a room.

If compared with the average room temperature of 7-blade air diffuser with 3.0 m/s inlet velocity and 287 K inlet temperature, the average temperature of current case was not as low as that of 7-blade air diffuser with 3.0 m/s inlet velocity since the latter air diffuser had higher air flow rate. Therefore, those occupants around the 7-blade air diffuser of current case might not feel uncomfortable. Meanwhile, the average room temperature of 5-blade air diffuser of current case did not exceed recommended room temperature of 296 K, and hence the occupants around the air diffuser might not feel warm.

In addition, line 1 of all the X-Y plots in Figure 4.26 showed that the fluctuation of temperature profile around the centre position due to air flow through the air gap (constricted area) between the air diffuser blades with Venturi effect where air velocity was increased and pressure was reduced, and air velocity could affect the temperature distribution. Furthermore, the temperature profile within the room of lines 2 to 5 for 5 or 7-blade air diffusers showed that the room temperature was within 291 – 292 K, which was slightly lower than that (292 – 293 K) of 5 or 7-blade air diffuser at 287 K inlet temperature.

Furthermore, the temperature distribution of 5 and 7-blade air diffusers with two outlets near wall bottoms at 285 K inlet temperature was slightly consistent if compared with the temperature distribution of round diffuser achieved by Mohammed (2013) as expressed in Figure 2.13 since the air flow distribution via the blades of the proposed diffusers was relatively more uniform although their inlet temperature was much lower than that of round diffuser established by Mohammed (2013).

The range of velocity magnitude, Y velocity and static temperature distribution within the room for round ceiling air diffuser with 285 K inlet air temperature are summarised in Table 4.5.

Table 4.5: Range of velocity magnitude, Y velocity and static temperature distribution within room for 285 K inlet temperature

Item	Diffuser Model	
	5-blade	7-blade
Velocity Magnitude (m/s)	0 – 0.60	0 – 0.60
Y Velocity (m/s)	-0.14 – 0.20	-0.14 – 0.20
Static Temperature (K)	291.6 – 293.8	291.6 – 293.8

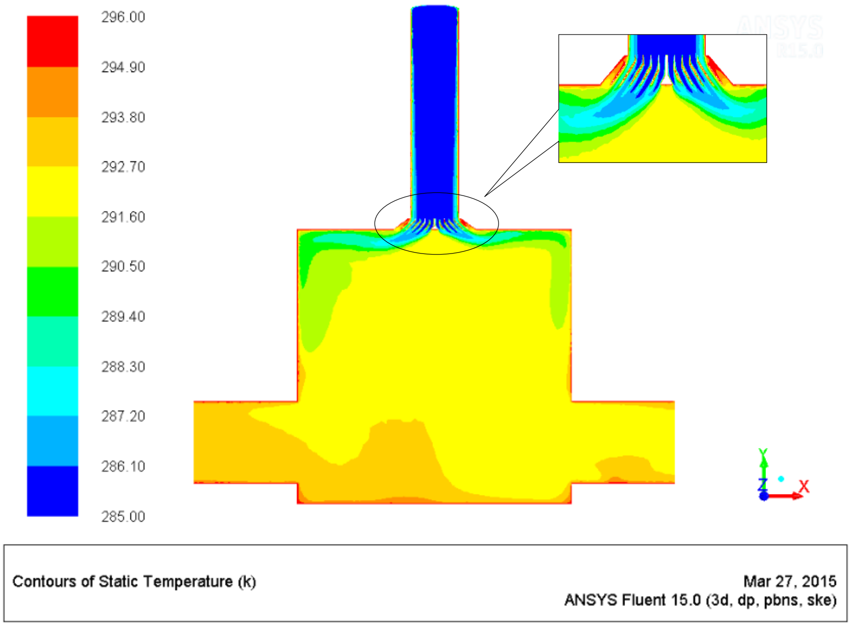

(a)

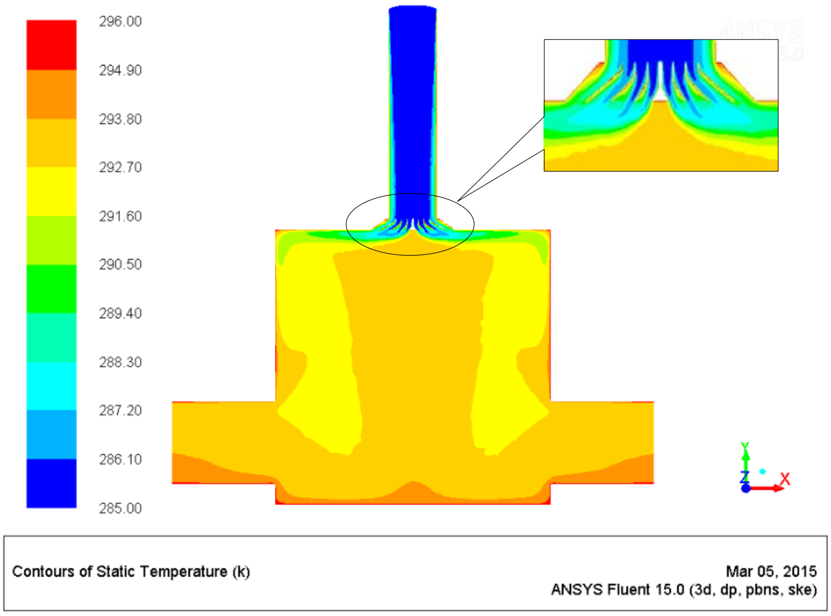

(b)

Figure 4.25: Contours of static temperature in the room with inlet on ceiling and 2 outlets near wall bottoms at 285 K inlet temperature: (a) 7-blade, & (b) 5-blade round ceiling air diffuser

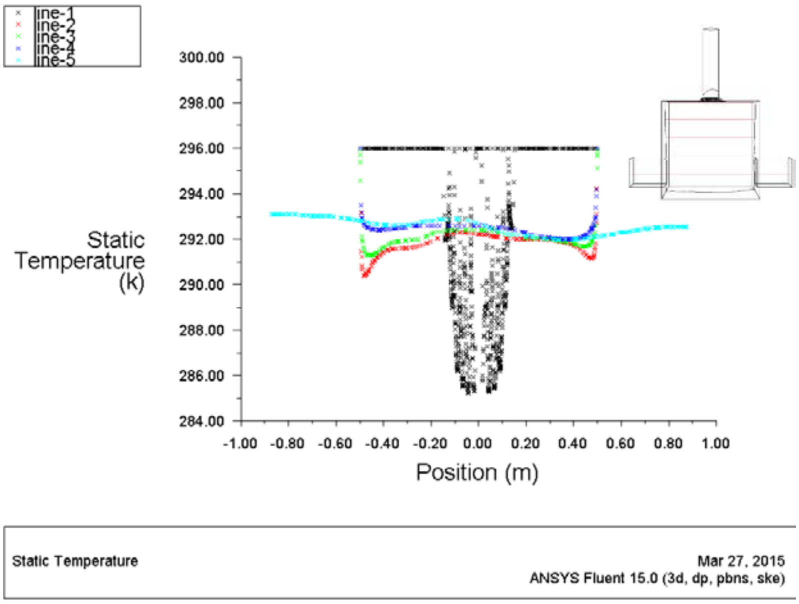

(a)

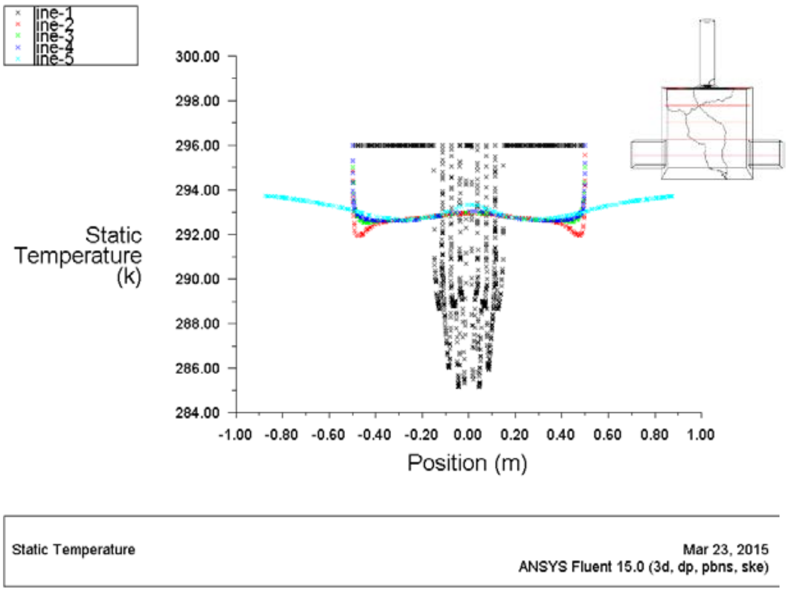

(b)

Figure 4.26: **X-Y plots of static temperature at section lines (red colour line 1 to 5 depicted in small figure beside the XY plot) on *x*-axis extending from the centre of the room to the edge of walls with 2 outlets near wall bottoms at 285 K inlet temperature: (a) 7-blade, & (b) 5-blade round ceiling air diffuser**

4.1.6 Inlet temperature of 289 K for the round ceiling air diffuser with two outlets near bottom of walls

Based on Figures 4.27 and 4.28, the 7-blade round ceiling air diffuser with inlet air temperature of 289 K produced lower temperature profile (293.2 – 293.9 K) within the room than that of 5-blade air diffuser (293.9 – 294.6 K) since air flow via the vanes of 7-blade air diffuser was consistent and associated with lower temperature. In addition, the velocity magnitude and Y velocity for current case were similar to those of other 5 or 7-blade air diffuser at 1.0 m/s inlet velocity, although their inlet temperatures were different. Therefore, the inlet air flow velocity could significantly affect the air condition in a room.

The average room temperature (293.2 – 293.9 K) generated by 7-blade air diffuser with inlet air temperature of 289 K was higher than that of 7-blade air diffuser with inlet air temperature of 287 K (292.4 – 293.3 K) in which the current case led to higher room temperature condition. Therefore, a higher temperature would be detected in the room. It was similar to the average room temperature of 5-blade air diffuser of current case (293.9 – 294.6 K), where the occupants around the air diffuser might feel warmer.

In addition, line 1 of all the X-Y plots in Figure 4.28 showed that the fluctuation of temperature profile around the centre position due to air flow through the air gap (constricted area) between the air diffuser blades with Venturi effect where air velocity was increased and pressure was reduced, and air velocity could affect the temperature distribution. In addition, the temperature profile within the room of lines 2 to 5 for 5 or 7-blade air diffusers showed that the room temperature was within 293 – 294 K, which was slightly higher than that (292 – 293 K) of 5 or 7-blade air diffuser at 287 K inlet temperature.

Furthermore, the temperature distribution of 5 and 7-blade air diffusers with two outlets near wall bottoms at 289 K inlet temperature were slightly consistent if compared with that of round diffuser obtained by Mohammed (2013) as revealed in Figure 2.13 since the air flow distribution via the blades of the proposed diffusers was relatively more uniform although their inlet temperature was lower than that of round diffuser established by Mohammed (2013).

The range of velocity magnitude, Y velocity and static temperature distribution within the room for round ceiling air diffuser with 289 K inlet air temperature are summarised in Table 4.6.

Table 4.6: Range of velocity magnitude, Y velocity and static temperature distribution within the room for 289 K inlet temperature

Item	Diffuser Model	
	5-blade	7-blade
Velocity Magnitude (m/s)	0 – 0.60	0 – 0.60
Y Velocity (m/s)	-0.14 – 0.20	-0.14 – 0.20
Static Temperature (K)	293.9 – 294.6	293.2 – 293.9

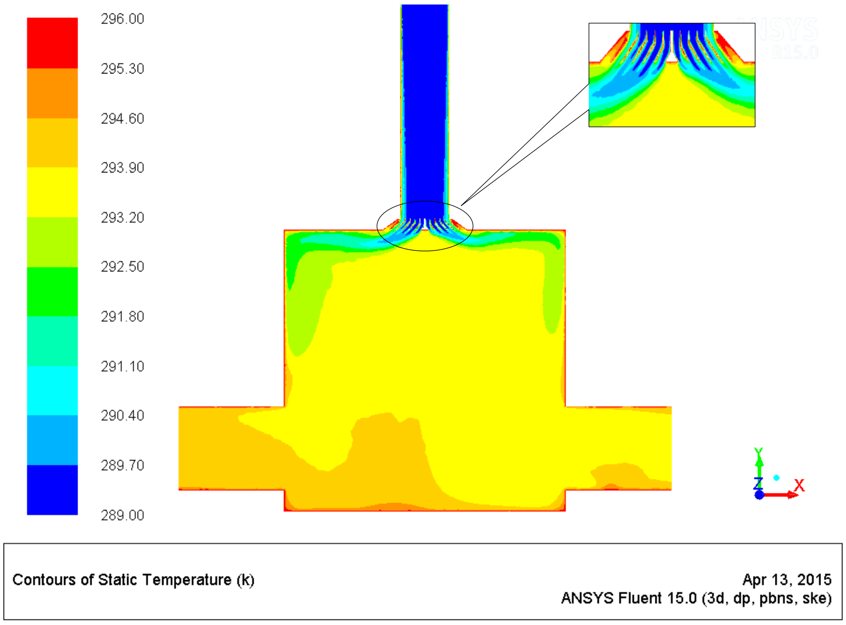

(a)

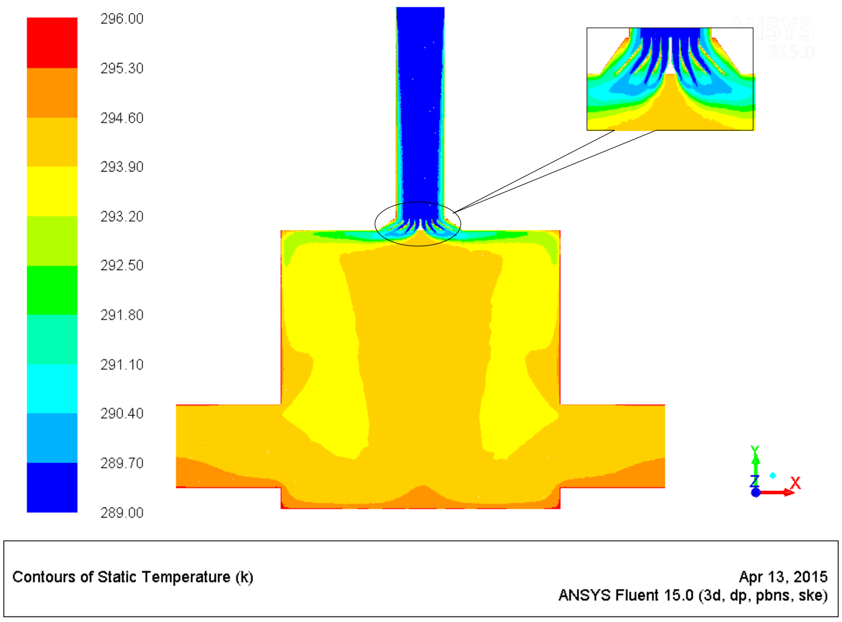

(b)

Figure 4.27: Contours of static temperature in the room with inlet on ceiling and 2 outlets near wall bottoms at 289 K inlet temperature: (a) 7-blade, & (b) 5-blade round ceiling air diffuser

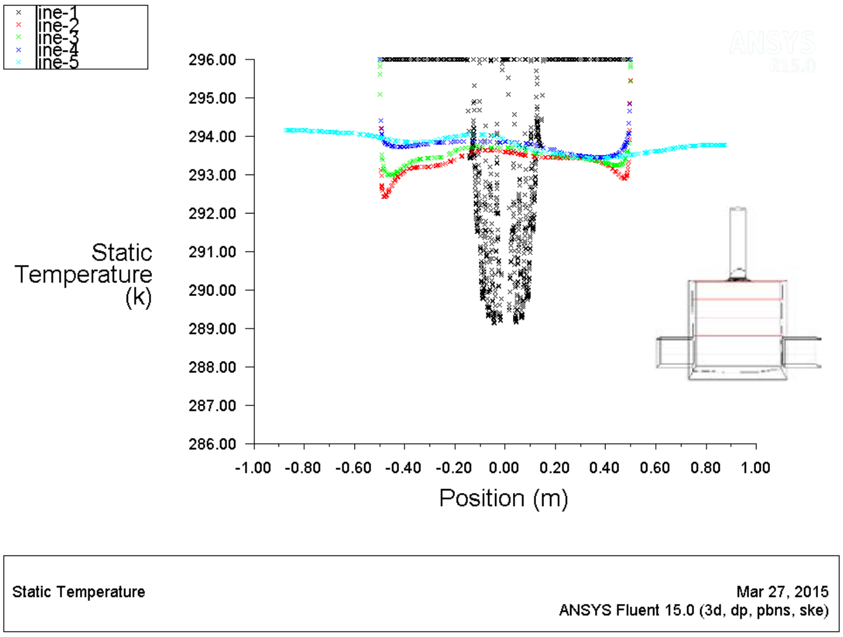

(a)

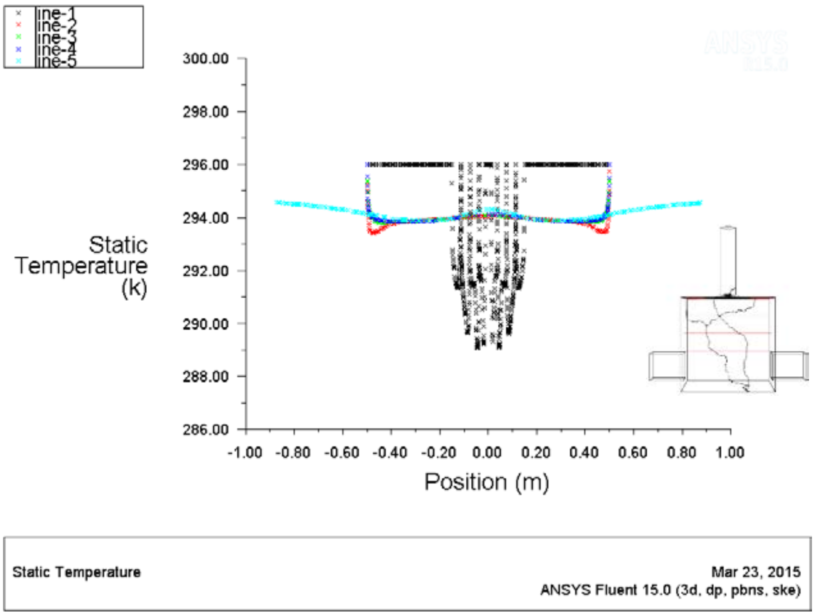

(b)

Figure 4.28: **X-Y plots of static temperature at section lines (red colour line 1 to 5 depicted in small figure beside the XY plot) on *x*-axis extending from the centre of the room to the edge of walls with 2 outlets near wall bottoms at 289 K inlet temperature: (a) 7-blade, & (b) 5-blade round ceiling air diffuser**

4.1.7 The round ceiling air diffuser with one outlet near wall bottom

The air flow behaviours and temperature distribution of round ceiling air diffusers in room with inlet on ceiling and one outlet near wall bottom for inlet velocity at 1.0 m/s and, inlet temperature of 287 K are revealed in Figures 4.29 to 4.34.

Based on sections (a) of Figures 4.29 and 4.30, the 4-blade/vane round ceiling air diffuser illustrated that the air flow distribution was not uniform throughout the room volume as most of the distributed air was concentrated around the central span of the room. It might be due to high volumetric flow rate or static pressure around the central core blade where the air tended to release from the air diffuser at a shorter distance. The occupants nearby the air diffuser might not feel comfortable due to higher air flow toward their body continuously.

From sections (b) of Figures 4.29 and 4.30, the air flow distribution from the 5-blade/vane round ceiling air diffuser was relatively more uniform (0 – 0.3 m/s) throughout the room volume than that of 4-blade/vane round ceiling air diffuser (0 – 0.6 m/s). They did not display any concentration of air distribution around the middle spot of the room volume, and Coanda effect of air distribution was noticed where the flow emerged radically and approached the wall and then turned into 90° downward, which implied the throw of air could be longer as shown in Figures 4.29 (b). In addition, those occupants around the air diffuser might feel comfortable as the air from diffuser was evenly distributed throughout the room.

Although the CFD results of sections (c) of Figures 4.29 and 4.30 showed that the air flow distribution from the 5-blade round ceiling air diffuser with an average blade angle of 30° was similar to that of those 5-blade round ceiling air diffuser with an average blade angle of 40° in sections (b) of Figures 4.29 to 4.30, the air diffuser with 40° blade angle exhibited slightly consistent air flow (0 – 0.3 m/s) than that (0 – 0.3 m/s) of diffusers with 30° blade angle since air flow via the air diffuser with 40° blade angle had less direct impact with the air diffuser blades, and was able to flow smoothly if compared with diffuser of 30° blade angle. The air flow from 5-blade round ceiling air diffuser with 30° blade angle was relatively uniform distributed throughout the room, leading to a more consistent velocity profile (0 – 0.3 m/s) within the room than that of 4-blade air diffuser (0 – 0.6 m/s) since it provided similar effect if compared to that of 5-blade air diffuser with 40° blade angle. A better thermal comfort will be experienced as the air from diffuser is uniformly distributed throughout the room without high flow concentration around the air diffuser.

The CFD results of sections (d) of Figures 4.29 and 4.30 for 7-blade/vane round ceiling air diffuser expressed that the air flow distribution (0 – 0.3 m/s) was slightly consistent than that of those of the 4 (0 – 0.6 m/s) or 5 (0 – 0.3 m/s) blades round ceiling air diffusers since air flow via the 7-blade air diffuser was relatively more uniform than that via 4 or 5-blade air diffuser. Coanda effect of air distribution was observed where the flow emerged radically and reached the wall and then directed into 90° downward, which revealed the throw of air could be longer in Figures 4.29 (d). The occupants nearby the air diffuser might not feel uncomfortable as the air from diffuser was uniformly distributed throughout the room without high flow concentration around the air diffuser.

In addition, line 1 of all the X-Y plots in Figure 4.30 revealed that the fluctuation of velocity profile around the centre position due to air flow through the air gap (constricted area) between the air diffuser blades with Venturi effect where air velocity was increased and pressure was reduced. The velocity profile within the room of lines 2 to 5 for 5 or 7-blade air diffuser reflected that the air velocity was within 0.1 m/s, while velocity profile within the room of lines 2 to 5 for 4-blade air diffuser indicated air velocity was up to 0.6 m/s around centre position due to uneven air distribution.

Furthermore, the air flow behaviours of 5 and 7-blade air diffusers with one outlet near wall bottom was slightly consistent if compared with that of round diffuser gained by other researcher as illustrated in Figure 2.13 since the air flow via the blades of proposed diffusers was relatively more uniform distributed, and less contact between the air flow and blade surfaces.

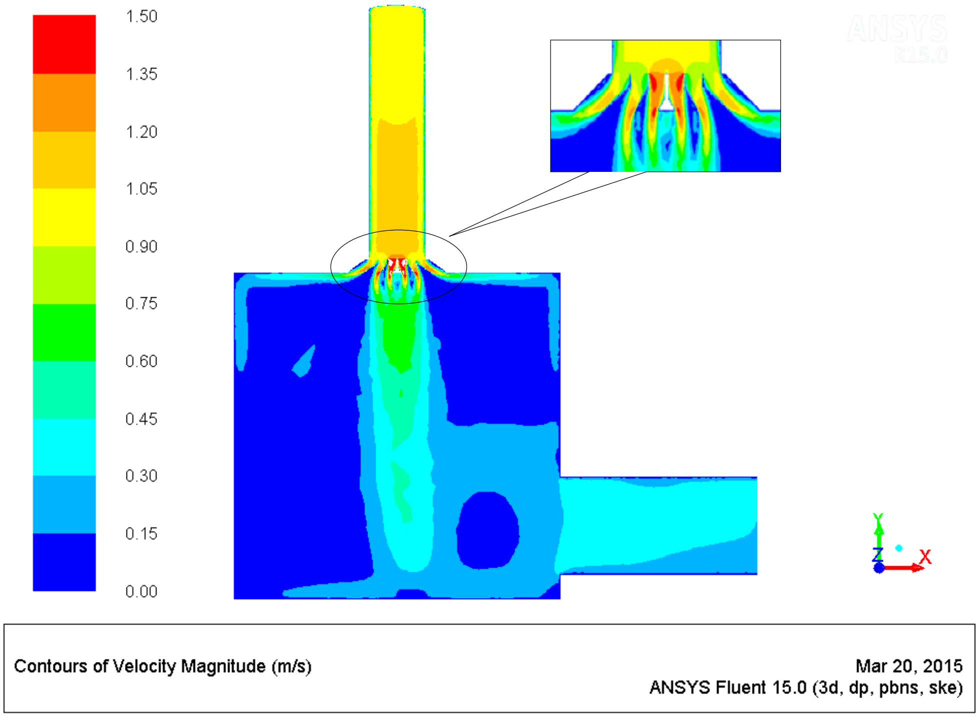
1.50
1.35
1.20
1.05
0.90
0.75
0.60
0.45
0.30
0.15
0.00
Y
Z
X
Contours of Velocity Magnitude (m/s)
Mar 20, 2015
ANSYS Fluent 15.0 (3d, dp, pbns, ske)

(a)

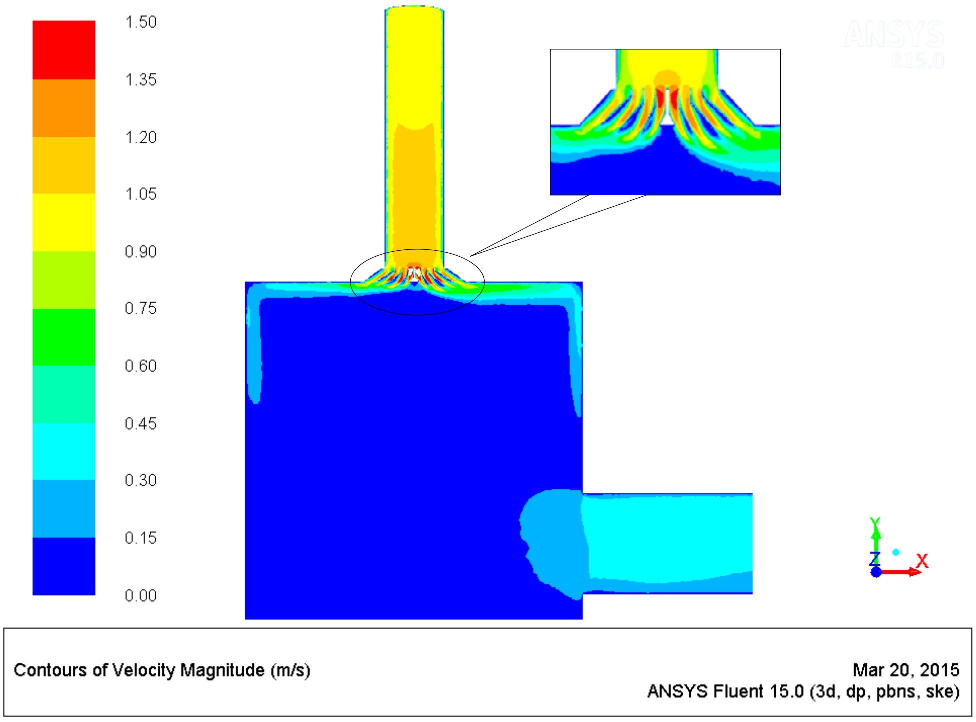
1.50
1.35
1.20
1.05
0.90
0.75
0.60
0.45
0.30
0.15
0.00
Y
Z
X
Contours of Velocity Magnitude (m/s)
Mar 20, 2015
ANSYS Fluent 15.0 (3d, dp, pbns, ske)

(b)

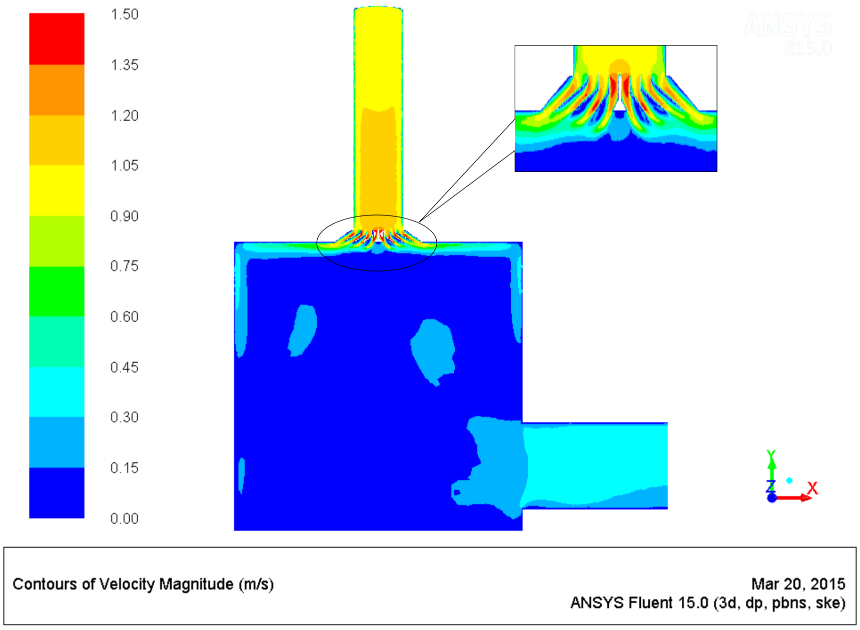

(c)

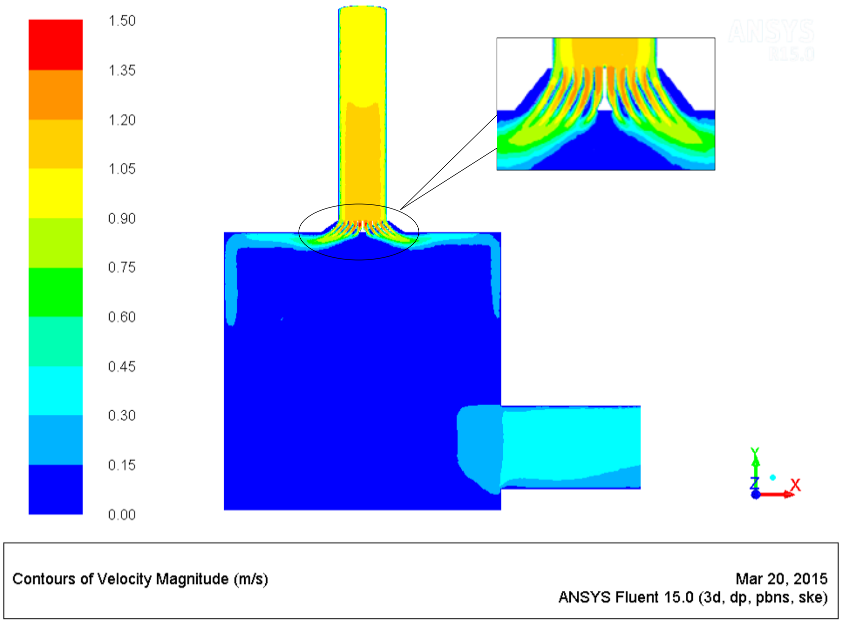

(d)

Figure 4.29: Contours of velocity magnitude in the room with inlet on ceiling and 1 outlet near wall bottom: (a) 4-blade, (b) 5-blade, (c) 5-blade with blade angle change, & (d) 7-blade round ceiling air diffuser

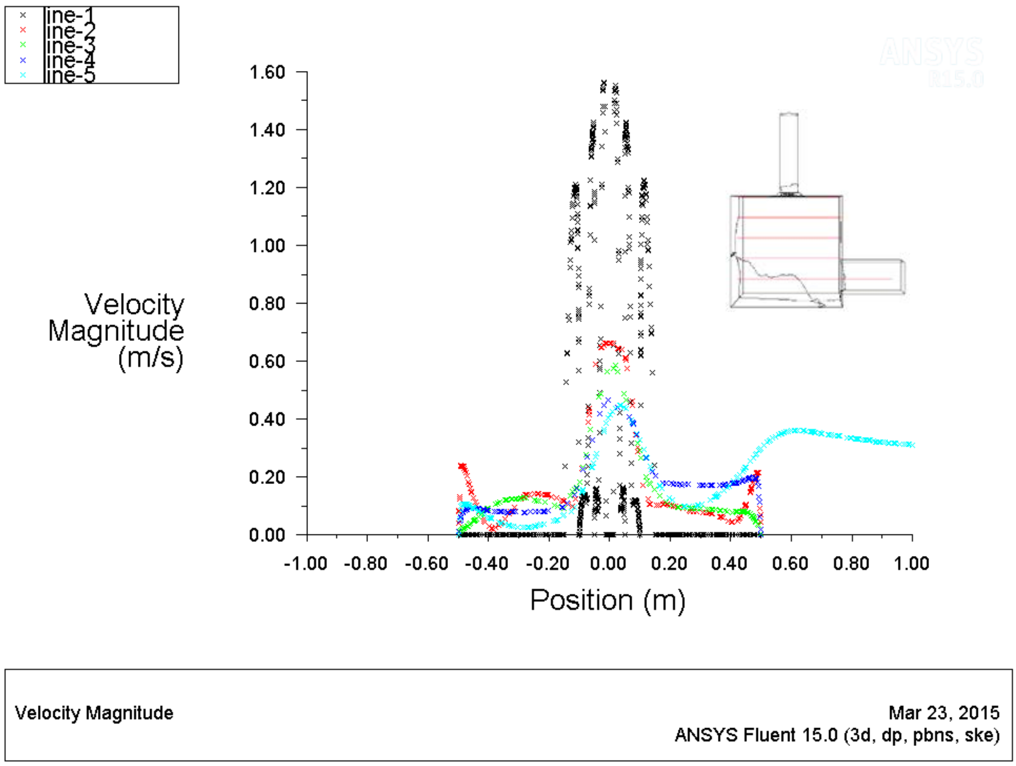
line-1
line-2
line-3
line-4
line-5
Velocity Magnitude (m/s)
Position (m)
Velocity Magnitude
Mar 23, 2015
ANSYS Fluent 15.0 (3d, dp, pbns, ske)

(a)

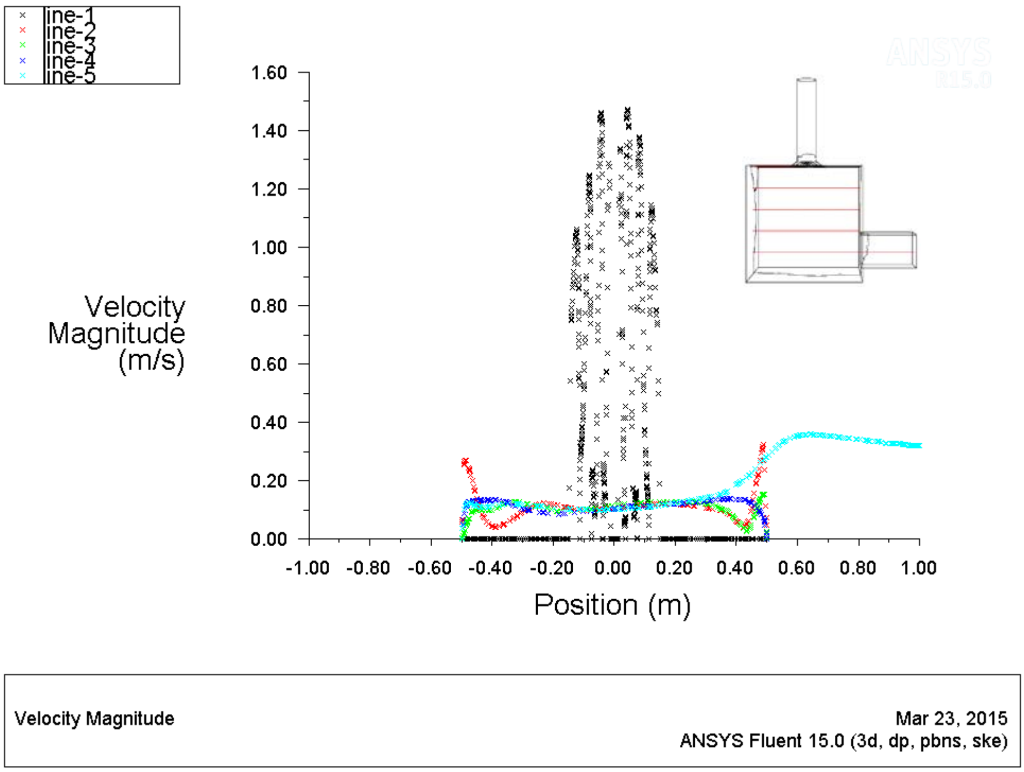
line-1
line-2
line-3
line-4
line-5
Velocity Magnitude (m/s)
Position (m)
Velocity Magnitude
Mar 23, 2015
ANSYS Fluent 15.0 (3d, dp, pbns, ske)

(b)

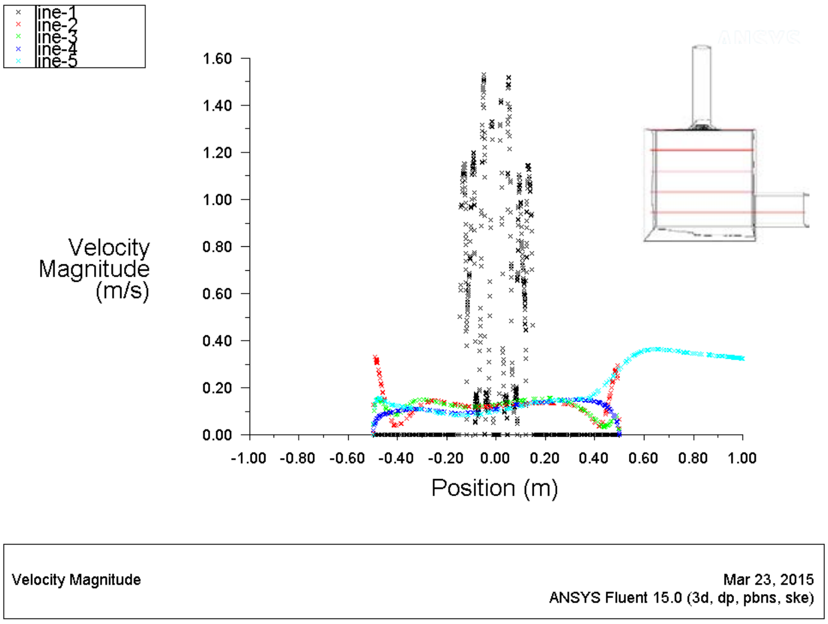

(c)

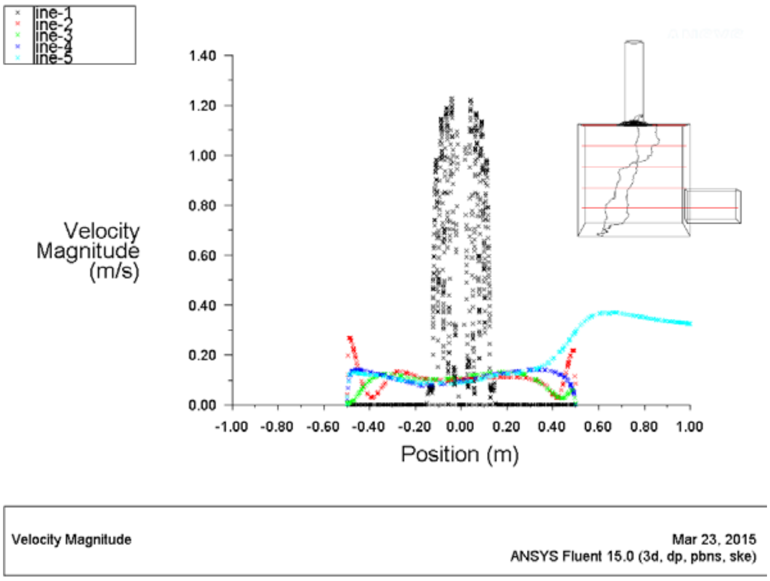

(d)

Figure 4.30: The X-Y plots of velocity magnitude at section lines (red colour line 1 to 5 depicted in small figure beside the XY plot) on *x*-axis extending from the centre of the room to the edge of walls with 1 outlet near wall bottom: (a) 4-blade, (b) 5-blade, (c) 5-blade with blade angle change, & (d) 7-blade round ceiling air diffuser

Based on sections (a) of Figures 4.31 and 4.32, the 4-blade/vane round ceiling air diffuser illustrated that the air flow distribution (-0.48 – 0.2 m/s) was not uniform throughout the room volume as most of the distributed air was concentrated around the central span of the room. It might be due to high volumetric flow rate or static pressure around the central core blade where the air tended to release from the air diffuser at a shorter distance. The occupants nearby the air diffuser might feel uncomfortable due to higher air flow toward their body continuously.

From sections (b) of Figures 4.31 and 4.32, the air flow distribution from the 5-blade/vane round ceiling air diffuser was relatively more uniform (0.03 – 0.2 m/s) throughout the room volume than that of 4-blade/vane round ceiling air diffuser (-0.48 – 0.2 m/s) since air flow via the blades of 5-blade air diffuser was smoother. In addition, those occupants nearby the air diffuser might feel comfortable as the air from diffuser was evenly distributed throughout the room without high flow concentration around the air diffuser.

The sections (c) of Figures 4.31 and 4.32 showed that the air flow distribution from the 5-blade round ceiling air diffuser with an average blade angle of 30° was similar to that of those 5-blade round ceiling air diffuser with an average blade angle of 40° in sections (b) of Figures 4.31 to 4.32, the air diffuser with 40° blade angle (0.03 – 0.2 m/s) exhibited slightly consistent air flow than that (0.03 – 0.2 m/s) of diffuser with 30° blade angle since air flow via the air diffuser with 40° blade angle have lesser contact surface with the air diffuser blades, and able to flow smoothly if compared with diffuser of 30° blade angle. The air flow of 5-blade air diffuser with 30° blade angle was able to distribute effectively throughout the room, leading to a more consistence room velocity profile (0.03 – 0.2 m/s) within the room than that of 4-blade air diffuser (-0.48 – 0.2 m/s) since it provided similar effect if compared to that of 5-blade air diffuser with 40° blade angle. The occupants nearby the air diffuser might not feel uncomfortable as the air from diffuser was uniformly distributed throughout the room without high flow concentration around the air diffuser.

The CFD results of sections (d) of Figures 4.31 and 4.32 for 7-blade/vane round ceiling air diffuser expressed that the air flow distribution (0.03 – 0.2 m/s) was slightly consistent than that of the 4 (-0.48 – 0.2 m/s) or 5- (0.03 – 0.2 m/s) blades round ceiling air diffusers since air flow via the 7-blade air diffuser was more uniform than that of 4 or 5-blade air diffuser. It implied that the 7-blade air diffuser might be able to create more thermal comfort for the occupants within the room since the air flow rate from the 7-blade air diffuser was relatively higher and was able to uniformly distribute to further space if compared with the other diffusers.

In addition, line 1 of all the X-Y plots in Figure 4.32 showed that the fluctuation of velocity profile around the centre position due to air flow through the air gap (constricted area) between the air diffuser blades with Venturi effect where air velocity was increased and pressure was reduced. The velocity profile within the room of lines 2 to 5 for 5 or 7-blade air diffuser reflected that the air velocity was within 0.1 m/s, while the velocity profile within the room of lines 2 to 5 for 4-blade air diffuser indicated air velocity up to -0.6 m/s around centre position due to uneven air distribution.

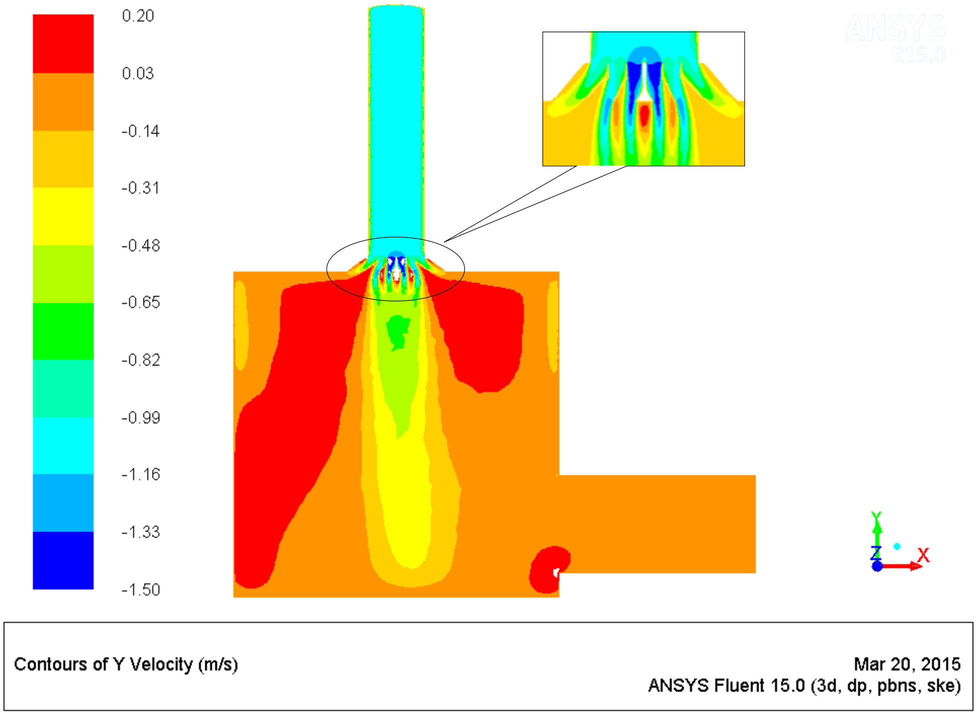
0.20
0.03
-0.14
-0.31
-0.48
-0.65
-0.82
-0.99
-1.16
-1.33
-1.50
Contours of Y Velocity (m/s)
Mar 20, 2015
ANSYS Fluent 15.0 (3d, dp, pbns, ske)

(a)

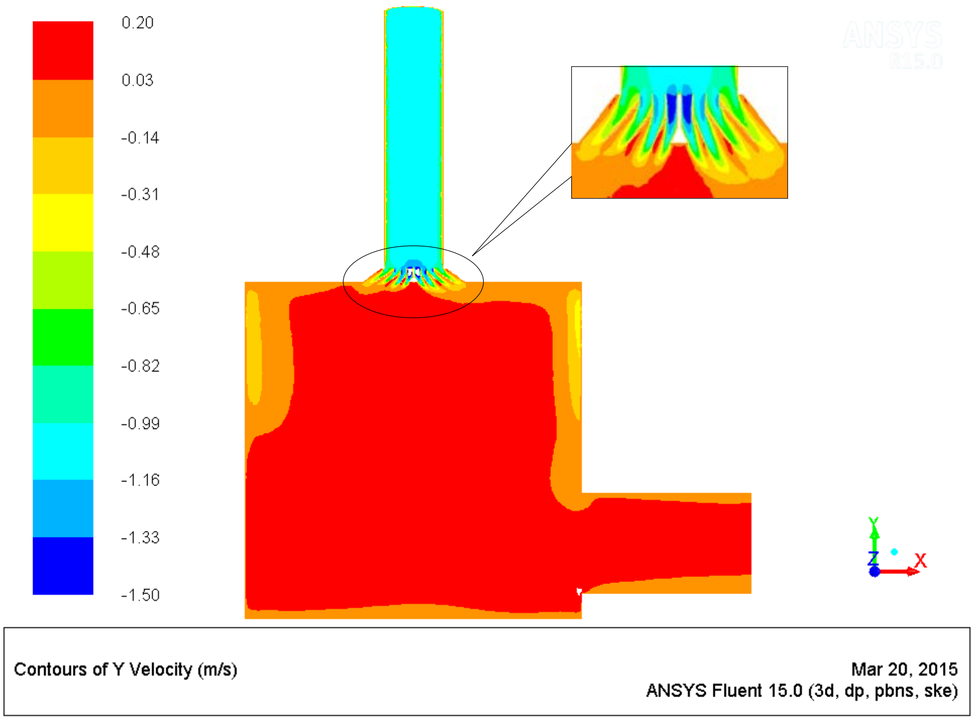
0.20
0.03
-0.14
-0.31
-0.48
-0.65
-0.82
-0.99
-1.16
-1.33
-1.50
Contours of Y Velocity (m/s)
Mar 20, 2015
ANSYS Fluent 15.0 (3d, dp, pbns, ske)

(b)

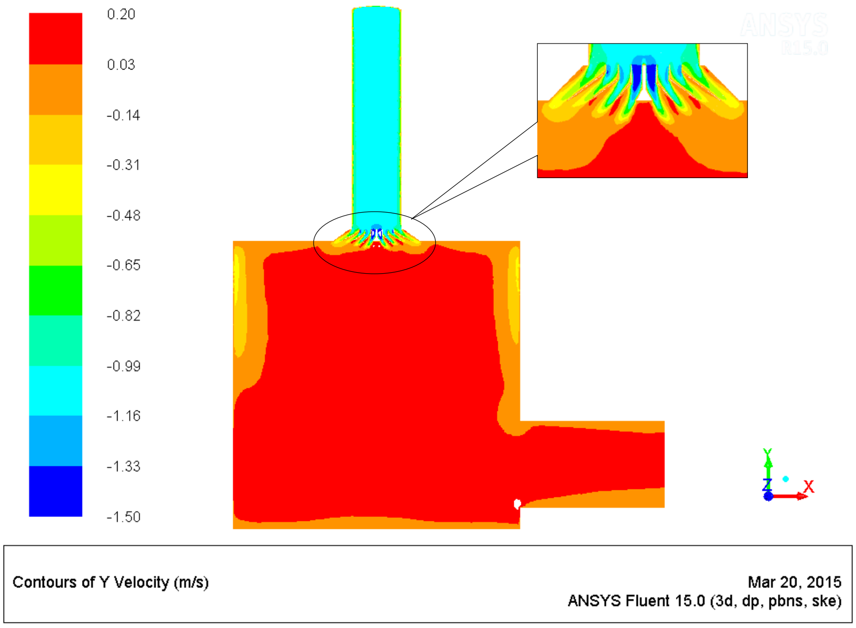

(c)

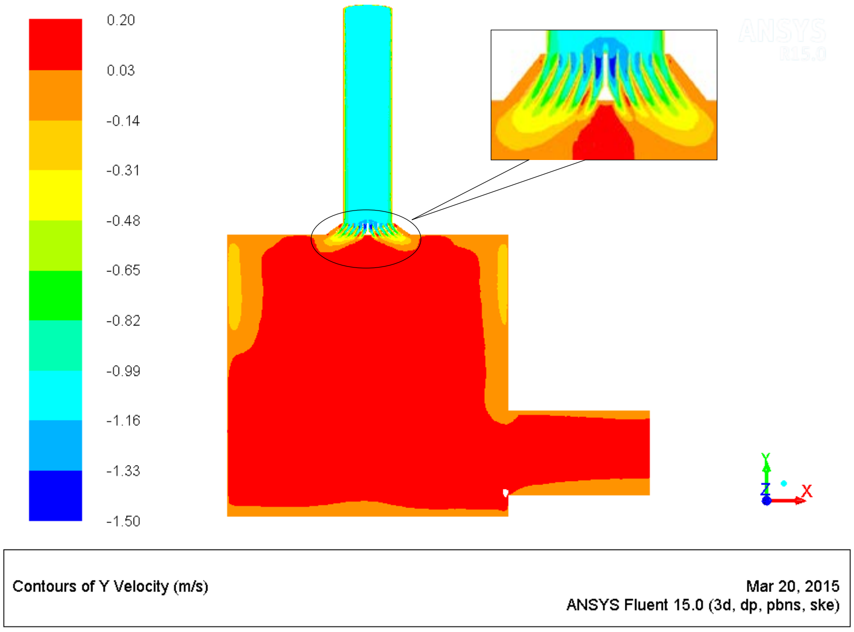

(d)

Figure 4.31: Contours of Y velocity in the room with inlet on ceiling and 1 outlet near wall bottom: (a) 4-blade, (b) 5-blade, (c) 5-blade with blade angle change, & (d) 7-blade round ceiling air diffuser

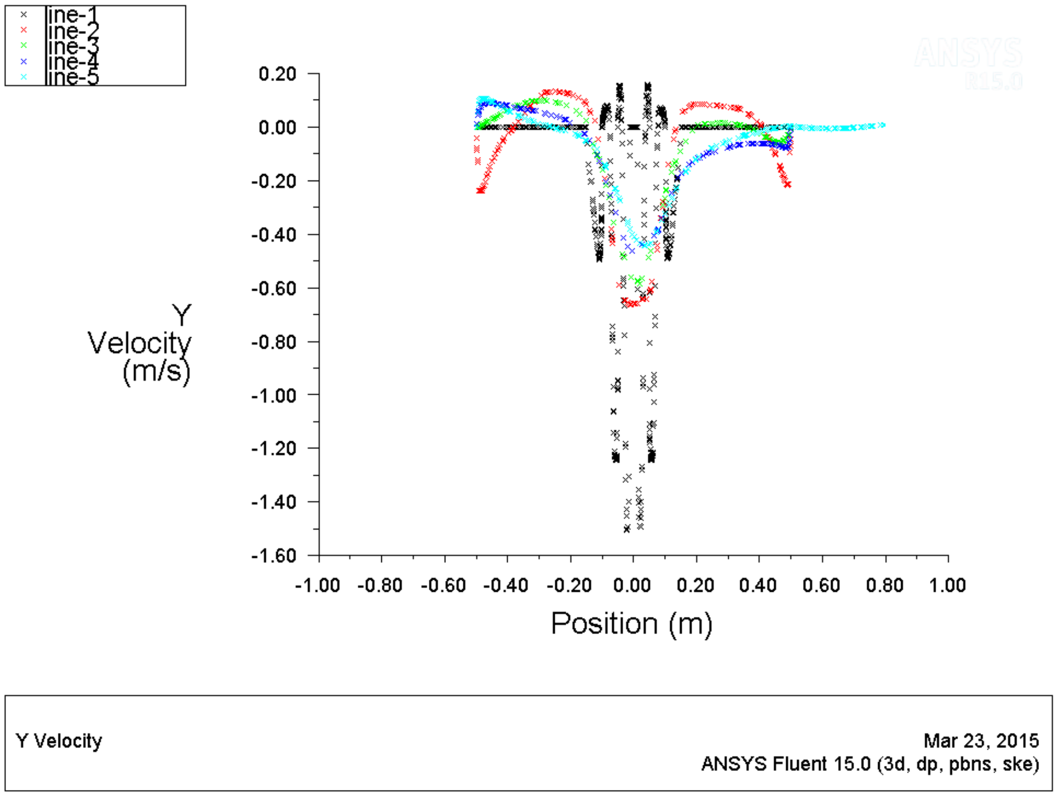

line-1
line-2
line-3
line-4
line-5
0.20
0.00
-0.20
-0.40
-0.60
-0.80
-1.00
-1.20
-1.40
-1.60
Y Velocity (m/s)
-1.00 -0.80 -0.60 -0.40 -0.20 0.00 0.20 0.40 0.60 0.80 1.00
Position (m)
Y Velocity
Mar 23, 2015
ANSYS Fluent 15.0 (3d, dp, pbns, ske)

(a)

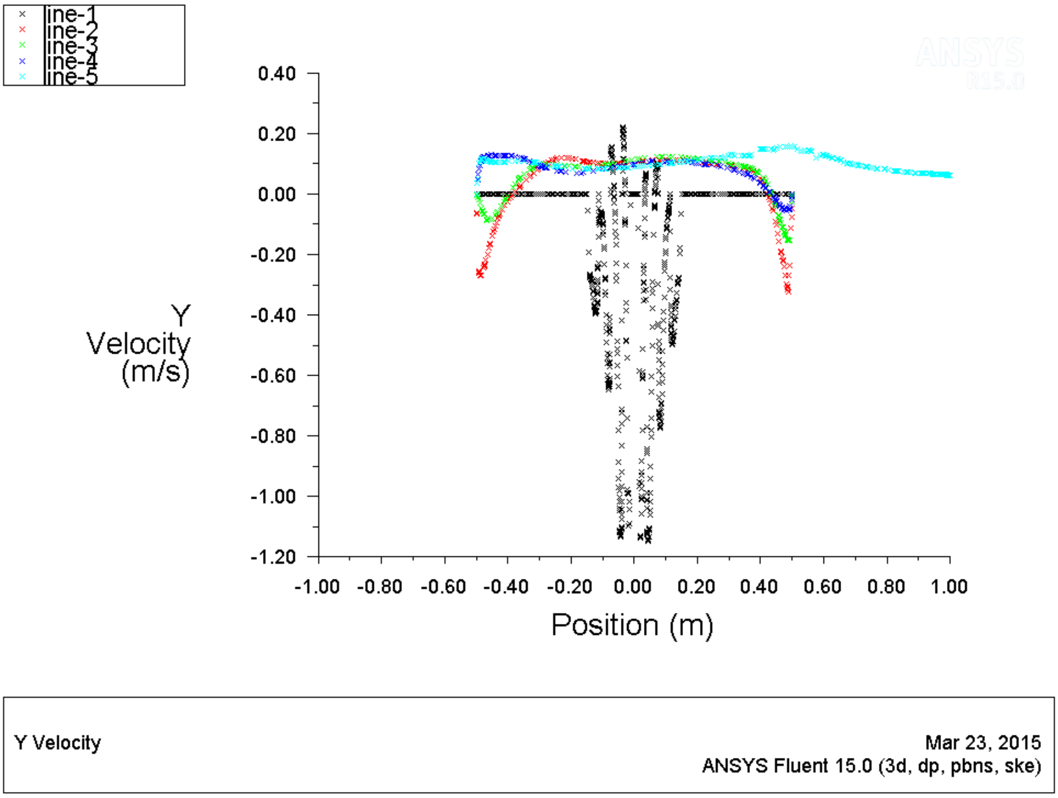

line-1
line-2
line-3
line-4
line-5
0.40
0.20
0.00
-0.20
-0.40
-0.60
-0.80
-1.00
-1.20
Y Velocity (m/s)
-1.00 -0.80 -0.60 -0.40 -0.20 0.00 0.20 0.40 0.60 0.80 1.00
Position (m)
Y Velocity
Mar 23, 2015
ANSYS Fluent 15.0 (3d, dp, pbns, ske)

(b)

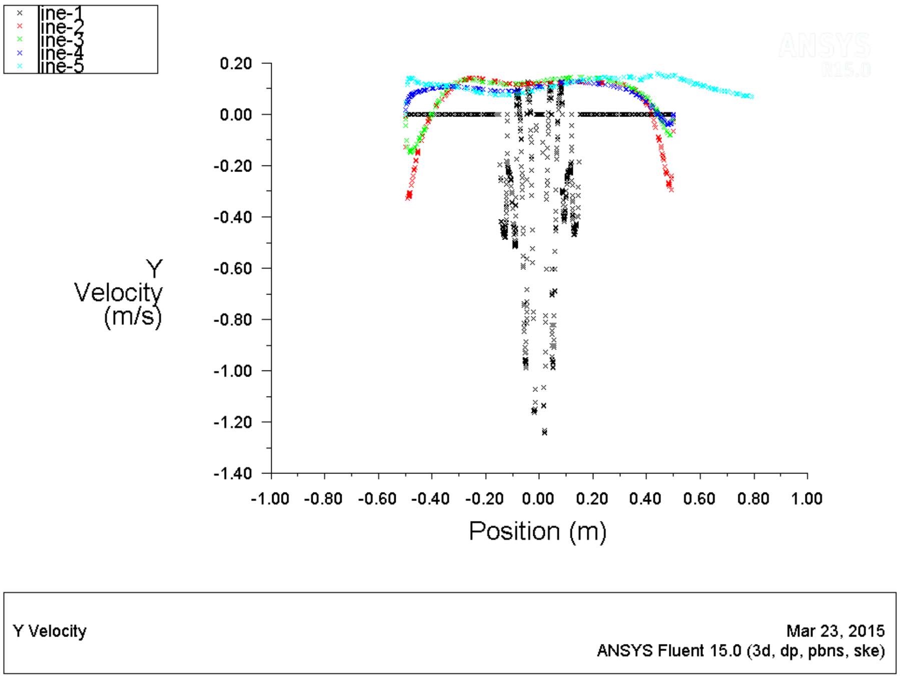

(c)

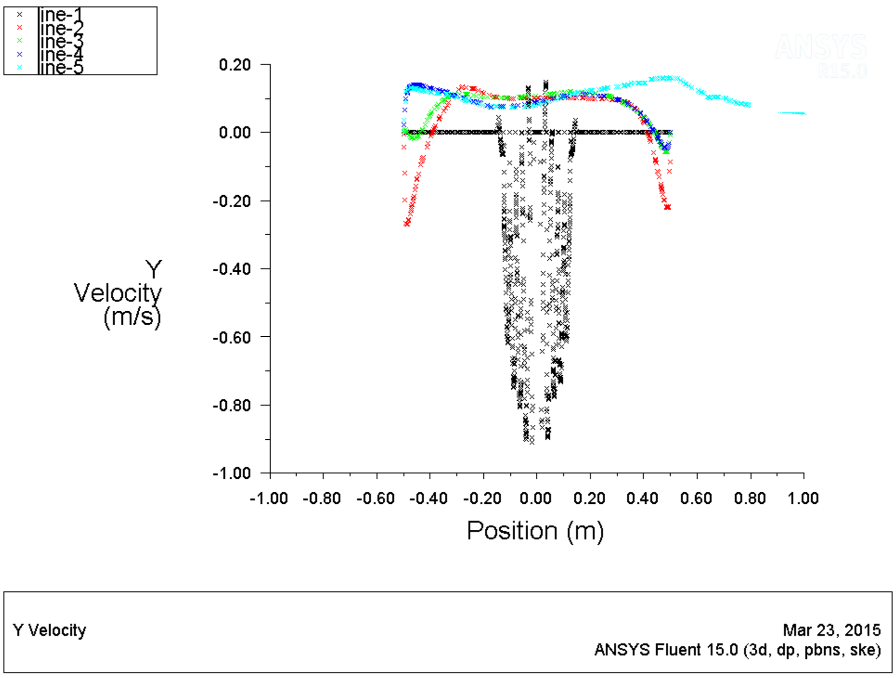

(d)

Figure 4.32: X-Y plots of Y velocity at section lines on *x*-axis extending from the centre of the room to the edge of walls with 1 outlet near wall bottom: (a) 4-blade, (b) 5-blade, (c) 5-blade with blade angle change, & (d) 7-blade round ceiling air diffuser

Based on sections (a) of Figures 4.33 and 4.34, the 4-blade/vane round ceiling air diffuser illustrated that the air flow distribution was not uniform throughout the room volume as most of the distributed air was concentrated around the central span of the room due to the reasons as stated in the previous section. The occupants nearby the air diffuser might experience cooler condition (289.7 – 290.6 K) due to aforesaid uneven air distribution.

From sections (b) of Figures 4.33 and 4.34, the temperature distribution from the 5-blade/vane round ceiling air diffuser was relatively more consistent (292.4 – 294.2 K) throughout the room than that (289.7 – 293.3 K) of 4-blade/vane round ceiling air diffuser (Figures 4.5 (a)) since air flow via the blades of 5-blade air diffuser are uniform. In addition, those occupants nearby the air diffuser might feel comfortable as the air from diffuser was evenly distributed throughout the room without high flow concentration around the air diffuser.

The sections (c) of Figures 4.33 and 4.34 showed that the air flow distribution from the 5-blade round ceiling air diffuser with an average blade angle of 30° was similar to that of those 5-blade round ceiling air diffuser with an average blade angle of 40° in sections (b) of Figures 4.33 and 4.34, However, the air diffuser with 40° blade angle (292.4 – 294.2 K) exhibited slightly consistent temperature distribution than that (292.4 – 294.2 K) of diffusers with 30° blade angle since air flow via the air diffuser with 40° blade angle had less contact surface with the air diffuser blades, and was able to flow smoothly if compared with diffuser of 30° blade angle. The air flow of 5-blade round ceiling air diffuser with 30° blade angle was able to distribute effectively throughout the room, leading to a more consistent temperature profile (292.4 – 294.2 K) within the room than that of 4-blade air diffuser (289.7 – 293.3 K) since it provided similar effect if compared to that of 5-blade air diffuser with 40° blade angle. The occupants nearby the air diffuser might not feel uncomfortable as the air from diffuser was uniformly distributed throughout the room without high flow concentration around the air diffuser.

The CFD results of sections (d) of Figures 4.33 to 4.34 for 7-blade/vane round ceiling air diffuser expressed that the temperature distribution (292.4 – 293.3 K) was slightly consistent if compared with that of the 4 (289.7 – 293.3 K) or 5- (292.4 – 294.2

K) blades round ceiling air diffusers since air flow via the 7-blade air diffuser was relatively more equal than that via 4 or 5-blade air diffuser. Meanwhile, the 7-blade air diffuser provided slightly more lower temperature profile of 292.4 – 293.3 K throughout the room (Figure 4.5 (d)) if compared with that of 4 or 5-blade air diffuser, implying that the 7-blade air diffuser might be able to create better thermal comfort for occupants within the room, and assist in reducing energy consumption by the air handling unit to cool the supply air since the air flow rate from the 7-blade air diffuser was relatively higher and able to distribute to more further space uniformly if compared with the other diffusers.

The line 1 of all the X-Y plots in Figure 4.34 reflected that the fluctuation of temperature profile around the centre position due to air flow through the air gap (constricted area) between the air diffuser blades with Venturi effect where air velocity was increased and pressure was reduced, and air velocity could affect the temperature distribution. The temperature profile within the room of lines 2 to 5 for 5 or 7-blade air diffusers reflected that the room temperature was within 293 K, while the velocity profile within the room of lines 2 to 5 for 4-blade air diffuser indicated room temperature up to 287 K around centre position due to uneven air distribution.

Furthermore, the temperature distribution of 5 and 7-blade air diffusers with one outlet near wall bottom were slightly consistent if compared with that of round diffuser gained by Mohammed (2013) as illustrated in Figure 2.13 since the air flow via the blades of proposed diffusers was relatively more uniform distributed, and less contact between the air flow and blade surfaces.

In addition, it can be noticed that the models with one number of air outlet near wall bottom could provide effective air flow behaviour and temperature distribution throughout the room but not as consistent as those models with two outlets near wall bottoms since it only directed the air from the inlet to the outlet in one direction. The air could be stagnant around the other wall before it was circulated (Figure 4.31). Nevertheless, its air flow distribution and temperature distribution were relatively effective than that of air outlet on ceiling level.

The range of velocity magnitude, Y velocity and static temperature distribution within the room volume for each model with one outlet near wall bottom are summarised in Table 4.7.

Table 4.7: Range of velocity magnitude, Y velocity and static temperature distribution within the room with one outlet near wall bottom

Item	Diffuser Model			
	4-blade	**5-blade (40°)**	**5-blade (30°)**	**7-blade**
Velocity Magnitude (m/s)	0 – 0.75	0 – 0.60	0 – 0.60	0 – 0.60
Y Velocity (m/s)	-0.65 – 0.20	-0.14 – 0.20	-0.14 – 0.20	-0.14 – 0.20
Static Temperature (K)	289.7 – 293.3	292.4 – 294.2	292.4 – 294.2	292.4 – 293.3

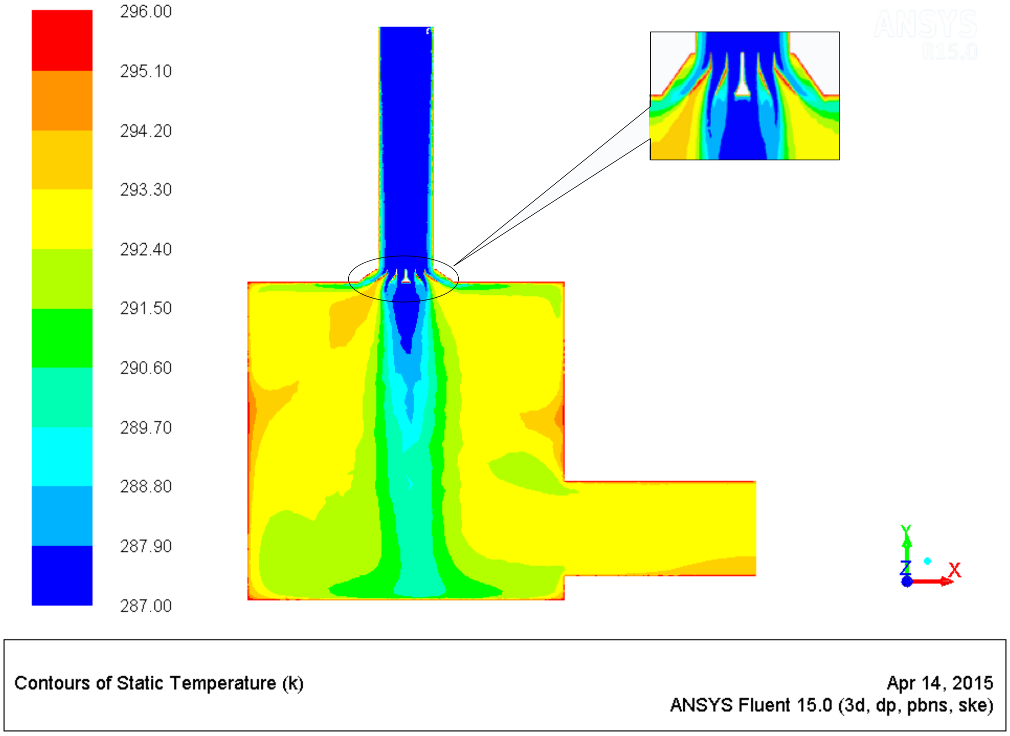
296.00
295.10
294.20
293.30
292.40
291.50
290.60
289.70
288.80
287.90
287.00
Y
Z
X
Contours of Static Temperature (k)
Apr 14, 2015
ANSYS Fluent 15.0 (3d, dp, pbns, ske)

(a)

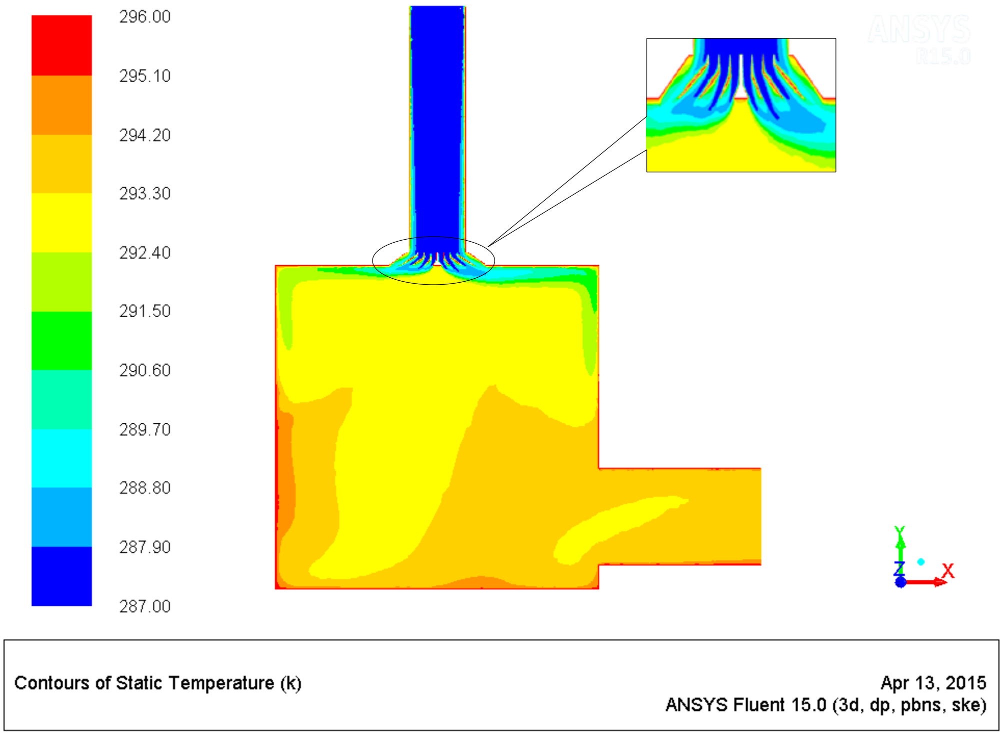
296.00
295.10
294.20
293.30
292.40
291.50
290.60
289.70
288.80
287.90
287.00
Y
Z
X
Contours of Static Temperature (k)
Apr 13, 2015
ANSYS Fluent 15.0 (3d, dp, pbns, ske)

(b)

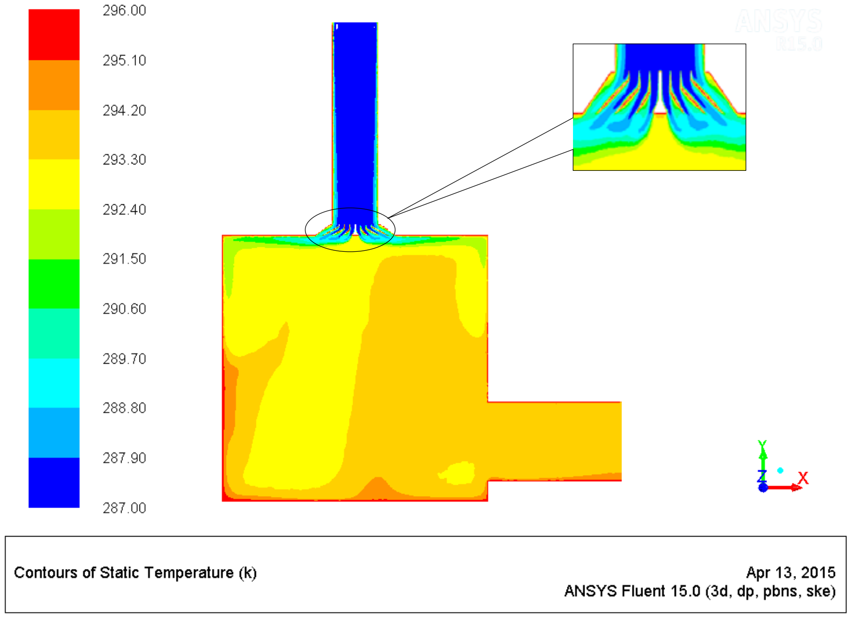

(c)

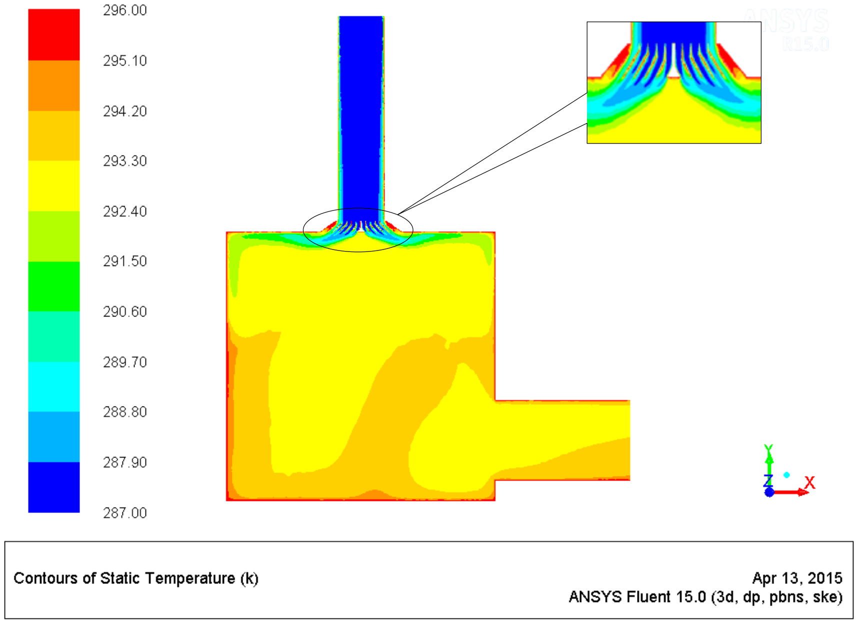

(d)

Figure 4.33: Contours of static temperature in the room with inlet on ceiling and 1 outlet near wall bottom: (a) 4-blade, (b) 5-blade, (c) 5-blade with blade angle change, & (d) 7-blade round ceiling air diffuser

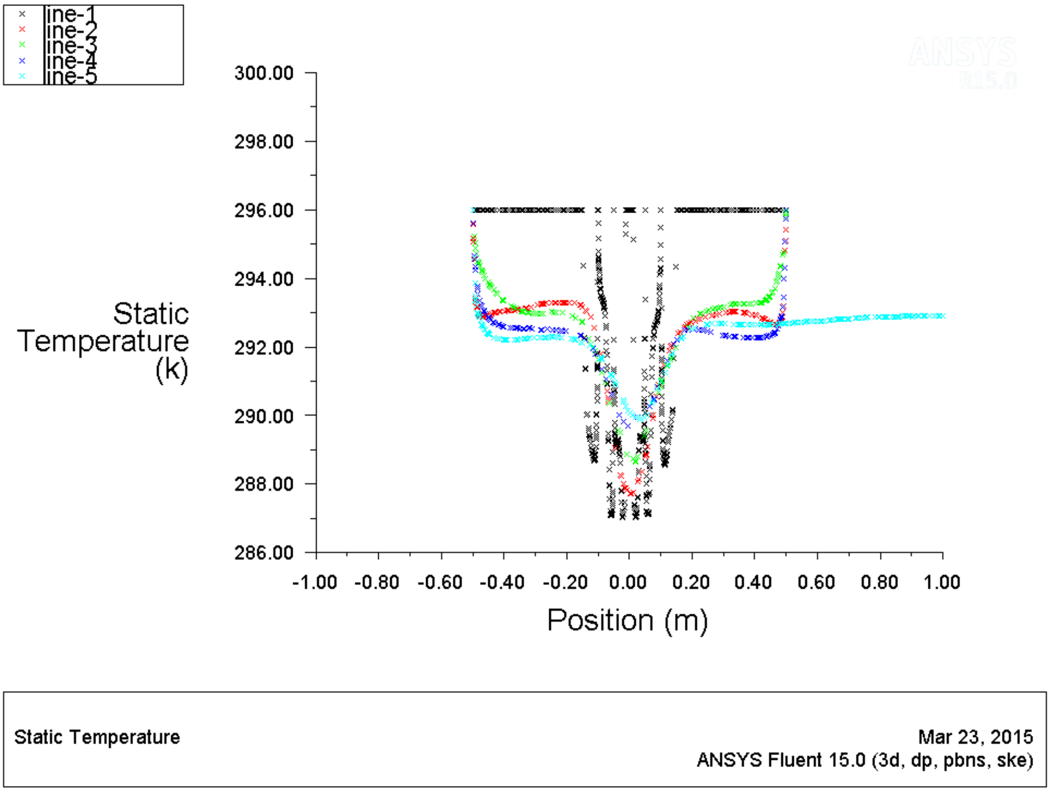
line-1
line-2
line-3
line-4
line-5
300.00
298.00
296.00
294.00
292.00
290.00
288.00
286.00
Static Temperature (k)
-1.00 -0.80 -0.60 -0.40 -0.20 0.00 0.20 0.40 0.60 0.80 1.00
Position (m)
Static Temperature
Mar 23, 2015
ANSYS Fluent 15.0 (3d, dp, pbns, ske)

(a)

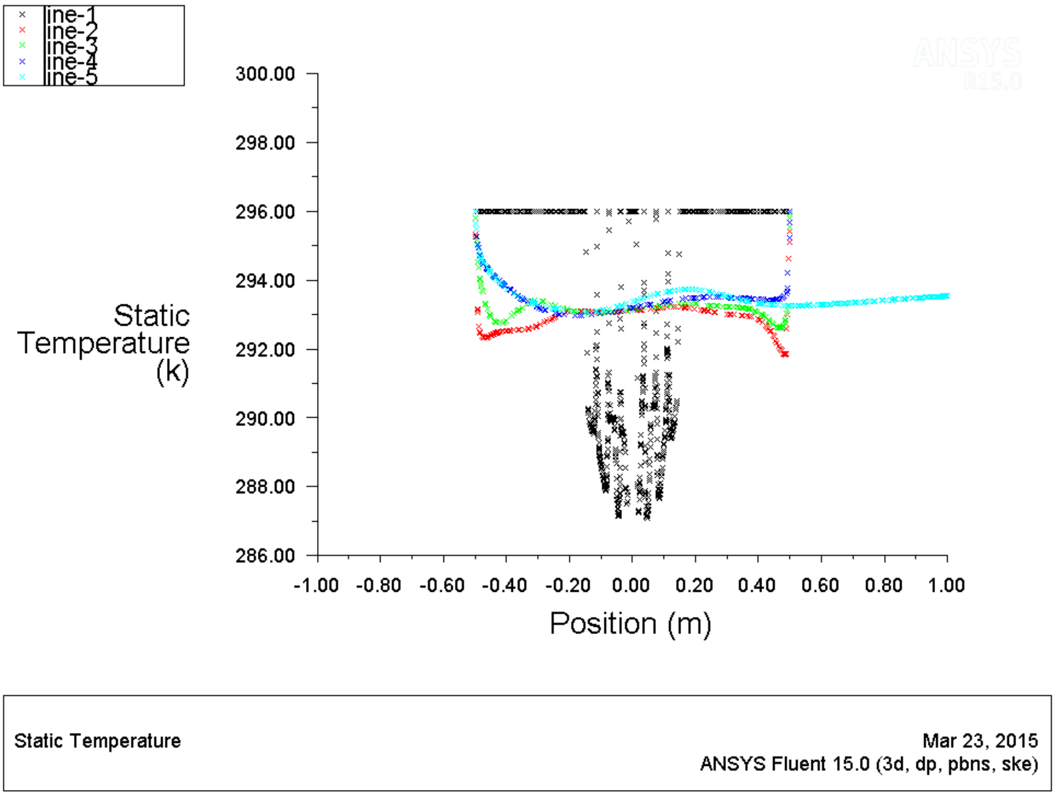
line-1
line-2
line-3
line-4
line-5
300.00
298.00
296.00
294.00
292.00
290.00
288.00
286.00
Static Temperature (k)
-1.00 -0.80 -0.60 -0.40 -0.20 0.00 0.20 0.40 0.60 0.80 1.00
Position (m)
Static Temperature
Mar 23, 2015
ANSYS Fluent 15.0 (3d, dp, pbns, ske)

(b)

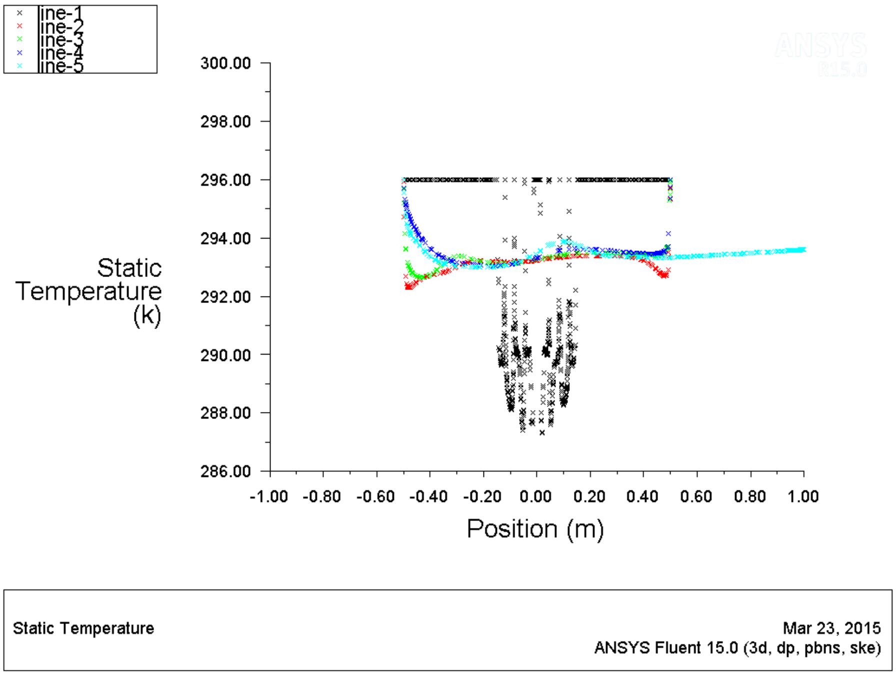

(c)

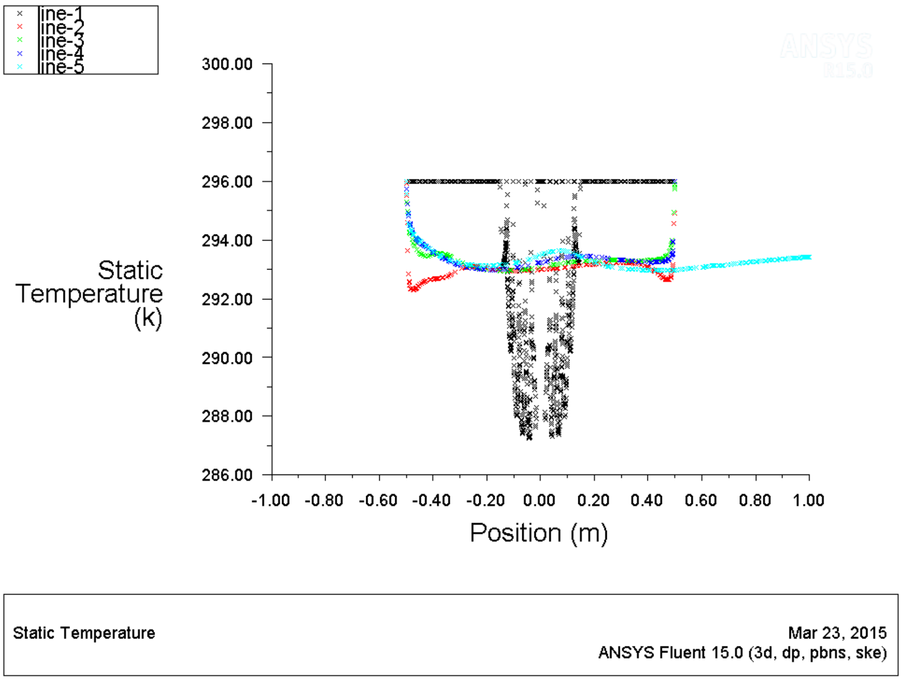

(d)

Figure 4.34: **X-Y plots of static temperature at section lines on *x*-axis extending from the centre of the room to the edge of walls with 1 outlet near wall bottom: (a) 4-blade, (b) 5-blade, (c) 5-blade with blade angle change, & (d) 7-blade round ceiling air diffuser**

4.1.8 The round ceiling air diffuser with one outlet on ceiling level

The air flow behaviours and temperature distribution of round ceiling air diffusers in room with inlet and outlet on ceiling level for inlet velocity at 1.0 m/s and, inlet temperature of 287 K are depicted in Figures 4.35 to 4.40.

Based on sections (a) of Figures 4.35 to 4.36, the 4-blade/vane round ceiling air diffuser reflected that the air flow was not evenly distributed throughout the room (0 – 0.6 m/s) as most of the air was concentrated around the middle spot of the room volume although the effect might not be as severe as those models with outlets near bottom of walls. It might be due to high volumetric flow rate or static pressure around the central core blade where the air tended to release from the air diffuser at a shorter distance, which was similar to those previous cases. The occupants nearby the air diffuser might not feel comfortable due to higher air flow toward their body continuously.

From sections (b) of Figures 4.35 to 4.36, the air flow distribution from the 5-blade/vane round ceiling air diffuser was relatively more uniform (0 – 0.3 m/s) throughout the room than that of 4-blade/vane round ceiling air diffuser (0 – 0.6 m/s) since the air flow via the blades of 5-blade air diffuser was smoother. They did not display any concentration of air distribution around the middle spot of the room, and Coanda effect of air distribution was observed where the flow emerged radically and approached the wall and then turned into 90° downward, suggesting that the throw of air could be longer as illustrated in Figures 4.35 (b). The occupants nearby the air diffuser might not feel uncomfortable as the air from diffuser was uniformly distributed throughout the room.

Although the CFD results of sections (c) of Figures 4.35 to 4.36 displayed that the air flow distribution from the 5-blade round ceiling air diffuser with an average blade angle of 30° was similar to those 5-blade round ceiling air diffusers with an average blade angle of 40° in sections of (b) of Figures 4.35 to 4.36, the air diffuser with 40° blade angle exhibited slightly consistent air flow (0 – 0.3 m/s) than that (0 – 0.3 m/s) of diffusers with 30° blade angle since air flow via the air diffuser with 40° blade angle had less contact surface with the air diffuser blades, and was able to flow smoothly if compared with diffuser of 30° blade angle. The air flow from 5-blade air diffuser with 30° blade angle was relatively uniform distributed throughout the room, leading to a more consistent room velocity profile (0 – 0.3 m/s) within the room than that of the 4-blade air diffuser (0 – 0.6 m/s) since it provided similar effect if compared to that of 5-blade air diffuser with 40° blade angle. The occupants nearby the air diffuser might not feel uncomfortable as the air from diffuser was uniformly distributed throughout the room without high flow concentration around the air diffuser.

The CFD results of item (d) of Figures 4.35 to 4.36 for 7-blade/vane round ceiling air diffuser reflected that the air flow behaviours (0 – 0.3 m/s) was slightly consistent than those of the 4 (0 – 0.6 m/s) or 5- (0 – 0.3 m/s) blades round ceiling air diffusers since air flow via the 7-blade air diffuser was relatively more equal than that via 4 or 5-blade air diffuser. Coanda effect of air distribution was noticed where the flow emerged radically and reached the wall and then directed into 90° downward, which revealed the throw of air could be longer in Figures 4.35 (d). The occupants nearby the air diffuser might not feel uncomfortable as the air from diffuser was uniformly distributed throughout the room without high flow concentration around the air diffuser.

In addition, line 1 of all the X-Y plots in Figure 4.36 revealed that the fluctuation of velocity profile around the centre position due to air flow through the air gap (constricted area) between the air diffuser blades with Venturi effect where air velocity was increased and pressure was reduced. The velocity profile within the room of lines 2 to 5 for 5 or 7-blade air diffuser reflected that the air velocity was within 0.1 m/s, while the velocity profile within the room of lines 2 to 5 for 4-blade air diffuser indicated air velocity was up to 0.6 m/s around centre position due to uneven air distribution.

Furthermore, the air flow behaviours of 5 and 7-blade air diffusers with one outlet on ceiling level was slightly consistent if compared with that of round diffuser achieved by Mohammed (2013) as displayed in Figure 2.13 since the air flow via the blades of proposed diffusers was relatively more uniform distributed, and less contact between the air flow and blade surfaces.

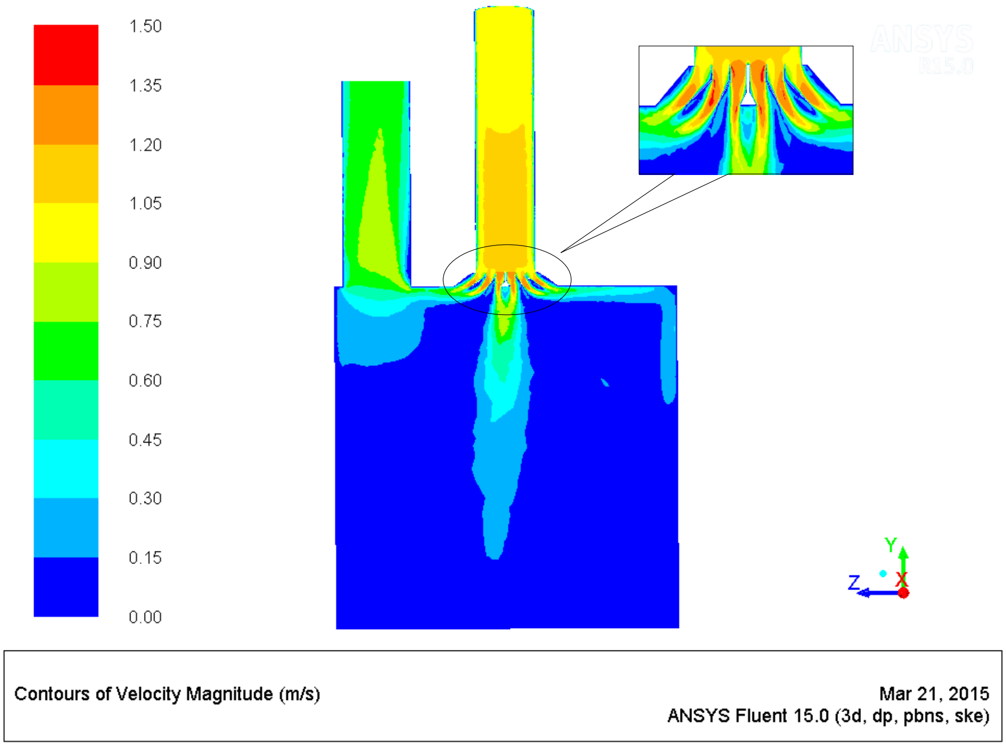
1.50
1.35
1.20
1.05
0.90
0.75
0.60
0.45
0.30
0.15
0.00
Y
Z
X
Contours of Velocity Magnitude (m/s)
Mar 21, 2015
ANSYS Fluent 15.0 (3d, dp, pbns, ske)

(a)

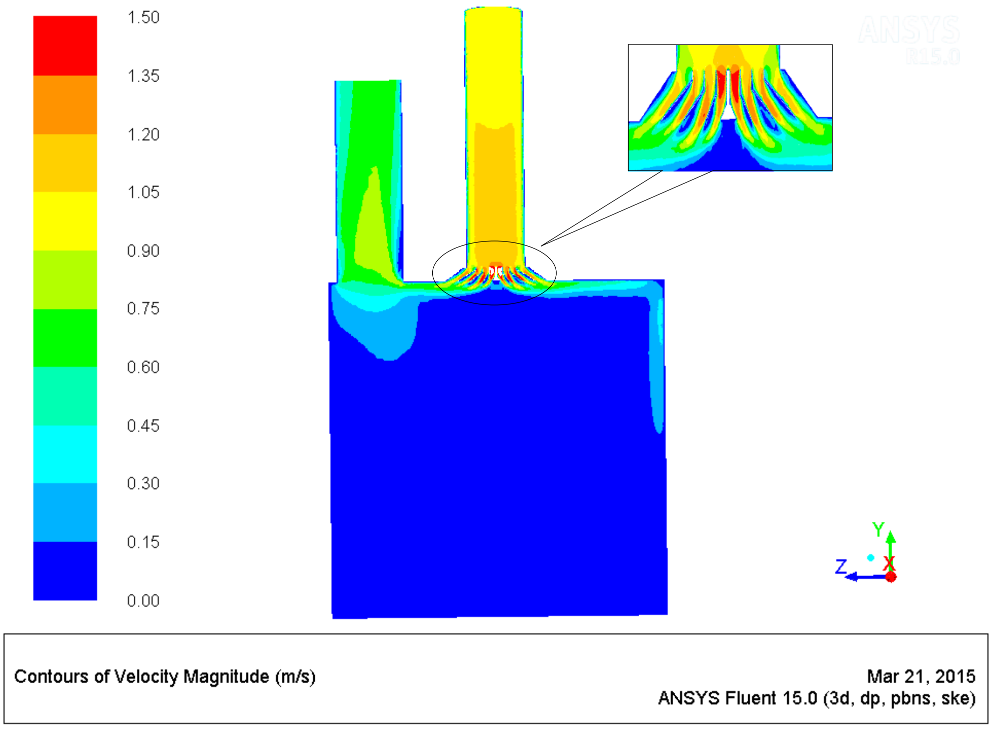
1.50
1.35
1.20
1.05
0.90
0.75
0.60
0.45
0.30
0.15
0.00
Y
Z
X
Contours of Velocity Magnitude (m/s)
Mar 21, 2015
ANSYS Fluent 15.0 (3d, dp, pbns, ske)

(b)

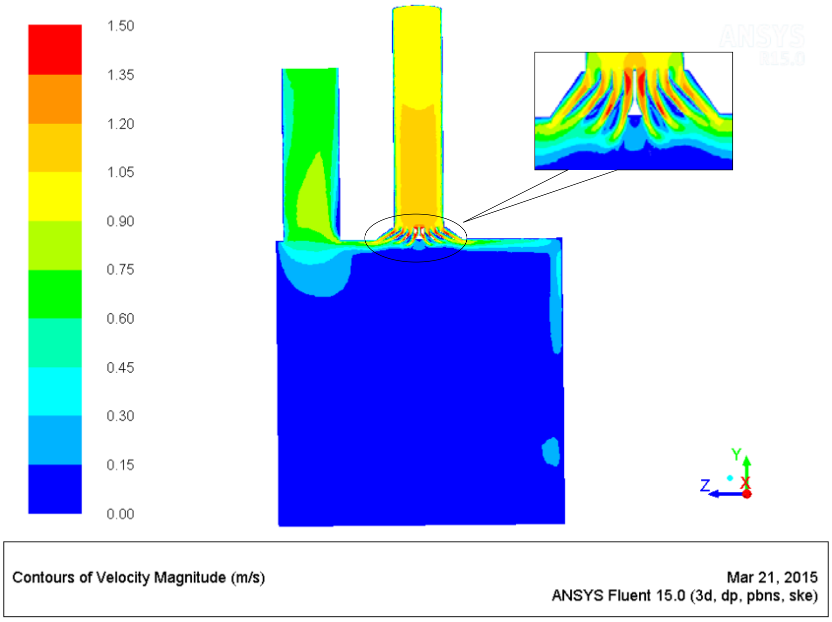

(c)

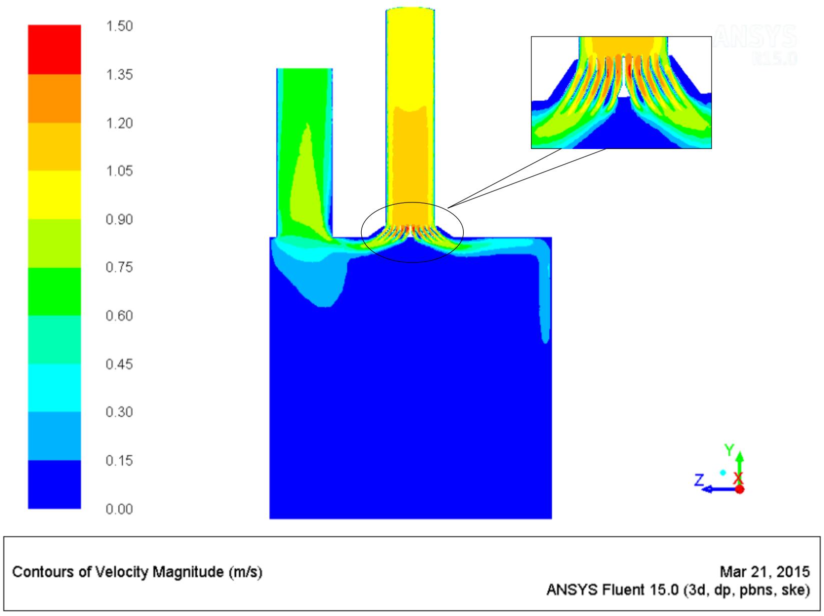

(d)

Figure 4.35: Contours of velocity magnitude in the room with inlet and outlet on ceiling level: (a) 4-blade, (b) 5-blade, (c) 5-blade with blade angle change, & (d) 7-blade round ceiling air diffuser

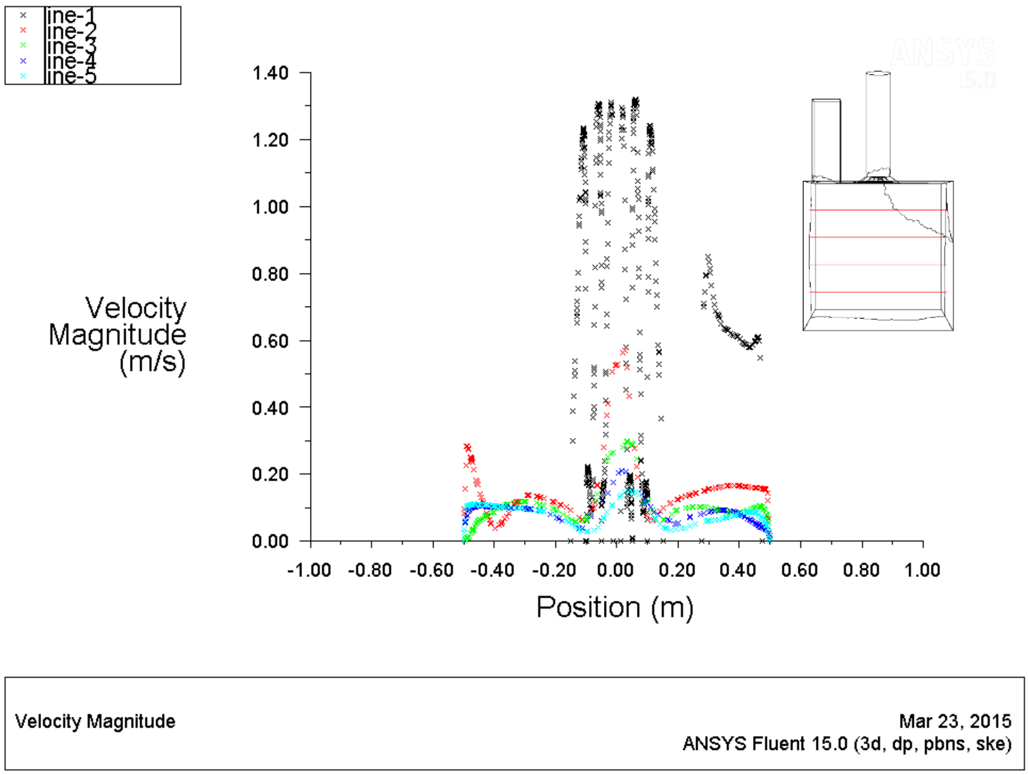
line-1
line-2
line-3
line-4
line-5
Velocity Magnitude (m/s)
1.40
1.20
1.00
0.80
0.60
0.40
0.20
0.00
-1.00 -0.80 -0.60 -0.40 -0.20 0.00 0.20 0.40 0.60 0.80 1.00
Position (m)
Velocity Magnitude
Mar 23, 2015
ANSYS Fluent 15.0 (3d, dp, pbns, ske)

(a)

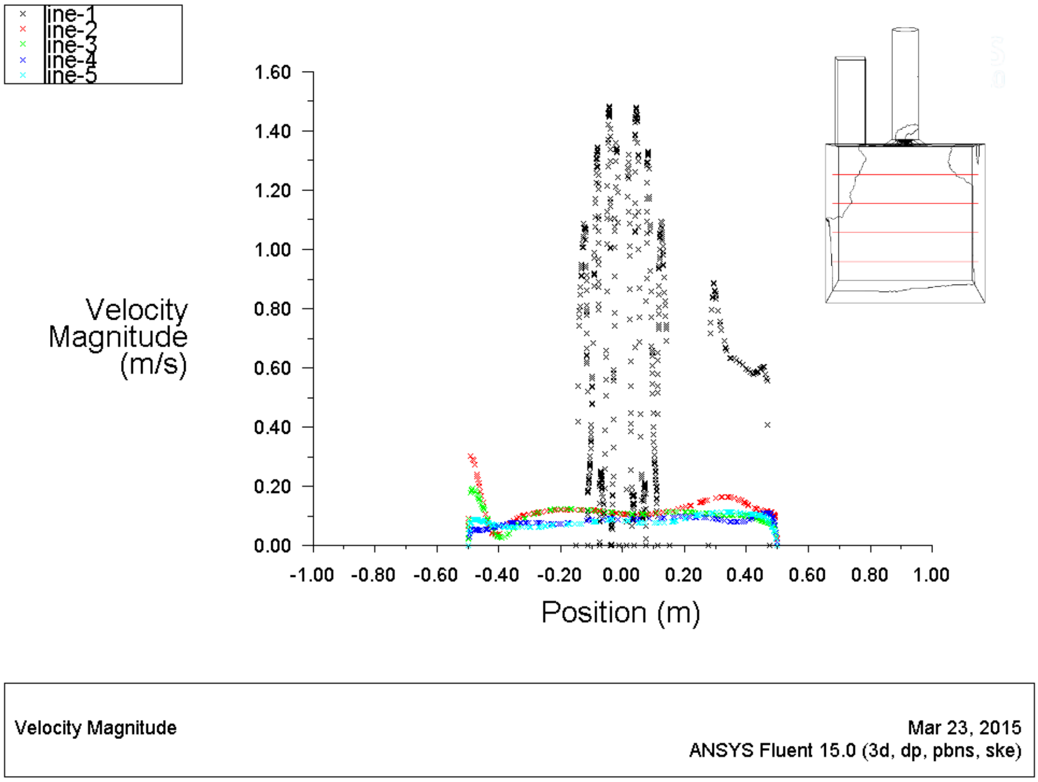
line-1
line-2
line-3
line-4
line-5
Velocity Magnitude (m/s)
1.60
1.40
1.20
1.00
0.80
0.60
0.40
0.20
0.00
-1.00 -0.80 -0.60 -0.40 -0.20 0.00 0.20 0.40 0.60 0.80 1.00
Position (m)
Velocity Magnitude
Mar 23, 2015
ANSYS Fluent 15.0 (3d, dp, pbns, ske)

(b)

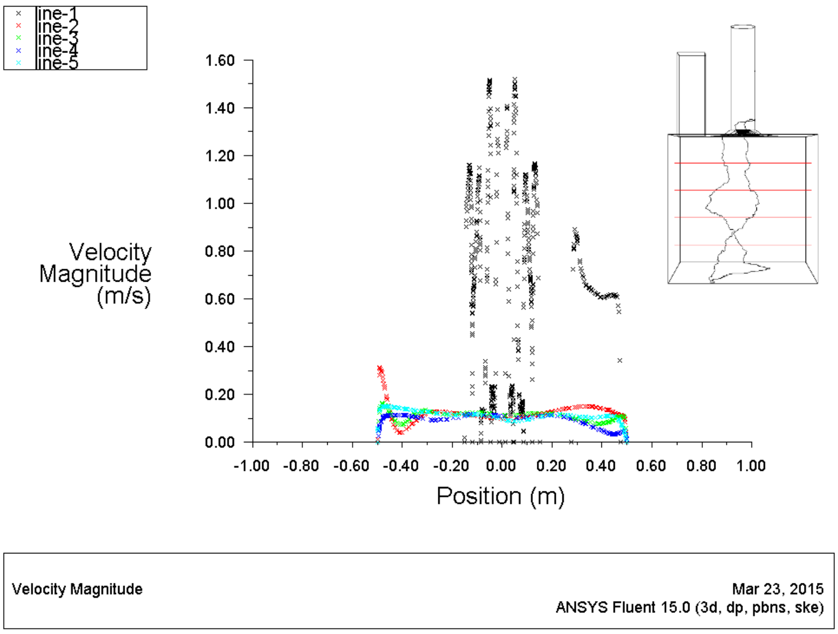

(c)

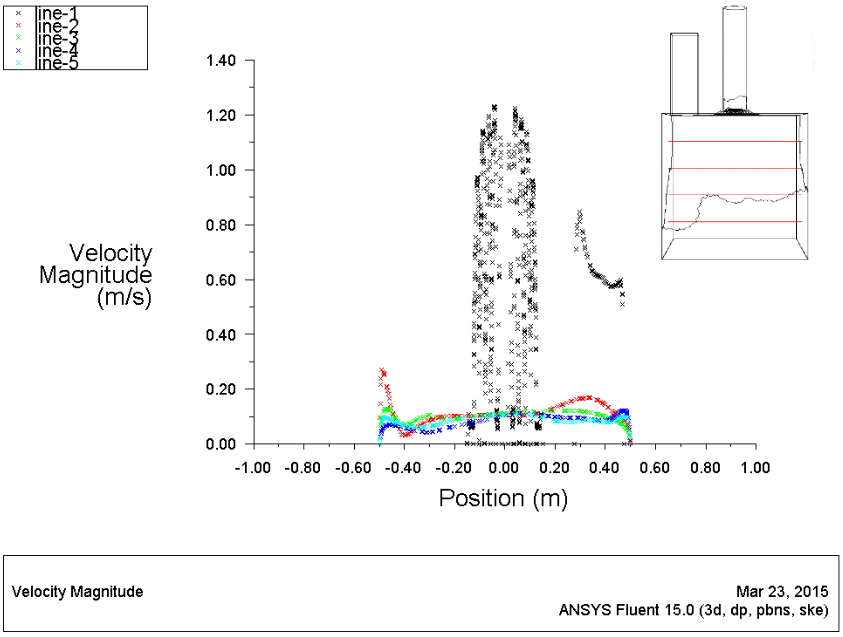

(d)

Figure 4.36: The X-Y plots of velocity magnitude at section lines (red colour line 1 to 5 depicted in small figure beside the XY plot) on *x*-axis extending from the centre of the room to the edge of walls with 1 outlet on ceiling: (a) 4-blade, (b) 5-blade, (c) 5-blade with blade angle change, & (d) 7-blade round ceiling air diffuser

Based on sections (a) of Figures 4.37 and 4.38, the 4-blade/vane round ceiling air diffuser indicated that the air flow distribution (-0.31 – 0.2 m/s) was not uniform throughout the room as most of the distributed air was concentrated around the middle spot of the room. It might be due to high volumetric flow rate or static pressure around the central core blade where the air tended to throw out from the air diffuser at a shorter distance. The occupants nearby the air diffuser might not feel comfortable due to higher air flow toward their body continuously.

From sections (b) of Figures 4.37 and 4.38, the air flow distribution from the 5-blade/vane round ceiling air diffuser was relatively more uniform (0.03 – 0.2 m/s) throughout the room than that of 4-blade/vane round ceiling air diffuser (-0.31 – 0.2 m/s) since the air flow via the blades of 5-blade air diffuser was smoother. In addition, those occupants nearby the air diffuser might feel comfortable as the air from diffuser was evenly distributed throughout the room without high flow concentration around the air diffuser.

The sections (c) of Figures 4.37 and 4.38 showed that the air flow distribution from the 5-blade round ceiling air diffuser with an average blade angle of 30° was similar to those of 5-blade round ceiling air diffuser with an average blade angle of 40° in sections (b) of Figures 4.37 to 4.38. However, the air diffuser with 40° blade angle exhibited slightly consistent air flow (0.03 – 0.2 m/s) than that (0.03 – 0.2 m/s) of diffuser with 30° blade angle since the air flow via the air diffuser with 40° blade angle had less contact surface with the air diffuser blades, and was able to flow smoothly if compared with diffuser of 30° blade angle. The air flow of 5-blade air diffuser with 30° blade angle was able to distribute effectively throughout the room, leading to a more consistent velocity profile (0.03 – 0.2 m/s) within the room than that of 4-blade air diffuser (-0.31 – 0.2 m/s) since it provided similar effect if compared to that of 5-blade air diffuser with 40° blade angle. The occupants nearby the air diffuser might not feel uncomfortable as the air from diffuser was uniformly distributed throughout the room without high flow concentration around the air diffuser.

The CFD results of sections (d) of Figures 4.37 and 4.38 for 7-blade/vane round ceiling air diffuser revealed that the air flow behaviours (0.03 – 0.2 m/s) was slightly consistent than those of the 4 (-0.31 – 0.2 m/s) or 5- (0.03 – 0.2 m/s) blades round ceiling air diffusers since the air flow via the 7-blade air diffuser was relatively more equal than that via 4 or 5-blade air diffuser. It suggested that the 7-blade air diffuser might be able to create more thermal comfort for occupants within the room since the air flow rate from the 7-blade air diffuser was relatively higher and was able to distribute to further space uniformly if compared with the other diffusers.

In addition, line 1 of all the X-Y plots in Figure 4.38 showed that the fluctuation of velocity profile around the centre position due to air flow through the air gap (constricted area) between the air diffuser blades with Venturi effect where air velocity was increased and pressure was reduced. The velocity profile within the room of lines 2 to 5 for 5 or 7-blade air diffuser reflected that the air velocity was within 0.1 m/s, while the velocity profile within the room of lines 2 to 5 for 4-blade air diffuser indicated air velocity up to -0.6 m/s around centre position due to uneven air distribution.

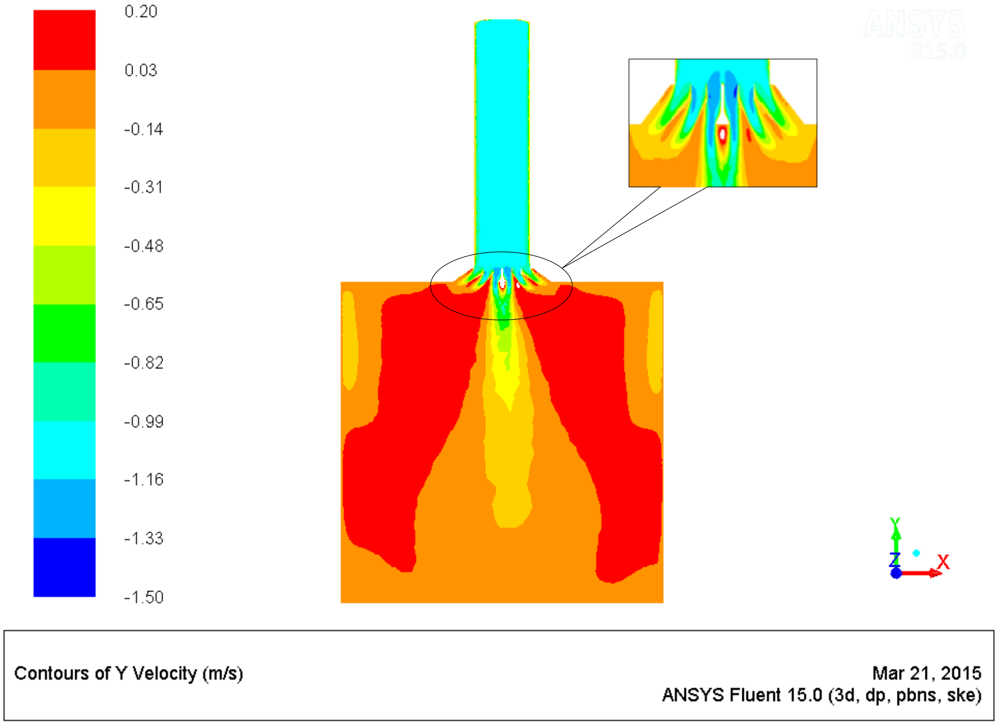

0.20
0.03
-0.14
-0.31
-0.48
-0.65
-0.82
-0.99
-1.16
-1.33
-1.50
Y
Z
X
Contours of Y Velocity (m/s)
Mar 21, 2015
ANSYS Fluent 15.0 (3d, dp, pbns, ske)

(a)

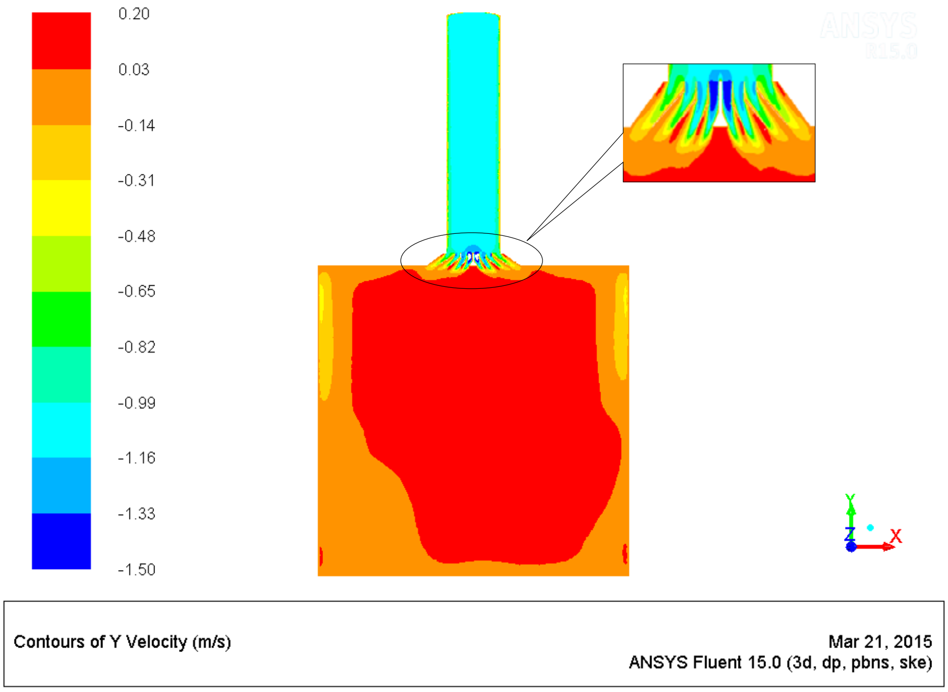

0.20
0.03
-0.14
-0.31
-0.48
-0.65
-0.82
-0.99
-1.16
-1.33
-1.50
Y
Z
X
Contours of Y Velocity (m/s)
Mar 21, 2015
ANSYS Fluent 15.0 (3d, dp, pbns, ske)

(b)

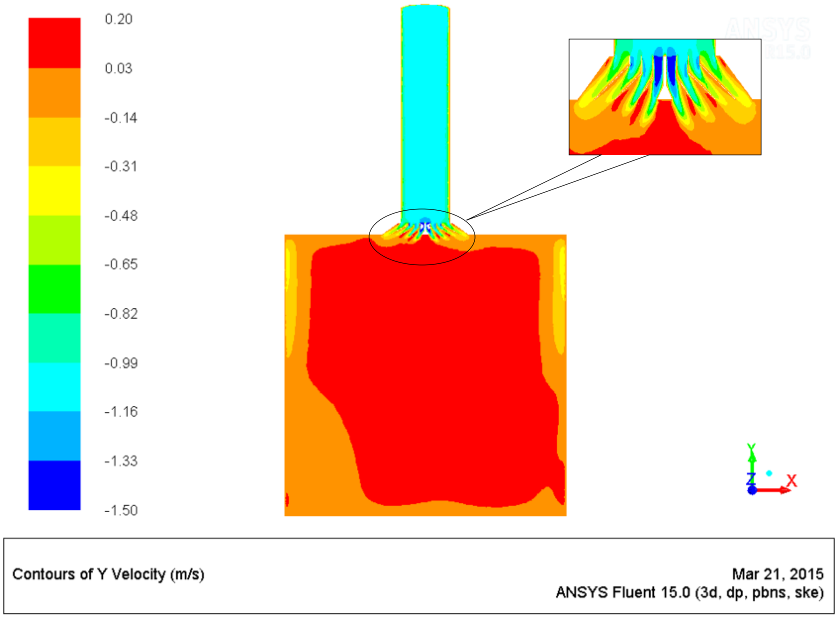

(c)

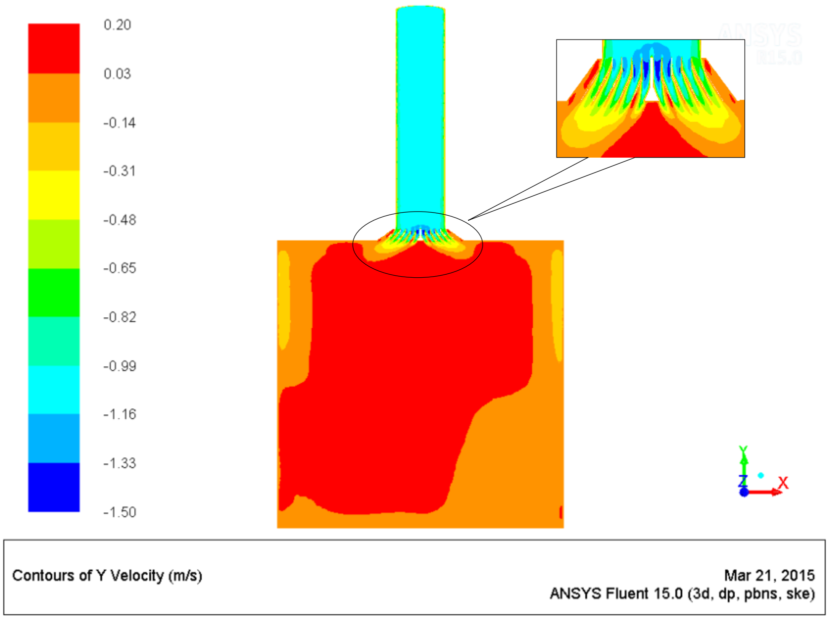

(d)

Figure 4.37: Contours of Y velocity in the room with inlet and outlet on ceiling level: (a) 4-blade, (b) 5-blade, (c) 5-blade with blade angle change, & (d) 7-blade round ceiling air diffuser

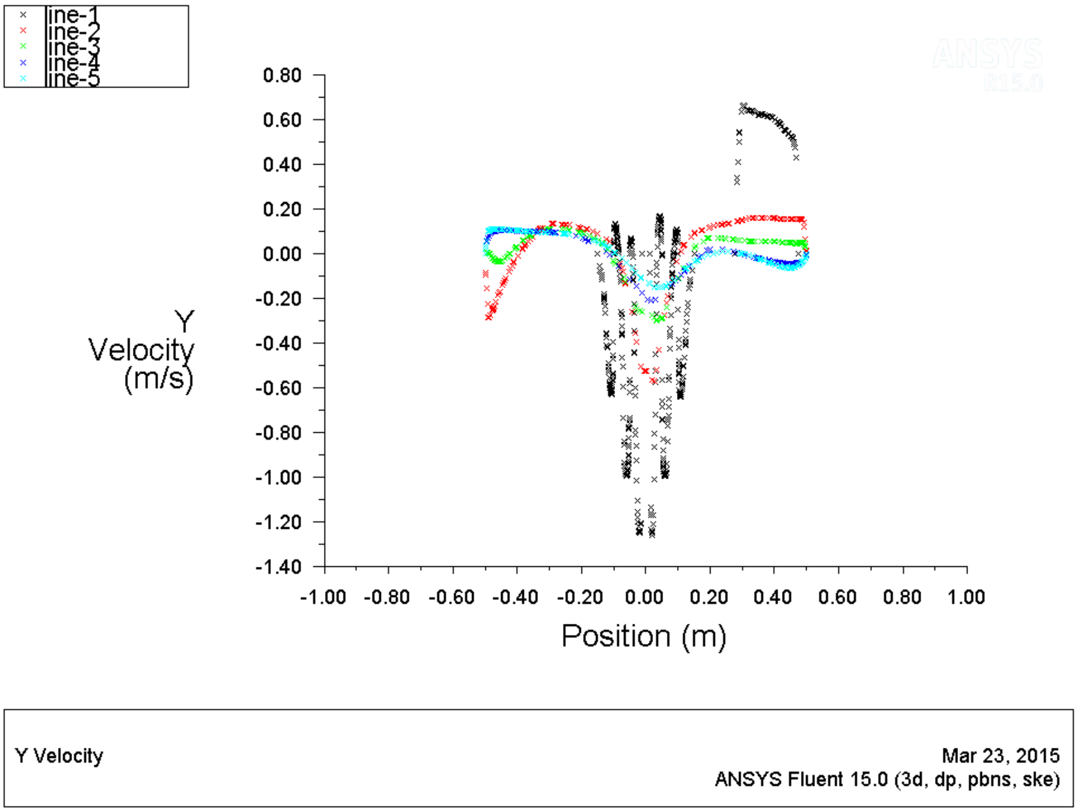
line-1
line-2
line-3
line-4
line-5
Y Velocity (m/s)
Position (m)
Y Velocity
Mar 23, 2015
ANSYS Fluent 15.0 (3d, dp, pbns, ske)

(a)

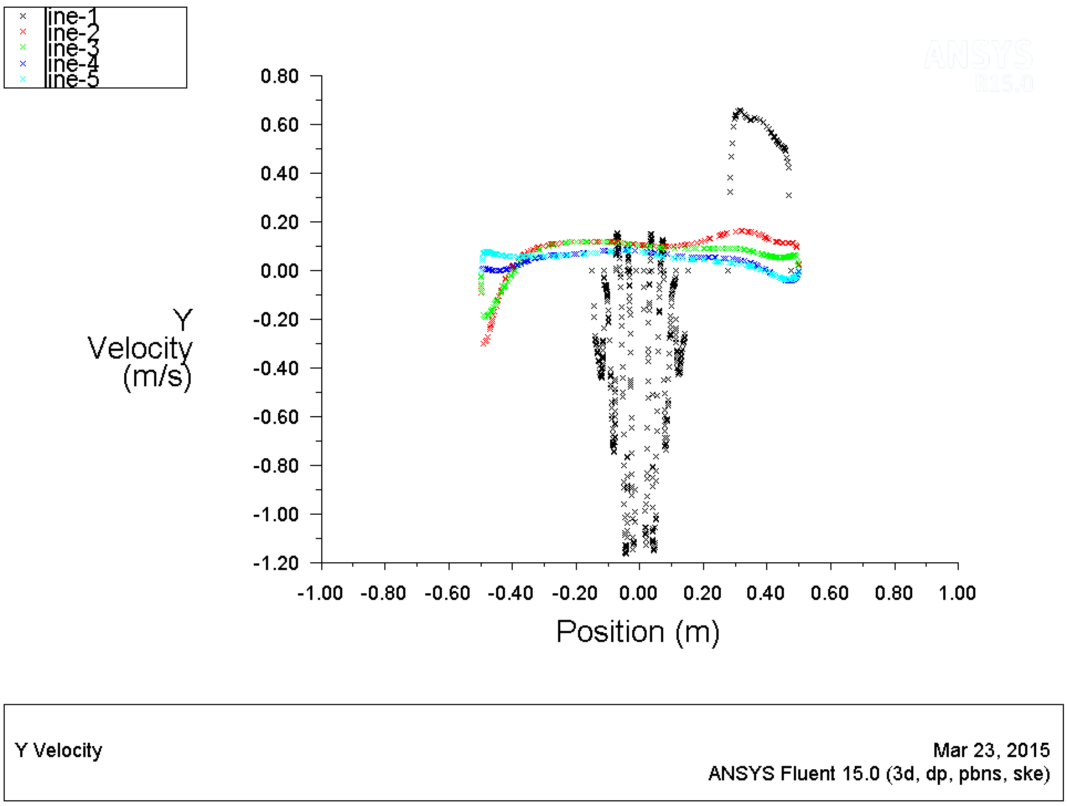
line-1
line-2
line-3
line-4
line-5
Y Velocity (m/s)
Position (m)
Y Velocity
Mar 23, 2015
ANSYS Fluent 15.0 (3d, dp, pbns, ske)

(b)

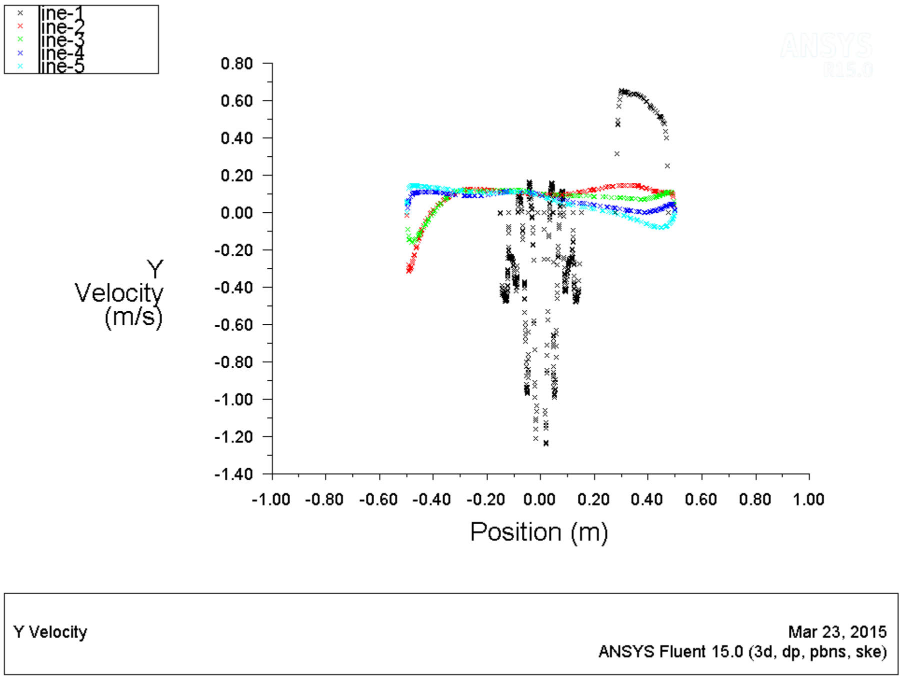

(c)

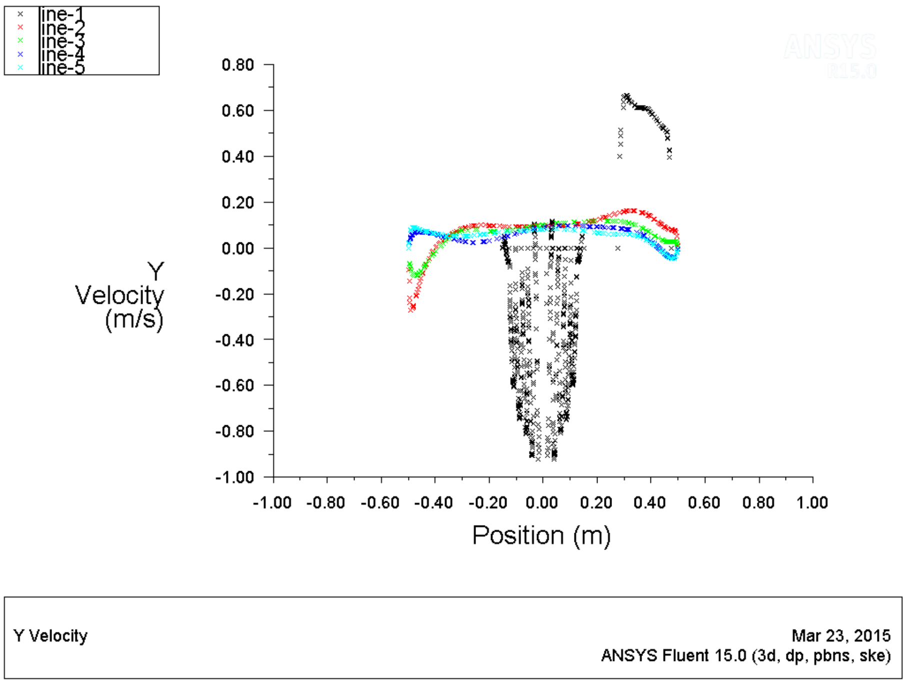

(d)

Figure 4.38: X-Y plots of Y velocity at section lines on *x*-axis extending from the centre of the room to the edge of walls with 1 outlet on ceiling: (a) 4-blade, (b) 5-blade, (c) 5-blade with blade angle change, & (d) 7-blade round ceiling air diffuser

Based on sections (a) of Figures 4.39 and 4.40, the 4-blade/vane round ceiling air diffuser indicated that the temperature distribution was not even throughout the room as most of the distributed air was concentrated around the middle spot of the room due to the reasons as stated in the previous section. The occupants nearby the air diffuser might feel uncomfortable (291.5 – 292.4 K) due to aforesaid uneven air distribution.

From sections (b) of Figures 4.39 and 4.40, the temperature distribution from the 5-blade/vane round ceiling air diffuser was relatively more consistent (292.4 – 294.2 K) throughout the room than that (291.5 – 294.2 K) of 4-blade/vane round ceiling air diffuser (Figures 4.39 (a)) since air flow via the blades of 5-blade air diffuser was uniform. In addition, the occupants nearby the air diffuser might feel comfortable as the air from diffuser was evenly distributed throughout the room without high flow concentration around the air diffuser.

The sections (c) of Figures 4.39 and 4.40 revealed that the air flow distribution from the 5-blade round ceiling air diffuser with an average blade angle of 30° was similar to those of 5-blade round ceiling air diffuser with an average blade angle of 40° in sections (b) of Figures 4.39 and 4.40. However, the air diffuser with 40° blade angle (292.4 – 294.2 K) exhibited slightly consistent temperature distribution than that (293.3 – 294.2 K) of diffusers with 30° blade angle since air flow via the air diffuser with 40° blade angle have lesser contact surface with the air diffuser blades, and was able to flow smoothly if compared with diffuser of 30° blade angle. The air flow of 5-blade round ceiling air diffuser with 30° blade angle was able to distribute effectively throughout the room, leading to a more consistent temperature profile (293.3 – 294.2 K) within the room than that of 4-blade air diffuser (291.5 – 294.2 K) since it provided similar effect if compared to that of 5-blade air diffuser with 40° blade angle. The occupants nearby the air diffuser might not feel uncomfortable as the air from diffuser was uniformly distributed throughout the room without high flow concentration around the air diffuser.

The CFD results of sections (d) of Figures 4.39 and 4.40 for 7-blade/vane round ceiling air diffuser revealed that the temperature distribution (292.4 – 294.2 K) was slightly consistent if compared with that of the 4 (291.5 – 294.2 K) or 5 (292.4 – 294.2

K) blades round ceiling air diffusers since air flow via the 7-blade air diffuser was relatively more equal than that via 4 or 5-blade air diffuser. Meanwhile, the 7-blade air diffuser provided more lower temperature profile of 292.4 – 294.2 K throughout the room (Figure 4.39 (d)) if compared with that of 4 or 5-blade air diffuser, implying that the 7-blade air diffuser might be able to create more thermal comfort for occupants within the room, and assist in reducing energy consumption by the air handling unit to cool the supply air since the air flow rate from the 7-blade air diffuser was relatively higher and was able to distribute to further space uniformly if compared with the other diffusers.

The line 1 of all the X-Y plots in Figure 4.40 reflected that the fluctuation of temperature profile around the centre position due to air flow through the air gap (constricted area) between the air diffuser blades with Venturi effect where air velocity was increased and pressure was reduced, and air velocity could affect the temperature distribution. The temperature profile within the room of lines 2 to 5 for 5 or 7-blade air diffusers reflected that the room temperature was within 293 – 294 K respectively, while velocity profile within the room of lines 2 to 5 for 4-blade air diffuser indicated room temperature up to 289 K around centre position due to uneven air distribution.

Furthermore, the temperature distribution of 5 and 7-blade air diffusers with one outlet on ceiling level were slightly consistent if compared with that of round diffuser achieved by Mohammed (2013) as displayed in Figure 2.13 since the air flow via the blades of proposed diffusers was relatively more uniform distributed, and lesser contact between the air flow and blade surfaces.

Although the model with air outlet on ceiling level might be able to provide effective air flow behaviour and temperature distribution throughout the room, it was not as consistent as those models with air outlets near bottom of walls as it directed the air from the inlet to the outlet which was close to each other on the ceiling level, and hence the air might be stagnant around the bottom space of the room before it could be circulated (Figures 4.37). The aforesaid scenario is short circuit of air occurred if the position of inlet and outlet is very close to each other, where the air will be extracted from the room immediately instead of being distributed throughout the room. Thus, the position of air outlet should be diligently located on the ceiling space and apart from any air inlet by around 1.5 – 2 m as recommended by the diffuser manufacturers.

The range of velocity magnitude, Y velocity and static temperature distribution within the room for each model with one outlet on ceiling level are summarised in Table 4.8.

Table 4.8: Range of velocity magnitude, Y velocity and static temperature distribution within the room with one outlet on ceiling level

Item	Diffuser Model			
	4-blade	5-blade (40°)	5-blade (30°)	7-blade
Velocity Magnitude (m/s)	0 – 0.90	0 – 0.60	0 – 0.60	0 – 0.60
Y Velocity (m/s)	-0.82 – 0.20	-0.14 – 0.20	-0.14 – 0.20	-0.14 – 0.20
Static Temperature (K)	291.5 – 294.2	292.4 – 294.2	293.3 – 294.2	292.4 – 294.2

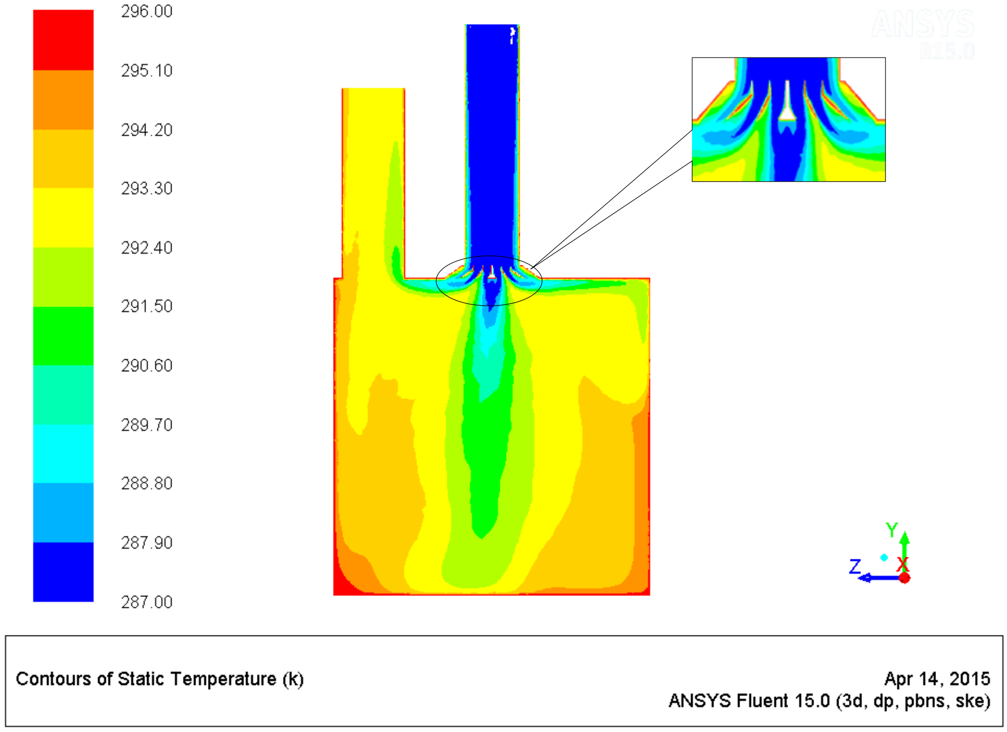
296.00
295.10
294.20
293.30
292.40
291.50
290.60
289.70
288.80
287.90
287.00
Y
Z
X
Contours of Static Temperature (k)
Apr 14, 2015
ANSYS Fluent 15.0 (3d, dp, pbns, ske)

(a)

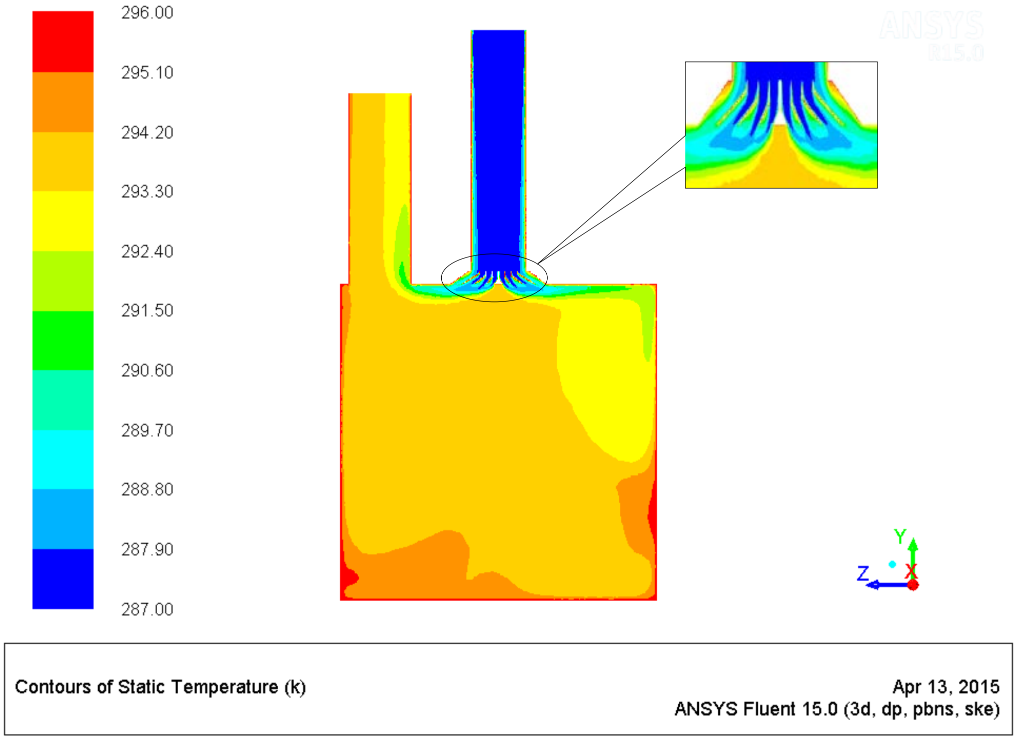
296.00
295.10
294.20
293.30
292.40
291.50
290.60
289.70
288.80
287.90
287.00
Y
Z
X
Contours of Static Temperature (k)
Apr 13, 2015
ANSYS Fluent 15.0 (3d, dp, pbns, ske)

(b)

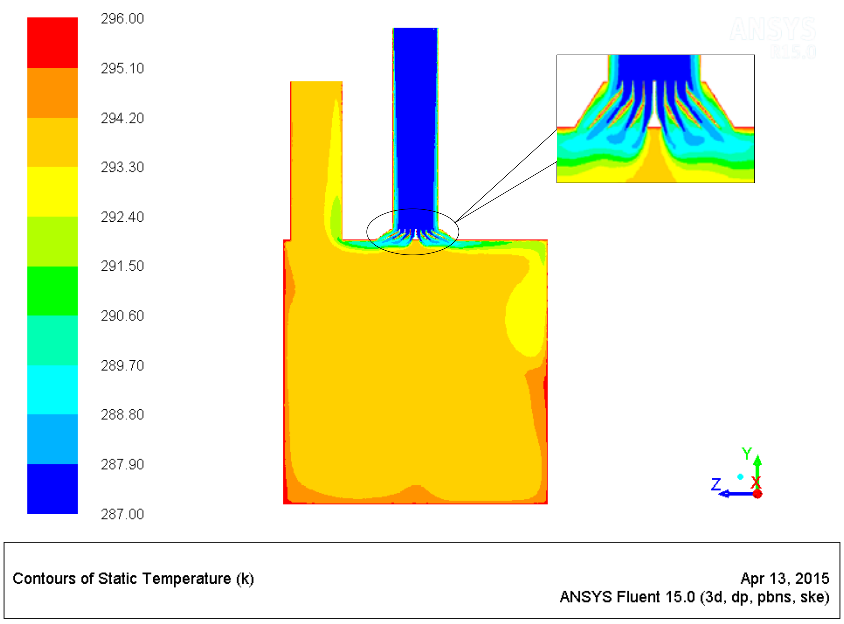

(c)

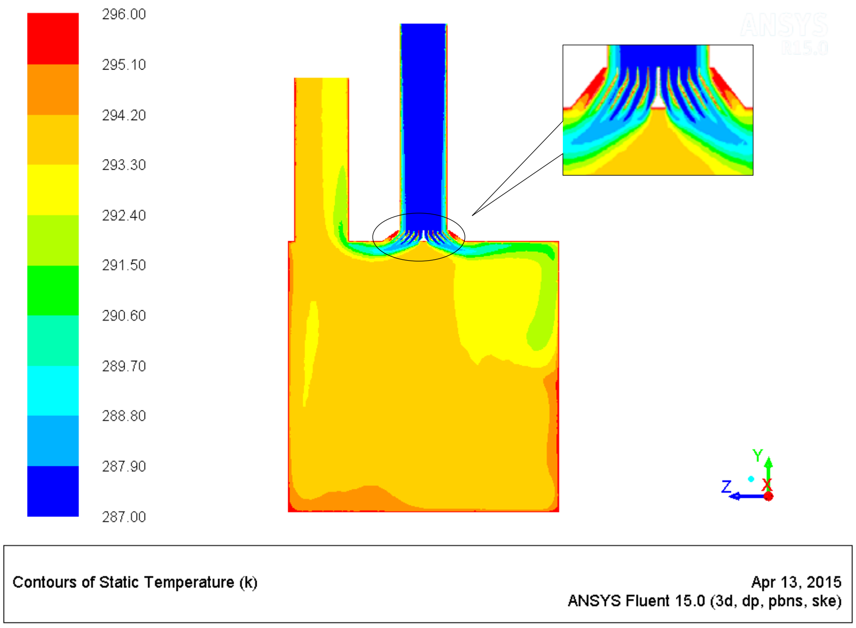

(d)

Figure 4.39: Contours of static temperature in the room with inlet and outlet on ceiling level: (a) 4-blade, (b) 5-blade, (c) 5-blade with blade angle change, & (d) 7-blade round ceiling air diffuser

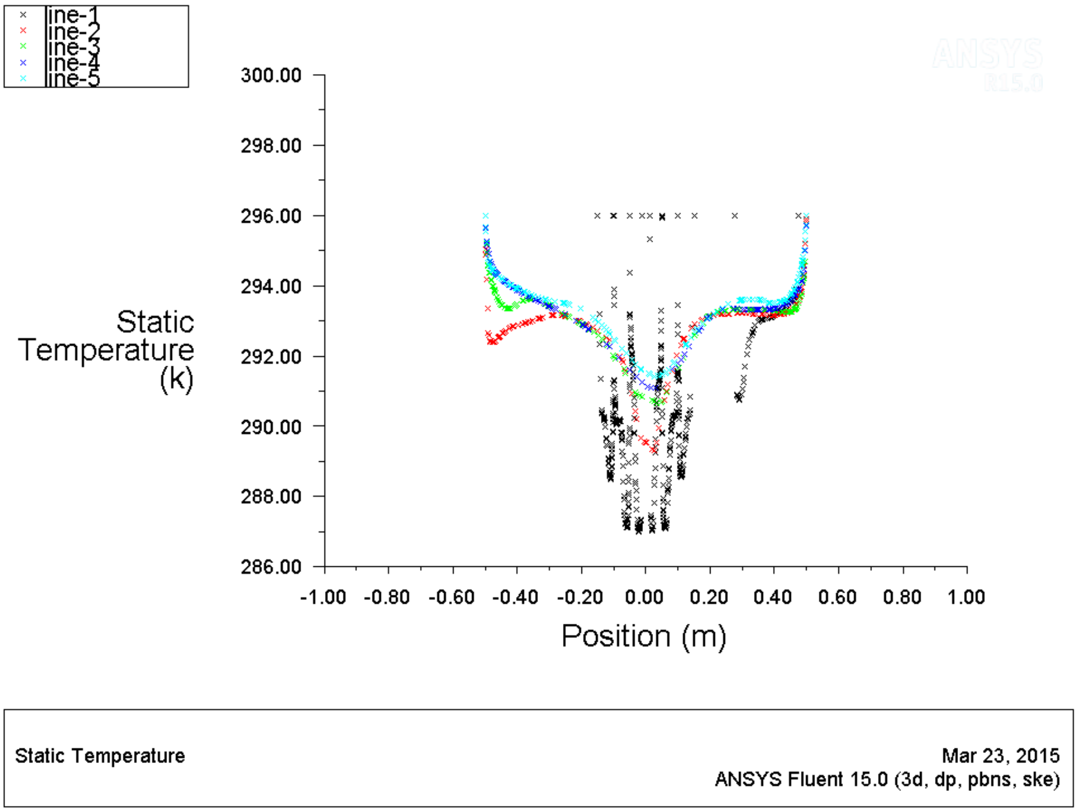
line-1
line-2
line-3
line-4
line-5
ANSYS
R15.0
Static Temperature (k)
300.00
298.00
296.00
294.00
292.00
290.00
288.00
286.00
-1.00 -0.80 -0.60 -0.40 -0.20 0.00 0.20 0.40 0.60 0.80 1.00
Position (m)
Static Temperature
Mar 23, 2015
ANSYS Fluent 15.0 (3d, dp, pbns, ske)

(a)

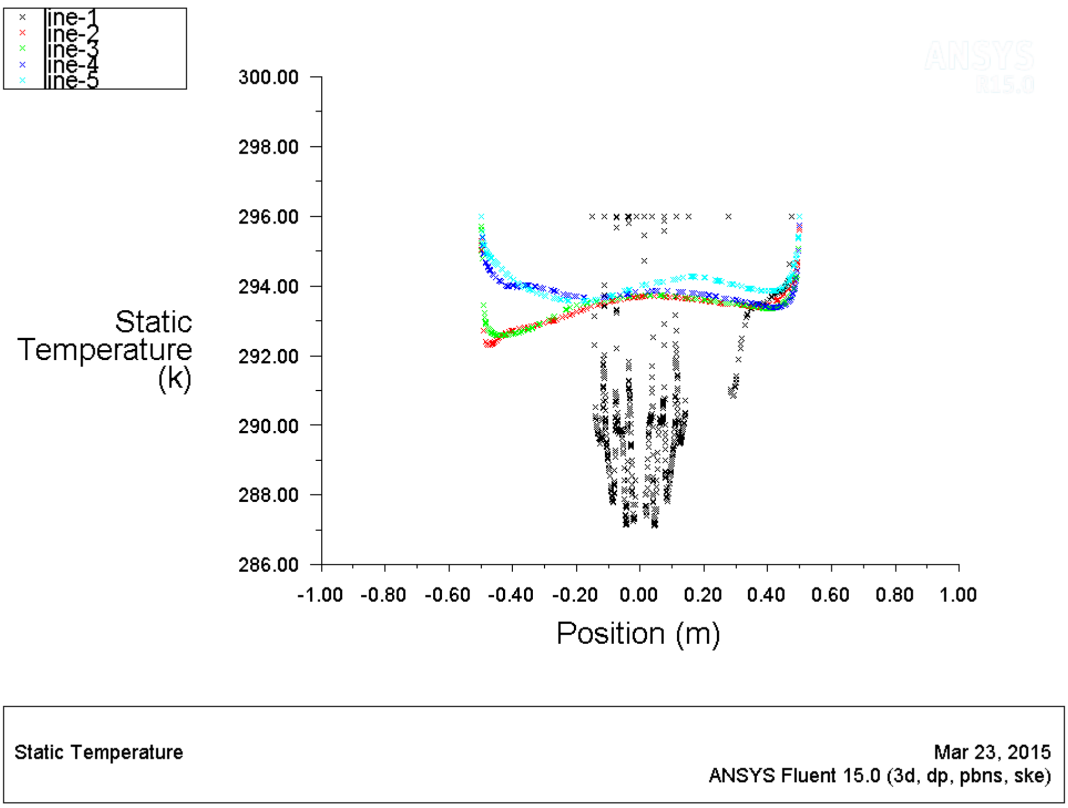
line-1
line-2
line-3
line-4
line-5
ANSYS
R15.0
Static Temperature (k)
300.00
298.00
296.00
294.00
292.00
290.00
288.00
286.00
-1.00 -0.80 -0.60 -0.40 -0.20 0.00 0.20 0.40 0.60 0.80 1.00
Position (m)
Static Temperature
Mar 23, 2015
ANSYS Fluent 15.0 (3d, dp, pbns, ske)

(b)

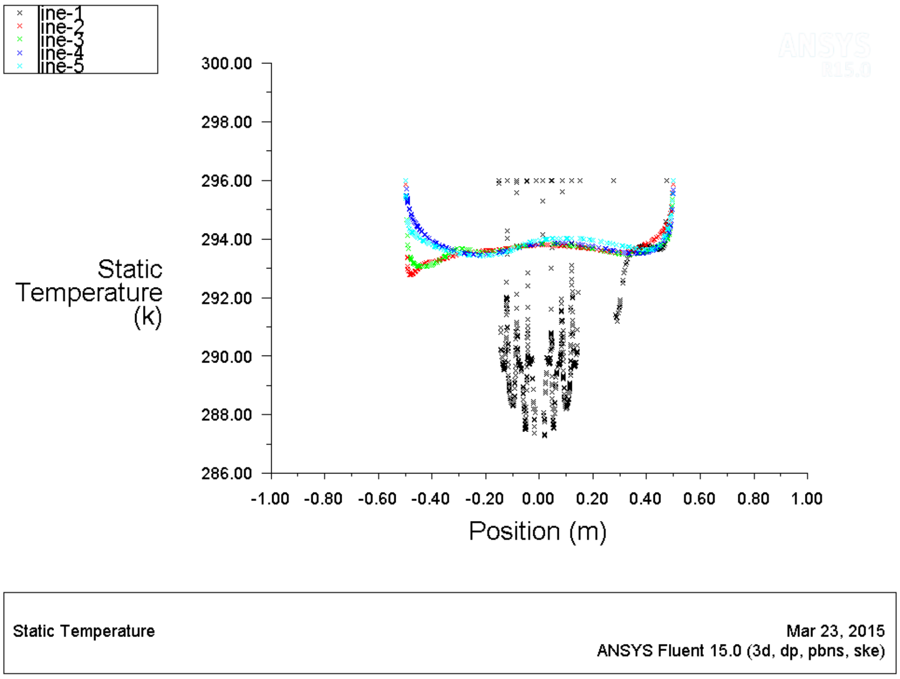

(c)

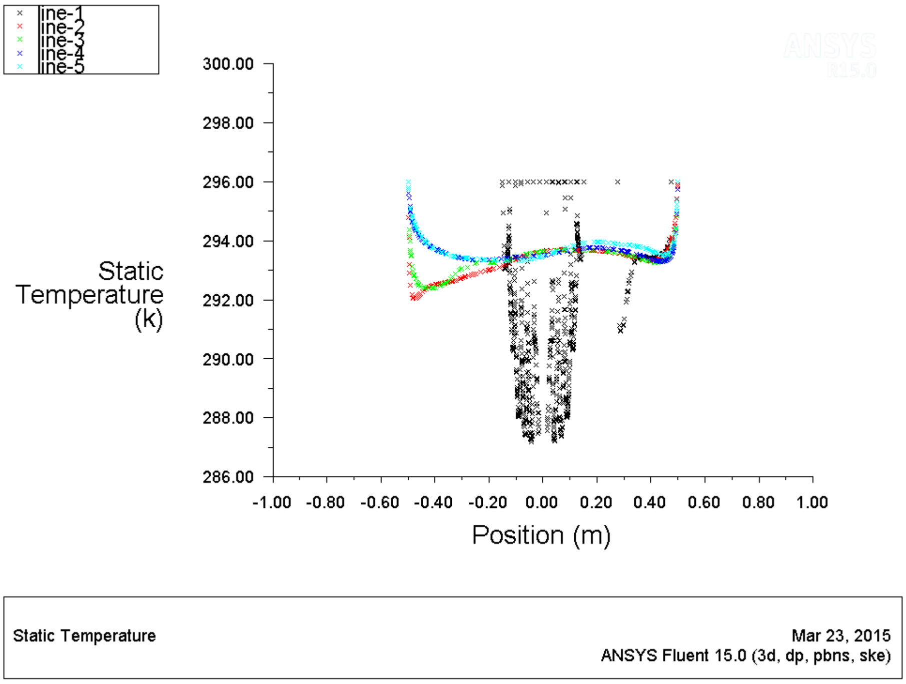

(d)

Figure 4.40: X-Y plots of static temperature at section lines on *x*-axis extending from the centre of the room to the edge of walls with 1 outlet on ceiling: (a) 4-blade, (b) 5-blade, (c) 5-blade with blade angle change, & (d) 7-blade round ceiling air diffuser

4.2 The dimensionless average room air velocity or temperature with Reynolds number

The relationship of dimensionless average room air velocity or temperature with Reynolds number was only discussed for 5 and 7-blade round ceiling air diffuser with 2 outlets near bottom of walls in this section since the 5 and 7-blade air diffusers provided relatively more consistent results than other diffuser models. The graphs were plotted for dimensionless average room velocity (V_a/V_i) or temperature (T_a/T_i) with Reynolds number (R*e*).

From Figure 4.41, the dimensionless average room velocity (V_a/V_i) for both 5 and 7-blade round air diffuser increased with Reynolds number, respectively since the average room air flow rate increased, resulting in increase in the dimensionless average room velocity. It was also observed that the dimensionless average room velocity of 7-blade air diffuser (approximate 11 – 14 %) increased slightly higher than that of 5-blade air diffuser since the air flow distribution from 7-blade air diffuser was slightly uniform than that of 5-blade air diffuser. The results of dimensionless average room velocity in this project were compatible with the CFD simulation predicted results on the velocity magnitude or Y velocity in the previous sections, where the average room air flow rate increased with increasing inlet velocity. The working detail tabulation of dimensionless average room velocity and Reynolds number can be found in Appendix C.1.

Furthermore, the dimensionless average room air velocity of both 5 and 7-blade air diffusers increased slightly more than that of round air diffuser obtained by Aziz et al. (2012) as illustrated in Figure 2.11. Thus, the proposed diffusers might be able to supply relatively higher air flow rate than that of previous study.

In Figure 4.42, the dimensionless average room temperature (T_a/T_i) for both 5 and 7-blade air diffusers were reduced, while the Reynolds number increased with the inlet velocity. On the other hand, the dimensionless average room temperature of 7-blade air diffuser (approximate 0.2 – 0.3 %) was reduced slightly more than that of 5-blade air diffuser, where colder room air temperature distribution could be provided by the 7-blade air diffuser, possibly assisting in reducing energy consumption by the air handling unit to cool the supply air. The results of dimensionless average room temperature in this project were compatible with the CFD simulation predicted results on the static temperature in the previous sections, where the average room air temperature could be reduced with increase of the inlet velocity. The working detail tabulation of dimensionless average room temperature and Reynolds number can be found in Appendix C.2.

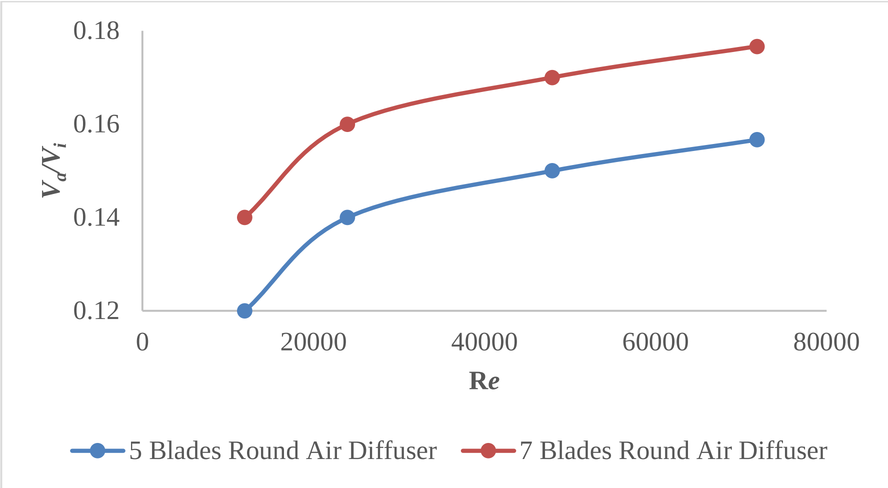

Figure 4.41: Dimensionless average room air velocity V_a/V_i with various inlet velocities and Reynolds numbers at inlet at same inlet air temperature

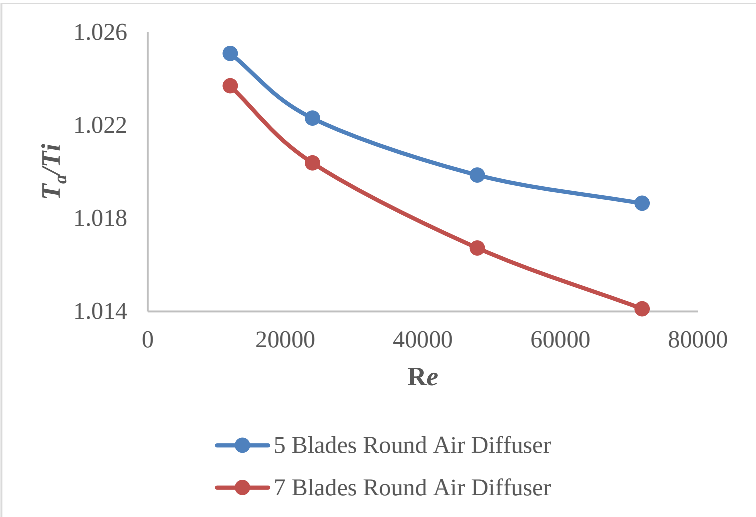

Figure 4.42: Dimensionless average room temperature T_a/T_i with various inlet velocities and Reynolds numbers at inlet at same inlet temperature

Furthermore, the dimensionless average room air temperature of both 5 and 7-blade round diffusers were lower than that of round air diffuser obtained by Aziz et al. (2012) and Mohammed (2013) as depicted in Figures 2.11 and 2.15, respectively. However, the proposed diffusers did not cause the room air temperature to be very low and make the occupants feel cold or uncomfortable if compared to previous study.

4.3 The overall ventilation effectiveness and effective draft temperature

The evaluations on overall ventilation effectiveness and effective draft temperature (*EDT*) were performed on 5 and 7-blade round ceiling air diffusers with 2 outlets near bottom of walls in this section since the 5 and 7-blade air diffusers provided relatively more consistent results than other diffuser models. The graphs were plotted for overall ventilation effectiveness and effective draft temperature with Reynolds number.

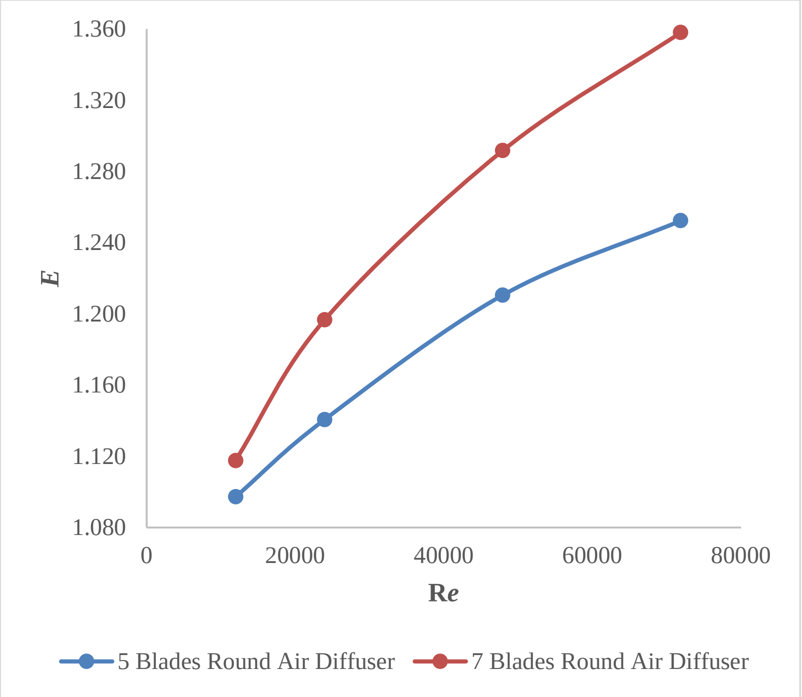

Figure 4.43: The overall ventilation effectiveness (*E*) in the room with various inlet velocities and Reynolds numbers at inlet at same inlet temperature

From Figure 4.43, the overall ventilation effectiveness in room increased with the Reynolds number, and 7-blade round air diffuser had higher overall ventilation effectiveness (approximate 2.2 – 3 %) than that of 5-blade round air diffuser. Since most of the calculated values of overall ventilation effectiveness were more than 1, it was denoted that the air distribution from 5 or 7- blade air diffusers were effective ventilation as stated in Section 3.7, leading to energy utilised for supplying the conditioned air via these diffusers was able to achieve satisfactory thermal comfort within the room. Besides, the 7-blade air diffuser could achieve effective energy utilisation that was slightly more than that of 5-blade air diffuser since the 7-blade air diffuser could provide more uniform air flow distribution within the room.

In addition, the levels of overall ventilation effectiveness of proposed 5 and 7-blade air diffusers were relatively higher if compared with that obtained by Aziz et al. (2012) as presented in Figure 2.12. Hence, the proposed diffusers could achieve effective air distribution for ventilation and energy utilisation that was slightly efficient than that of round diffuser achieved by Aziz et al. (2012).

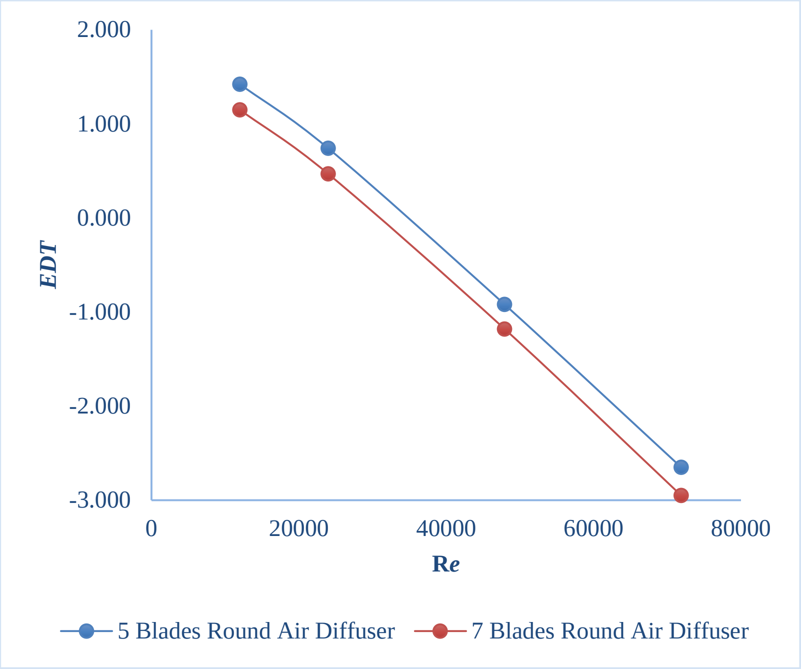

Figure 4.44: The effective draft temperature (*EDT*) in the room with various inlet velocities and Reynolds numbers at inlet

From Figure 4.44, the *EDT* in room was reduced with increase of Reynolds number, and the 7-blade air diffuser had lower *EDT* (approximate 19 – 22 %) than that of 5-blade round air diffuser. Meanwhile, the *EDTs* for inlet air velocity at 1.0 and 2.0 m/s ranged between -1.7 and 1.1, which was considered as thermal comfort zone as stated in Section 2.2.1. However, the *EDTs* for inlet air velocity at 0.5 and 3.0 m/s were out of the thermal comfort zone. Therefore, the proposed 5 and 7-blade air diffusers were able to achieve thermal comfort within the room for inlet air velocity at 1.0 and 2.0 m/s, whereas the 7-blade air diffuser could achieve room temperature that was slightly lower than that of 5-blade air diffuser since the 7-blade air diffuser could provide more uniform air flow distribution within the room. In addition, the optimum thermal comfort zone could be achieved based on inlet velocity at 1 m/s and inlet temperature of 287 K for both 5 and 7-blade air diffusers with an *EDT* range of 0 – 1.1.

Furthermore, the *EDT* values of the proposed 5 and 7-blade air diffusers with inlet air velocity at 1.0 and 2.0 m/s was relatively higher if compared with the *EDT* of round air diffuser obtained by Aziz et al. (2012) as showed in Figure 2.12, indicating that the lower room temperature was achieved compared to this project.

CHAPTER 5

CONCLUSIONS AND RECOMMENDATIONS

5.1 Conclusions

The study has revealed that the issue of uneven air distribution occurred at the existing 4-blade round ceiling air diffuser was due to high volumetric flow rate or static pressure around the air gap of the central core blades where the air tended to release from the air diffuser within the shorter distance as identified via CFD simulation. This defect was minimised by the proposed 5 and 7-blade round ceiling air diffusers with an average blade angle of 40°, which were able to improve the air flow behaviours and temperature distribution within the room as revealed by the CFD predicted results according to the various parameters such as diffuser blades configuration, blade angles, air outlets position, inlet air velocities and air temperatures.

The CFD results identified that the performance of 5-blade air diffuser with an average blade angle of 30° might be not as effective as that of 5-blade air diffuser with an average blade angle of 40° because the air flow via the air diffuser with 40° blade angle was relatively more uniform and smoother than that of diffuser with 30° blade angle, and the air flow had lesser direct impact with the blade surface sloped at 40° blade angle.

By increasing the inlet velocity to 1.0, 2.0 or 3.0 m/s or reducing the inlet temperature to 285 or 287 K, cooler air could be supplied by the proposed air diffusers and mainly via the 7-blade air diffuser since it could allow relatively more consistent air flow distribution compared to the 5–blade air diffuser. Hence, it is concluded that the proposed air diffusers would be capable of achieving required thermal comfort and assisting in reducing energy consumption by air handling unit for cooling the supply air at 1.0 or 2.0 m/s inlet velocity and 285 or 287 K inlet temperature if compared with the 4-blade air diffuser or those round air diffusers studied by others. In addition, the CFD results of the proposed air diffusers were compatible with those of the dimensionless average room velocity and temperature, as well as overall ventilation effectiveness and *EDT*.

Furthermore, the proposed air diffusers with two air outlets near the bottom of walls were able to provide slightly more effective air flow pattern and temperature distribution within the room if compared with that of one outlet either near the bottom of wall or on the ceiling level since the air flow could be directed to the respective outlet equally throughout the room.

In summary, the proposed model of 7-blade round ceiling air diffuser with 2 outlets near the bottom of walls could achieve optimal thermal comfort environment in a room at 1.0 m/s inlet velocity and 287 K inlet temperature.

Least or not last, these project results can be useful reference data for any air diffuser designer to exploit further whether it can be used for developing new air diffuser configuration that can assist in reducing energy consumption by air handling unit for cooling supply air, while the air flow throw length is enhanced to further location which is further than those of similar type of diffusers, and the thermal comfort level required is not compromised.

5.2 Future work

Future work can be feasibility study on whether the performance of proposed air diffusers can maintain the room relative humidity at 50 – 60% RH according to ASHRAE design guideline as indicated on Appendix A for avoiding electrostatic condition due to very dry air or mould grow due to very moisture air.

Feasibility study can also be conducted on whether the proposed air diffusers can generate the noise level at NC 40 – 50 according to ASHRAE design guideline as indicated on Appendix A for not affecting any occupant’s audibility to ensure that the proposed diffusers can meet the requirement of aforesaid criteria as desired, in addition to the thermal comfort requirement.

Furthermore, the CFD predicted data obtained in this project can be verified or validated with the experimental results of the tested prototype models for supporting the statement of achieving the optimum room condition by the proposed air diffusers.

REFERENCES

ANSYS. (2015, January). Retrieved January 26, 2015, from ANSYS Web site: http://www.ansys.com/Industries/Academic.

ASHRAE (2013). *ASHRAE Standard – Ventilation for Acceptable Indoor Air Quality*, pp. 16.

ASHRAE (2005). *ASHRAE Pocket Guide for Air Conditioning, Heating, Ventilation, Refrigeration (SI Edition)*, pp. 244-245.

Aziz, MA, Gad, IAM, Mohammed, ESFA, & Mohammed, RH, 2012. Experimental and numerical study of influence of air ceiling diffusers on room air flow characteristics. *Energy and Buildings*, [e-journal] 55 (4), pp. 738-746.

Claude-Alain Roulet (2008), *Ventilation and Airflow in Buildings - Methods for Diagnosis and Evaluation,* Earthscan, 1st Edition, pp. 40.

Halton (2014). Retrieved February 5, 2015, from Halton Web site: http://www.halton.be/halton/images.nsf/files/CCB396F99CD34748C22571D9004B122E/$file/linear_slot_diffusers_en.pdf.

Hart & Cooley (2014). Retrieved February 5, 2015, from Hart & Cooley Web site: http://www.hartandcooley.com/grilles-registers-and-diffusers-grd/commercial-grds/ceiling-diffusers.

Hart & Cooley (2014). Retrieved February 5, 2015, from Hart & Cooley Web site: http://www.limaregister.com/products/1400-al1400/square-rectangular-ceiling-diffuser.

HC Barcol-Air. (2012). Retrieved February 5, 2015, from HC Barcol-Air Web site: http://barcolair.nl/airdistribution.asp.

JPR Services (2015). Retrieved February 5, 2015, from JPR Services Web site: http://jprservices.co.uk/wp-content/uploads/2013/06/DWS-Brochure-JPR.pdf.

Mohammed, RH, 2013. A simplified method for modelling of round and square ceiling diffusers. *Energy and Buildings*, [e-journal] 64, pp. 473-482.

Moukalled, F, Verma, S, & Darwish, M, 2011. The use of CFD for predicting and optimising the performance of air conditioning equipment. *International Journal of Heat and Mass Transfer,* [e-journal] 54 (1-3), pp. 549-563.

PrudentAire. (2014). Retrieved February 5, 2015, from PrudentAire Web site: http://www.prudentaire.com/product_pdf/Supply_Air_Diffusers.pdf.

PrudentAire. (2014). Retrieved February 5, 2015, from PrudentAire Web site: http://www.prudentaire.com/images/pdf/Swirl_Diffuser.pdf.

PrudentAire. (2014). Retrieved February 5, 2015, from PrudentAire Web site: http://www.prudentaire.com/images/pdf/Jet_Diffuser.pdf.

Ruskin. (2014, June). Retrieved February 3, 2015, from Ruskin Web site: http://www.air-diffusion.co.uk/PDF/Circular_Diffusers.pdf.

Sajadi, B, Saidi, MH, & Mohebbian, A, 2011. Numerical investigation of the swirling air diffuser: Parametric study and optimization. *Energy and Buildings,* [e-journal] 43 (6), pp. 1329-1333.

Scottaire. (2014). Retrieved February 3, 2015, from Scottaire Web site: http://www.scottaire.co.uk/linearslot2.html.

Stamou, A, & Katsiris, I, 2006. Verification of a CFD model for indoor airflow and heat transfer. *Building and Environment,* [e-journal] 41 (9), pp. 1171-1181.

Sun, Y, & Smith, TF, 2005. Air flow characteristics of a room with square cone diffusers. *Building and Environment,* [e-journal] 40 (5), pp. 589-600.

Tavakoli, E, & Hosseini, R, 2013. Large eddy simulation of turbulent flow and mass transfer in far-field of swirl diffusers. *Energy and Buildings,* [e-journal] 59, pp. 194-202.

Wang, H, & Zhai, Z, 2012. Analyzing grid independency and numerical viscosity of computational fluid dynamics for indoor environment applications. *Building and Environment*, [e-journal] 52, pp. 107-118.

Zhao, B, Li, X, & Yan, Q, 2003. A simplified system for indoor airflow simulation. *Building and Environment*, [e-journal] 38 (4), pp.543-552.

APPENDICES

APPENDIX A: ASHRAE design guideline on room temperature and relative humidity (ASHRAE, 2005)

General Design Criteria

General Category	Specific Category	Inside Design Conditions: Winter	Inside Design Conditions: Summer	Air Movement	Circulation, air changes per hour
Dining and Entertainment Centers	Cafeterias and Luncheonettes	21 to 23°C 20 to 30% rh	26°C 50% rh	0.25 m/s at 1.8 m above floor	12 to 15
	Restaurants	21 to 23°C 20 to 30% rh	23 to 26°C 55 to 60% rh	0.13 to 0.15 m/s	8 to 12
	Bars	21 to 23°C 20 to 30% rh	23 to 26°C 50 to 60% rh	0.15 m/s at 1.8 m above floor	15 to 20
	Nightclubs and Casinos	21 to 23°C 20 to 30% rh	23 to 26°C 50 to 60% rh	below 0.13 m/s at 1.5 m above floor	20 to 30
	Kitchens	21 to 23°C	29 to 31°C	0.15 to 0.25 m/s	12 to 15
Office Buildings		21 to 23°C 20 to 30% rh	23 to 26°C 50 to 60% rh	0.13 to 0.23 m/s 4 to 10 L/(s·m²)	4 to 10
Museums, Libraries, and Archives	Average	20 to 22°C 40 to 55% rh		below 0.13 m/s	8 to 12
	Archival	(Specific Requirements)		below 0.13 m/s	8 to 12
Bowling Centers		21 to 23°C 20 to 30% rh	24 to 26°C 50 to 55% rh	0.25 m/s at 1.8 m above floor	10 to 15
Communication Centers	Telephone Terminal Rooms	22 to 26°C 40 to 50% rh	22 to 26°C 40 to 50% rh	0.13 to 0.15 m/s	8 to 20
	Radio and Television Studios	21 to 23°C 40 to 50% rh	23 to 26°C 45 to 55% rh	0.13 to 0.15 m/s	15 to 40
Transportation Centers	Airport Terminals	23 to 26°C 30 to 40% rh	23 to 26°C 40 to 55% rh	below 0.13 m/s at 3.7 m above floor	8 to 12
	Ship Docks	21 to 23°C 20 to 30% rh	23 to 26°C 50 to 60% rh	0.13 to 0.15 m/s at 1.8 m above floor	8 to 12
	Bus Terminals	21 to 23°C 20 to 30% rh	23 to 26°C 50 to 60% rh	0.13 to 0.15 m/s at 1.8 m above floor	8 to 12
	Garages	4 to 13°C	27 to 38°C	0.15 to 0.38 m/s	4 to 6
Warehouses		Often depend on the materials stored.			1 to 4

General Design Criteria

Noise	Filtering Efficiencies (ASHRAE *Standard* 52.1)	Load Profile	Comments
NC 40 to 50	35% or better	Peak at 1 to 2 P.M. 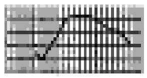	Prevent draft discomfort for patrons waiting in serving lines
NC 35 to 40	35% or better	Peak at 1 to 2 P.M. 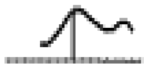	
NC 35 to 50	Use charcoal for odor control with manual purge control for 100% outside air to exhaust ±35% prefilters	Peak at 5 to 7 P.M. 	
NC 35 to 45[f]	Use charcoal for odor control with manual purge control for 100% outside air to exhaust ±35% prefilters	Nightclubs peak at 8 P.M. to 2 A.M. Casinos peak at 4 P.M. to 2 A.M. Equipment, 24 h/day	Provide good air movement but prevent cold draft discomfort for patrons
NC 40 to 50	10 to 15% or better	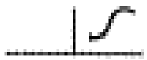	Negative air pressure required for odor control. (See also Chapter 30, Kitchen Ventilation.)
NC 30 to 45	35 to 60% or better	Peak at 4 P.M. 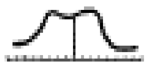	
NC 35 to 40	35 to 60% or better	Peak at 3 P.M. 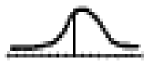	
NC 35	35% prefilters plus charcoal filters 85 to 95% final	Peak at 3 P.M. 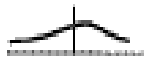	
NC 40 to 50	10 to 15%	Peak at 6 to 8 P.M. 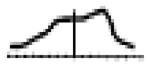	
to NC 60	85% or better	Varies with location and use	Constant temperature and humidity required
NC 15 to 25	35% or better	Varies widely due to changes in lighting and people	Constant temperature and humidity required
NC 35 to 50	35% or better and charcoal filters	Peak at 10 A.M. to 9 P.M. 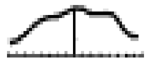	Positive air pressure required in terminal
NC 35 to 50	10 to 15%	Peak at 10 A.M. to 5 P.M. 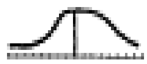	Positive air pressure required in waiting area
NC 35 to 50	35% with exfiltration	Peak at 10 A.M. to 5 P.M. 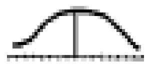	Positive air pressure required in terminal
NC 35 to 50	10 to 15%	Peak at 10 A.M. to 5 P.M. 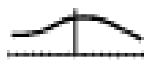	Negative air pressure required to remove fumes; positive air in pressure adjacent occupied spaces
to NC 75	10 to 35%	Peak at 10 A.M. to 3 P.M. 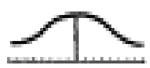	

APPENDIX B: Velocity vectors in the room for each diffuser models

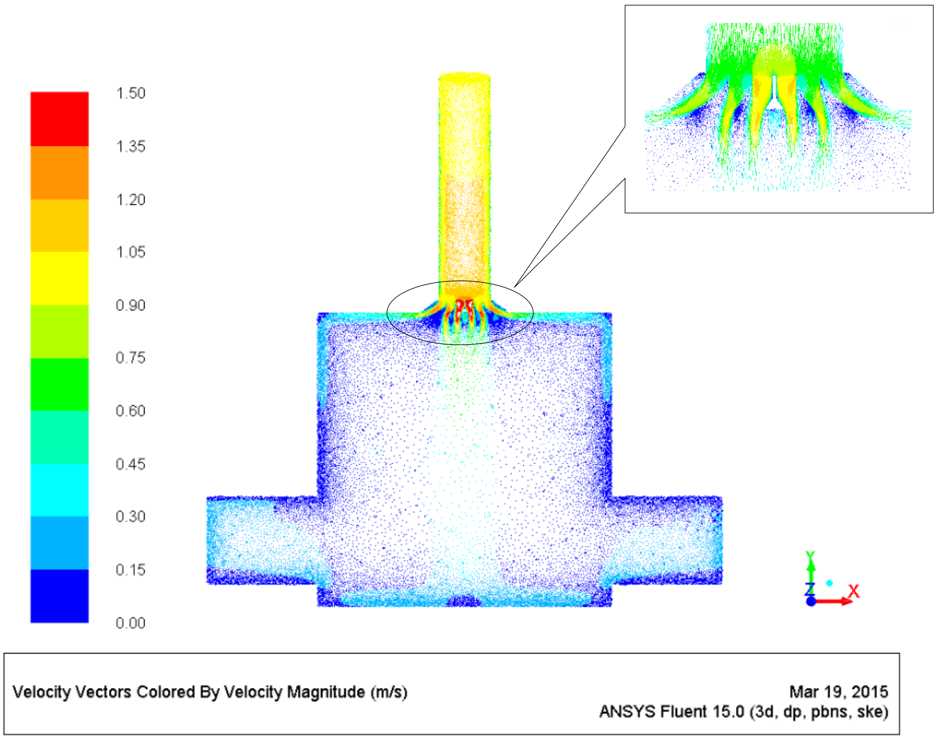

(a)

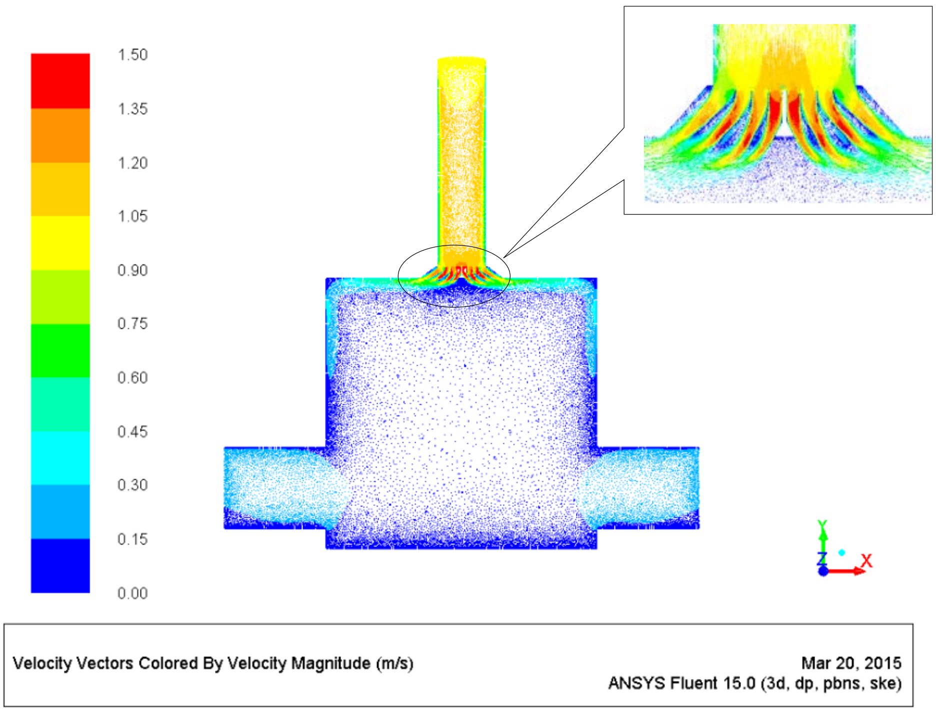

(b)

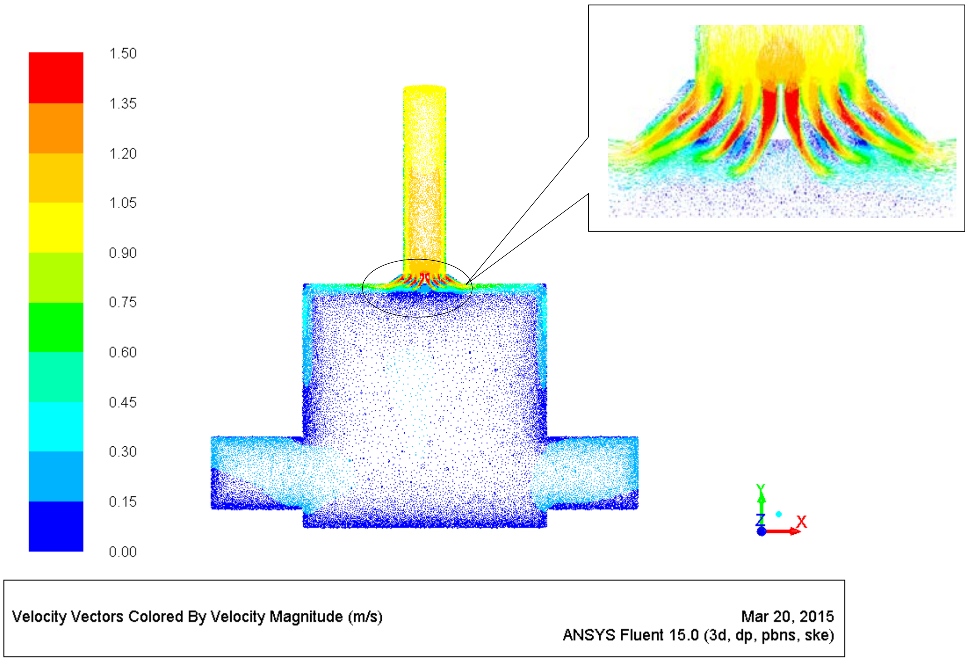

(c)

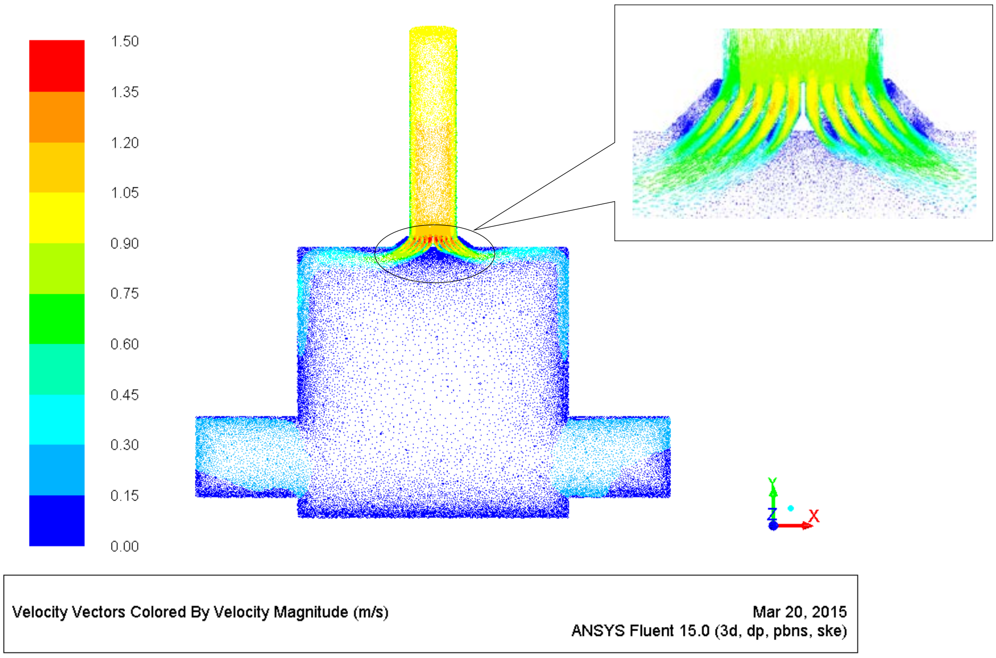

(d)

Figure B.1: **Velocity vectors in the room with inlet on ceiling and 2 outlets near wall bottoms: (a) 4-blade, (b) 5-blade, (c) 5-blade with blade angle change, & (d) 7-blade round ceiling air diffuser**

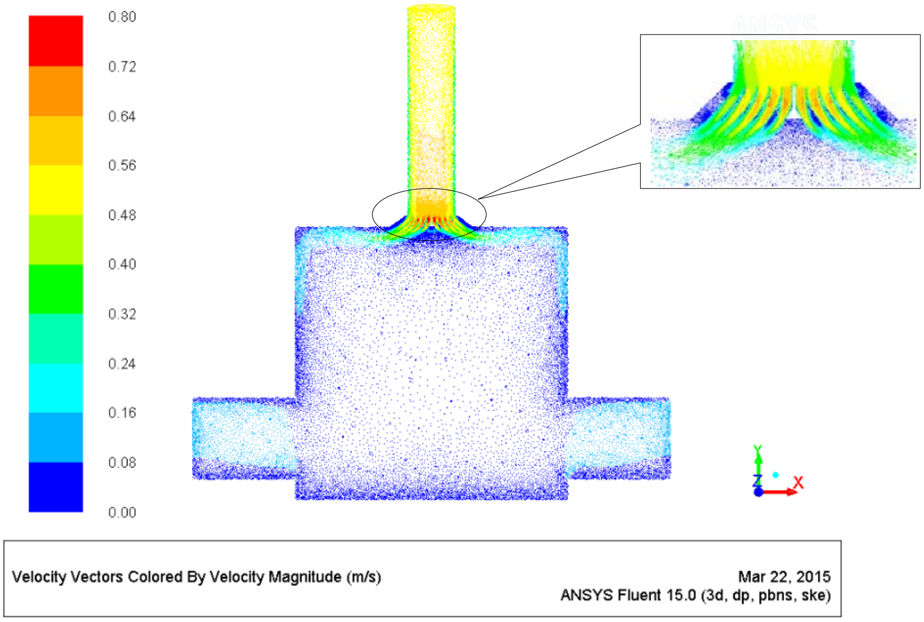

(a)

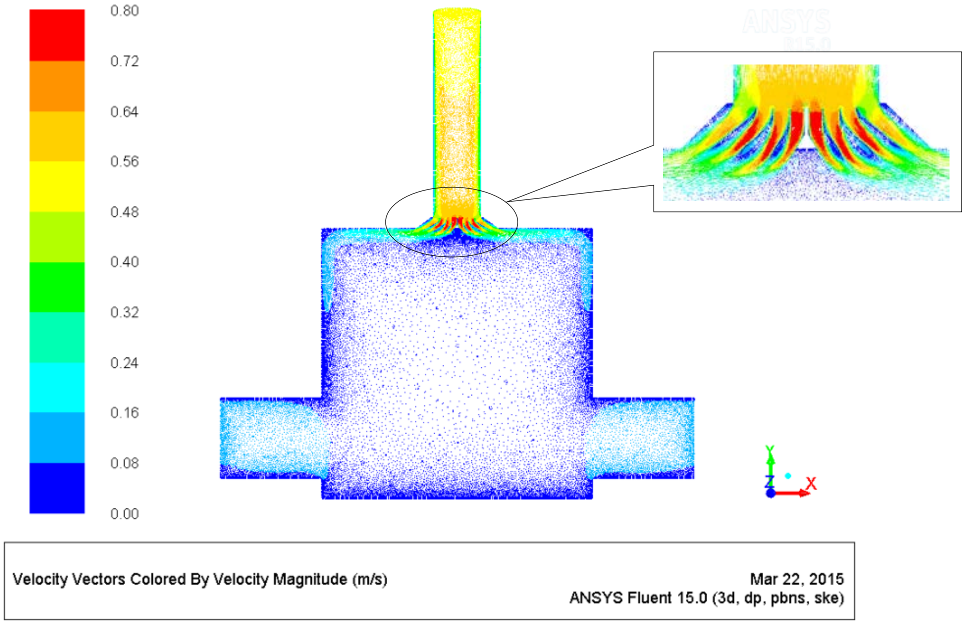

(b)

Figure B.2: **Velocity vectors in the room with inlet on ceiling and 2 outlets near wall bottoms at 0.5 m/s inlet velocity: (a) 7-blade, & (b) 5-blade round ceiling air diffuser**

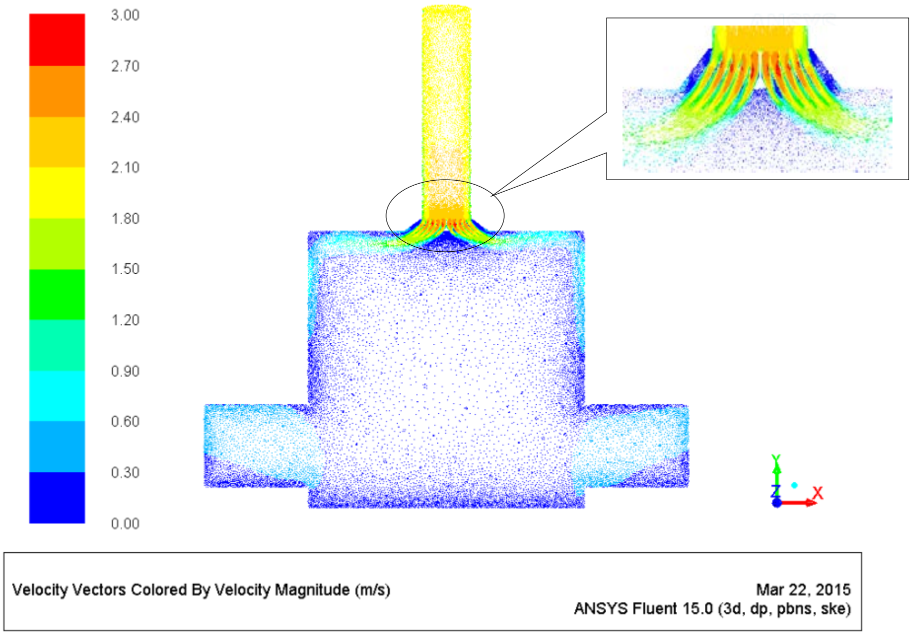

(a)

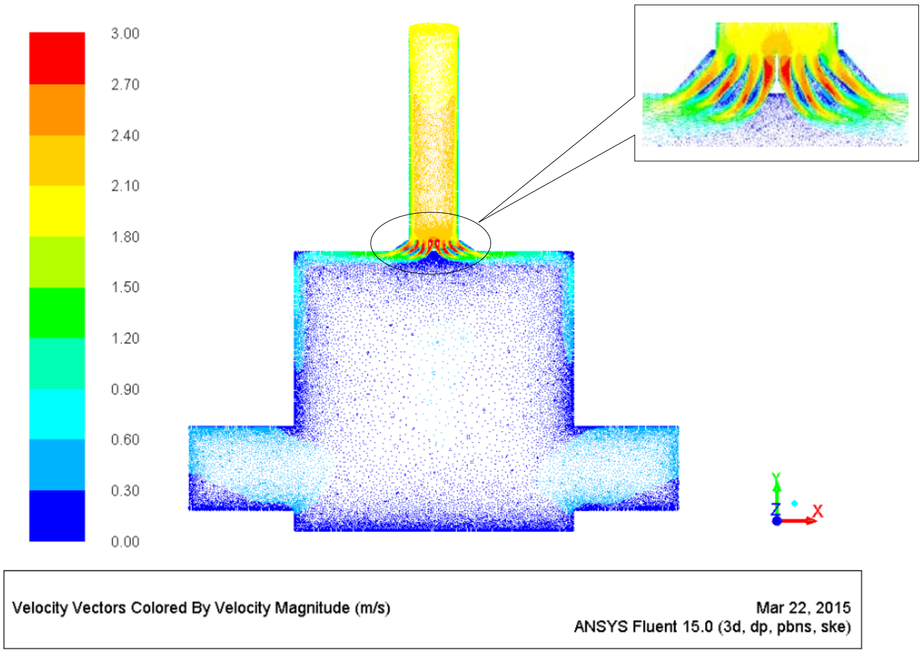

(b)

Figure B.3: **Velocity vectors in the room with inlet on ceiling and 2 outlets near wall bottoms at 2.0 m/s inlet velocity: (a) 7-blade, & (b) 5-blade round ceiling air diffuser**

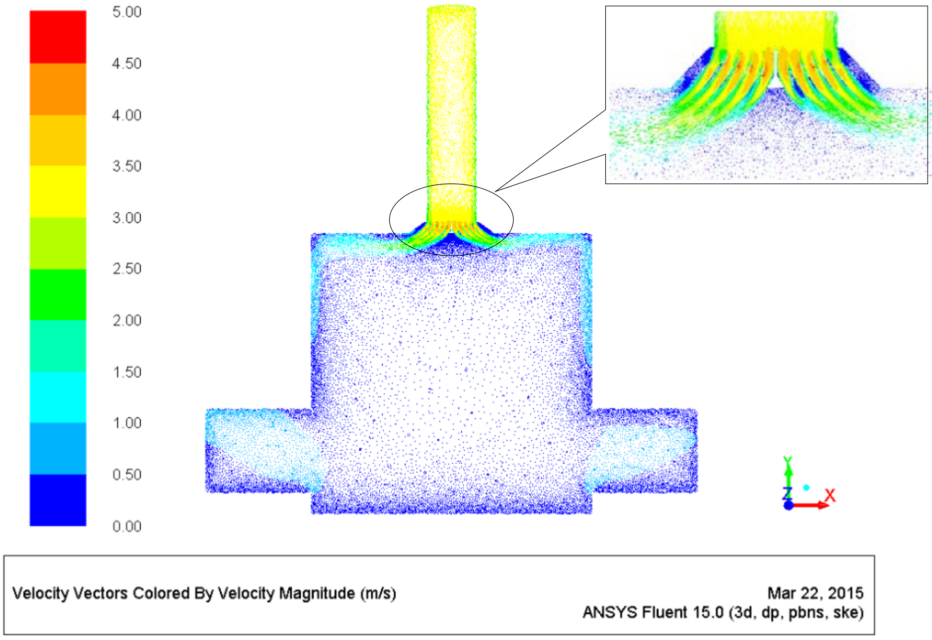

(a)

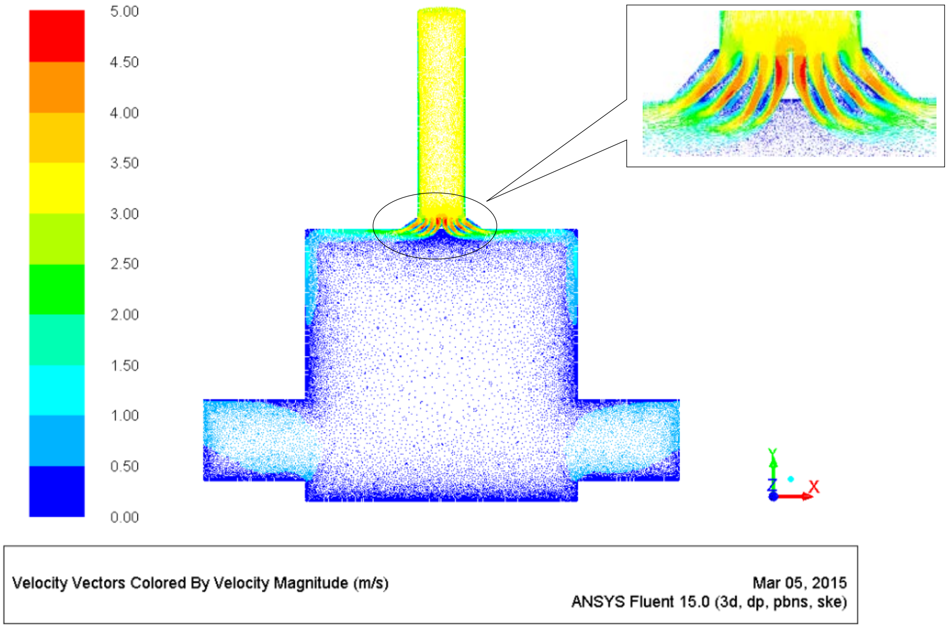

(b)

Figure B.4: Velocity vectors in the room with inlet on ceiling and 2 outlets near wall bottoms at 3.0 m/s inlet velocity: (a) 7-blade, & (b) 5-blade round ceiling air diffuser

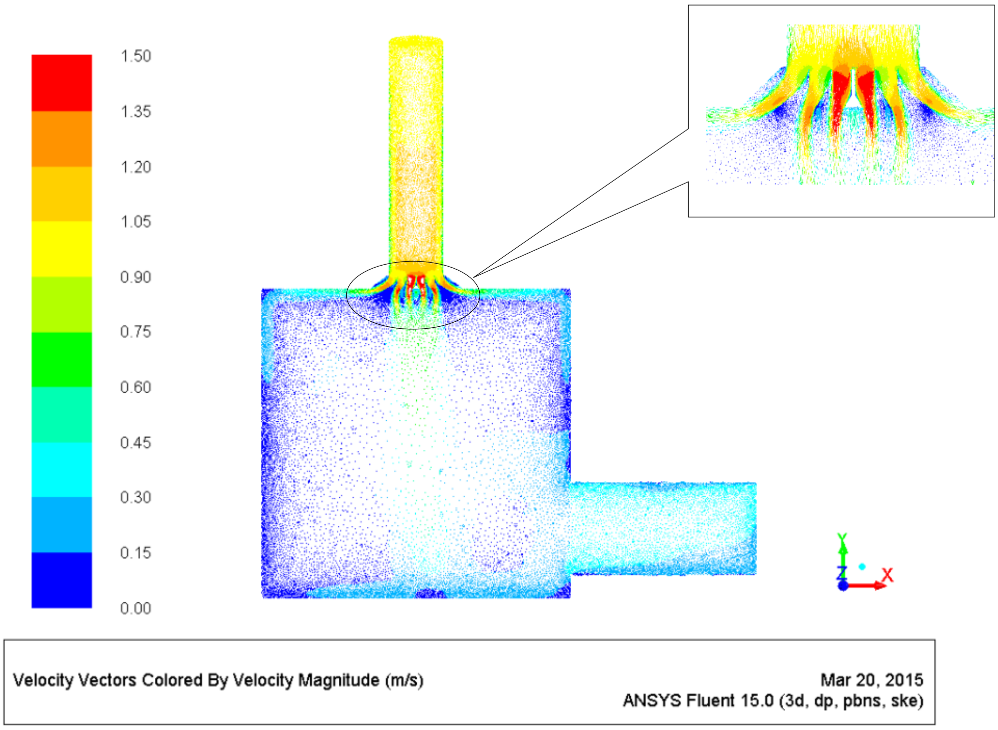
1.50
1.35
1.20
1.05
0.90
0.75
0.60
0.45
0.30
0.15
0.00
Velocity Vectors Colored By Velocity Magnitude (m/s)
Mar 20, 2015
ANSYS Fluent 15.0 (3d, dp, pbns, ske)

(a)

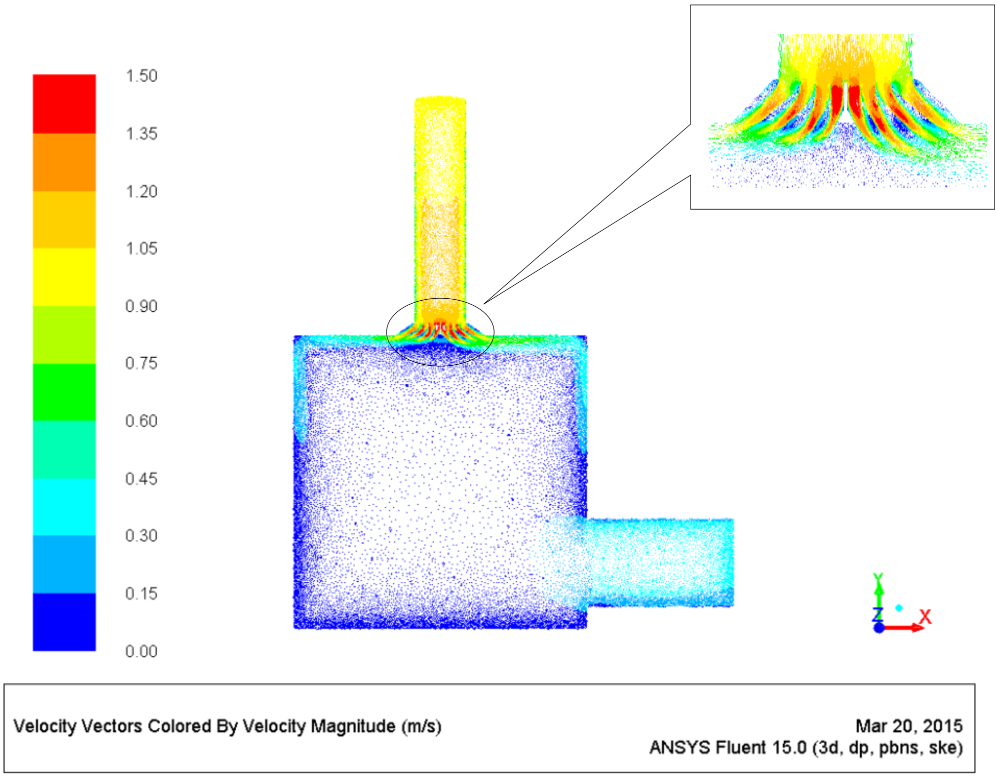
1.50
1.35
1.20
1.05
0.90
0.75
0.60
0.45
0.30
0.15
0.00
Velocity Vectors Colored By Velocity Magnitude (m/s)
Mar 20, 2015
ANSYS Fluent 15.0 (3d, dp, pbns, ske)

(b)

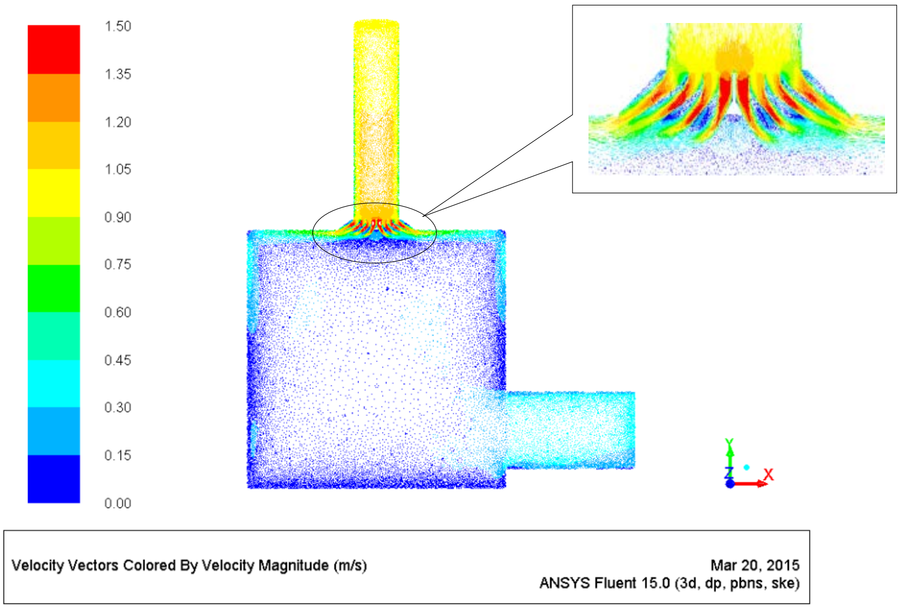

(c)

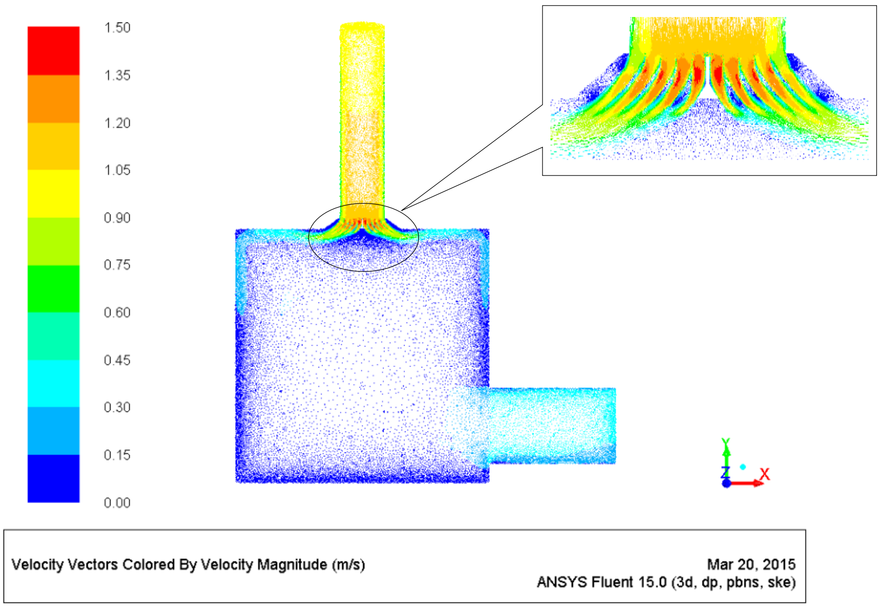

(d)

Figure B.5: **Velocity vectors in the room with inlet on ceiling and 1 outlet near wall bottom: (a) 4-blade, (b) 5-blade, (c) 5-blade with blade angle change, & (d) 7-blade round ceiling air diffuser**

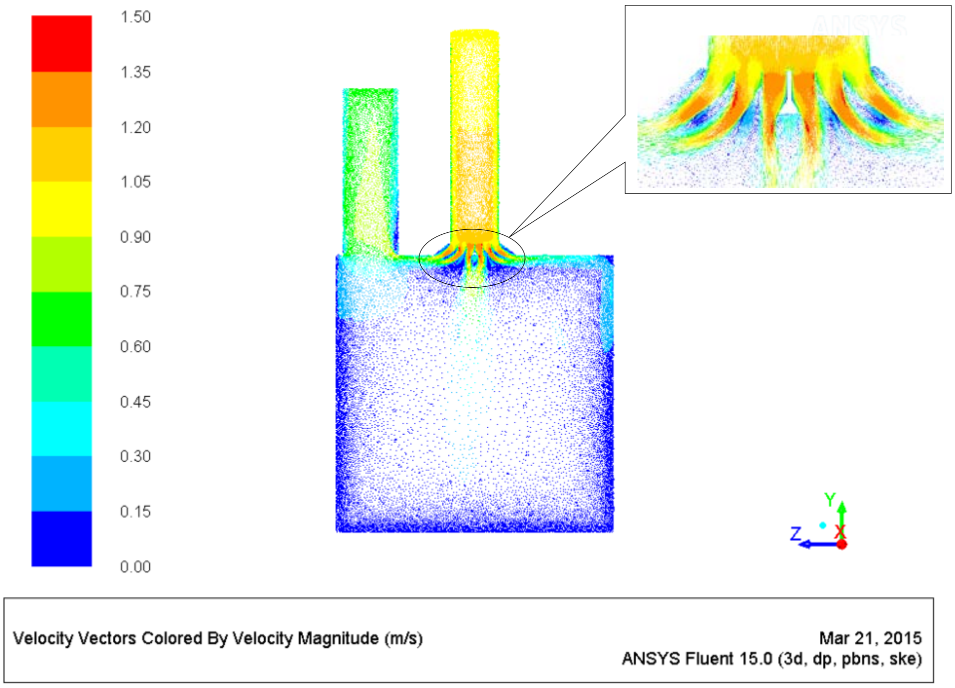
1.50
1.35
1.20
1.05
0.90
0.75
0.60
0.45
0.30
0.15
0.00
Velocity Vectors Colored By Velocity Magnitude (m/s)
Mar 21, 2015
ANSYS Fluent 15.0 (3d, dp, pbns, ske)

(a)

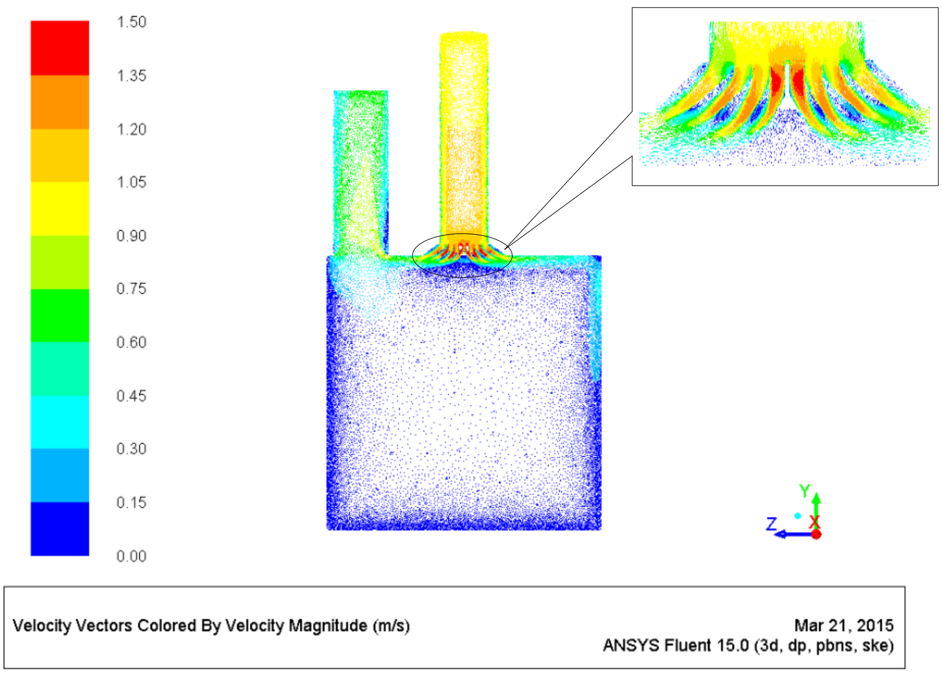
1.50
1.35
1.20
1.05
0.90
0.75
0.60
0.45
0.30
0.15
0.00
Velocity Vectors Colored By Velocity Magnitude (m/s)
Mar 21, 2015
ANSYS Fluent 15.0 (3d, dp, pbns, ske)

(b)

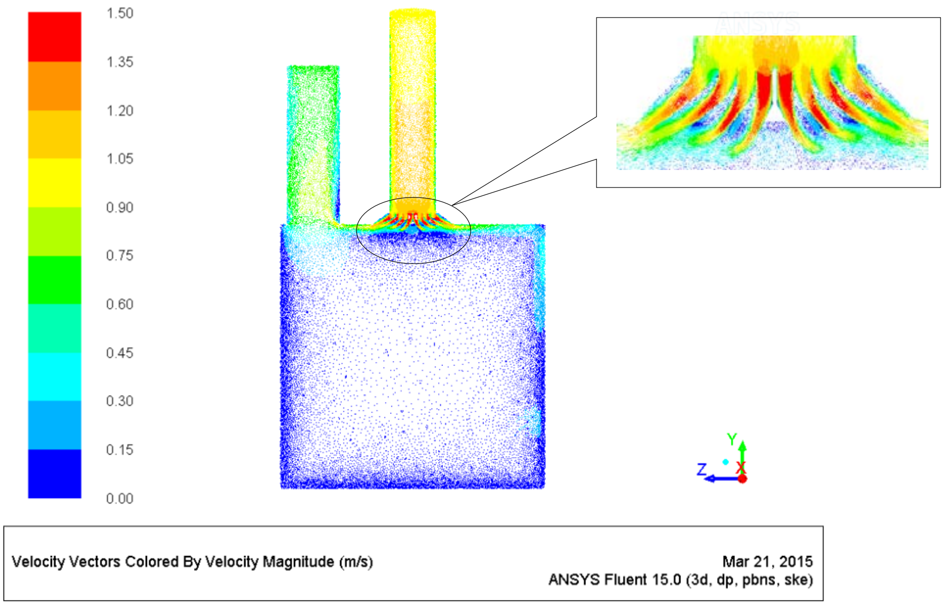

(c)

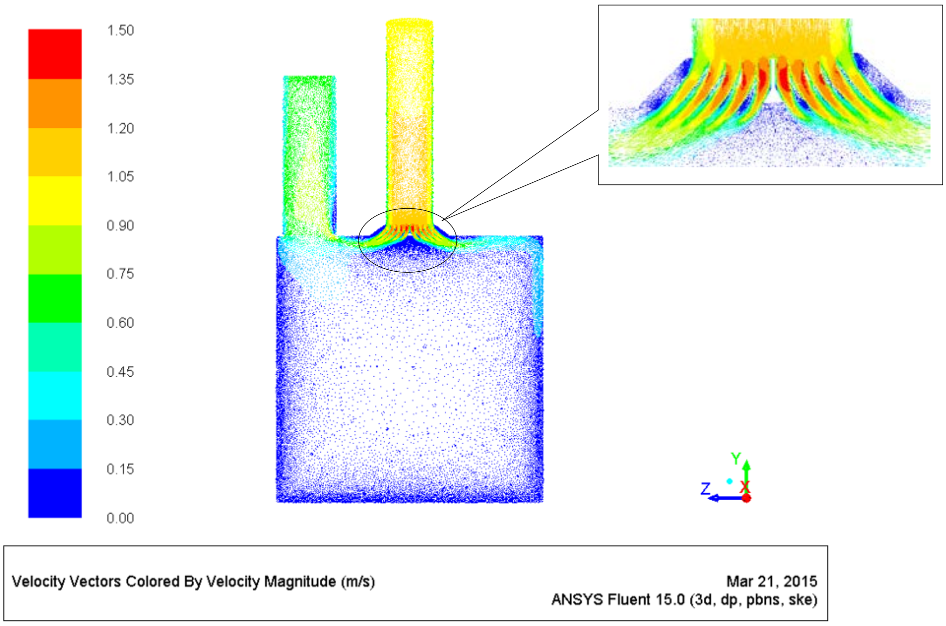

(d)

Figure B.6: **Velocity vectors in the room with inlet and outlet on ceiling level: (a) 4-blade, (b) 5-blade, (c) 5-blade with blade angle change, & (d) 7-blade round ceiling air diffuser**

APPENDIX C: Tabulation for detail working on dimensionless average room air velocity and temperature

Table C.1: Dimensionless average room air velocity at various inlet velocities and Reynolds number at same inlet temperature in the room with 2 outlets near bottom of walls for round ceiling air diffuser

Item	5-blade			
	Average Room Air Velocity, V_a (m/s)	**Inlet Air Velocity, V_i (m/s)**	**Dimensionless Average Room Air Velocity, V_a/V_i**	**Reynolds Number at Inlet, Re (= $\rho V_i d_i/\mu$)**
1	0.06	0.50	0.12	11980
2	0.14	1.00	0.14	23961
3	0.30	2.00	0.15	47921
4	0.47	3.00	0.16	71882

Item	7-blade			
	Average Room Air Velocity, V_a (m/s)	**Inlet Air Velocity, V_i (m/s)**	**Dimensionless Average Room Air Velocity, V_a/V_i**	**Reynolds Number at Inlet, Re (= $\rho V_i d_i/\mu$)**
1	0.07	0.50	0.14	11980
2	0.16	1.00	0.16	23961
3	0.34	2.00	0.17	47921
4	0.53	3.00	0.18	71882

Table C.2: Dimensionless average room air temperature at various inlet velocities and Reynolds number at same inlet temperature in the room with 2 outlets near bottom of walls for round ceiling air diffuser

Item	5-blade			
	Average Room Air Temperature, T_a (K)	**Inlet Air Temperature, T_i (K)**	**Dimensionless Average Room Air Temperature, T_a/T_i**	**Reynolds Number at Inlet, Re (= $\rho V_i d_i/\mu$)**
1	294.2	287.0	1.025	11980
2	293.4	287.0	1.022	23961
3	292.7	287.0	1.020	47921
4	292.4	287.0	1.019	71882

Item	7-blade			
	Average Room Air Temperature, T_a (K)	**Inlet Air Temperature, T_i (K)**	**Dimensionless Average Room Air Temperature, T_a/T_i**	**Reynolds Number at Inlet, Re (= $\rho V_i d_i/\mu$)**
1	293.8	287.0	1.024	11980
2	292.9	287.0	1.020	23961
3	291.8	287.0	1.017	47921
4	291.1	287.0	1.014	71882

APPENDIX D: Tabulation for detail working on overall ventilation effectiveness and effective draft temperature

Table D.3: The overall ventilation effectiveness (*E*) in room at various inlet velocities and Reynolds number at same inlet temperature in the room with 2 outlets near bottom of walls for round ceiling air diffuser

	5-blade				
Item	**Average Room Air Temperature, T_a (K)**	**Inlet Air Temperature, T_i (K)**	**Outlet Air Temperature, T_o (K)**	**Overall Ventilation Effectiveness, *E***	**Reynolds Number at Inlet, Re (= $\rho V_i d_i/\mu$)**
1	294.2	287.0	294.9	1.097	11980
2	293.4	287.0	294.3	1.141	23961
3	292.7	287.0	293.9	1.211	47921
4	292.4	287.0	293.7	1.252	71882

	7-blade				
Item	**Average Room Air Temperature, T_a (K)**	**Inlet Air Temperature, T_i (K)**	**Outlet Air Temperature, T_o (K)**	**Overall Ventilation Effectiveness, *E***	**Reynolds Number at Inlet, Re (= $\rho V_i d_i/\mu$)**
1	293.8	287.0	294.6	1.188	11980
2	292.9	287.0	294.0	1.197	23961
3	291.8	287.0	293.2	1.292	47921
4	291.1	287.0	292.5	1.358	71882

Table D.4: The effective draft temperature (*EDT*) in the room at various inlet velocities and Reynolds number at inlet with 2 outlets near bottom of walls for round ceiling air diffuser

Item	5-blade				
	Average Room Air Temperature, T_a (K)	**Local Airstream Temperature, T_x (K)**	**Local Airstream Velocity, V_x (m/s)**	**Effective Draft Temperature, EDT**	**Reynolds Number at Inlet, R*e* (= $\rho V_i d_i/\mu$)**
1	294.2	294.9	0.06	1.42	11980
2	293.4	293.9	0.12	0.74	23961
3	292.7	293.3	0.34	-0.92	47921
4	292.4	292.9	0.55	-2.65	71882

Item	7-blade				
	Average Room Air Temperature, T_a (K)	**Local Airstream Temperature, T_x (K)**	**Local Airstream Velocity, V_x (m/s)**	**Effective Draft Temperature, EDT**	**Reynolds Number at Inlet, R*e* (= $\rho V_i d_i/\mu$)**
1	293.8	294.8	0.13	1.15	11980
2	292.9	293.4	0.16	0.47	23961
3	291.8	292.7	0.41	-1.18	47921
4	291.1	292.1	0.65	-2.95	71882

APPENDIX E: Zone air distribution effectiveness for ventilation (ASHRAE, 2013)

Air Distribution Configuration	E_z
Ceiling supply of cool air	1.0
Ceiling supply of warm air and floor return	1.0
Ceiling supply of warm air at least 8°C (15°F) above space temperature and ceiling return.	0.8
Ceiling supply of warm air less than 8°C (15°F) above space temperature and ceiling return provided that the 0.8 m/s (150 fpm) supply air jet reaches to within 1.4 m (4.5 ft) of floor level. **Note**: For lower velocity supply air, $E_z = 0.8$.	1.0
Floor supply of cool air and ceiling return provided that the 0.8 m/s (150 fpm) supply jet reaches at least 1.4 m (4.5 ft) above the floor. **Note**: Most underfloor air distribution systems comply with this proviso.	1.0
Floor supply of cool air and ceiling return, provided low-velocity displacement ventilation achieves unidirectional flow and thermal stratification	1.2
Floor supply of warm air and floor return	1.0
Floor supply of warm air and ceiling return	0.7
Makeup supply drawn in on the opposite side of the room from the exhaust and/or return	0.8
Makeup supply drawn in near to the exhaust and/or return location	0.5